Universidad Autónoma de Madrid

Universidad Autónoma de Madrid

Facultad de Medicina

Departamento de Bioquímica

Doctoral thesis

Functional validation of DNA glycosylases as cancer risk modifiers in *BRCA1* and *BRCA2* mutation carriers. Potential use of OGG1 inhibitors as a novel strategy for cancer treatment

Juan Miguel Baquero López

Madrid, 2020

Programa de Doctorado en Biociencias Moleculares
Departamento de Bioquímica
Facultad de Medicina
Universidad Autónoma de Madrid

Functional validation of DNA glycosylases as cancer risk modifiers in *BRCA1* and *BRCA2* mutation carriers. Potential use of OGG1 inhibitors as a novel strategy for cancer treatment

Tesis doctoral presentada por:

Juan Miguel Baquero López
Graduado en Biología por la Universidad Complutense de Madrid

Directores de tesis:

Dr. Javier Benítez Ortiz
Jefe del Grupo de Genética Humana y Director del Programa de Genética del Cáncer Humano (CNIO)

Dra. Ana Osorio Cabrero
Investigadora del Grupo de Genética Humana (CNIO)

Grupo de Genética Humana
Programa de Genética del Cáncer Humano
Centro Nacional de Investigaciones Oncológicas (CNIO)

This doctoral thesis, submitted for the degree of Doctor of Philosophy at the Autonomous University of Madrid, has been elaborated in the Human Genetics Group at the Spanish National Cancer Research Center (CNIO) in Madrid, under the supervision of Dr. Javier Benítez Ortiz and Dra. Ana Osorio Cabrero.

This research was supported by the following grants and fellowships:

- University Professor Training grant FPU15/01978 from the Spanish Ministry of Education, Culture, and Sport. 2016-2020: Juan Miguel Baquero López.
- Spanish Ministry of Economy and Competitiveness SAF2014-57680-R, the Spanish Network of Rare Diseases (CIBERER).
- FIS PI16/00440 supported by FEDER funds and HORIZON 2020-BRIDGES (2015-2019)

A mi abuelo

AGRADECIMIENTOS

Estoy aprendiendo a morderme la lengua y voy a intentar aquí ser lo más diplomático posible. En cualquier caso, creo que unos agradecimientos pierden todo su significado si no se redactan con franqueza. En consecuencia, garantizo que las siguientes palabras son plenamente sinceras.

Durante estos cuatro largos años de tesis, he sufrido un profundo desarrollo personal en gran parte gracias a toda la gente que se ha cruzado en mi camino. A pesar de las adversidades que han ido surgiendo, en todo momento me he sentido un privilegiado de poder haber formado parte de una institución de primer nivel como es el CNIO. Como es lógico, me he encontrado de todo en esta etapa: desde brillantes investigadores, hasta auténticos fraudes, desde personas extraordinarias, a extremadamente tóxicas. Esto lo valoro como algo muy positivo, ya que me ha ayudado a reflexionar acerca de cómo debo actuar para llegar a ser un buen científico y, principalmente, una mejor persona.

Antes de pasar a los agradecimientos personales, querría darle las gracias a los responsables de concederme la ayuda FPU (convocatoria 2015), así como la prórroga de tres meses este último año, que me han permitido subsistir durante este tiempo. Gracias por haberme posibilitado vivir esta experiencia y confío en haber dado un buen uso del dinero público destinado a mi formación.

Como no puede ser de otra manera, agradezco a mis directores el apoyo y dedicación que me han prestado en todo momento. Javier, te estoy muy agradecido por toda la confianza depositada en mí desde el primer día. No podía haberme presentado más verde a la entrevista y aun así no dudaste en dirigirme. Desde entonces, te has preocupado a diario por los progresos en mi trabajo, mostrando interés por cualquier novedad y concediéndome siempre total libertad para organizarme. Esto último, que aunque a veces me resultase algo caótico, echando la vista atrás considero que ha sido algo fundamental para hacerme crecer como investigador. Ana, te agradezco tu actitud constructiva frente a cualquier situación, tu cercanía y compresión. Gracias también por tus correcciones constantes, que han mejorado enormemente todo lo que ha pasado por tus manos. Muchas gracias a los dos por todo, ha sido un placer.

Esta tesis es en gran parte deudora del trabajo del doctor Carlos Benítez-Buelga. Hoy nos encontraríamos ante un manuscrito muy diferente de no haber sido por su ayuda constante. Le agradezco facilitarme continuar sus líneas de investigación y la estrecha colaboración mantenida en todo momento.

A todo el personal del CNIO y la UAM implicado en el progreso de esta tesis a nivel administrativo. A las secretarias Irene, Celia y Gema, sois encantadoras. Agradezco a Ana Sánchez, Rocío Gómez y a mi tutora María Monsalve su buena disposición siempre que les he molestado por cuestiones burocráticas.

Muchas gracias a todos los miembros del grupo de Genética Humana por acogerme tan amablemente desde el primer día y haberme transmitido que disponía de ayuda para cualquier cosa que pudiera necesitar en todo momento. Ali, me encanta tu mentalidad en relación a que “hay que tener recursos” para salir al paso en cualquier circunstancia, sabes muchísimo y ha sido un alivio enorme tenerte cerca para consultarte cualquier duda, siempre me quedaba más tranquilo después de preguntarte. Toya, te agradezco la paciencia que tuviste conmigo enseñándome técnicas y protocolos, eres muy meticulosa y aprendí muchísimo el primer año gracias a ti. Y sobretodo, muchas gracias por tus consejos y tu preocupación sincera hacia cuestiones personales, eres una excelente compañera. Ana Cora, me dio mucha pena que te tuvieras que ir, no solo eres muy divertida, sino también una profesional extraordinaria. Nunca estuvo tan bien organizado el laboratorio como cuando te teníamos por aquí.

Paloma, tú entiendes mejor que nadie lo que nos ha supuesto esta experiencia que hemos vivido en paralelo. Gracias por tu complicidad y predisposición a ayudarme para cualquier cosa que necesitase. Te deseo lo mejor tras el doctorado y no tengo ninguna duda de que te irá estupendamente con independencia del camino que elijas. Oriol, gracias por tus consejos y los buenos momentos fuera del laboratorio. María, gracias por tu simpatía y por permitirme trabajar con tu serie de muestras de ovario. Bea y Javi, sois unos currantes natos, contribuisteis a incrementar exponencialmente el buen rollo del grupo. Estoy seguro de que hay un excelente ambiente laboral allí donde estéis.

Ale, sin duda la ausencia que más noté fue la tuya. A pesar de que te he echado de menos por aquí, me alegra mucho saber que todo te va bien por casa. Gracias por ser tan buena compañera y transmitirme vitalidad cuando la necesitaba. Te admiro como científica y sobretodo por ser una luchadora incansable.

A Alexandra, Afshan, Eneida y todas las estudiantes que pasaron por el grupo y tuvieron que tener que soportarme. Particularmente me compadezco de Mónica y Rocío, quienes me concedieron el privilegio de dirigir sus TFGs. He aprendido muchísimo gracias a vosotras y ojalá haya sido recíproco, ya que contribuir con vuestra formación me produce mucha más satisfacción que el resultado de cualquier experimento.

Gracias a los compañeros de la Unidad de Cáncer Familiar. Laura, muchas gracias por estar siempre disponible, por todas las confidencias y momentos de desahogo. Le agradezco al doctor Miguel Urioste permitirme vivir la extraordinaria experiencia que fue acompañarle a su consulta y, principalmente, su predisposición a colaborar con el reclutamiento de los pacientes, siendo de vital importancia para el desarrollo de esta tesis. Aprovecho aquí para dar las gracias a todas las personas, pacientes y familiares, que colaboraron desinteresadamente en este proyecto. Nos debemos a vosotros y el objetivo último de toda investigación biomédica debe estar orientado hacia su aplicación clínica.

A todos los integrantes del grupo de Cáncer Endocrino, que han tenido que padecer mis visitas constantes por su laboratorio. Meme, te felicito por haber cohesionado un grupo extraordinario. Bruna, no he visto a nadie que se preocupe tanto por todos sus compañeros, eso dice mucho más de ti que todas tus publicaciones. Juanma, que reconozco que te he dado particularmente la lata, gracias por toda la paciencia que has tenido conmigo siempre, tu sentido del humor y ser experto en levantar el ánimo de la gente. María, me gustaría dejar aquí claro la horrible persona que eres, pero para que nadie lo malinterprete, prefiero darte las gracias por ser tan amable, buena compañera y por alegrar con tu simpatía cualquier situación. Rocío, Cristina, Alberto, Javi, Rafa, Laura, Lucía, Sara… de verdad que sois todos majísimos y unos investigadores excepcionales. Alfonso, aunque no hubo día en el que no quisiera que me dejaras tranquilo, en cuanto te fuiste sentí mucho que no siguieras por aquí molestándome.

Gracias a los miembros del CEGEN. Guille y Hugo sois unos compañeros estupendos. A la Unidad de Citogenética, especialmente a Raúl y a Patri, por vuestra ayuda y por ser unas personas maravillosas.

A Fer por su amor incondicional, eres el mejor científico que conozco. Celeste, tienes un corazón enorme, gracias por preocuparte hasta de las plantas. A todos los integrantes del Programa de Genética, así como al resto de trabajadores del CNIO que me han apoyado durante estos años o, simplemente, transmitido su simpatía con cualquier gesto, como una sonrisa sincera por el pasillo, ayudándome a ignorar por un momento el sufrimiento que caracteriza la existencia humana.

Muchas gracias a todos los alumnos y profesores de la Facultad de Ciencias de la UAM con los que he compartido clases a lo largo de estos cursos. Habéis hecho que participar en la docencia universitaria haya sido una de las experiencias más enriquecedoras que he vivido en estos años y que más pena me da que se termine. Agradezco especialmente a la profesora Begoña Fernández toda su amabilidad y ayuda. Fijándome en ti he observado cuales son todas las cualidades que debe tener un buen profesor.

A mis padres. A toda mi familia y amigos, confío en que no vais a leer esto y así no os decepcionaréis por haberme retirado sin encontrar la vacuna contra el cáncer. Mis agradecimientos hacia vosotros no van a consistir en unas pomposas palabras protocolarias, sino en la promesa de ofreceros todo el tiempo y cariño que no os he dado estos últimos años. Lo siento mucho, no volverá a ocurrir.

A Ana (que tú si vas a leer esto), te escriba aquí lo que te escriba, solo sé que me voy a quedar muy corto. No te puedes hacer a la idea de todo lo que has hecho por mi y cómo me has ayudado a sobrevivir a la tesis. Gracias por todo tu amor y la paciencia que has demostrado cada día que me has tenido que soportar abatido, desganado y de mal humor. Por muy abstraído que estuviera a veces por el trabajo, en todo momento he tenido clarísimo que un segundo a tu lado vale infinitamente más que todos los resultados y publicaciones del mundo.

Quiero dedicarle mi tesis doctoral a mi abuelo Agustín, por haberme transmitido todos los valores que me hicieron crecer como persona. Cuando tengo que afrontar una decisión importante, me gusta pararme a pensar cual sería la decisión que te hubiera hecho sentirte más orgulloso de mí. En esta tesis he puesto todo lo mejor de mí para que haya sido así.

ABSTRACT

Women carrying germline deleterious mutations in the *BRCA1* and *BRCA2* genes have a high lifetime risk of developing breast and ovarian cancer. However, mutation carriers show considerable differences in disease manifestation, and this suggests the existence of genetic or environmental factors that modify the risk of cancer development. The identification of these factors would allow obtaining accurate cancer risk prediction models and providing personalized genetic counselling.

The *BRCA* genes are involved in the homologous recombination (HR) DNA repair pathway and, consequently, cells with deleterious mutations in these genes are highly dependent on other repair pathways. In particular, tumors with *BRCA1* or *BRCA2* mutations are selectively sensitive to the treatment with inhibitors of the protein PARP1 from the base excision repair (BER) pathway. This phenomenon is referred to as synthetic lethality and has positioned PARP1 inhibitors as promising drugs for the treatment of breast or ovarian cancers deficient in *BRCA1* or *BRCA2*.

Bearing in mind these facts, our research group previously carried out a study that analysed genes involved in BER as candidate cancer risk modifiers in women carrying germline mutations in the *BRCA* genes. The polymorphisms identified with higher statistical evidence as risk modifiers were localized in glycosylase genes. The first objective of this thesis has been the characterization, by using functional studies, of the molecular basis through which the studied genetic variants, localized in regulatory regions of the *NEIL2* and *UNG* genes, contribute to modify cancer risk.

NEIL2 SNP rs804271, linked to higher breast cancer risk in *BRCA2* mutation carriers, is associated with *NEIL2* overexpression and higher accumulation of oxidative damage in the telomeric DNA of women harbouring a *BRCA2* mutation. On the other hand, *UNG* SNP rs34259, linked to a protective effect for ovarian cancer risk in *BRCA2* mutation carriers, is associated with a lower *UNG* expression and lower uracil levels at telomeres in *BRCA2* mutations carriers. These and other findings, reported in the present thesis, help to explain the association of these SNPs with cancer risk, highlighting the importance of genetic changes in glycosylase genes as modifiers of cancer susceptibility for *BRCA* genes mutation carriers.

Secondly, because of the essential role of the BER pathway in maintaining telomere integrity, we aimed to analyse the consequences of pharmacological inhibition of OGG1 glycosylase at the telomeres of tumoral cells as a possible therapeutic strategy. Our results show that, upon oxidative stress conditions, OGG1 inhibition blocks BER at telomeres. As a consequence, telomere instability, post-mitotic defects, and lower cell proliferation are generated. Therefore, these results show that OGG1 is necessary to preserve telomere homeostasis and present OGG1 inhibitors as a tool to induce oxidative DNA damage at telomeres, with potential implications in cancer and aging research.

Finally, we have studied the possible synthetic lethality relationship between *OGG1* and *BRCA1* on breast tumoral cells with silenced *BRCA1*, as well as the impact of the combined treatment of PARP1 and OGG1 inhibitors. The OGG1 inhibitor TH5487 decreases cell viability in a higher proportion when *BRCA1* is silenced. Besides, TH5487 increases the therapeutic effect of the PARP1 inhibitor olaparib. These findings could lead to a new framework for the treatment of hereditary breast and ovarian cancer.

RESUMEN

Las mujeres portadoras de mutaciones germinales deletéreas en los genes *BRCA1* y *BRCA2* presentan un riesgo relativo elevado de desarrollar cáncer de mama y ovario a lo largo de su vida. Sin embargo, existen diferencias considerables en la manifestación de la enfermedad entre estas mujeres, lo que sugiere la existencia de factores genéticos y ambientales modificadores del riesgo de desarrollo del cáncer. La identificación de dichos factores permitiría obtener modelos predictivos del riesgo de cáncer más precisos y ofrecer un consejo genético personalizado.

Los genes *BRCA* participan en la vía de reparación del ADN por recombinación homóloga (HR) y, en consecuencia, las células con mutaciones deletéreas en estos genes son altamente dependientes de otras vías de reparación. En particular, los tumores con mutaciones en *BRCA1* o *BRCA2* son selectivamente sensibles al tratamiento con inhibidores de la proteína PARP1 de la vía de reparación por escisión de bases (BER). Este fenómeno se conoce como letalidad sintética y ha situado a los inhibidores de PARP1 como agentes muy prometedores para el tratamiento de cánceres de mama u ovario deficientes en *BRCA1* o *BRCA2*.

Teniendo en cuenta estos hechos, nuestro grupo de investigación llevo a cabo un estudio donde se analizaron los miembros de la vía BER como posibles modificadores del riesgo de cáncer en mujeres portadoras de mutaciones germinales en los genes *BRCA*. Los polimorfismos que se encontraron con una mayor evidencia estadística como modificadores del riesgo se localizaban en genes de glicosilasas. El primer objetivo de esta tesis ha consistido en la caracterización, mediante estudios funcionales, de las bases moleculares a través de las cuales las variantes genéticas identificadas, situadas en regiones reguladoras de los genes *NEIL2* y *UNG*, contribuyen a modificar el riesgo de cáncer.

El SNP de *NEIL2* rs804271, vinculado con un mayor riesgo de cáncer de mama en portadoras de mutaciones en BRCA2, se asocia a una sobreexpresión de *NEIL2* y una mayor acumulación de daño oxidativo en el ADN telomérico de las mujeres portadoras de mutación en *BRCA2*. Por su parte, el SNP de *UNG* rs34259, vinculado a un menor riesgo de cáncer de ovario en portadoras de mutaciones en *BRCA2*, se asocia una menor expresión de *UNG* y menores niveles de uracilo en los telómeros de portadoras de mutaciones en *BRCA2*. Estos, junto a otros resultados expuestos en esta tesis, ayudan a explicar las asociaciones entre estos SNPs y el riesgo de cáncer, subrayando la importancia de los cambios genéticos en los genes de glicosilasas como modificadores del riesgo de cáncer para las portadoras de mutaciones en los genes *BRCA*.

En segundo lugar, debido al papel fundamental de la vía BER en el mantenimiento de la integridad telomérica, nos propusimos analizar las consecuencias de la inhibición farmacológica de la glicosilasa OGG1 sobre los telómeros de células tumorales como posible estrategia terapéutica. Nuestros resultados muestran que, bajo condiciones de estrés oxidativo, la inhibición de OGG1 bloquea la vía BER en los telómeros. A raíz de ello, se genera inestabilidad telomérica, defectos post-mitóticos y una menor proliferación celular. En consecuencia, estos resultados demuestran que OGG1 es necesaria para preservar la homeostasis telomérica y presentan a los inhibidores de OGG1 como una nueva herramienta para inducir daño oxidativo en el ADN telomérico, con potenciales implicaciones en la investigación del cáncer y el envejecimiento.

Finalmente, hemos estudiado la posible relación de letalidad sintética entre *OGG1* y *BRCA1* sobre células tumorales de mama con *BRCA1* silenciado, así como el impacto del tratamiento combinado de inhibidores de PARP y OGG1. El inhibidor de OGG1 TH5487 disminuye la viabilidad celular en una mayor proporción cuando *BRCA1* está silenciado y, además, potencia la acción del inhibidor de PARP1 olaparib. Estos descubrimientos podrían conducir hacia un nuevo marco para el tratamiento del cáncer de mama y ovario hereditario.

TABLE OF CONTENTS

Table of contents:

ABBREVIATIONS

5'-dRP	5'-deoxyribose Phosphate
8-oxoG	8-oxoguanine
ANOVA	Analysis of Variance
AP	Apurinic/Apyrimidinic
APE1	Apurinic/Apyrimidinic Endonuclease 1
AU	Arbitrary Units
BC	Breast Cancer
BER	Base Excision Repair
BRCA1	Breast Cancer Susceptibility Gene 1
BRCA2	Breast Cancer Susceptibility Gene 2
BSA	Bovine Serum Albumin
CG	Candidate Gene
ChIP	Chromatin Immunoprecipitation
CNIO	Spanish National Cancer Research Centre
CIMBA	The Consortium of Investigators of Modifiers of BRCA1/2
COGS	Collaborative Oncological Gene-environment Study
DAPI	4',6-Diamidino-2-Phenylindole
DDR	DNA Damage Response
dGTP	Deoxyguanosine Triphosphate
DMSO	Dimethyl Sulfoxide
DNA	Deoxyribonucleic Acid
DNPH	2,4-Dinitrophenylhidrazine
dNTP	Deoxyribonucleic Triphosphate
DSB	Double-Strand Break
dTTP	Deoxythymidine Triphosphate
dUTP	Deoxyuridine Triphosphate
EMA	European Medicines Agency
eQTL	expression Quantitative Trait Locus
FA	Fanconi Anemia
FBOC	Familial Breast and Ovarian Cancer
FBS	Fetal Bovine Serum
FDA	Food and Drug Administration
FEN1	Flap Endonuclease 1
FISH	Fluorescence in situ Hybridization
FPG	Formamidopyrimidine DNA Glycosylase
GFP	Green Fluorescence Protein
Gh	Guanidinohydantoin
GTEx	Genotype-Tissue Expression
GWAS	Genome-Wide Association Study
HBOC	Hereditary Breast and Ovarian Cancer
HR	Homologous Recombination
HT-Q	High-throughput quantitative
IC_{50}	Half-maximal inhibitory concentration
IDIBELL	Bellvitge Biomedical Research Institute
IF	Immunofluorescence
LCLs	Lymphoblastoid Cell Lines
LD	Linkage Disequilibrium
MAF	Minor Allele Frequency
MBD4	Methyl-CpG-Binding Domain Protein 4
MMR	Mismatch Repair
MPG	N-Methylpurine DNA Glycosylase
mRNA	Messenger Ribonucleic Acid
MTT	3-(4,5-dimethylthiazol-2-yl)-2,5-diphenyltetrazolium
MUTYH	MutY Homolog
NEIL1	Nei-like DNA Glycosylase 1
NEIL2	Nei-like DNA Glycosylase 2
NEIL3	Nei-like DNA Glycosylase 3
NS	Not Significant
NT	Non-targeting control/Non-treated
NTH1	Endonuclease III Homolog 1
OC	Ovarian Cancer
OCT	Optimal Cutting Temperature medium
OGG1	8-Oxoguanine Glycosylase 1
OGG1i	OGG1 inhibitor
OLP	Olaparib
OS	Oxidative Stress
P/S	Penicillin-Streptomycin
PARP-1	Poly ADP-ribose polymerase 1
PARPi	PARP inhibitor
PBMC	Peripheral Blood Mononuclear Cells
PBS	Phosphate-Buffered Saline
PCNA	Proliferating Cell Nuclear Antigen
PFA	Paraformaldehyde
POL 2	RNA polymerase 2
Pol β	DNA polymerase β
PRS	Polygenic Risk Score
ROS	Reactive Oxygen Species
SEM	Standard Error of the Mean
SEOM	Spanish Society of Medical Oncology
sgNT	single guide non-targeting
SL	Synthetic Lethality
SMUG1	Single Strand Selective Monofunctional Uracil DNA Glycosylase
SNP	Single Nucleotide Polymorphism
SSB	Single-Strand Break
SSC	Saline-Sodium Citrate buffer
STR	Short Tandem Repeat
TDG	Thymine DNA Glycosylase
TF	Transcription Factor
TIDE	Tracking of Indels by Decomposition
TL	Telomere Length
TNBC	Triple-Negative Breast Cancer
TSS	Transcriptional Start Site
UNG	Uracil DNA Glycosylase
UTR	Untranslated Region
XRCC1	X-ray Repair Cross-Complementing 1

INTRODUCTION

1. Hereditary breast and ovarian cancer

1.1 General features

Breast cancer (BC) is the most commonly diagnosed and the leading cause of cancer death among women worldwide, with an estimated 2.1 million new cases and 630,000 deaths annually (Bray et al., 2018). On the other side, epithelial ovarian cancer (OC) is the most lethal gynaecological cancer, with over 295,000 new cases and 185,000 deaths globally per year (Reid et al., 2017; Bray et al., 2018). BC and OC are highly heterogeneous diseases, composed of different subtypes developed through multiple molecular pathways, each of which represents a very different biological entity associated with distinct clinical outcomes (Waks and Winer, 2019; Lheureux et al., 2019).

Multiple risk factors for BC and OC have been identified, including lifestyle, hormonal, and genetic factors (Reid et al., 2017). The majority of cases are considered as sporadic, which are characterized by a later age of onset and by lacking an evident family history. However, up to 15% of all cases report a positive family history of cancer and are thus considered as having a "familial cancer". These families are characterized by a higher number of cancer cases than statistically expected, variable age of onset and unknown inheritance model (Daly et al., 2017). Nevertheless, given that the familial clustering can be a consequence of several non-genetic factors, this category does not reliably identify hereditary cases, that is, women carrying a germline mutation responsible for the predisposition to cancer development. Conversely to familial cancer, hereditary breast and ovarian cancer (HBOC) is associated with inherited risk alleles in susceptibility genes. HBOC represents about 5-10% of all BC and OC cases and is characterized by an autosomal dominant pattern of inheritance, young age of onset and multiple primary and/or bilateral cancers (Samadder et al., 2019; Kobayashi et al., 2013).

1.2. Susceptibility genes

Individuals who carry an inherited pathogenic mutation in the HBOC susceptibility genes have an increased lifetime risk of developing cancer. Therefore, the presence of germline mutations in these genes is a prognostic and predictive factor (Kotsopoulos, 2018). Identifying these germline mutations in a woman with BC and/or OC is important because it can influence her immediate and long-term management and has important implications for other family members. Also, the identification of asymptomatic carriers of such mutations offers a remarkable opportunity for cancer prevention (Girolimetti et al., 2014).

Pathogenic mutations in genes from the DNA repair machinery can cause genomic instability which triggers tumorigenesis and cancer progression (Jeggo et al., 2016). Certainly, the majority of

the HBOC susceptibility genes are involved in DNA damage response (DDR) and are members of the different DNA repair pathways (Tomasova et al., 2020).

HBOC susceptibility genes are divided into three groups depending on the frequency and the associated risk of their pathogenic mutations: high, moderate and low susceptibility genes. As reflected in **Figure 1A**, pathogenic variants in the high susceptibility genes are very rare in the population with a minor allele frequency (MAF) <0.005 and they confer a relative risk of cancer higher than 4 fold. Risk variants in moderate susceptibility genes confer a relative risk of cancer of 2-4 fold and are rare in population (MAF of 0.005-0.01). Finally, mutations in low-susceptibility loci are frequent in the population (MAF >0.05) but the conferred risk of cancer of less than 1.5 fold (Wendt and Margolin, 2019).

Up to date, different approaches have led to the identification of a considerable number of HBOC risk loci (Lilyquist et al., 2018; Mavaddat et al., 2019). However, as shown in **Figure 1B**, there is still around 50% of the familial cases in which the genetic cause is not known, with the consequent detriment to the patients (Couch et al., 2014; Rudolph et al., 2016; Mavaddat et al., 2019). Currently, only approximately 10% to 24% of patients referred for breast or ovarian cancer risk assessment with genetic testing are found to harbour known pathogenic variants identified by multigene panel testing (Lu et al., 2019). Around 15% of familial cases are attributed to germline pathogenic mutations in *BRCA1* or *BRCA2* genes (breast cancer susceptibility gene 1 and 2, described in the next section). Additional high-penetrance genes (*P53*, *PTEN*, *STK11*, *CDH1* and *PALB2*) linked to diferent familial syndromes, as well as moderate and low susceptibility loci, explain other significant percentage of the HBOC cases (Couch et al., 2014; Willoughby et al., 2019; Yang et al., 2020) (**Figure 1B**). Genome-wide association studies (GWAS) have identified more than 300 genomic loci harbouring BC low susceptibility variants, which are mainly common single nucleotide polymorphisms (SNPs) that would explain up to 40% of the familial cancer risk (Michailidou et al., 2017; Ferreira et al., 2019; Mavaddat et al., 2019). Regarding OC, GWAS have identified 35 risk loci to date (Phelan et al., 2017; Lu et al., 2018).

Familial breast cancer families that are negative for mutations in any of the known risk genes are commonly classified as BRCAX families, and their inheritance pattern can be explained by a polygenic inheritance model of several low-penetrance loci, or an unknown mutation in a yet undiscovered moderate susceptibility gene (Melchor and Benítez, 2013).

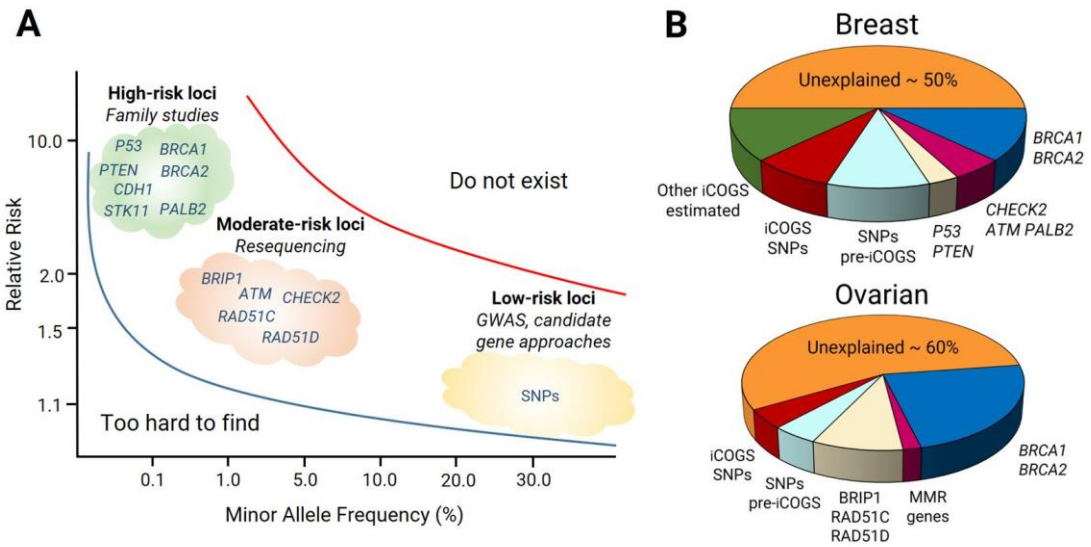

Figure 1 - HBOC suspectibility genes. A) Relative risk in relation to minor allele frequency of high, moderate and low susceptibility genes for HBOC (adapted from Foulkes, 2008). The main genetic technique used for the characterization of the different type of susceptibility loci is marked in italics. **B)** Relative contribution of mutations in high susceptibility (e.g., *BRCA1/2*, *P53, PTEN*), moderate susceptibility (e.g., *CHEK2*, *ATM*) genes and common low-penetrance genetic variants (SNPs) to breast and ovarian familial cancer risk. Adapted from Rudolph et al., 2016.

1.3 High susceptibility HBOC genes: *BRCA1* and *BRCA2*

Family-based linkage analysis identified in the early 1990s the two major HBOC genes: *BRCA1*, located on chromosome 17, and *BRCA2* on chromosome 13 (Miki et al., 1994; Wooster et al., 1994). *BRCA1* and *BRCA2* are tumor suppressor genes encoding multifunctional proteins that are essential for the repair of DNA double-strand breaks (DSBs) by homologous recombination (HR) DNA repair pathway. BRCA1 is a pleiotropic DDR protein that acts in both checkpoint activation and DNA repair, whereas BRCA2 assists the recruitment of the essential HR factor RAD51 onto RPA-coated single-stranded DNA (Roy et al., 2012; Jasin and Rothstein, 2013; Prakash et al., 2015). However, both proteins participate in numerous other central processes to maintaining genome stability, including regulation of the cell cycle progression, apoptosis, various transcriptional pathways, DNA replication, and telomere homeostasis (Fradet-Turcotte et al., 2016; Takaoka and Miki, 2018). As a result, the loss of function of either BRCA protein leads to an accumulation of genetic defects and a dramatic increase in genomic instability (Zámborszky et al., 2017).

The estimated cumulative risk of developing breast cancer to age 80 years is in the range of 65-79% for *BRCA1* and 61-77% for *BRCA2* female pathogenic mutation carriers (**Figure 2A**). For ovarian cancer, the corresponding estimated cumulative risk differs significantly between both genes: is in the range of 36-53% for *BRCA1* and 11%-25% for *BRCA2* carriers (**Figure 2B**) (Kuchenbaecker, Hopper, et al., 2017). Nevertheless, these estimates vary considerably depending on the target population and the design of the study. As an example, in Spanish population, the average

estimated cumulative risk of breast cancer to age 70 years is 52% for *BRCA1* and 47% for *BRCA2* mutation carriers (Milne et al., 2008). In the case of ovarian cancer, the corresponding estimates are 22% for *BRCA1* and 18% for *BRCA2* mutation carriers (Milne et al., 2008).

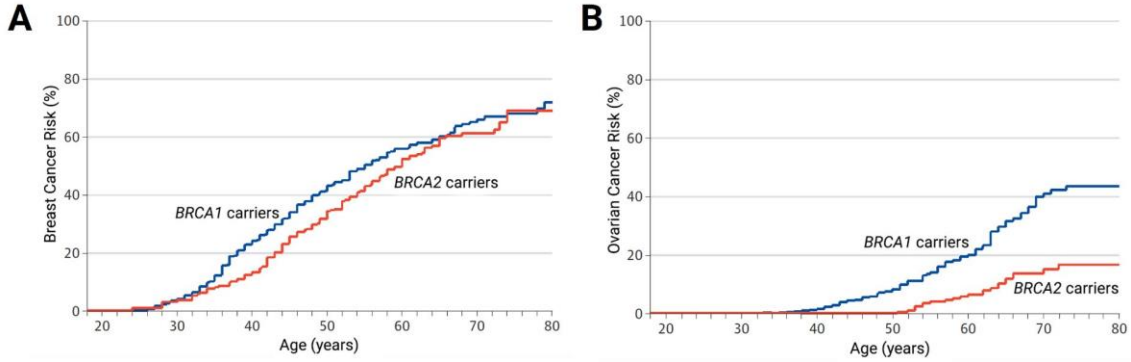

Figure 2 - Kaplan-Meier estimated cumulative risk of breast (A) and ovarian (B) cancer in *BRCA1/2* mutation carriers. Breast cancer incidences grow quickly in early adulthood until ages 30 to 40 years for *BRCA1* and until ages 40 to 50 years for *BRCA2* carriers, then remained at a similar and constant incidence until age 80 years. For ovarian cancer, there is an increase in incidence with age up to 70 years for both *BRCA1* and *BRCA2* carriers. The earliest follow-up started at age 18 years. Adapted from Kuchenbaecker *et al.*, 2017.

Genetic testing for *BRCA1* and *BRCA2* mutations is broadly available and has become an integral part of genetic counselling, gynaecologic and oncologic practice (Karlan et al., 2007; Easton et al., 2015). Given their significant implications for performing a correct diagnosis, prognosis and cancer treatment, the accurate identification of *BRCA1/2* mutation carriers results essential (Stoppa-Lyonnet, 2016). To this end, the selection of appropriate candidates for genetic testing to identify potential germline pathogenic variants in *BRCA1/2* is based on widely accepted clinical inclusion criteria (Bradbury and Olopade, 2007). As an example, the current selection criteria for germline testing recommended by the Spanish Society of Medical Oncology (SEOM) are summarized in **Table 1** (González-Santiago et al., 2020).

Table 1 – SEOM selection criteria for germline testing in HBOC risk assessment

a) Regardless of family history:
▪ Women with synchronous or metachronous breast and ovarian cancer
▪ Breast cancer ≤ 40 years
▪ Bilateral breast cancer (the first diagnosed ≤ 50 years)
▪ Triple-negative breast cancer ≤ 60 years
▪ High-grade epithelial non-mucinous ovarian cancer or fallopian tube or primary peritoneal cancer
▪ Ancestry with founder mutations
▪ BRCA somatic mutation detected in any tumor type with a allele frequency > 30%
▪ Metastatic HER2-negative breast cancer patients eligible to consider PARP inhibitor therapy
b) 2 or more first degree relatives with any combination of the following high-risk features:
▪ Bilateral breast cancer + another breast cancer < 60 years
▪ Breast cancer < 50 years and prostate or pancreatic cancer < 60 years
▪ Male breast cancer
▪ Breast and ovarian cancer
▪ Two cases of breast cancer diagnosed before age 50 years
c) 3 or more direct relatives with breast cancer (at least one premenopausal) and/or ovarian cancer and/or, pancreatic cancer or high Gleason (≥ 7) prostate cancer

1.4 Genetic modifiers of cancer risk in *BRCA1* and *BRCA2* mutation carriers

The high variability in cancer manifestation in *BRCA1/2* mutation carriers is consequence of several lifestyle, hormonal and genetic factors (Rudolph et al., 2016). In addition to the location and type of mutations in *BRCA1/2* genes (Rebbeck et al., 2015), the disease penetrance is also influenced by mutations in many other loci, considered such as genetic modifers of cancer risk (Mavaddat et al., 2010; Milne and Antoniou, 2011; Barnes and Antoniou, 2012; Friebel et al., 2014; Milne and Antoniou, 2016).

In 2005, the Consortium of Investigators of Modifiers of BRCA1/2 (CIMBA) was established to discover genetic cancer risk modifiers in BRCA1/2 pathogenic variant carriers (Chenevix-Trench et al., 2007). Since then, several GWAS have led to identifying numerous cancer risk-associated loci. Despite most of these variants show evidence of association with breast or ovarian cancer risk in the general population (Lu et al., 2018; Ferreira et al., 2019), some SNPs modify breast or ovarian cancer risk specifically for *BRCA1* or *BRCA2* mutation carriers (Milne and Antoniou, 2016). The associated effect sizes of these genetic modifiers are small (estimated hazard ratio per copy of the minor allele <1.5) and are estimated to account for a low proportion (<10%) of the modifying genetic variance for *BRCA1/2* mutation carriers (Couch et al., 2013; Milne and Antoniou, 2016). Nonetheless, it is no longer appropriate to counsel *BRCA1/2* mutation carriers accordingly average population risk estimates. Alternatively, the incorporation of polygenic risk scores (PRS) into risk prediction models is predicted that will improve cancer risk management in *BRCA1/2* mutation carriers (Kuchenbaecker, McGuffog, et al., 2017; Mavaddat et al., 2019; A. Lee et al., 2019).

Prior and in parallel to GWAS, the search for genetic modifiers of cancer risk in *BRCA1/2* mutation carriers has been also carried out through candidate gene (CG) approaches. CGs are hypothesis-based association studies focused on genes considered biologically likely to be involved in disease etiology, therefore, the interpretation of positive findings is relatively straightforward (Amos et al., 2011). CG studies for genetic modifiers in *BRCA1/2* mutation carriers have assessed variants in genes of candidate pathways, such as DNA repair or steroid hormone metabolism (Milne and Antoniou, 2016).

The search for genetic modifiers of cancer risk in *BRCA1/2* mutation carriers has been mainly focused on the different DNA repair pathways because cells harbouring pathogenic mutations in *BRCA* genes manifest defective HR and, they are thus crucially dependent on other members of the DNA repair machinery. Moreover, as indicated previously, BRCA1 and BRCA2 are multifunctional proteins involved in diverse processes, including other DNA repair pathways, as is summarized in **Figure 3** (Kobayashi et al., 2013). In particular, BRCA proteins play a role in the base excision repair

(BER) DNA repair pathway through transcription regulation and protein-protein interactions (Saha et al., 2010; Alli and Ford, 2015). The interaction between BRCA1/2 proteins and the BER pathway, as well as the identification of genetic variants in BER genes as HBOC risk modifiers in *BRCA1/2* mutation carriers, are the main focus of this thesis and are reviewed in the following sections.

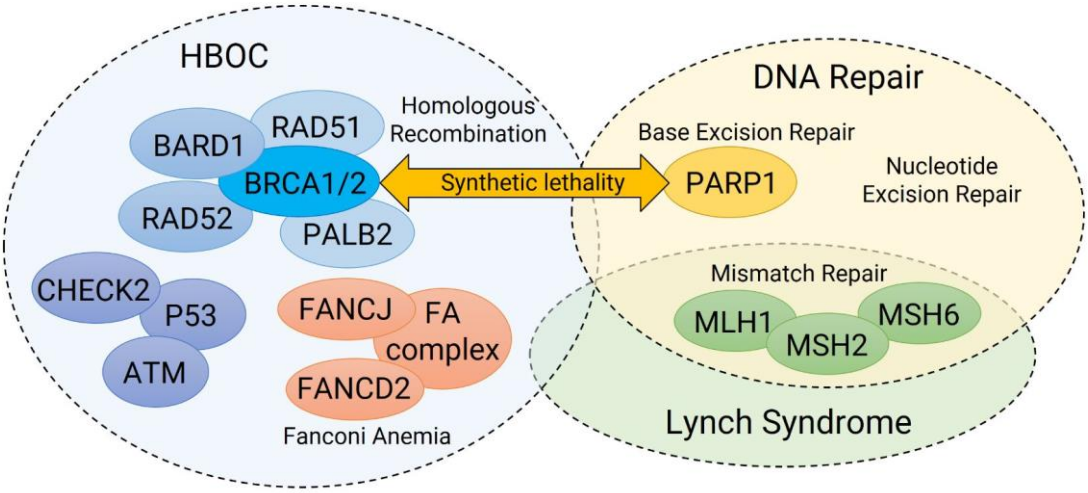

Figure 3 - BRCA proteins involvement in multiple DNA repair networks. Apart from their role in HR, they interact with the BER, the Fanconi Anemia (FA), the DNA mismatch repair (MMR) and, other DNA repair genes harbouring pathogenic variants related to HBOC (Adapted from Kobayashi et al., 2013).

2. Base excision repair pathway

2.1 Overview of the BER pathway

The genome of all cells is continuously exposed to a wide variety of exogenous and endogenous sources of DNA damage, for example, reactive oxygen species (ROS), UV light, and ionizing radiation (Hegde et al., 2008). Consequently, DNA bases suffer from oxidation, deamination, and alkylation. To maintain genome integrity, these injuries are repaired by the BER pathway. BER is a fundamental DNA damage response pathway responsible for repairing DNA base lesions, as well as single-strand breaks (SSBs). This is a highly conserved pathway from bacteria to humans, which involves different types of enzymes working in four sequential steps: lesion recognition, excision of damaged nucleotide, DNA resynthesis and ligation (Lee and Kang, 2019).

BER is initiated by the DNA glycosylases, enzymes that recognize and eliminate the damaged bases. There are eleven glycosylases known in humans, each removing a few related lesions, often with some overlap in substrate specificity (Wallace, 2014) (**Table 2**). Particularly, glycosylase action consists of flipping the affected base out of the DNA helix followed by the catalysis of the cleavage of the N-glycosidic bond, generating an abasic (apurinic/apyrimidinic, AP) site (Dizdaroglu et al., 2017). Furthermore, glycosylases can be either monofunctional, which possess only the glycosylase

activity, or bifunctional that have an additional lyase activity that incises the AP-site (Hegde et al., 2008).

Table 2 - Human DNA Glycosylases

Enzyme	Abbreviation	Type	Substrates
Single strand selective monofunctional uracil DNA glycosylase	SMUG1	Monofunctional	U, 5-FU, 5-hmU, ssU
Uracil DNA glycosylase	UNG or UDG	Monofunctional	U, 5-FU
Thymine DNA glycosylase	TDG	Monofunctional	T and U paired with G
MutY homolog	MUTYH	Monofunctional	A paired with G, C and 8-oxoG
Methyl-CpG binding domain protein 4	MBD4	Monofunctional	T and U paired with G, 5-hmU
N-Methylpurine DNA glycosylase	MPG or AAG	Monofunctional	Alkylated and deaminated purines
8-Oxoguanine glycosylase 1	OGG1	Bifunctional	8-oxoG paired with C
Endonuclease III homolog 1	NTH1	Bifunctional	Oxidized bases
Nei-like DNA glycosylase 1, 2 and 3	NEIL (1, 2 and 3)	Bifunctional	Oxidized bases

Abbreviations: A, adenine; C, cytosine; G, guanine; T, thymine; U, uracil; 5-FU, 5-Fluorouracil; 5-hmU, 5-hydroxymethyluracil; ssU, single-strand uracil. Adapted from Krokan and Bjøras, 2013

The abasic site created by monofunctional glycosylases is further processed by apurinic/apyrimidinic-endonuclease 1 (APE1) that incises the DNA backbone, leaving a single nucleotide gap in double-stranded DNA containing a 3‘-hydroxyl and a 5’-deoxyribose phosphate (5’-dRP) flap at the margins. Thus, the repair of damaged DNA bases converges with SSB repair (Dianov and Hübscher, 2013). The generated gap represents a single-templating base for DNA synthesis on the non-lesion strand where the accessory factors poly (ADP-ribose) polymerase 1 (PARP-1) and X-ray repair cross-complementing 1 (XRCC1) bind to promote repair. Depending on the physiological state of the cell and nature of the deoxyribose fragment, the gap is finally repaired through two different sub-pathways that differ based on the size of the re-synthesis patch that occurs after strand-incision (Maynard et al., 2009). In the short-patch BER, to repair the gap a single nucleotide is incorporated while in long-patch BER, replicative polymerases, such as DNA polymerase δ and ε, insert from 2 to 8 nucleotides, displacing the pre-existing bases 3´ to the original lesion. In short-patch, DNA polymerase β or λ (Pol β or Pol λ) removes the 5’-dRP group and inserts a single nucleotide that is sealed in a ligation step by DNA ligase I or III in association with XRCC1. When the 5’-dRP group in the gap is a weak substrate for the lyase activity of Pol β or Pol λ, these or other polymerases conduct strand displacement DNA synthesis in the long-patch BER subpathway. Long-patch BER requires the assistance of flap endonuclease 1 (FEN1) to remove the displaced single-strand flap generated. Finally, the intervention of the proliferating cell nuclear antigen (PCNA) associated DNA Ligase I seals the nick (Krokan and Bjøra, 2013; Wallace, 2014; Beard et al., 2019). **Figure 4** summarizes BER steps and its two different sub-pathways.

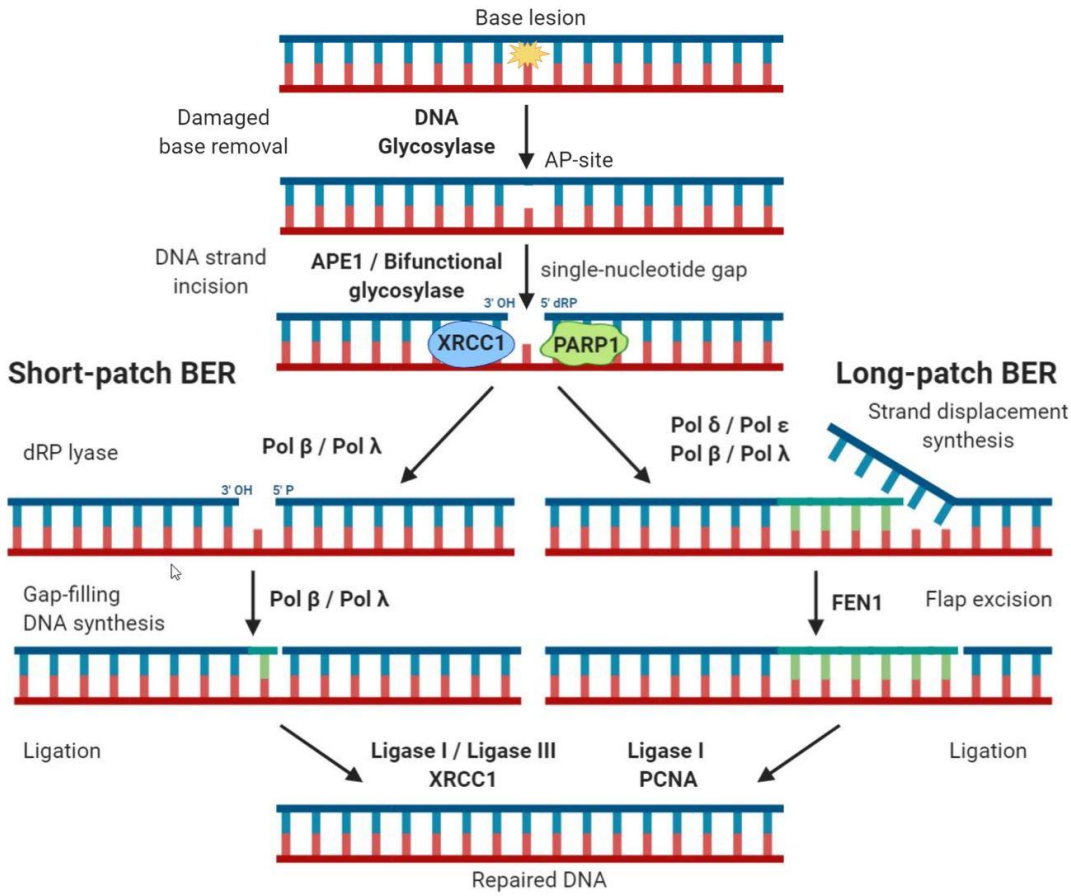

Figure 4 - Base excision repair pathway. Schematic representation of consecutive BER steps, including its two different subpathways. Adapted from Beard et al., 2019.

2.2 BER and cancer

The vast majority of cancers display defects in DNA repair (Gavande et al., 2016). The BER pathway is crucial for the maintenance of genome integrity and mutations in BER genes have been associated with cancer (Jeggo et al., 2016; Whitaker et al., 2017). *In vitro* studies have demonstrated that in the absence of BER enzymes, cells accumulate mutations and are hypersensitive to damaging agents (Wallace et al., 2012). Knockout mouse models have shown that the lesions repaired by the BER pathway can trigger carcinogenesis since when more than one glycosylase is knocked out, the mice develop tumors at an early age. Moreover, single glycosylase knockout mice have less severe phenotypes, reflecting that some glycosylases exhibit redundant functions, that is, overlapping substrate specificities. In contrast, the proteins involved in the next BER steps are required for development, given that attempts at generation knockout mice for APE1, XRCC1, FEN1, Pol β, and Ligase III result in embryonic lethality (Xanthoudakis et al., 1996; Tebbs et al., 1999; Larsen et al., 2003; Gu et al., 1994; Puebla-Osorio et al., 2006), except for PARP1, for which knockout mice are viable and fertile (Wang et al., 1995).

Besides, many of the BER proteins have been shown to be dysregulated in a large diversity of cancers (Wallace, 2014). As two examples, XRCC1 is overexpressed in triple-negative breast cancer (TNBC) (K. J. Lee et al., 2019), and overexpression of APE1 is associated with high grade serous epithelial ovarian cancer and correlates with poor overall survival (Al-Attar et al., 2010). This overexpression of BER proteins, as a negative prognosis factor, is explained based on the hypothesis that these enzymes may help cancer cells to overcome therapeutically induced DNA damage, modulating the treatment efficacy (Gavande et al., 2016). All these findings have led to consider the BER pathway as a promising target for cancer treatment, motivating the development of inhibitors to BER proteins (O'Connor, 2015).

2.3 BER inhibitors

2.3.1 Targeting BER enzymes in cancer therapy

The observations regarding BER knockout mice indicate that inhibitors to the core BER enzymes may have unpredicted on-target toxicities in normal tissues. However, inhibitors of DNA glycosylases and PARP1 may be well-tolerated by non-cancer cells, whose DNA repair machinery is unharmed (Visnes, Grube, et al., 2018). In consequence, the use of inhibitors of these BER enzymes in cancer treatment is a promising research field (Mechetin et al., 2020). This premise is based on the hypothesis that the inhibitors would trigger irreparable DNA damage and cell death in cancer cells, which are deficient in compensatory repair pathways. At the same time, normal cells would escape from inhibition consequences because they are proficient in the compensatory repair mechanisms and also, have lower levels of DNA lesions. This idea represents the concept of synthetic lethality (SL): a synthetic lethal interaction takes place between two genes when the disturbance of either gene alone is viable but, the perturbation of both genes simultaneously leads to the loss of viability (O'Neil et al., 2017).

In addition to synthetic lethality, there are at least another two potentially therapeutic strategies for BER inhibitors: sensitization to chemotherapy or irradiation and sensitization to endogenous cancer-specific stress (Visnes, Grube, et al., 2018). The three possible therapeutic strategies are outlined in **Figure 5**.

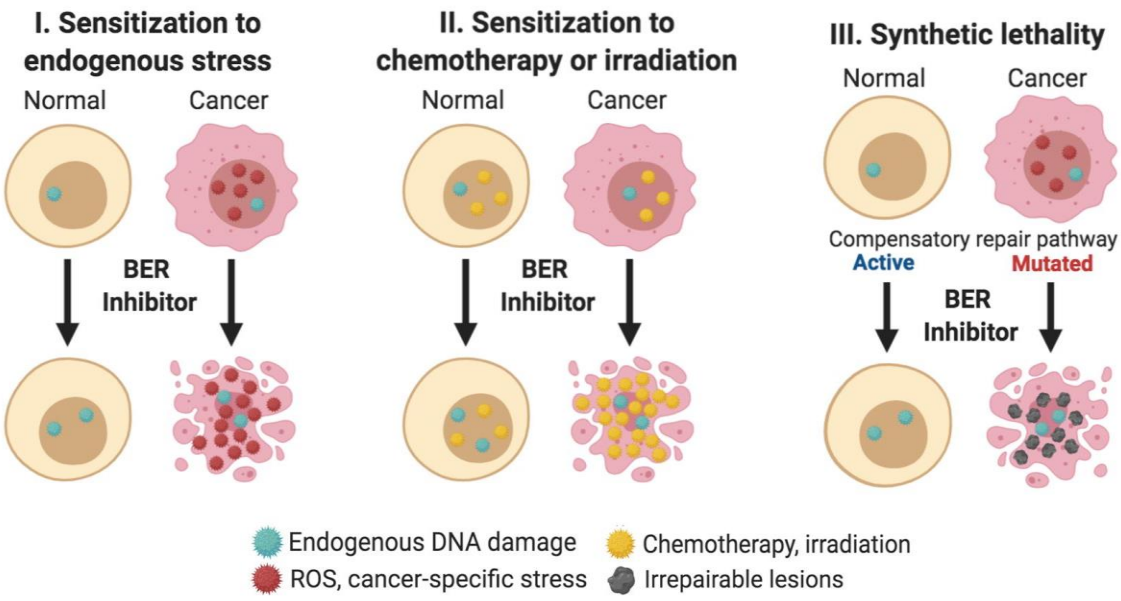

Figure 5 – Therapeutic strategies for BER inhibitors. I. Sensitization to endogenous cancer-specific stress; II. Sensitization to chemotherapy or irradiation; III. Synthetic lethality. Adapted from Visnes, Grube, et al., 2018.

2.3.2 PARP inhibitors: Synthetic lethality in *BRCA1/2* mutation carriers

In 2005, the concept of synthetic lethality was demonstrated between *BRCA1/2* genetic defects and pharmacologic PARP inhibition (Bryant et al., 2005; Farmer et al., 2005). PARPs are a family of nuclear enzymes whose actions include the synthesis of poly(ADP-ribose) chains on residues of target proteins as post-translational modification (poly ADP-ribosylation) and DNA damage recognition through binding to SSBs (Krishnakumar and Kraus, 2010). The most characterized family member is PARP1, which participates in DNA repair via multiple pathways including BER and in the maintenance of genomic integrity (Sousa et al., 2012; Ray Chaudhuri and Nussenzweig, 2017). The inhibition of PARP1 triggers the accumulation of SSBs that are converted to DSBs during DNA replication. BRCA1 or BRCA2-deficient cells can not repair these DSBs resulting in selective cell death (Rouleau et al., 2010; Drost and Jonkers, 2014).

Since these first preclinical observations were published, the synthetic lethality approach has been exploited for the treatment of BRCA-deficient breast or ovarian cancer (Cipak and Jantova, 2010). Multiple clinical trials with PARP inhibitors have been carried out, demonstrating the PARP inhibitors efficacy in several cancers, mainly HBOC (Faraoni and Graziani, 2018). In 2014, the PARP inhibitor olaparib was approved by the European Medicines Agency (EMA) and the Food and Drug Administration (FDA) as maintenance therapy for platinum-sensitive advanced ovarian cancer patients with pathogenic germline mutations in *BRCA1/2* genes (Deeks, 2015). Currently, PARP inhibitors are the only approved drugs targeting the BER pathway for cancer treatment. Up to four different PARP inhibitors (olaparib, rucaparib, niraparib, and talazoparib) have been approved for

specific breast or ovarian cancer subtypes harbouring *BRCA1/2* germline mutations, as single agents or in combination therapies with DNA damaging agents (Yap et al., 2019; Slade, 2020). Nevertheless, BRCA1/2-deficient tumor cells can become resistant to PARP inhibitors through multiple mechanisms (D'Andrea, 2018). Hence, it is important to find alternative treatments and, in this regard, inhibitors of other members of the BER pathway may be an alternative therapeutic strategy (Visnes, Grube, et al., 2018).

2.3.3 OGG1 inhibitors

Oxidative stress (OS) is defined as excess production of reactive oxygen species (ROS) relative to antioxidant defense (Shankar and Mehendale, 2014). Oxidative DNA damage represents the most prevalent DNA damage in human genome (Poetsch, 2020) and cancer cells display high levels of oxidized bases (Nakabeppu, 2014; Dizdaroglu, 2015). In human cells, the most common base lesion generated as a consequence of OS is 8-oxoguanine (8-oxoG) (De Bont and van Larebeke, 2004; Cadet and Wagner, 2013), whose accumulation leads to genome instability (Fouquerel et al., 2019). The role of the glycosylase OGG1 is essential to achieve the repair of oxidative base lesions. OGG1 specifically recognizes and excises 8-oxoG in double-stranded DNA when it is base-paired with cytosine (Ba and Boldogh, 2018).

Recently, two chemically distinct classes of OGG1 inhibitors have been developed (Tahara et al., 2018; Visnes, Cázares-Körner, et al., 2018). In particular, it has been reported that the OGG1 inhibitor TH5487 decreases proinflammatory gene expression, suggesting that OGG1 inhibition could be used for the prevention and treatment of inflammatory conditions (Visnes, Cázares-Körner, et al., 2018). Nonetheless, the application of OGG1 inhibitors for cancer treatment has not been investigated yet. It has been hypothesized that OGG1 inhibition may be a way to increase 8-oxoG levels in cancer cells, which would lead to specific death of cancer cells (Visnes, Grube, et al., 2018). From the opposite point of view, a recent study has proposed that OGG1 inhibitors could attenuate the SL interaction caused by PARP inhibition in BRCA1-deficient cells (Giovannini et al., 2019). These researches argue that blocking the BER pathway through OGG1 inhibition might prevent the generation of SSBs during the BER repairing process, which are recognized by PARP1. Thus, this lower accumulation of DNA breaks would mitigate PARP inhibition in a HR-deficient context (Giovannini et al., 2019). Independently of the final consequences of OGG1 inhibition in specific situations, owing to their unique characteristics, the telomeres of cancer cells are genome regions prone to harbour DNA damage, and therefore may be particularly susceptible to suffer the effects of OGG1 inhibition.

2.4 BER at the telomeres

2.4.1 Telomeres as a hotspot for DNA damage

The telomeres are nucleoprotein complexes that protect the ends of linear eukaryotic chromosomes. In mammals, the telomeric DNA sequence is commonly 9-15 kilobases (kb) and is composed of tandemly 5'-(TTAGGG)n-3' hexanucleotide repeats (**Figure 6A**) that are coated by the telomere capping complex called shelterin (Blackburn, 2001; De Lange, 2005; O'Sullivan and Karlseder, 2010) (**Figure 6B**). Functional telomeres maintain chromosome stability, promote cellular survival and, prevent degenerative diseases and cancer (Blackburn et al., 2015). In all dividing normal cells, taking place a progressive telomere shortening, which eventually results in cellular growth arrest. This shortening is considered an initial proliferative barrier to tumor formation (Shay and Wright, 2019). Indeed, most human tumors express telomerase, the enzyme which elongates the telomeres, whereas most normal tissues are deficient in telomerase activity (Shay, 2016). On the other hand, loss of telomere protection can lead to telomere crisis, which is a state of extensive genome instability that can promote cancer progression (Maciejowski and De Lange, 2017). Indeed, individuals with short telomeres display a higher cancer risk. However, individuals with long telomeres also present an increased risk for several cancers, which creates the cancer-telomere length paradox (Aviv et al., 2017).

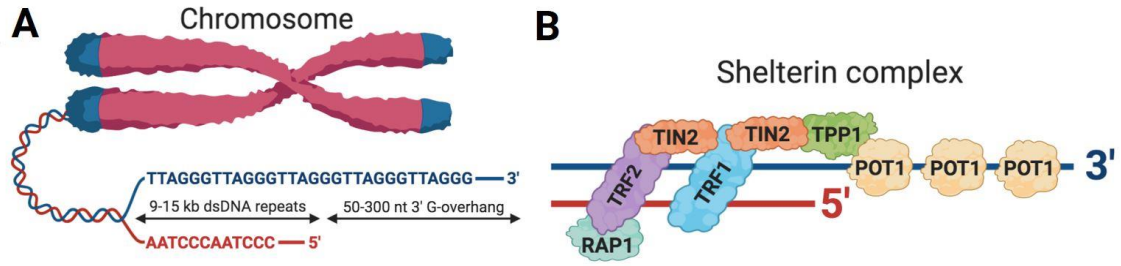

Figure 6 – Structure of human telomeres. A) Human telomeric DNA consist of many kb of TTAGGG repeats, with a G-rich leading strand forming the G-overhang. **B)** The shelterin complex is composed of the telomeric repeat-binding factor proteins TRF1, TRF2, the TRF2-interacting factor RAP1, the bridging molecules TIN2 and TPP1 and the telomeric protection factor POT1. Figures adapted from O'Sullivan and Karlseder, 2010.

An additional threat to the telomeres is the ineffective repair of its DNA when damaged. In the first place, telomeres are dynamic structures that usually stay in a highly compact chromatin state, which block access to DNA repair machinery (Blasco, 2007). Secondly, DNA repair at telomeres is tightly regulated to avoid chromosome fusions during DNA replication and thus, DSB repair pathways are generally repressed by the shelterin at intact telomeres (Sfeir and de Lange, 2012). However, the BER pathway is active at telomeres, being essential for telomere maintenance (Jia et al., 2015). Specifically, the most frequent base lesions at telomeric DNA corrected by BER enzymes are uracil residues and oxidized bases (Fouquerel, Parikh, et al., 2016).

2.4.2 Oxidative DNA damage at telomeres

The genomic distribution of oxidative base lesions is not random along the chromosomes (Amente et al., 2019). Indeed, telomeres harbour more oxidized bases than other genome regions upon oxidative stress conditions (Hewitt et al., 2012). Guanine has the lowest redox potential among nucleobases and is, therefore, the base most easily oxidized (Cadet et al., 2008). The high guanine incidence as triplets in the telomere DNA sequence makes telomeric DNA especially prone to the 8-oxoG formation (Oikawa and Kawanishi, 1999; Rhee et al., 2011; An et al., 2015). The accumulation of 8-oxoG at telomeres decreases the binding affinity of the shelterin, triggering telomere uncapping and leading potentially to telomere crisis (Opresko et al., 2005). Furthermore, 8-oxoG regulates telomerase activity: when 8-oxoG is present in the dNTP pool as 8-oxodGTP inhibits telomere elongation. Conversely, 8-oxoG lesions within the telomeric DNA sequence destabilizes telomere structure, promoting telomerase activity (Fouquerel, Lormand, et al., 2016). Considering these observations, as is summarized in **Figure 7**, it has been proposed a hormesis-like model whereby low basal levels of DNA damage at telomeric DNA may be beneficial for telomere lengthening, whereas higher accumulated levels are detrimental (Wang et al., 2010).

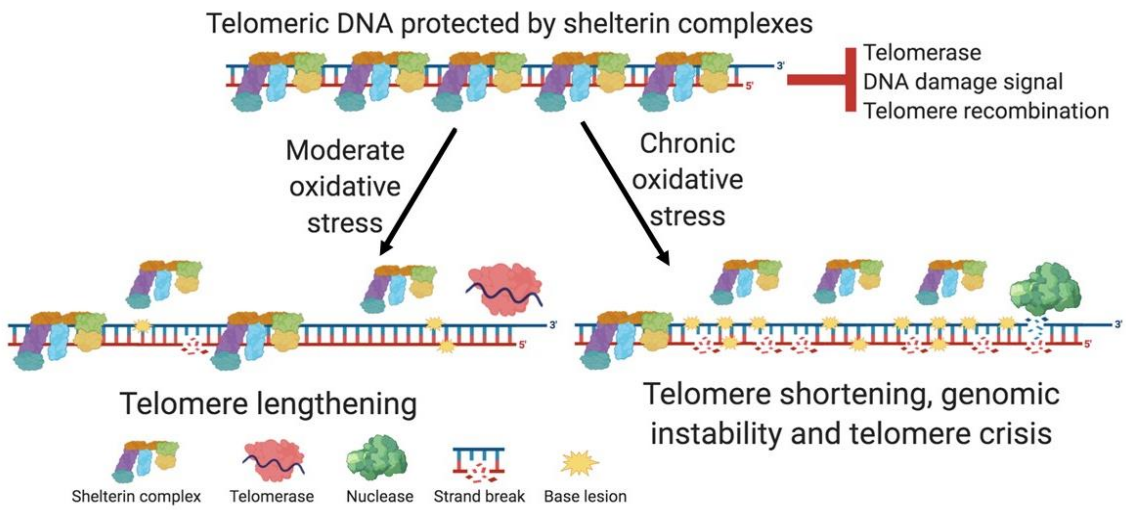

Figure 7 - The levels of DNA damage may regulate telomere length. Under moderate DNA damage conditions base lesion levels are low, which might slightly reduce sheltering binding, promoting telomerase-mediated telomere lengthening. On the contrary, high oxidative stress increases oxidative DNA damage that may lead to telomere uncapping, hence causing telomere shortening. Figure modified from Wang et al., 2010.

The DNA glycosylases responsible for removing oxidized DNA bases are necessary to preserve telomere integrity (Ahmed and Lingner, 2018; Barnes et al., 2019). In particular, the glycosylase OGG1 is critical in maintaining telomere length homeostasis through telomeric guanine damage repair (Lu and Liu, 2010). Moreover, OGG1 knockout mice accumulate 8-oxoG in their telomeres, which was associated with multiple telomere defects (Wang et al., 2010). Recently, it has been demonstrated that the targeted 8-oxoG generation at telomeric DNA in cells lacking functional

OGG1 triggers telomere fragility and, when this 8-oxoG formation becomes chronic, results into telomere losses and post-mitotic defects, such as micronuclei generation, anaphase bridge formation, chromosome fusions and finally, proliferation defects (Fouquerel et al., 2019). Hence, all these observations suggest that OGG1 inhibitors might be employed as a tool to induce the accumulation of oxidative DNA damage at telomeres of cancer cells that may lead to cancer cell death or arrest tumoral progression.

Besides OGG1, the NEIL glycosylases repair oxidized DNA bases in telomeric DNA (Zhou et al., 2013). Further oxidation of 8-oxoG results in the formation of guanidinohydantoin (Gh) that blocks the DNA replication at telomeres (Aller et al., 2010). Hydantoin lesions in telomeric sequences only can be removed by the NEIL enzymes (Zhou et al., 2015). It has been shown that NEIL3 is specifically active at telomeres during late S phase in human cells, and its depletion causes telomere dysfunction and mitotic defects (Zhou et al., 2017). Furthermore, fibroblasts derived from *NEIL2* knockout mice show higher frequency in telomere loss than from the wild-type (Chakraborty et al., 2015).

2.4.3 Uracil at telomeres

Uracil arises in the genome from the deamination of cytosine to uracil or polymerase misincorporation of deoxyuridine triphosphate (dUTP) instead of deoxythymidine triphosphate (dTTP) during DNA synthesis (Krokan et al., 2002). This gives rise to G:C to A:T transversions, a common signature in human tumors (Visnes et al., 2009). The telomeres are prone to uracil accumulation, which is mainly recognized and removed by the uracil-DNA glycosylase (UNG) (Cortizas et al., 2016). In a similar way to oxidative lesions, the amount of uracil in telomeric DNA could modulate telomere length (**Figure 7**), because its accumulation decreases the binding affinity of the shelterin component POT1 (Vallabhaneni et al., 2015). Further, in mouse UNG-deficient cells uracil has been detected at telomeres resulting in abnormal telomere lengthening (Vallabhaneni et al., 2015). In conclusion, these findings highlight the necessity of UNG-initiated BER for the preservation of telomere integrity.

3. DNA glycosylases as genetic modifiers of cancer risk in *BRCA1/2* mutation carriers

As mentioned above, the high variability in disease manifestation among *BRCA1/2* pathogenic germline mutation carriers is modulated by genetic factors. The identification of these genetic cancer risk modifiers is of utmost importance to develop accurate cancer risk prediction models and provide personalized genetic counselling to healthy women carrying pathogenic variants in *BRCA* genes (Lesueur et al., 2018). In the view of mutations in DNA repair genes can modulate its

DNA repair capacity, and promote numerous diseases including cancer (D'Errico et al., 2016), DNA repair genes are potential candidates to act as cancer risk modifiers.

In particular, considering the interaction of synthetic lethality between the two BRCA proteins and the BER pathway component PARP1, genetic variation in BER genes may modify cancer risk in the carriers of pathogenic mutations in *BRCA* genes. To address this hypothesis, our group designed a candidate gene study to search for new genetic modifiers of cancer risk, focusing on BER genes (Osorio et al., 2014). In this work was followed a tagging SNP approach using a large series of *BRCA1* and *BRCA2* mutation carriers (n=23.463) from the CIMBA consortium, included in the Collaborative Oncological Gene-environment Study (COGS) (Bahcall, 2019). Eleven SNPs of BER genes showed evidence of association with breast or ovarian cancer (p.value<0.05). Interestingly, the SNPs with the strongest evidence of association were localized in DNA glycosylases genes. Specifically, the most significant associations found were between three common SNPs in *OGG1*, *NEIL2* and *UNG*, with ovarian cancer risk in *BRCA1*, breast cancer risk in *BRCA2* and ovarian cancer risk in *BRCA2* mutation carriers, respectively (information detailed in **Table 3**). Furthermore, these associations were subsequently confirmed in a larger series of BRCA1 and BRCA2 mutation carriers from the OncoArray Consortium (Amos et al., 2017).

Table 3 - SNPs in glycosylase genes associated with HBOC cancer risk from Osorio et al., 2014

SNP name	MAF[1]	Gene	Location	Cancer	Mut. Group	HR[2] per allele	p-value
rs2304277	0.182	*OGG1*	Downstream 3'-UTR	Ovarian	*BRCA1*	1.12 (1.03-1.21)	4.8×10^{-3}
rs804271	0.435	*NEIL2*	Upstream 5´-UTR	Breast	*BRCA2*	1.09 (1.03-1.16)	2.7×10^{-3}
rs34259	0.201	*UNG*	Downstream 3'-UTR	Ovarian	*BRCA2*	0.80 (0.69-0.94)	7.6×10^{-3}

[1]Minor allele frecuency (MAF) reported in the 1000 Genomes Project for the Iberian subpopulation (Zerbino et al., 2018).
[2]The hazard ratio (HR) refer to the increase or the reduction in risk coferred by the rare allele of each polymorphism.

The associations found are not surprising results since SNPs in DNA glycosylase genes have been previously identified as susceptibility factors for a wide disease spectrum, including several cancer types, cochlear/ocular disorders, myocardial infarction and neurodegenerative disorders (D'Errico et al., 2016). Continuously, there are described new associations between glycosylase polymorphisms and cancer risk (Ye et al., 2020; Mimouni et al., 2020), highlighting their role as cancer risk modifiers.

The three cancer risk modifiers SNPs identified in glycosylase genes are localized into their regulatory regions (Osorio et al., 2014), so they could be disturbing their expression level. Taking into account the data previously summarized here, aberrant glycosylases expression levels might interfere with telomere maintenance and thus contribute to the risk of developing cancer. Supporting this idea, our group has already carried out the functional validation of the *OGG1* SNP

(Benitez-Buelga et al., 2016). This variant causes transcriptional down-regulation of *OGG1* and is associated with higher levels of DSBs and short telomeres. Therefore, these results may help to explain the higher ovarian cancer risk of *BRCA1* mutation carriers that harbour the SNP (Benitez-Buelga et al., 2016). However, functional analysis concerning *NEIL2* and *UNG* SNPs still needs to be addressed.

OBJECTIVES

Our research group has previously identified a series of SNPs in DNA glycosylase genes from the BER pathway as modifiers of breast or ovarian cancer susceptibility in *BRCA1* and *BRCA2* mutation carriers. The primary objective of this work was to explain the molecular basis of these associations. Given that the BER pathway is essential for maintaining telomere integrity, we hypothesized that SNPs in DNA glycosylase genes might interfere with telomere maintenance and thus contribute to the risk of developing cancer.

On the other hand, telomeres are more susceptible than other genome regions to oxidative stress. Indeed, the most common oxidative DNA lesion at telomeric DNA is 8-oxoG which is mainly removed by the glycosylase OGG1. Therefore, we hypothesized that OGG1 inhibition may induce oxidative telomeric DNA damage in cancer cells and might represent a novel potential therapeutic strategy.

Moreover, considering the well-known synthetic lethal interaction caused by PARP inhibition in BRCA1 or BRCA2-deficient cells, we thought that inhibitors of other BER enzymes might also cause this phenomenon in this particular cellular context.

The specific objectives of this thesis were:

1. To gain molecular insight into the SNPs in the *NEIL2* and *UNG* genes identified as cancer risk modifiers for *BRCA1/2* mutation carriers by functional assays.
2. To evaluate the role of OGG1 DNA repair activity at telomeres and characterize the defects associated with OGG1 inhibition or depletion in these genomic regions.
3. To investigate the possible synthetic lethal interaction between *BRCA1* and *OGG1* using the recently developed OGG1 inhibitor TH5487 and its effect in combination with the PARP inhibitor olaparib.

MATERIAL AND METHODS

1. Materials description

1.1 Patient-derived series

1.1.1 Familial breast and ovarian cancer series

A familial breast and ovarian cancer (FBOC) series was collected to perform the functional validation of the SNPs in glycosylase genes as cancer risk modifiers in *BRCA1* and *BRCA2* mutation carriers (Results Part I). The series was composed of 344 individuals from 173 families meeting high-risk criteria (González-Santiago et al., 2020), and screened for deleterious mutations in the *BRCA1* and *BRCA2* genes by next generation sequencing methods. Thirty-two families carried a deleterious mutation in *BRCA1*, 31 in *BRCA2*, and 110 did not carry any mutation in either of these two genes, which were classified as BRCAX families. As controls, were considered 111 members of the *BRCA1/2* families who did not harbour the corresponding familial mutation in the *BRCA1* or *BRCA2* genes and without personal cancer antecedents.

All patients and controls signed an appropriate informed consent form and the proposal was approved by the ethics committee at the Fuenlabrada Hospital (Madrid, Spain). Peripheral whole blood from FBOC members was obtained by venipuncture, preserved in cold, and processed for different purposes (detailed below) within the next 8 hours after the blood collection. The number of individuals from the FBOC series that could be included for the different functional studies is detailed in **Supplementary Table S1**. The average age was not significantly different between the different groups included in the FBOC series (BRCA1, BRCA2, BRCAX, and controls).

1.1.2 Lymphoblastoid patient-derived cell lines

In order to validate the functional studies carried out with the FBOC series, a set of 20 lymphoblastoid cell lines (LCLs) was also included in some analysis. LCLs were established by Epstein-Barr virus transformation of peripheral blood mononuclear cells (PBMCs). Summarily, peripheral whole blood was collected in heparin and diluted with an equal amount of phosphate-buffered saline (PBS; Lonza). Next, blood was centrifuged with Histopaque®-1077 (Sigma) at 400 x g for 30 min at room temperature. The PBMC layer was recovered, washed with PBS (Lonza), and resuspended in freezing media (complete growth medium with 10% DMSO; detailed information in the Cell culture and treatments section). PBMCs immortalization was carried out by our collaborators from the Bellvitge Biomedical Research Institute (IDIBELL; Barcelona, Spain).

To establish the panel of LCLs, blood was collected from 13 healthy women carrying heterozygous mutations in *BRCA1* and 7 non-carrier relatives used as controls. None of the women included in the series had personal antecedents of cancer. This LCL panel has been previously

described by our research group (Vaclova et al., 2015). LCLs series description is detailed in **Supplementary Table S2**.

1.1.3 Set of prophylactic oophorectomies

As another series included to perform validation of functional studies carried out in the FBOC series, we collected a set of 17 prophylactic oophorectomies from *BRCA1* and *BRCA2* mutation carriers. The oophorectomies panel description is detailed in **Supplementary Table S3**. The ovarian biopsies were preserved at -80°C in Optimal Cutting Temperature medium (OCT, Agar Scientific) until DNA and RNA extraction.

1.2 Other cell lines

U2OS osteosarcoma cell line was used to study the role of OGG1 at the telomeres and the consequences of OGG1 inhibition in these genome regions (Results Part II). The parental U2OS cell line was obtained from the Science for Life Laboratory at the Karolinska Institutet (Stockholm, Sweden). This cell line was employed to generate cells with OGG1 protein fused to Green Fluorescence Protein (GFP; OGG1-GFP), and *OGG1* knockout (OGG1-KO) cells by CRISPR/Cas9 (described below).

TNBC cell line MDA-MB-231 was used to analyse the possible SL between BRCA1 and OGG1 (Results Part III). This cell line was used to obtain *BRCA1* knockout (BRCA1-KO) single colony clones by CRISPR/Cas9 (described below). BRCA1-deficient TNBC cell line MDA-MB-436 was included as negative control in *BRCA1* mRNA and protein expression analysis. HEK293T cells were used for lentiviral production. All commercial cell lines were authenticated by short tandem repeat (STR) profiling analysis (**Supplementary Table S4**) in collaboration with the Genomics Unit at the CNIO (Madrid, Spain).

2. Nucleid acids based analysis

2.1 DNA extraction and SNPs genotyping

DNA was extracted from peripheral blood of FBOC members using the Maxwell® FSC Instrument (Promega), and from cultured cells and ovarian biopsies using the DNeasy® Blood & Tissue Kit (Qiagen), in both cases, following the manufacturer's instructions. Subsequently, extracted DNA was quantified by the PicoGreen® fluorometric assay (Thermo Fisher Scientific).

SNPs genotyping was carried out using a KASPar probe specifically designed for rs34259 (G>C; LGC genomics), and a specific Taqman probe for rs804271 (Thermo Fisher Scientific). Probe design for rs804271 is G>T (reverse strand) instead of C>A. Allelic discrimination assays were performed in duplicate using the 7900HT Fast Real-Time PCR System (Applied Biosystems) and the ABI

QuantStudio 6 Flex Real-Time PCR System (Applied Biosystems) following the instrument-specific conditions detailed by the manufacturer.

2.2 Relative quantification of base lesions in specific genome regions

The protocol for the quantification of telomeric oxidative DNA damage (O'Callaghan et al., 2008) was adapted to measure the relative accumulation of different kinds of base lesions in specific genomic regions. This is a qPCR method based on differences in PCR kinetics between template DNA digested by a determinate glycosylase and undigested DNA. Each glycosylase recognizes and cuts specific base lesions, generating abasic sites that are then converted in SSBs by its AP lyase activity (bifunctional glycosylases) or by APE1 (monofunctional glycosylases). These SSBs inhibit the PCR, thus, the increment in the cycle threshold after glycosylase incubation (ΔCt; Ct digested–Ct undigested) is proportional to the amount of base lesions in the amplified region (detailed in **Figure 8**).

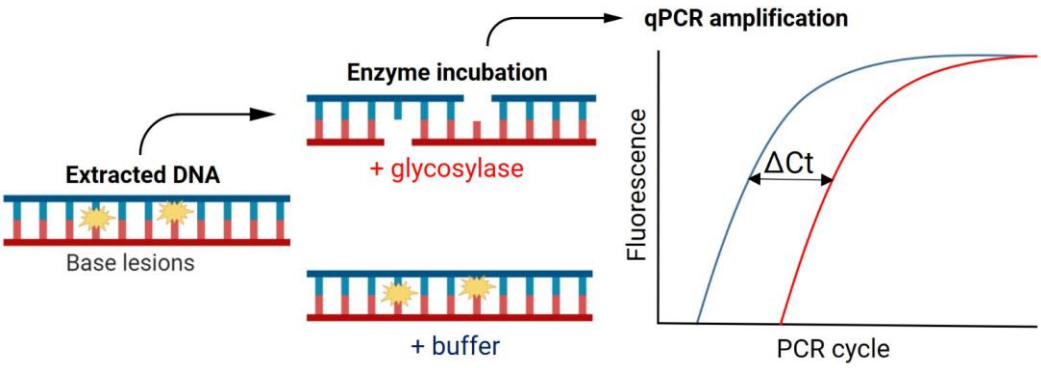

Figure 8 – Base lesions measurement protocol. Schematic representation of the qPCR-based method to measure relative DNA damage levels within specific DNA amplified regions.

The incubations with human glycosylases (provided by T. Helleday, Karolinska Institutet, Stockholm, Sweden) were performed at 37°C in glycosylase buffer (25mM Tris-HCl, 15mM NaCl, 2mM $MgCl_2$, 0.0025% Tween at pH 8.0). Incubations with bacterial formamidopyrimidine DNA glycosylase (FPG; New England Biolabs) were performed at 37°C in 1 x NEBuffer™ (10 mM Bis-Tris-propane-HCl, 10 mM $MgCl_2$, 1 mM dithiothreitol, pH 7.0; New England Biolabs). Specific incubation conditions for each glycosylase are detailed in **Supplementary Table S5**. The reactions were stopped by incubation at 95°C for 5 min. Each 10 µL of qPCR reaction was composed of 10 ng of digested or undigested genomic DNA, GoTaq® qPCR MasterMix 1x (Promega), and 100nM of forward and reverse selected primers (**Supplementary Table S6**). Samples were run on the ABI QuantStudio 6 Flex Real-Time PCR System (Applied Biosystems). Cycling conditions were 10 min at 95ºC, followed by 40 cycles of 95°C for 15 s and 60°C for 1 min. Each sample was analysed in triplicate.

2.3 RNA expression analysis

RNA was extracted from PBMC of FBOC samples, ovarian biopsies or cultured cells using TRIzol® Reagent (Thermo Fisher Scientific) according to the manufacturer´s instructions. RNA quantity and quality were assessed by NanoDrop® (Thermo Fisher Scientific). The High Capacity cDNA Reverse Transcription Kit (Applied Biosystems) was utilized for cDNA synthesis following the manufacturer's instructions using 1000 ng of total RNA.

For the determination of mRNA expression levels, cDNAs were amplified by quantitative RT-PCR. Two µL of cDNA at a final concentration of 10 ng/µL was mixed with 1x GoTaq® qPCR MasterMix (Promega) and 1 µM cDNA primers of each pair of primers (F/R) in a final volume reaction of 10 µL. Primers used are listed in **Supplementary Table S6**. Regarding *UNG* expression, considering that the human *UNG* gene encodes both nuclear (UNG2) and mitochondrial (UNG1) forms of human UNG (Nilsen et al., 1997; Akbari et al., 2007), we designed specific primers to quantify total *UNG* mRNA expression and the relative expression of each isoform. The amplification conditions consisted of an initial step at 95°C for 10 min, followed by 40 cycles of 10 s at 95°C and 1 min at 65°C. Each qPCR was performed in triplicate including no-template controls in an ABI QuantStudio S6 Flex System (Applied Biosystems). Relative mRNA expression was calculated using the 2ΔΔCt method for qPCR analysis after normalization with the housekeeping gene *GAPDH* using the QuantStudioTM Real-Time PCR Software (Applied Biosystems).

3. Protein-based assays

3.1 Protein extraction and Western blotting

Protein expression was determined by Western blotting. Briefly, cell pellets from PBMC of FBOC samples or cultured cells were lysed in RIPA buffer (Sigma) in the presence of Complete Protease Inhibitor Cocktail (Roche). Total protein concentration was determined using the Pierce BCA Protein Assay Kit (Thermo Fisher Scientific) following the manufacturer's instructions. Sixty micrograms of protein were electrophoresed on 12% SDS/PAGE and transferred to Immobilon-FL membranes (Millipore). Membranes were blocked in TBS-T (50 mM Tris-HCl, 150 mM NaCl, pH 7.5, 0.1% Tween-20) and 5% non-fat milk for 1 h at room temperature. Blots were probed over-night at 4ºC with the following primary antibodies: rabbit anti-NEIL2 (HPA064460; Atlas Antibodies) at 1/1,000 dilution, mouse anti-UNG (TA503563; Origene) at 1/1,000 dilution, rabbit anti-OGG1 (ab124741; Abcam) at 1/2,500 dilution, rabbit anti-BRCA1 (sc-6954; Santa Cruz) at 1/200 dilution, mouse anti-GAPDH (ab8245; Abcam) at 1/3,000, and mouse anti-β-Actin (A5441; Sigma) at 1/10,000 dilution in blocking solution. Anti-mouse and anti-rabbit IgG-HRP (Dako) were used as the secondary antibodies at 1/10,000 dilution in blocking solution 1 h at room temperature. Immunoblots were developed using

Immobilon Classico Western HRP substrate (Millipore). Each western blot was performed at least in duplicate. Images were analysed using ImageJ software (NIH Image) and NEIL2, UNG, OGG1, and BRCA1 protein levels were normalized by β-Actin or GAPDH.

3.2 Immunodetection of oxidized proteins

Oxidized proteins in plasma samples were detected by measuring the levels of carbonylated proteins as previously described (García-Giménez et al., 2012). Briefly, 5 µg of proteins were denatured with 5 µl of 12% SDS. Next, 10 µl of 10 mM 2,4-dinitrophenyl hydrazine (DNPH) in 10% (v/v) trifluoroacetic acid was added to the protein solution. The reaction mixture was neutralized and prepared for SDS–PAGE by adding 7.5 µl of 2 M Tris base containing 30% (v/v) glycerol. Derivatized samples were spotted onto a nitrocellulose membrane and was blocked with 5% bovine serum albumin (BSA) prepared in PBS 0.1% Tween-20 for 1 h. Then, the membrane was incubated with a rabbit anti-DNP antibody as described by the manufacturer of the OxyBlot Protein Oxidation Detection Kit (Millipore). Images were captured using an ImageQuant LAS-4000 (GE Healthcare Life Sciences). The signal density of each sample was analysed with ImageJ software (NIH Image). This protocol was carried out in collaboration with the Cell and Organ Pathophysiology of Oxidative Stress research group at the Health Research Institute INCLIVA (Valencia, Spain).

3.3 Telomerase activity assay

PBMC from FBOC members were cultured in RPMI supplemented with 20 % fetal bovine serum and phytohemagglutinin during 4–5 days. Next, telomerase activity was measured using the TRAPeze Telomerase Detection Kit (Merck Millipore) according to the manufacturer's instructions. The average telomerase activity was determined in each sample using 0.5, 0.25, and 0.125 µg of protein extract and normalized with the internal control included in the assay. This protocol was carried out in collaboration with the Department of Experimental Models of Human Disease at the Biomedical Research Institute Alberto Sols (Madrid, Spain).

4. Functional and cell-based assays

4.1. Cell culture and treatments

LCLs were cultured in RPMI-1640 (Sigma-Aldrich) supplemented with 20% non-heat-inactivated fetal bovine serum (FBS, Sigma-Aldrich), 1% penicillin-streptomycin (P/S, Gibco) and 0.5 % Fungizone (Gibco). U2OS, HEK293T, and MDA-MB-231 cell lines were cultured in DMEM (Lonza) growth medium supplemented with 10% of FBS (Biowest), 1% P/S and 0.5 % Fungizone. All the cultures were carried out at 37°C in 5% CO_2 atmosphere and mycoplasma testing was performed regularly.

To induce oxidative DNA damage, cells at about 80% of confluence were treated with H_2O_2 (Sigma) at 200 µM in serum-free DMEM for the indicated periods in each experiment. After oxidative treatment, the cells were allowed to recover in complete growth medium for 1 h when mentioned. To perform OGG1 inhibition, cells were released into fresh medium containing the OGG1 inhibitor TH5487 (Visnes, Cázares-Körner, et al., 2018) at the indicated times and concentrations. PARP inhibition was carried out incubating cells with olaparib (OLP, Axon Medchem) for the indicated periods and concentrations. Dimethyl sulfoxide (DMSO, Sigma-Aldrich) dissolvent was used as a control in treatments with TH5487 and/or OLP.

4.2 Plasmid construction OGG1-GFP and transfection

To generate the hOGG1-GFP vector, OGG1 ORF (GenBank accession number AB000410.1) was amplified by PCR without including the termination codon (Visnes, Cázares-Körner, et al., 2018). This was followed by restriction digestion and ligation into pENTR1A-GFP-N2 (FR1) (plasmid #19364, Addgene). After sequence verification, the entry clones were shuttled into pLENTI-PGK Puro DEST vector (w529 2) (plasmid #19068, Addgene) with ampicillin resistance using Gateway cloning LR Clonase reaction (Thermo Fisher Scientific). The destination vectors were verified by sequencing. U2OS cells were then transfected with the destination construct and selected with 1 ug/ml puromycin for 10 days. Clonal expansion was carried out to generate a single clone of U2OS cells constitutively expressing OGG1-GFP, and thus variability in expression levels was minimized. This protocol was performed by our collaborators from the Science for Life Laboratory at the Karolinska Institutet (Stockholm, Sweden).

4.3 CRISPR/Cas9 knockout of *OGG1* and *BRCA1*

sgRNAs were designed using the Benchling CRISPR sgRNA Design tool (*http://www.benchling.com*). Specifics sgRNA were tested against *OGG1* gene (exon 2), *BRCA1* gene (exon 11) and also a non-targeting control (NT) was used (sgOGG1: GTGTACTAGCGGATCAAGTA, sgBRCA1: GCTCATTACAGCATGAGAAC and sgNT: CCGCGCCGTTAGGGAACGAG). Those sequences were cloned into the lentiCRISPRv2 vector (plasmid #52961, Addgene) and verified by Sanger sequencing (primers listed in **Supplementary Table S6**). Viruses were produced by transient plasmid transfection into HEK293T cells by the calcium phosphate method, as previously described (Torres-ruiz et al., 2017). Briefly, cells were seeded at 1.1×10^7 cells/dish in 15-cm dishes the day before transfection. Cells were transfected using second-generation packaging plasmids (psPAX2 and pMD.2G, #12260 and #12259, respectively, Addgene) and the appropriate transfer plasmid (pLV CRISPR sgOGG1 or sgBRCA1 or sgNT). The medium was collected after 48 h, cleared by low-speed centrifugation, and filtered through 0.45 µm-pore-size PVDF filters (Millipore). Viral titers

were calculated and values range around 107 to 108 TU/ml. In order to carry out transductions, cells were split and 24 hours later were transduced using a multiplicity of infection = 5 to ensure a high rate of transduced cells. Cells were incubated at 37ºC for 12 hours. After that viral supernatant was replaced with fresh cell medium.

OGG1 knockout was performed in U2OS-GFP cells. A sorting step of the GFP negative cells was carried out to obtain the final pool of OGG1-KO cells used in the different experiments (Results Part II). On the other hand, *BRCA1* knockout cells were generated using the MDA-MB-231 cell line. Several single colony clones were established, some of which displayed reduced *BRCA1* mRNA expression. Then, these clones were selected for Western blotting validation (detailed in Results Part III). *BRCA1* knockout clones were validated by Sanger sequencing of the targeted region, followed by analysis using Tracking of Indels by Decomposition (TIDE) (*https://tide.nki.nl*), confirming *BRCA1* gene disruption (**Supplementary Figure S1**). CRISPR/Cas9 gene knockouts were carried out in collaboration with the Cytogenetics Unit of the CNIO (Madrid, Spain).

4.4 Cell sorting

U2OS-GFP cells were trypsinized, resuspended at a concentration of 5×10^6 cells/ml and incubated with 5 µg/ml Hoechst (Thermo Fisher Scientific) for 15 min at 37°C in the dark. Cells were sorted based on the amount of DNA by defining three regions for sorting: G1, S, and G2/M cell-cycle phases. A post-sorting purity check was used to confirm the purities of the resulting sorted populations that were higher than 90% in all cases (**Supplementary Figure S2**). The sorting was performed with the use of a BD Influx™ (BD Biosciences). The separated cells (at least 1×10^6 cells from each sorted population) were collected in tubes containing 0.5 ml culture medium and, after centrifugation, cell pellets were stored at -20ºC until used for DNA or protein extraction.

4.5 Evaluation of DNA repair by confocal microscopy

To study DNA repair at the telomeres, U2OS OGG1-GFP cells were used to measure mean signal intensity for OGG1-GFP, XRCC1, γH2AX, and 53BP1 contained within the telomeric region defined by the TRF2 foci. Besides, γH2AX mean signal intensity in the MDA-MB-231 cell line was measured as a marker of DSBs and replication stress.

U2OS cells were seeded in 12-well plates for 24 h before the start of the indicated treatments and followed by the following immunofluorescence (IF) protocol. Before fixation, cells were previously extracted with 0.2% Triton X-100 (Sigma) in PBS (Sigma) for 2 min (pre-extraction step). Cells were fixed with 4% paraformaldehyde (PFA, Agar Scientific) for 10 min. After washing with PBS (Sigma), cell permeabilization was performed with 0.5% Triton X-100 in PBS for 15 min. Blocking with 3% BSA (Sigma) in PBS for 1 hour was followed by staining with primary (over night) and

secondary antibodies (1h) and 0.5 µg/ml 4',6-Diamidino-2-Phenylindole (DAPI; Sigma) to visualize nuclei. After each staining, a washing step was performed three times (5 min in PBS each). All steps were performed at room temperature. Primary antibodies used were: mouse anti-TRF2 (ab13579, Abcam) at 1/200, rabbit anti-γH2AX (#2577, Cell Signalling) at 1/500, rabbit anti-53BP1 (ab36823, Abcam) at 1/1,000, and rabbit anti-XRCC1 (ab134056; Abcam) at 1/200. Secondary antibodies used were: anti-mouse Alexa 555 (TermoFisher Scientific) and anti-rabbit Alexa 647 (TermoFisher Scientific). Image acquisition was performed with a Leica confocal microscope TCS-SP5 using the oil immersion objective Leica ACS APO 40.0x1.15. Image treatment was done with Leica and ImageJ software (NIH Image), and the analysis was performed using automatic CellProfiler software (Broad Institute).

Regarding MDA-MB-231, cells were grown on uCLEAR bottom 96-well plates (Greiner Bio-One). The next steps were performed in the same way as for U2OS cells. Antibodies used were primary rabbit anti phospho-histone H2AX (#9718, Cell Signalling) and secondary anti-rabbit Alexa 555 (TermoFisher Scientific). Images were automatically acquired from each well using an Opera High-Content Screening System (Perkin Elmer). Images were segmented based on the DAPI staining to generate masks matching cell nuclei, from which mean signal intensities were calculated. We considered γH2AX positive cells those with a pan-nuclear H2AX signal intensity higher than an arbitrarily chosen threshold.

4.6 Telomere fluorescence in situ hybridization (Telo-FISH)

U2OS cells were treated with 0.2 µg/ml Colcemide (Life Technologies) for 4 h to enrich cells at metaphase. Then, cell pellets were exposed to hypotonic treatment with 75 mM KCl solution, fixed in cold Carnoy's solution [methanol:acetic acid (3:1)], and spread onto glass slides. The samples were fixed again in PBS containing 3.7% PFA and dehydrated by successive incubations in 70%, 80%, and 100% ethanol before FISH hybridization. DNA was denatured at 72°C in 1 M HCl, 20 x saline-sodium citrate (SSC) buffer, deionized formamide hybridization mixture, and hybridized with Cy3-labeled (CCCTAA)3 peptide nucleic acid (PNA) telomere probe (0.5 µg/ml) [PNA BIO/F1001 (TelC-FAM) Panagene]. Finally, the slides were washed with a buffer containing formamide to remove the non-specifically bound probe, and DNA was stained with 0.5 µg/ml DAPI/Antifade solution (Palex Medical). Telomere FISH images were digitally acquired with a CCD camera (Photometrics SenSys) connected to a Leica DM5500B microscope using a 100x objective and the CytoVision software 7.2 (Leica). Images were blinded analysed to score for chromosome signal-free ends (telomere losses) and multi-telomeric signals (telomere fragility). This protocol was carried out in collaboration with the Cytogenetics Unit of the CNIO (Madrid, Spain).

4.7 Telomere length measurement by high-throughput quantitative FISH

Telomere length (TL) was quantified in the FBOC series by high-throughput quantitative FISH (HT-QFISH) with automated fluorescence microscopy as previously described (Canela et al., 2007). Briefly, PBMCs were separated by Histopaque-1070 (Sigma-Aldrich) gradient centrifugation. Cells were counted and plated (80,000 – 100,000 cells/well) in clear bottomed black-well 96-well plates precoated with 0.001% (poly) L-lysine solution (Sigma-Aldrich) for 30 min at 37°C. DAPI was used for nucleus staining and a fluorescent peptide nucleic acid Cy3 probe against telomeric repeats was used for telomere detection. TL values were analysed using individual telomere spots on a per-cell basis (Approximately 90,000 telomere spots per sample, which represents around 3,500 cells). Fluorescence intensities were then converted into Kb using L5178-R, L5178-S, and CCRF-CEM cells as calibration standards, which have stable TL of 79.7 Kb, 10.3 Kb and 7.5 kb, respectively. Samples were analysed in duplicate, or triplicate in the case of calibration standards. A TL < 3 Kb was defined as a short telomere. The load of short telomeres was estimated as the percentage of short telomeres (short telomeres/ total number of measured telomeres). Because TL is strongly heritable (Pooley et al., 2013), BRCA status, the presence or absence of the SNP, and TL were assessed in the same member of each family. Whenever possible the index case was used, and if this sample was not available, the most recently genotyped individual was included. Given that chemotherapy affects TL (Benitez-Buelga et al., 2015), patients who were undergoing this treatment were excluded from the analysis. This protocol was carried out in collaboration with the Telomeres and Telomerase Group at the CNIO (Madrid, Spain).

4.8 Colony formation assay

MDA-MB-231 cells (WT or KO clones) were seeded at a density of 350 cells/well in 6-well plates. Twenty-four hours after seeding, the medium was replaced and cells were treated with DMSO or with the indicated concentrations of PARP inhibitor OLP and/or OGG1 inhibitor TH5487 and were incubated until colony size surpassed a minimum of 50 cells (≈12-14 days).

Concerning U2OS cells (OGG1-GFP or OGG1-KO), seeding was performed at a density of 500 cells/well in 6-well plates. Six days after seeding, the medium was removed and cells were challenged with a single pulse of H_2O_2 (Sigma) at 200 µM in serum-free DMEM for 1 h. Next, treatment was removed and replaced with complete medium with DMSO or with TH5487 (10 µM) for 6 additional days until colony size surpassed a minimum of 50 cells.

Finally, U2OS or MDA-MB-231 cells were washed twice with PBS, fixed with ice-cold methanol (Sigma) for 10 min, and stained with 1% crystal violet solution (Sigma) for 20 min, followed by

extensive washes in tap water and air drying. The plates were scanned and colony number and relative colony area were measured with ImageJ software (NIH Image).

4.9 MTT colorimetric assay

The effect of PARP and OGG1 inhibition on cell viability was assessed in the MDA-MB-231 cell line using the MTT colorimetric assay. Cells were seeded in 96-well plates at a density of 2,500 cells per well and, after 8 h, treated with olaparib, TH5487, or a combination of drugs at different concentrations for 72 h. Six replicates for each concentration were used, with a 1% DMSO final concentration, in at least two independent plates. MTT (Sigma-Aldrich) dissolved in PBS was added to a final concentration of 1 g/l and incubated 4 h at 37ºC. Afterwards, the media was removed and cells lysed with DMSO. Compounds were added to the plates using the Biomeck NP^X Laboratory Automation Workstation (Beckman Coulter). Absorbance at 5444 nm was read on a spectrophotometer (VICTOR Multilabel Plate Reader; PerkinElmer). The data were normalized to a mean absorbance detected in wells containing media without cells, and the results were expressed as a percentage (%) of the control (DMSO-treated cells). Curves were fitted using GraphPad Prism 8 (GraphPad Software Inc) and half-maximal inhibitory concentration (IC_{50}) values were determined.

4.10 Detection of intracellular ROS during cell cycle phases by flow cytometry

The generation of intracellular ROS in U2OS cells during the cell cycle was determined using the fluorescent probe 2',7'-dichlorodihydrofluorescein diacetate (H2DCFDA, Molecular Probes), combined with Hoechst staining for detecting DNA content. The non-fluorescent H2DCFDA passively diffuses into cells and is converted to the highly fluorescent 2',7'-dichlorofluorescein (DCF) upon oxidation by ROS. U2OS cells were harvested using Trypsin for 5 min, pelleted and resuspended in PBS containing Hoechst (1µg/ml) for 15 min. Then, cells were washed with PBS and pelleted by centrifugation. Next, pellets were resuspended in DMEN without serum containing H2DCFDA to a final concentration of 10 Mm. Cells were incubated for 30 min at 37°C and analysed by flow cytometry (Navios, Beckman Coulter) using the FL1 (525/540nm) or FL9 (450/460nm) channels. We used the median value of H2DCFDA intensity as a threshold to stratify negative (below median) or positive (above median) cells. Then, the percentage of ROS positive cells in G1, S, or G2/M phases was calculated.

4.11 Chromatin Immunoprecipitation

Chromatin Immunoprecipitation (ChIP) was performed in U2OS OGG1-GFP cells as has been previously described (Carey et al., 2009). Chromatinized OGG1-GFP protein fraction was enriched by using GFP-Trap for Immunoprecipitation (IP) (Chromotek). DNA bound to OGG1-GFP was heated

to reverse crosslinking. The purified OGG1-GFP DNA was amplified by PCR both telomere sequence and the single-copy gene *36B4* using specific primers (listed in **Supplementary Table S6**). Fold enrichment was calculated over the 10% input DNA. This protocol was performed by our collaborators from the Science for Life Laboratory at the Karolinska Institutet (Stockholm, Sweden).

5. *In silico* studies

HaploReg v4.1 (Ward and Kellis, 2012) was used to search for more plausible causal variants within those in high linkage disequilibrium with the SNPs previously described as cancer risk modifiers in BRCA1/2 mutation carriers (Osorio et al., 2014). Haploreg is hosted by the Broad Institute (*https://pubs.broadinstitute.org/mammals/haploreg/haploreg.php*).

The Genotype-Tissue Expression (GTEx) portal (Ardlie et al., 2015) was consulted to check whether the studied SNPs act as expression quantitative trait loci (eQTL) in specific human tissues. The GTEx project is supported by the National Institutes of Health (*http://www.gtexportal.org*).

6. Statistical analysis

To evaluate the effect of the SNPs for each of the studied variables, we considered heterozygotes and homozygotes (GT/TT for rs804271 and GC/CC for rs34259) as a single group, as the cancer modifier effect of the SNPs acts in a dominant fashion in *BRCA2* mutation carriers (Osorio et al., 2014). Along this thesis the term “SNP effect” is used to denote the effect caused by the alternative allele of each SNP compared to non-carriers of the variant.

We performed linear regression analysis to test whether cancer antecedents in *BRCA1* and *BRCA2* mutation carriers from the FBOC series were associated with any of the variables evaluated in this study, but we did not find significant differences ($p<0.05$) between healthy *BRCA1* and *BRCA2* carriers or cancer cases. Hence, we did not stratify for cancer status in these groups (**Supplementary Table S7**). Pearson's chi-squared test was used for testing Hardy-Weinberg equilibrium and to calculate whether the frequencies of the SNPs among the FBOC groups were significantly different from the frequencies reported in the 1000 Genomes Project for the Iberian sub-population (Zerbino et al., 2018).

The Kolmogorov-Smirnov test was used to evaluate if the data sets were normally distributed. For comparative analyses between two groups of data, statistically significant differences were assessed by Student´s unpaired t-test for normally distributed variables and the Mann-Whitney U test for non-normal data distribution. For comparative analyses between three or more groups, statistically differences were analysed with the one-way analysis of variance (ANOVA) test. The

Spearman correlation test was used to establish whether correlations between variables were statistically significant.

Statistical calculations and graphs were done using the SPSS software package version 19.0 (IBM) and GraphPad Prism 8 (GraphPad Software Inc). In all analyses, a 2-tailed p-value ≤0.05 was considered statistically significant: *P≤0.05; **P≤0.01; ***P≤0.001 and ****P≤0.0001.

RESULTS PART I

1. SNPs in DNA glycosylase genes as cancer risk modifiers in *BRCA2* mutation carriers: functional validation

In the present thesis, we aimed to explain the molecular basis of the cancer risk modifier effect in *BRCA2* mutation carriers exerted by the SNPs located in the 5' untraslated region (UTR) of the *NEIL2* gene (rs804271), and in the 3'-UTR of the *UNG* gene (rs34259) (Osorio et al., 2014). For that purpose, we explored the effects of the SNPs on NEIL2 or UNG activity and expression levels and their possible involvement in telomere integrity. All these analyses were performed with the FBOC series, and some findings were also confirmed using the LCLs panel.

1.1 Association study, validation, and fine mapping

In a previous study of our research group (Osorio et al., 2014), the SNPs rs804271 and rs34259 showed the strongest association with breast or ovarian cancer risk, respectively, for *BRCA2* mutation carriers, among all SNPs (genotyped or imputed) covering the BER pathway genes (**Table 3**). The functional validation of the OGG1 SNP rs2304277 as ovarian cancer risk modifier in *BRCA1* mutation carriers has already been performed (Benitez-Buelga et al., 2016). These associations were obtained using a large series of *BRCA1/2* mutation carriers (n = 23,463) from the CIMBA consortium (Chenevix-Trench et al., 2007). Thereafter, we have confirmed these initial associations in a larger series of *BRCA2* mutation carriers (4291 new cases) from the OncoArray Consortium (Amos et al., 2017): rs804271: HR= 1.06, P=5.5X10^{-3}; rs34259 HR= 0.84, P = 6.7x10^{-3} (Baquero et al., 2019).

The SNP rs804271 is located at the 5'-UTR region of the *NEIL2* gene, within a transcriptional regulatory domain at the Transcriptional Start Site (TSS) of the gene. On the other hand, the SNP rs34259 is located in the 3'UTR of the *UNG* gene, 2.4 kb downstream of the translation termination codon. We explored the possible phenotypic effects of these SNPs by using HaploReg v4.1 (Ward and Kellis, 2012). The two SNPs affect the binding of RNA polymerase 2 (POL 2), and the rs804271 also altered the binding of other 17 different proteins. Additionally, in the presence of the rs804271, 3 binding motifs for transcription factors (TFs) (E2F1, SIN3A, and YY1) are predicted to be altered. We did not detect a better causal SNP among those in high linkage disequilibrium (LD) with each SNP according to their predicted regulatory features (**Supplementary Table S8**). Indeed, the two SNPs have been previously identified as a trans expression quantitative trait loci (eQTL), that modify *NEIL2* (rs804271) or *UNG* (rs34259) gene expression in two independent eQTL studies (Westra et al., 2013; Ardlie et al., 2015). Taking all these findings into consideration, we selected the initially postulated SNPs as the best candidates to carry out the functional validation studies.

1.2 SNPs frequencies

We genotyped the SNPs rs804271 and rs34259 in the FBOC series and in the panel of LCLs to evaluate their associations with the studied variables. Genotype and allele frequencies in the FBOC series are summarized in **Table 4**. Genotype distributions were in Hardy–Weinberg equilibrium in the FBOC series (rs804271: $\chi^2 = 0.11$, P = 0.74; rs34259: $\chi^2 = 0.03$, P = 0.86). The different groups of cases and controls presented similar genotype and allele frequencies, not statistically different from the frequencies reported in the 1000 Genomes Project for the Iberian subpopulation (Zerbino et al., 2018). SNPs genotypes for each LCL are detailed in **Supplementary Table S2**. Because of the reduced size of the LCLs panel (n=20), statistical analyses regarding frequencies were not performed with this series.

Table 4 - Frequencies distribution of the studied SNPs among FBOC groups

	Allele Frequencies			Genotype Frequencies				
	rs804271 (*NEIL2*)							
	G	T	p-value[2]	GG	GT	TT	GT/TT	p-value[2]
IBS[1]	121 (56.5%)	93 (43.5%)	-	30 (28.0%)	61 (57.0%)	16 (15,0%)	77 (72.0%)	-
BRCA1	52 (65.0%)	28 (35.0%)	0.1897	17 (42.5%)	18 (45.0%)	5 (12.5%)	23 (57.5%)	0.3229
BRCA2	60 (65.2%)	32 (34.8%)	0.1653	20 (43.5%)	20 (43.5%)	6 (13.0%)	26 (56.5%)	0.2222
CONTROLS	95 (59.4%)	65 (40.6%)	0.5983	29 (36.3%)	37 (46.2%)	14 (17.5%)	51 (63.7%)	0.4823
FBOC	207 (62.3%)	125 (37.7%)	0.1762	66 (36.7%)	75 (45.2%)	25 (15.1%)	100 (60.3%)	0.1623
	rs34259 (*UNG*)							
	G	C	p-value[2]	GG	GC	CC	GC/CC	p-value[2]
IBS[1]	171 (79.9%)	43 (20.1%)	-	69 (64.5%)	33 (30.8%)	5 (4.7%)	38 (34.0%)	-
BRCA1	75 (73.5%)	27 (26.5%)	0.2018	25 (49.0%)	25 (49.0%)	1 (2.0%)	26 (51.0%)	0.0943
BRCA2	96 (77.4%)	28 (22.6%)	0.5885	39 (62.9%)	18 (29.0%)	5 (8.1%)	23 (37.1%)	0.8402
BRCAX	186 (77.5%)	54 (22.5%)	0.5323	70 (58.3%)	46 (38.3%)	4 (3.3%)	50 (41.7%)	0.5888
CONTROLS	167 (75.2%)	55 (24.8%)	0.2417	65 (58.6%)	37 (33.3%)	9 (8.1%)	46 (41.4%)	0.6196
FBOC	524 (76.2%)	164 (23.8%)	0.2553	199 (57.8%)	126 (36.6%)	19 (5.5%)	145 (42.2%)	0.5146

[1]Set of samples of the Iberian Populations in Spain of the 1000 Genomes Project Phase 3
[2]χ^2 vs IBS

1.3 *NEIL2* and *UNG* mRNA expression levels

Given that the SNPs rs804271 and rs34259 are located in regulatory regions of the *NEIL2* and *UNG* genes respectively, we explored their potential implication as modulators of mRNA expression levels. Firstly, using the GTEx Portal (Ardlie et al., 2015), we examined the effect of the SNPs on transcriptional regulation in different human tissues (n=49). The two variants were significantly associated ($p<0.05$) with expression changes in several tissues (**Supplementary Table S9**). The SNP rs804271 was significantly associated with increased *NEIL2* mRNA levels in 46 different tissues, including whole blood (effect size= 0.29; P = 2.9×10^{-17}), ovary (effect size= 0.50; P= 1.3×10^{-15}), and

breast (effect size= 0.22; P = $5.5x10^{-11}$). On the other hand, the SNP rs34259 was significantly associated with decreased *UNG* mRNA levels in a total of 13 tissues, including whole blood (effect size= -0.184; P = $2.5x10^{-16}$).

To determine whether there were any differences in *NEIL2* or *UNG* expression associated with the two SNPs, we measured by RT-PCR *NEIL2* and *UNG* mRNA expression level in the FBOC series and the LCLs panel. With respect to *NEIL2* mRNA expression levels in the FBOC series, we did not find significant differences among the mutational groups (BRCA1 and BRCA2) or controls (**Figure 9A**). However, stratifying by the SNP rs804217, we found a significant *NEIL2* mRNA up-regulation associated with this variant in the whole series (**Figure 9B**), which was particularly significant in *BRCA1* mutation carriers. Complementary, we also measured *NEIL2* mRNA levels in the LCLs panel. We observed a higher *NEIL2* expression in the LCLs harbouring the polymorphism although the difference was not significant (**Supplementary Figure S3A**).

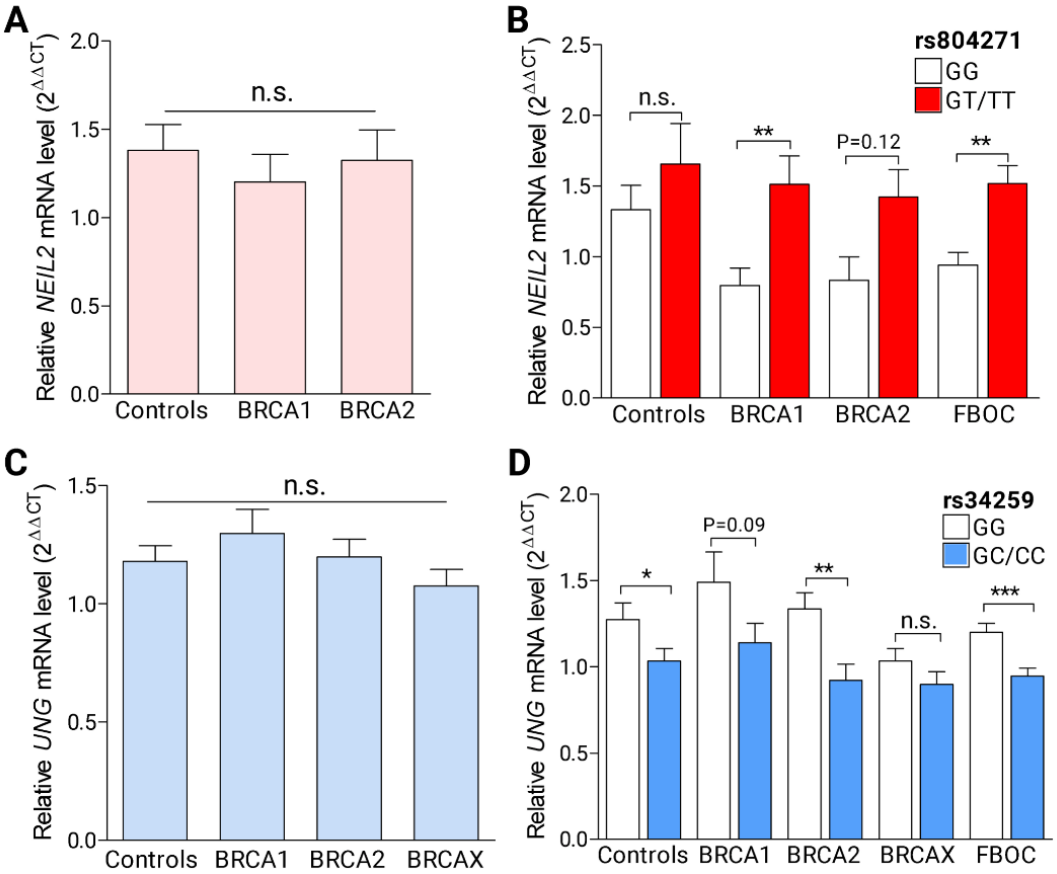

Figure 9 – *NEIL2* and *UNG* mRNA levels in the FBOC series. A) *NEIL2* mRNA levels among the FBOC groups. **B)** *NEIL2* mRNA levels according to the SNP rs804271 status [non-carriers (GG)/carriers (GT/TT)]. **C)** *UNG* mRNA levels among FBOC groups. **D)** *UNG* mRNA levels according to the SNP rs34259 status [non-carriers (GG)/carriers (GC/CC)]. Bars show the mean and the standard error of the mean (SEM). One-way ANOVA tests were performed for statistical significance in (A) and (C), Unpaired t-tests were used in (B) and (D).

Regarding *UNG* mRNA expression, firstly we used a subgroup of samples from the FBOC series (integrated by *BRCA2* mutation carriers and controls; n=97) to confirm that the mRNA levels of both UNG isoforms (mitochondrial UNG1 and nuclear UNG2) were significantly correlated, and also that total *UNG* mRNA expression was correlated with each of the two isoforms (**Supplementary Figure S4**). Consequently, the measures obtained for total *UNG* mRNA expression were representative of both isoforms. Then, we analysed *UNG* expression level in the whole FBOC series and we found no significant differences considering the BRCA status (**Figure 9C**). When we stratified regarding the rs34259, we found significantly lower *UNG* mRNA expression in individuals carrying the SNP (**Figure 9D**). Interestingly, this down-regulation was particularly pronounced in the BRCA2 group. Besides, the down-regulation associated with the SNP remained significant when analysing both isoforms (nuclear and mitochondrial) separately in BRCA2 mutation carriers (**Supplementary Figure S5**).

In the LCLs panel, we did not find differences in *UNG* mRNA expression regarding the presence/absence of the rs34259 (**Supplementary Figure S3B**). Nevertheless, considering that the SNP protective effect is for ovarian cancer, we also determined *UNG* mRNA expression in tissues of 17 prophylactic oophorectomies from *BRCA1* and *BRCA2* mutation carriers. Despite the reduced sample size, we found a trend toward lower total *UNG* mRNA expression associated with the rs34259 in this cohort (p=0.056), which was significant for the UNG1 isoform (**Supplementary Figure S6**). These results suggest that the intensity of the SNP effect on transcriptional regulation might be tissue-specific, supporting the tissue variability previously observed in the data provided by the GTEX portal.

1.4 NEIL2 and UNG protein levels

To analyse whether the SNPs effects on mRNA expression levels were translated into significant differences in protein expression, we determined by Western blotting NEIL2 and UNG protein levels in the LCLs panel (**Supplementary Figures S7A and S7B**). In the case of UNG, we also could analyse its protein level (UNG1 isoform) in a subset of individuals (n=30) from the FBOC series, composed by 10 controls (4 harbouring the SNP), and in 20 BRCA2 carriers (10 were harbouring SNP) (**Supplementary Figure S7C**). First, we tested whether *NEIL2* or *UNG* mRNA expression was correlated with their respective protein levels. We confirmed that *NEIL2* mRNA and protein levels were significantly correlated in the LCLs panel (**Figure 10A**). Similarly, *UNG1* mRNA levels correlated significantly with UNG1 protein levels in the subset from the FBOC series (**Figure 10B**). Additionally, we verified in the LCLs panel that both UNG isoforms remained highly correlated at the protein level (**Figure 10C**).

Concerning NEIL2 levels, we did not find significant differences associated with the rs804271 in the panel of LCLs. On the contrary, despite the reduced sample size, we could find a trend toward lower UNG1 and UNG2 protein levels in the LCL series associated with the *UNG* SNP (**Figure 10D)**. In the subset from the FBOC series we only could determine UNG1 isoform protein levels due to the low expression of the UNG2 isoform in these samples. Here, we showed that *BRCA2* mutation carriers harbouring SNP rs34259 had significantly lower UNG1 protein levels (**Figure 10E)**. This SNP effect remained significant when controls and BRCA2 carriers were combined, confirming that the downregulation associated with the rs34259 was translated into a lower expression of the UNG protein.

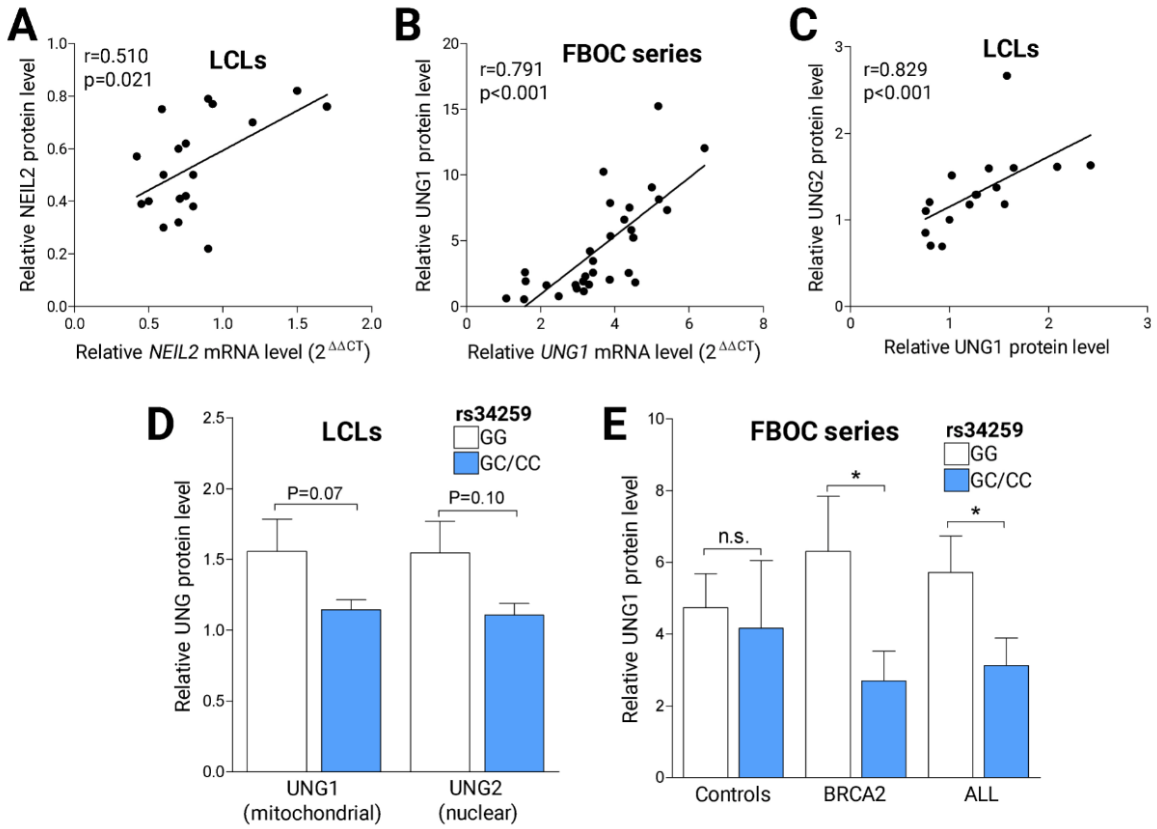

Figure 10 – *NEIL2* and *UNG* protein levels. A) Correlation analysis between *NEIL2* mRNA and protein levels in the panel of LCLs (n=20). **B)** Correlation analysis between *UNG1* mRNA and protein levels in a subset of individuals (n=30) from the FBOC series. **C)** Correlation analysis between UNG1 and UNG2 protein expression levels in LCLs (n=18). **D)** UNG1 and UNG2 expression levels in the LCL series (n=18) according to the SNP rs34259 status [non-carriers (GG)/carriers (GC/CC)]. **E)** Quantification of UNG1 protein levels in the patients shown in (B) according to the SNP rs34259. Spearman's test was used to assess the significance of the correlations in (A), (B), and (C). Unpaired t-tests were performed for statistical significance in (D) and (E). Bars show the mean and the SEM.

1.5 Accumulation of DNA damage at the telomeres

Glycosylases have an important role in the repair of base lesions from telomeric DNA (Jia et al., 2015). To analyse whether the studied SNPs have an impact on enzyme performance, we measured the relative accumulation of two kinds of lesions at the telomeres in the FBOC series: oxidized bases

and uracil. Telomeric DNA is prone to accumulate oxidative base lesions, which are recognized and excised by the glycosylases of the Fpg/Nei family (Prakash et al., 2012). We incubated the DNA from the members of the FBOC series with the glycosylases of this family NEIL2 and FPG, and then we determined by qPCR the relative amount of oxidized bases at the telomeric DNA in each sample. After qPCR analysis, we found a significantly higher accumulation of oxidative lesions in telomeric DNA from *BRCA1* and *BRCA2* mutation carriers compared with controls (**Figure 11A**). Furthermore, when we stratified according to the *NEIL2* SNP rs804271, we found that SNP carriers from the *BRCA1* or *BRCA2* mutational groups presented significantly higher oxidative DNA damage compared to their counterparts without the SNP (**Figure 11B**). Moreover, the *UNG* SNP rs34259 was also associated with lower oxidative DNA damage at the telomeres in the whole series (**Figure 11C**). Indeed, this association was found specifically pronounced in the group of controls (P=0.009), suggesting that the rs34259 is associated with lower oxidative DNA damage at telomeres independently of the BRCA status.

Telomeric DNA is also susceptible to uracil misincorporation, which is removed by the UNG glycosylase initiating the BER pathway (Vallabhaneni et al., 2015). Therefore, we decided to incubate the DNA of the FBOC series individuals, for the subsequent determination of the relative uracil accumulation in telomeric DNA. We did not find significant differences in uracil levels at telomeres among BRCA groups or controls. Interestingly, when we stratified according to the *UNG* SNP rs34259 status, we detected a significantly lower uracil accumulation at telomeric DNA when the SNP was present specifically for *BRCA2* mutation carriers (**Figure 11D**). These lower uracil levels could reflect an increased UNG activity which could explain the protective effect for ovarian cancer risk associated with this SNP in *BRCA2* mutation carriers.

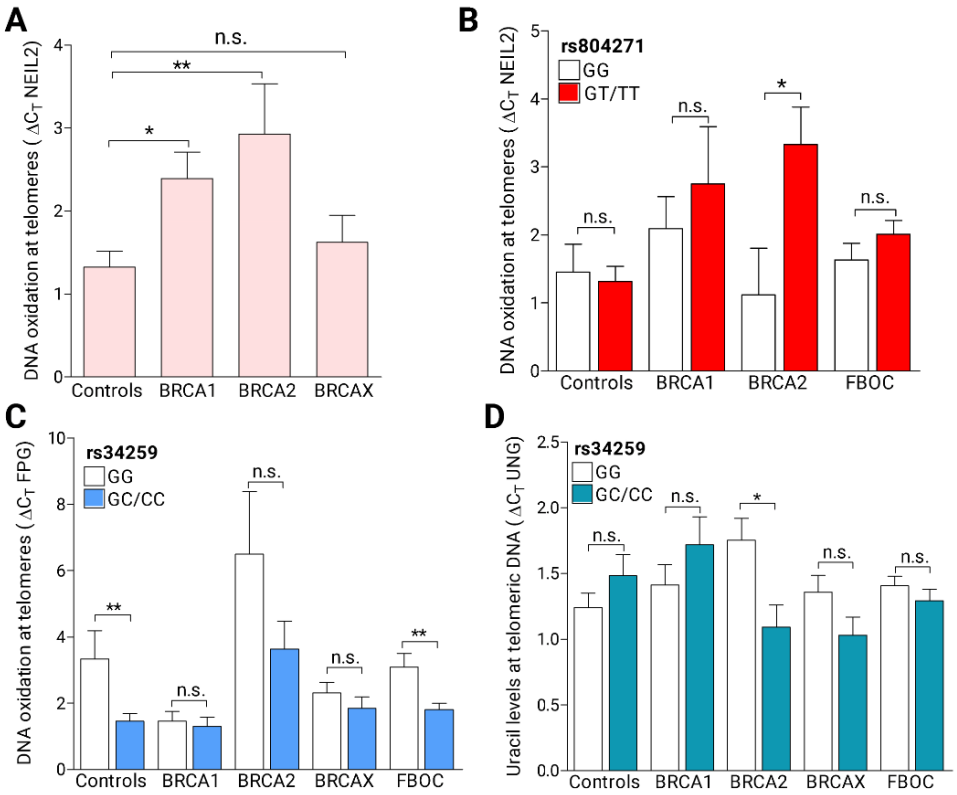

Figure 11 – Base lesions at telomeric DNA in the FBOC series. A) Comparative analysis of the relative accumulation of oxidative lesions among FBOC groups. **B)** Relative amount of oxidative lesions according to the NEIL2 SNP rs804271 status [non-carriers (GG)/carriers (GT/TT)]. **C)** DNA oxidation at telomeres according to the UNG SNP rs34259 status [non-carriers (GG)/carriers (GC/CC)]. **D)** Uracil accumulation at telomeres according to the UNG SNP rs34259 status. Bars show the mean and the SEM. Mann–Whitney U-test was used in (A), (B), and (C), unpaired t-test was used in (D).

1.6 Additional functional studies performed regarding the *UNG* SNP rs34259

1.6.1 Protein carbonylation

Oxidative stress (OS) induces oxidative DNA damage (Toyokuni et al., 1995). To analyse whether DNA oxidation at the telomeres may be explained by OS susceptibility, we used plasma from FBOC individuals to measure carbonylated proteins, a widely used biomarker of chronic OS (Fedorova et al., 2013). No significant differences were found in carbonylation levels among FBOC groups (**Figure 12A**). Nevertheless, carriers of the UNG variant showed a trend toward lower carbonylation levels (**Figure 12B**). Indeed, we observed a significantly lower protein carbonylation level for *BRCA2* mutation carriers harbouring the *UNG* SNP. This result suggests that the lower DNA oxidation associated with the rs34259 could be related to chronic OS susceptibility, which becomes more pronounced in *BRCA2* mutation carriers.

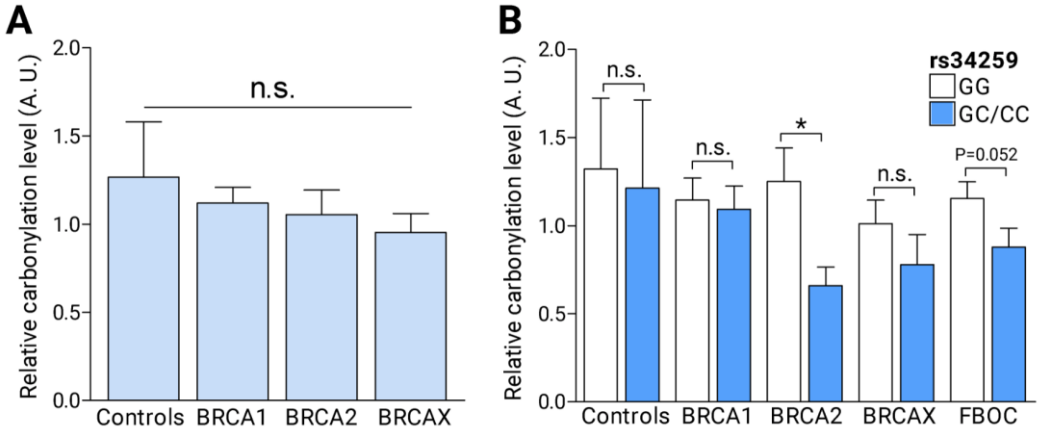

Figure 12 – Immunodetection of protein-bound carbonyl groups in plasma samples from the FBOC series. A) Protein carbonylation levels among FBOC groups in arbitrary units (A. U.) **B)** Protein carbonylation levels in the different groups stratified according to the presence or absence of the *UNG* SNP rs34259 [non-carriers (GG)/carriers (GC/CC)]. Bars show the mean and the SEM. One-way ANOVA test was performed for statistical significance in (A) and unpaired t-tests were performed in (D).

1.6.2 Telomere homeostasis

The accumulation of uracil or oxidative base lesions in the telomeric DNA interferes with the preservation of telomere integrity and thus can modulate telomere length (TL) (Zhou et al., 2015; Vallabhaneni et al., 2015). Because we had shown that the *UNG* SNP is associated with lower DNA damage at the telomeres, we decided to explore the possible involvement of the *UNG* SNP on telomere instability by measuring TL using PBMC from the individuals of the FBOC series. Besides, considering that shorter telomeres have been associated with an increased incidence of diseases such as cancer (Okamoto and Seimiya, 2019), we also estimated the percentage of short telomeres (TL < 3 Kb) in the series.

Given that TL shortens with age (Müezzinler et al., 2013), we first analysed the TL distribution in 91 healthy women (controls of the FBOC series) as a function of age to generate the regression line to adjust TL in the series. As expected, we obtained a decrease in TL with age (**Supplementary Figure S8**). Next, we examined TL and the percentage of short telomeres in the different groups of the FBOC series (**Figure 13**). We only detected a significant reduction in TL and an increase in the pertentage of short telomeres in the BRCAX cases compared to controls.

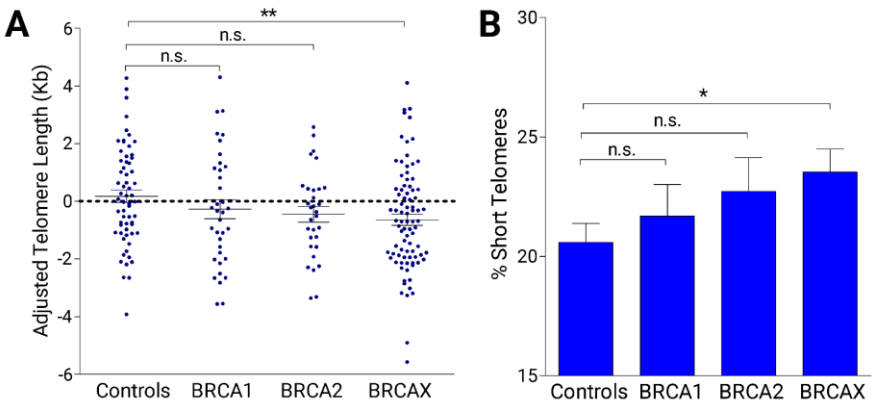

Figure 13 - Telomere length (A) and the percentage of short telomeres (B) among FBOC groups. Bars show the mean and the SEM. Numbers in brackets indicate sample size. Unpaired t-tests were performed for statistical significance.

Interestingly, when we studied the possible effect of the UNG SNP on TL, we were not able to detect significant differences within each mutational group, except for *BRCA2* mutation carriers, where the SNP is associated with a reduced age-adjusted TL (**Figure 14A**). Indeed, these patients also showed a trend toward a higher accumulation of short telomeres (**Figure 14B**).

TL can be regulated by telomerase activity. To evaluate whether the lower TL associated with the UNG SNP in *BRCA2* mutation carriers could be partially explained by telomerase activity, we measured this variable in the FBOC series. Mean telomerase activity was lower in all mutational groups and controls when the SNP was present, however, it did not reach statistical significance (**Figure 14C)**. Finally, we found a significant positive correlation between TL and telomerase activity (**Figure 14D**), reflecting how the telomerase action promotes telomere maintenance.

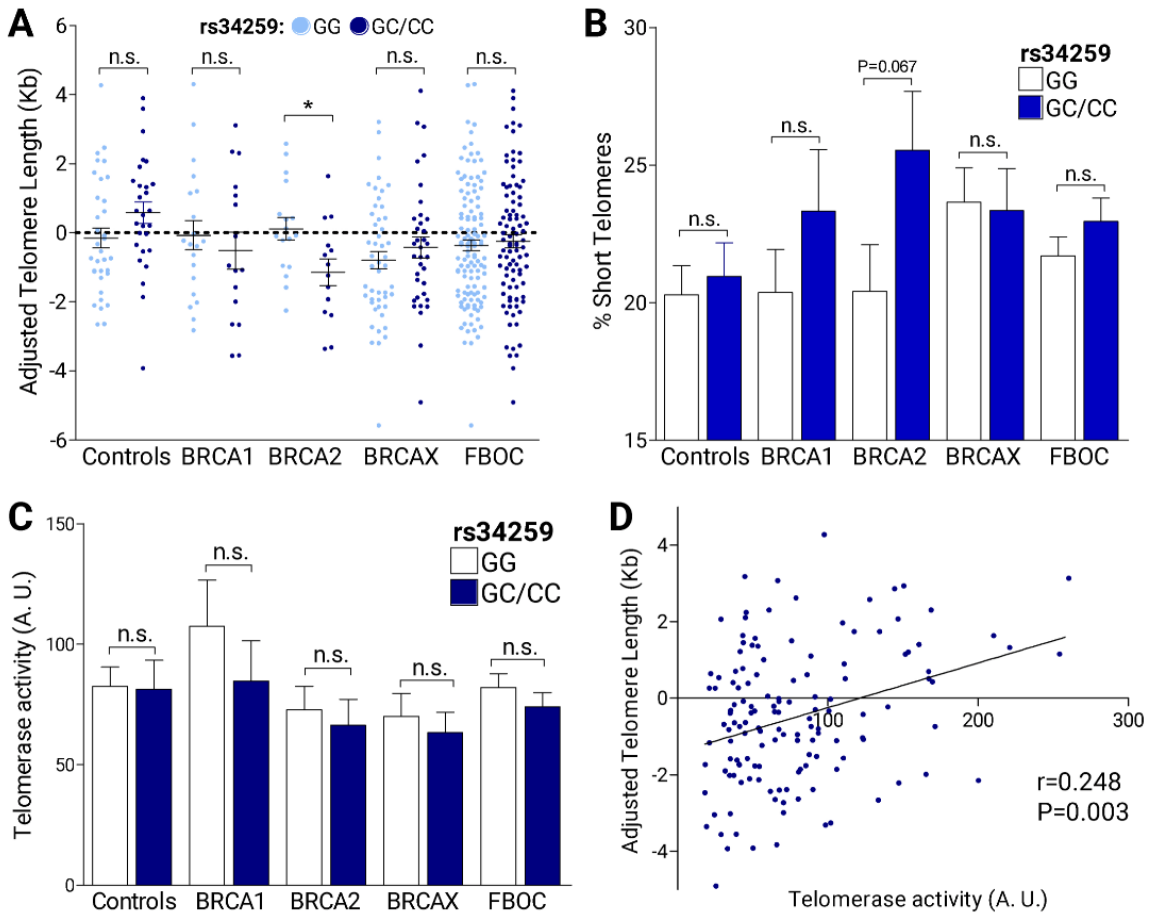

Figure 14 - Evaluation of the effect of the UNG SNP rs34259 on telomere integrity. A) Distribution of TL (kb) values adjusted for age in the FBOC series according to the presence or absence of the *UNG* SNP rs34259 [noncarriers (GG)/carriers (GC/CC)]. **B)** Percentage of short telomeres in the FBOC groups stratifying by the UNG SNP. **C)** Comparative analysis of telomerase activity in the FBOC series according to the presence or absence of the UNG SNP. **D)** Correlation analysis between telomerase activity and adjusted telomere length. Spearman's test was used to assess the significance of the correlation.

RESULTS PART II

2. Consequences of BER inactivation at telomeres by OGG1 dysfunction

The results presented in the previous section of this thesis show that functional variants in glycosylase genes can affect the levels of telomeric DNA damage. Considering also that the telomeres are particularly sensitive to oxidative stress, the second objective of this thesis was to explore the role of the glycosylase OGG1 in DNA repair activity at the telomeres and characterize the telomere defects generated as a consequence of OGG1 dysfunction. To achieve these goals, we first described spatial-temporal OGG1 DNA repair activity in U2OS osteosarcoma cells, a well-established model in telomere biology (Molenaar et al., 2003). Afterward, to analyse the consequences of OGG1 inhibition, we treated the cells with the novel OGG1 inhibitor TH5487 (Visnes, Cázares-Körner, et al., 2018). In parallel, we silenced the *OGG1* gene in U2OS to compare the effects at telomeres between OGG1 depletion or inhibition.

2.1. Telomeres are a hotspot for oxidation

Oxidative DNA lesions are not randomly distributed in the genome (Ding et al., 2017; Amente et al., 2019). To evaluate whether telomeric DNA is prone to accumulate these lesions, we incubated DNA extracted from U2OS cells with OGG1 and measured by qPCR oxidative DNA damage at three different genomic regions: the telomeric DNA, the *36B4* locus and the mitochondrial gene *MT-TF*. We found that U2OS cells accumulate higher levels of oxidized bases at telomeres compared to the other two analysed regions (**Figure 15A**). This result reflects that even in basal conditions, telomeric DNA harbours significantly higher amounts of oxidative damage. Next, to test if the amount of oxidative lesions may change along the cell cycle, we measured the relative accumulation of oxidized bases in cells sorted by cell cycle phase (G1, S, or G2/Mitosis). In the 3 analysed regions, we found significant differences between the cell phases, and also for the 3 regions, we detected the highest level of oxidative DNA damage in the S phase (**Figure 15B**).

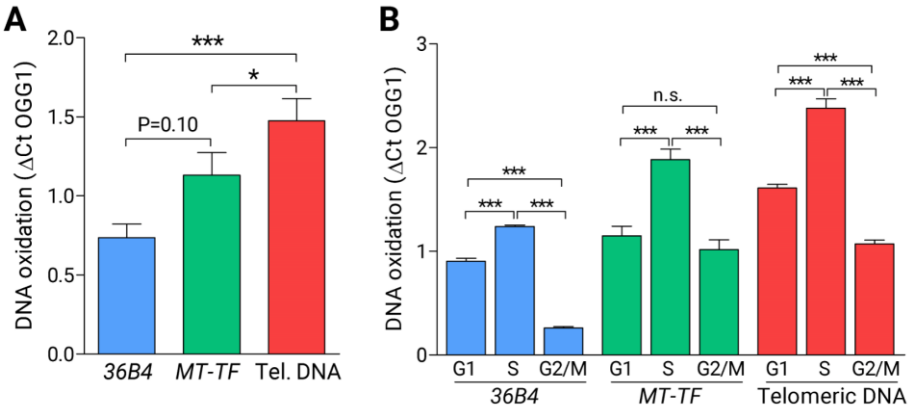

Figure 15 – Relative accumulation of oxidative lesions in different genomic regions. A) Comparative analysis of the relative level of oxidative lesions in three different regions (*36B4* locus, *MT-TF* mitochondrial gene, and telomeric DNA) determined in DNA from non-sorted U2OS cells. **B)** Relative level of oxidative lesions during the different cell cycle phases (G1, S, or G2/Mitosis) in the 3 regions defined in (A). Mann-Whitney tests were performed for statistical significance. Bars show the mean and the SEM of six independent experiments.

We hypothesized that the different accumulation of oxidative lesions along the cell cycle could be partially explained by differences in *OGG1* expression or variation in endogenous ROS levels throughout the cell cycle phases. To test these hypotheses, we measured OGG1 protein expression by Western blotting and intracellular ROS production by flow cytometry analysis in U2OS cell-cycle sorted cells. However, we found that OGG1 protein levels remained constant throughout the cell cycle (**Figure 16A**). In contrast, we observed a trend to higher endogenous ROS levels during the progression of the cell cycle, until reaching maximum values during G2/M (**Figure 16B**).

Complementary, we performed ChIP coupled to qPCR amplification to evaluate whether OGG1 binds *in vivo* to the telomeric DNA. Enrichment analysis showed that OGG1 was significantly enriched at telomeres compared to the *36B4* locus (**Figure 16C**), confirming the presence of OGG1 at telomeres under basal conditions.

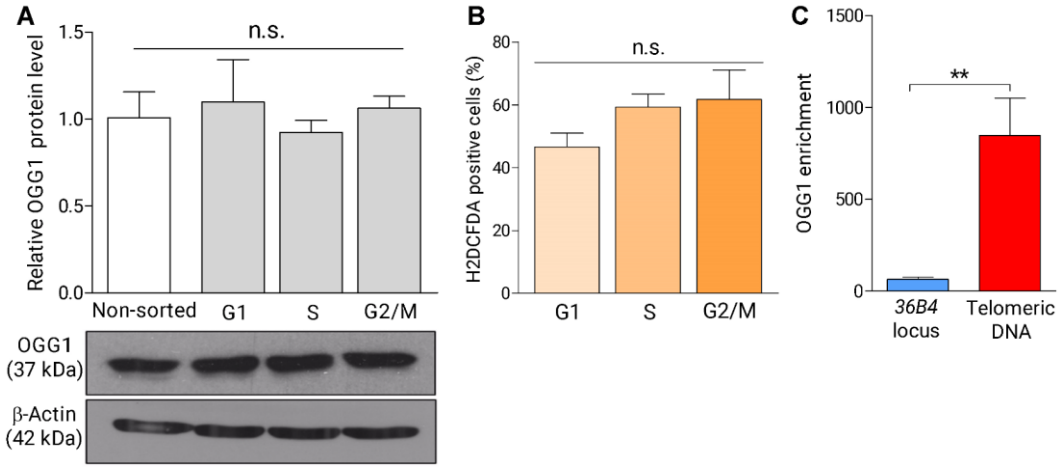

Figure 16 – OGG1 expression and ROS levels during the cell cycle and ChIP of OGG1. A) Quantification of OGG1 protein expression level along the cell cycle. Beta-Actin levels were used to normalize for protein loading. **B)** Percentage of cells with intracellular ROS levels above the median of the whole U2OS population in different cell cycle stages. **C)** OGG1-GFP pulldown followed by chromatin immunoprecipitation coupled to q-PCR for amplification of either *36B4* locus or the telomeric DNA. Statistical differences were tested by unpaired t-test in (A) and (B) and Mann-Whitney U tests in (C). Bars show the mean and the SEM of at least three independent experiments per condition.

2.2 OGG1 initiates BER at telomeres upon OS

After showing that telomeric DNA harbours more oxidative base lesions than other regions at basal conditions, we wondered whether OS conditions exacerbate these differences. To evaluate this idea, we measured the relative level of oxidative lesions per region in U2OS cells treated with H_2O_2 (200 µM/1h), followed by a recovery period (fresh medium/1h). We saw that the treatment with H_2O_2 significantly increases oxidative lesions in the three analysed regions (**Figure 17A**), demonstrating its efficacy to generate OS. Furthermore, we found that the recovery period caused a reduction in the levels of oxidized bases in the 3 regions, reflecting that DNA is being repaired. In parallel, we determined OGG1 protein levels in the same conditions to check whether OGG1

increases its expression in response to OS. However, no significant differences were detected in OGG1 expression compared to untreated cells (**Figure 17B**).

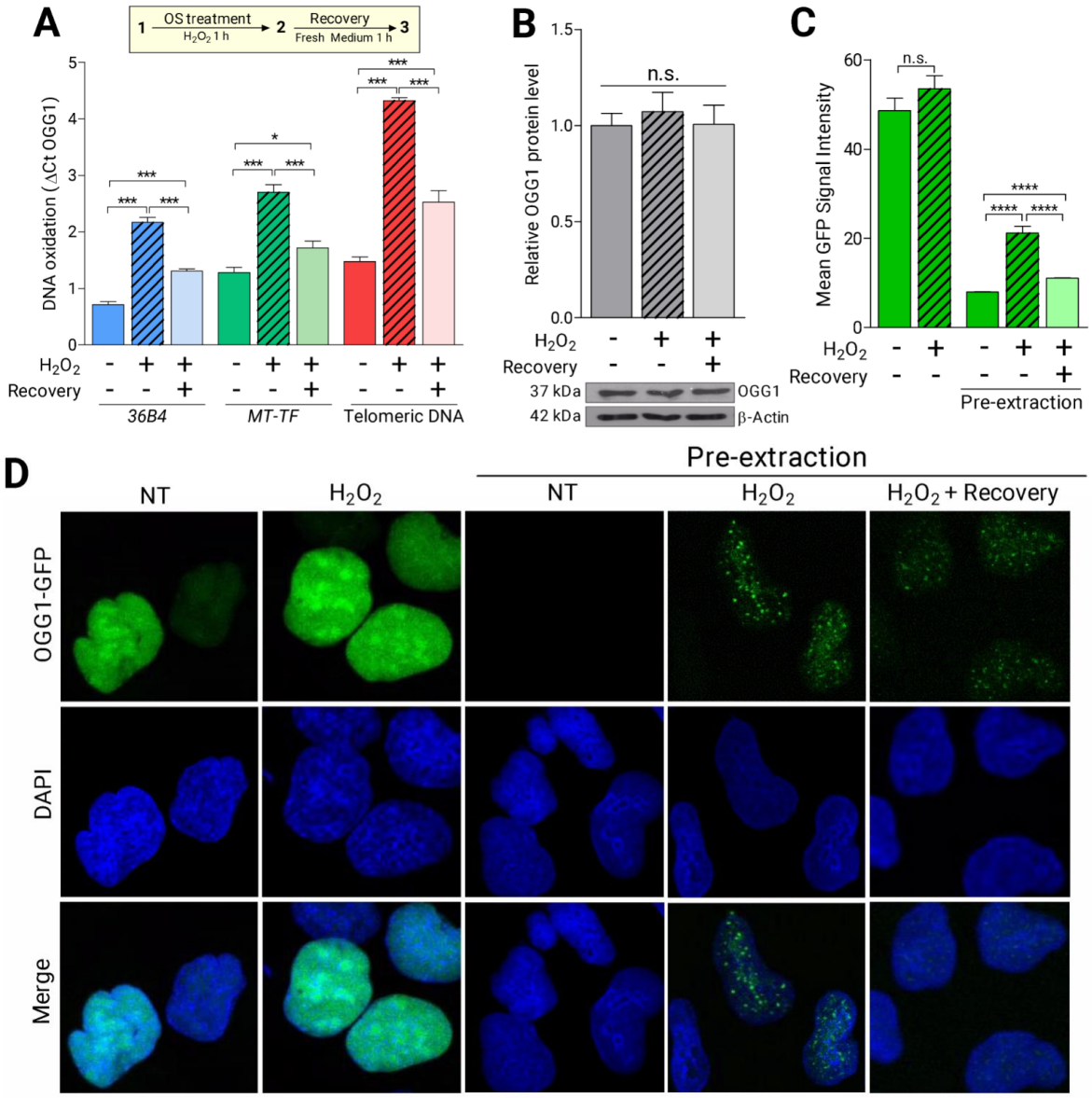

Figure 17 – Oxidative DNA damage accumulation and OGG1 recruitment induced by OS. A) Relative level of oxidative DNA lesions in 3 different genomic regions (*36B4* locus, *MT-TF* mitochondrial gene, and telomeric DNA) upon OS treatment (H_2O_2 200 µM/1h) and after a recovery period (fresh medium/1h). **B)** Quantification of OGG1 protein expression level in U2OS cells upon OS. Beta-Actin levels were used to normalize for protein loading. **C)** Quantification of OGG1-GFP signal intensity in response to OS in at least 1000 nuclei per condition. After pre-extraction, soluble proteins are removed enabling the detection of OGG1-GFP foci formation in response to OS. **D)** Confocal microscopy images for the conditions analysed in (C) showing OGG1-GFP staining pattern (green) within the nucleus, which is stained in blue with DAPI. Statistical differences were tested by unpaired t-test in (A) and (B) and Mann-Whitney U tests in (C). Bars show the mean and the SEM of at least three technical replicates per condition from three independent experiments.

To characterize spatial-temporal OGG1 DNA repair activity in response to OS, we used U2OS cells expressing OGG1 fused to GFP (OGG1-GFP) and analysed its expression pattern by Confocal IF. As we expected, images showed that OGG1 is a pan-nuclear protein distributed in patches, but we

did not detect an increase in GFP signal intensity after OS treatment (**Figures 17C and 17D**). Then, to follow whether OGG1 was recruited to damaged DNA upon OS, we performed a pre-extraction step to remove soluble proteins. Interestingly, nuclear OGG1-GFP foci were detected only in cells exposed to OS (**Figure 17D**), reflecting the OGG1 recruitment to chromatin in response to oxidative DNA damage. Indeed, the recovery period after oxidative treatment significantly decreased the GFP signal (**Figure 17C**). This finding together with the reduction in the levels of oxidized bases after the recovery time (**Figure 17A**), evidences the repair of oxidative lesions by the BER pathway.

Furthermore, to study whether the BER DNA repair pathway was specifically activated at the telomeres, we measured by IF OGG1-GFP signal intensity within the foci of the shelterin protein TRF2. We found that OS treatment significantly increases OGG1 at TRF2 foci, supporting the activation of the BER pathway at telomeres (**Figure 18**).

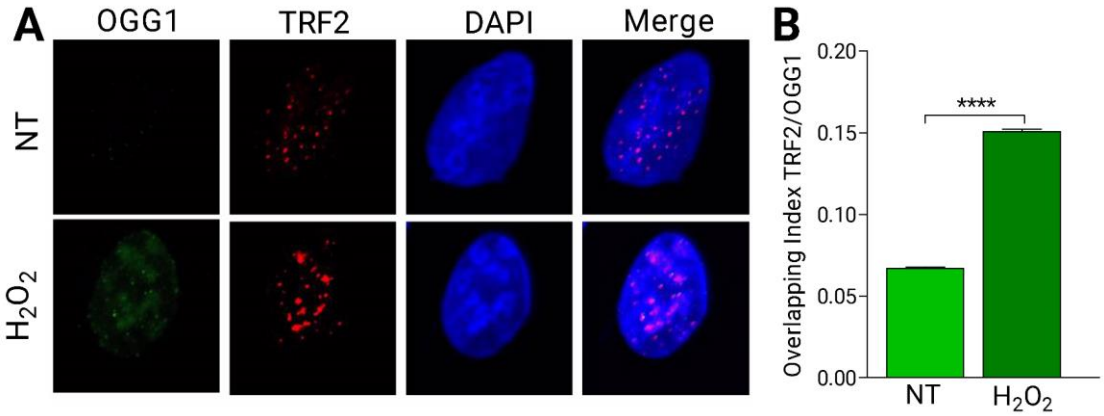

Figure 18 – OGG1 recruitment to telomeres upon OS. A) Confocal images showing OGG1-GFP staining pattern (green) and telomere TRF2 (red) within the nucleus, stained in blue with DAPI. **B)** Comparative analysis of OGG1-GFP signal intensity contained within TRF2 foci in non-treated (NT) or in response to OS from more than 200 nuclei per condition. Statistical differences were evaluated using unpaired T-test. Bars show the mean and the SEM.

2.3 *OGG1* gene knockout or Pharmacological OGG1 inhibition disrupts BER at telomeres

Once we showed that OS induces the activation of the BER pathway at the telomeres, we aimed to study the consequences of OGG1 inactivation in these regions. For this purpose, U2OS OGG1-GFP cells were used to generate a knockout for the OGG1 gene by CRISPR/Cas9 (OGG1-KO, detailed in material and methods). OGG1 knockout efficacy was validated by fluorescence microscopy and Western blotting (**Figures 19A and 19B**).

In order to analyse the impact of *OGG1* knockout, we first determined the level of oxidative DNA damage at basal conditions in the telomeres of these cells. We found that the telomeric DNA of OGG1-KO cells accumulates a higher level of oxidized bases compared to OGG1-proficient cells (**Figure 19C**). In parallel, we incubated U2OS OGG1-GFP cells with the OGG1 inhibitor TH5487 (10

µM) and measured the level of oxidized bases at telomeres each 24h for 4 days. Similarly to OGG1-KO cells, the treatment with TH5487 leads to a progressive accumulation of oxidized bases at the telomeres (**Figure 19D**). Taking together, these results reflect the essential role of OGG1 to preserve relative lower levels of oxidative damage in telomeric DNA.

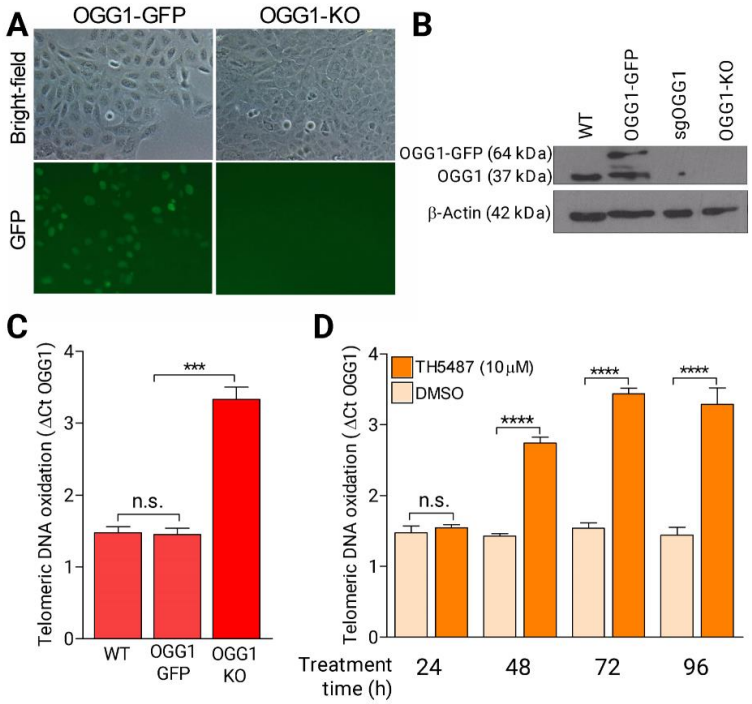

Figure 19 – OGG1 inactivation increases oxidative base lesions in the telomeric DNA. A) Bright-field and fluorescence microscope images showing OGG1-GFP depletion in OGG1-KO cells. **B)** CRISPR/Cas9 OGG1 knockout validation by Western blotting in U2OS OGG-GFP cells. A sorting step of the GFP-negative cells from sgOGG1 transfected cells was carried out to obtain the pool of GFP negative cells validated as OGG1-KO. β-actin was included as the loading control. **C)** Relative accumulation of oxidative DNA damage at the telomeric DNA in U2OS parental (WT), U2OS OGG1-GFP, and U2OS OGG1-KO cells. **D)** Relative accumulation of oxidative DNA damage at the telomeric DNA in U2OS OGG1-GFP cells treated with TH5487 (10 µM) during the indicated periods (hours). Unpaired t-tests were performed for statistical significance in (C) and (D). Bars show the mean and the SEM of at least three independent experiments.

Additionally, to check the ability of the OGG1 inhibitor to inactivate the BER pathway at telomeres, we induced we induced OS to stimulate the BER pathway. Then, we analysed by IF the signal intensity of the BER enzyme XRCC1 within the foci of TRF2. Both in basal and upon OS treatment, OGG1 inhibition (TH5487) or depletion (OGG1-KO cells) resulted in a decrease in XRCC1 signal intensity at the telomeres (**Figures 20A and 20B**), reflecting the disruption of the BER pathway in these genomic regions.

Subsequently, we hypothesized that the inhibition or depletion of OGG1 may cause more severe effects when the cells are exposed to OS conditions. To test this hypothesis, we carried out an oxidative treatment (H_2O_2 200 µM/1h) in the OGG1-KO cells and OGG1-GFP cells treated with the OGG1 inhibitor, and we measured the levels of oxidized bases at telomeric DNA. We validated that

the OS treatment exacerbates the accumulation of oxidative DNA damage at telomeres of OGG1 inhibited or depleted cells (**Figure 20C**). Furthermore, a recovery period (fresh medium/1h) after OS treatment, which was coupled to a decrease in oxidative base lesions at telomeric DNA from U2OS-proficient cells (**Figure 17A**), did not cause a reduction in the amount of oxidative lesions when *OGG1* is silenced, confirming that the activity of this glycosylase is essential for the repair of oxidative DNA damage at the telomeres.

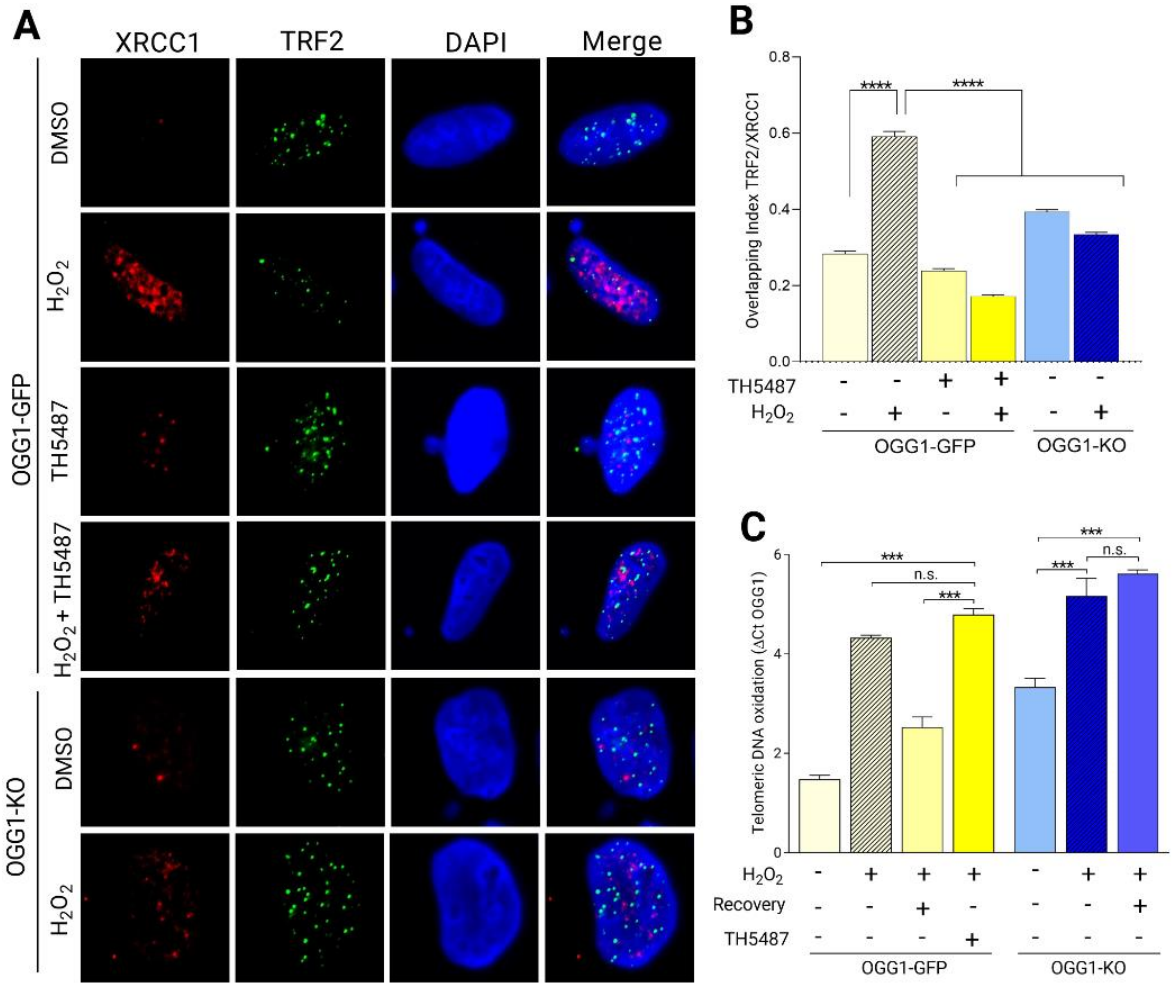

Figure 20 - OGG1 inactivation disrupts BER at telomeres upon OS. A) Confocal imaging of XRCC1 (red) and TRF2 (green) by IF after OS induction (H_2O_2 200 µM/1h) combined with OGG1 inhibition (TH5487) or knockout. DAPI was used to stain the cell nucleus (blue). **B)** Quantification of XRCC1 signal intensity integrated within telomeres (TRF2 foci) for the conditions presented in (A) from more than 200 nuclei per condition. **C)** Relative level of oxidized bases at telomeres in OGG1 inhibited/depleted U2OS cells upon oxidative stress treatment (H_2O_2 200 µM/1h) or followed by a recovery period (fresh media/1h). Mann–Whitney U-test was used in (B) and unpaired t-test was used in (C). Bars show the mean and the SEM of at least three independent experiments per condition.

Finally, we proposed to investigate whether the accumulation of oxidative lesions associated with the inactivation of OGG1 could evolve to DSBs. To examine this assumption, we measure by IF the activation at the telomeres of the DSBs markers γH2AX and 53BP1 (Mah et al., 2010; Panier and Boulton, 2014). We exposed U2OS cells to OS (H_2O_2 200uM/1h), and after we allowed cells to

recover for 16 hours since unrepaired SSBs generated via BER can be converted into DSBs after DNA replication (Schipler and Iliakis, 2013). As it was expected, after the oxidative treatment we found a significantly higher overlapping index of both YH2AX and 53BP1 foci with telomere TRF2 foci (**Figure 21**). However, no significant differences were detected regarding OGG1 inhibition/depletion in basal or under OS conditions.

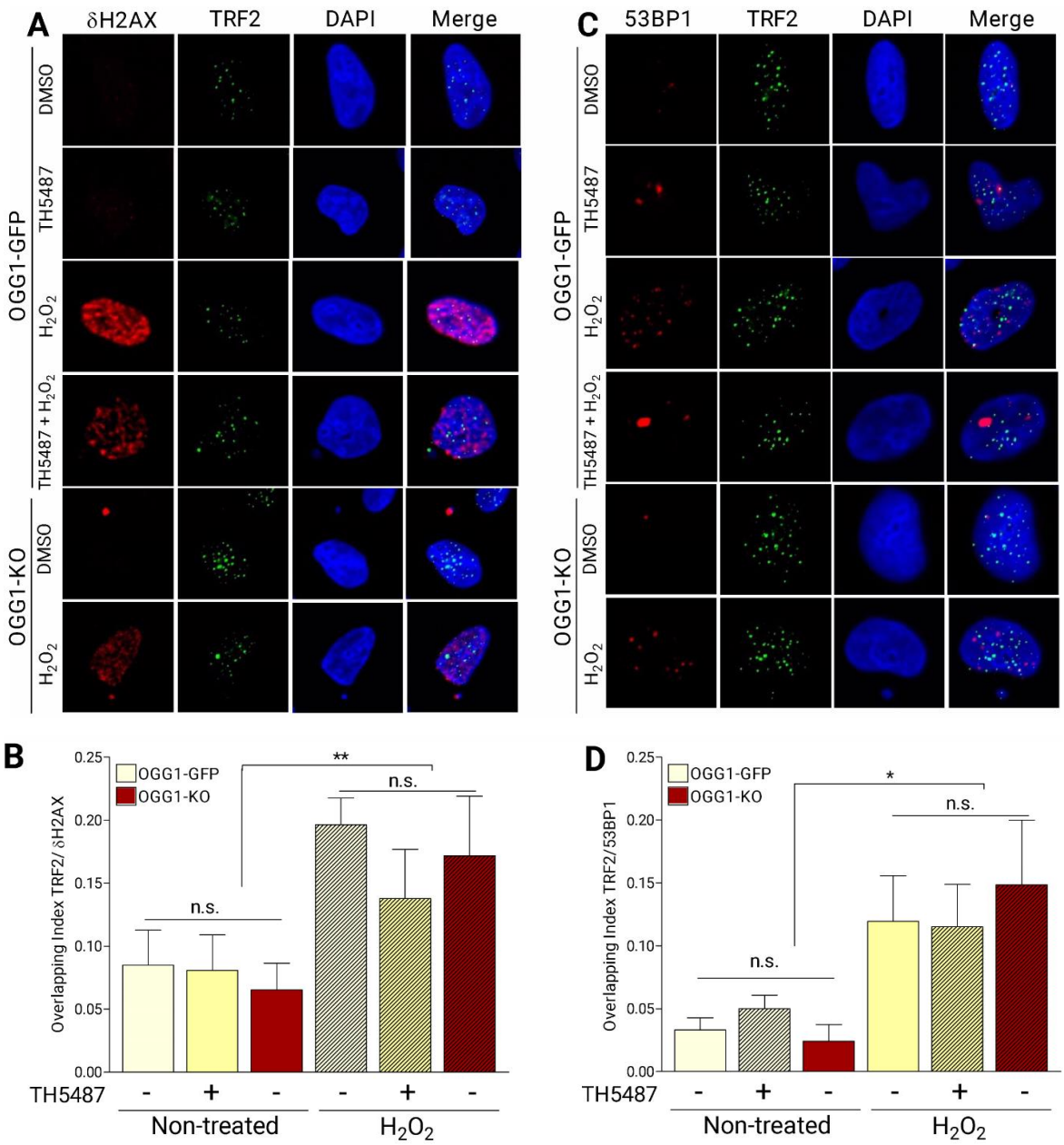

Figure 21 - DSBs at the telomeres. A) Confocal imaging at single cells representative for each treatment condition and stained for γH2AX (red) and TRF2 (green) using specific antibodies or DAPI to stain cell nucleus (blue). **B)** Confocal imaging at single cells representative for each treatment condition and stained for 53BP1 (red) and TRF2 (green) using specific antibodies or DAPI to stain cell nucleus (blue). **C)** Quantification of γH2AX signal intensity integrated within telomeres for the conditions presented in (A). **D)** Quantification of 53BP1 signal intensity integrated within telomeres for the conditions presented in (B). Mann-Whitney tests were performed for statistical significance. Bars show the mean and the SEM from 2 independent experiments incluiding at least 200 cells per condition.

2.4 OGG1 inactivation results in telomere losses, post-mitotic and proliferation defects

To study the impact of BER disruption on telomere integrity, we examined by telomere fluorescence *in situ* hybridization (Telo-FISH) whether OGG1 inhibition or silencing might compromise telomere stability. After incubating U2OS OGG1-GFP and OGG1-KO cells with the OGG1 inhibitor TH5487 (10 µM/24h), or with H_2O_2 (200 µM/1h) to generate OS, we analysed metaphase chromosomes to assess the number of chromosome signal-free ends and multi-telomeric signals, indicators of telomere losses and fragile telomeres, respectively (**Figure 22A**).

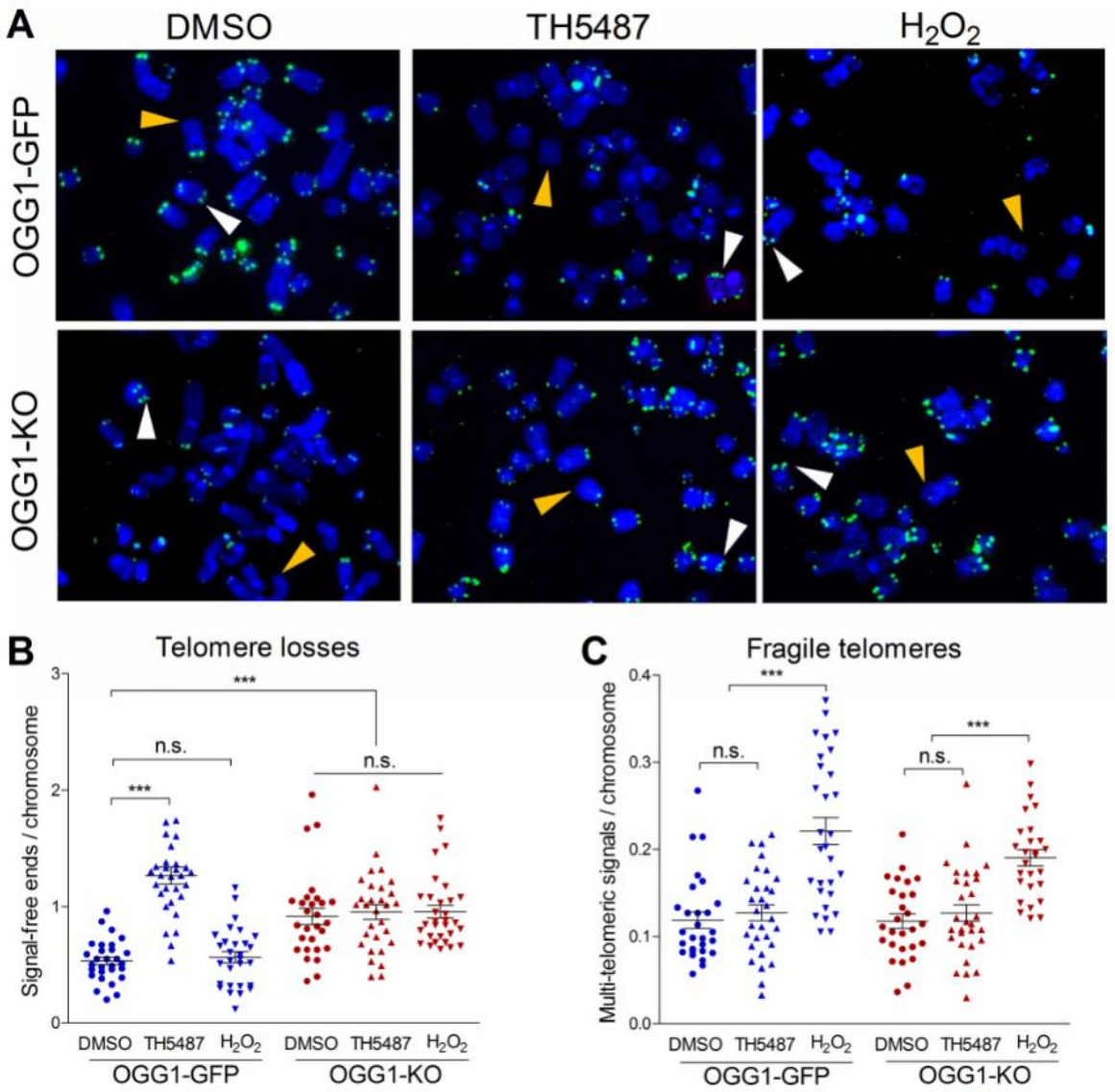

Figure 22 – The inactivation of OGG1 causes telomere losses. A) Representative telo-FISH images of metaphase chromosomes from U2OS OGG1-GFP or OGG1-KO cells for each studied condition [non-treated (DMSO), TH5487, and oxidative treatment (H_2O_2 200 µM/1h)]. Chromosomes were stained with DAPI (blue) and telomeres were stained with PNA telomeric probe (green). An example of a telomere loss (orange arrowhead) and a fragile telomere (white arrowhead) are indicated in each image. **B)** Quantification of telomeric signal-free ends for the conditions shown in (A). **C)** Quantification of fragile telomeres. Comparative analysis for the frequency of multi-telomeric signals for the conditions shown in (A). Each dot represents a metaphase. Statistical significance was determined using unpaired T-test. Bars show the mean and the SEM for events/metaphase. More than 30 metaphases per condition from two independent experiments.

We found that 24h of exposure to TH5487 was enough to observe a significant increase in telomere losses compared to the control treatment (DMSO) in OGG1-proficient cells (**Figure 22B**). Interestingly, OGG1-KO cells presented a higher number of telomere losses than OGG1-GFP cells at basal conditions, and the TH5487 treatment did not cause additional telomere loses in these cells, suggesting that telomere loss is a specific phenotype caused by OGG1 inactivation.

On the contrary, we did not observe significant differences in telomere fragility after OGG1 depletion or inhibition at basal conditions (**Figure 22C**). However, after OS treatment, we could detect a significant increase in the frequency of chromosomes with multi-telomeric signals for both groups regardless of the OGG1 status, and no additional effect on the telomere losses. These results reflect that telomere losses might be associated with OGG1 deficiency, while telomere fragility is a general phenotype occurring in OS conditions.

Next, we evaluated whether the telomere loss associated with OGG1 dysfunction might promote chromosome instability. To this end, we estimated by IF the frequency of micronuclei, which are markers of cell division defects, including errors in DNA replication and mitosis, whose formation is higher in cells with a defective DNA damage repair system (Crasta et al., 2012). U2OS OGG1-KO cells showed significant increases in micronuclei frequency compared with OGG1-proficient cells (**Figure 23A**). Similarly, the treatment with the OGG1 inhibitor (TH5487 10 µM/24h), induces micronuclei formation in an equivalent proportion than the OGG1 knockout. Importantly, OS conditions also caused a significant formation of micronuclei in both OGG1-proficient and deficient cells (**Figure 23A**).

Lastly, in order to analyse whether all these cellular defects associated with OGG1 dysfunction could impair the proliferation potential of U2OS cells, we evaluate the ability to form colonies and changes in proliferation after OGG1 inhibition or depletion. We did not find significant differences in the number of colonies that OGG1-KO cells or OGG1-GFP cells incubated with TH5487 (5 µM) were able to form 14 days after plating compared to OGG1-proficient cells (**Figure 23B**), which indicates no changes in clonogenic potential associated with OGG1 dysfunction. However, when we checked cell proliferation by measuring the area of the colonies, we found a significant decrease in the size of the colonies of OGG1-KO cells and OGG1-GFP cells treated with the OGG1 inhibitor compared to OGG1-proficient cells non-treated (incubated with DMSO, **Figure 23C**). Complementary, we inflicted OS conditions transiently during colony formation (H_2O_2 200uM/1h 6 days after seeding), and we found that the reduction in colony area caused by the oxidative treatment, was higher in OGG1-KO cells than in OGG1-GFP cells (**Figure 23D**). Overall, these data show that OGG1 dysfunction may lead to proliferation defects that are more pronounced after OS.

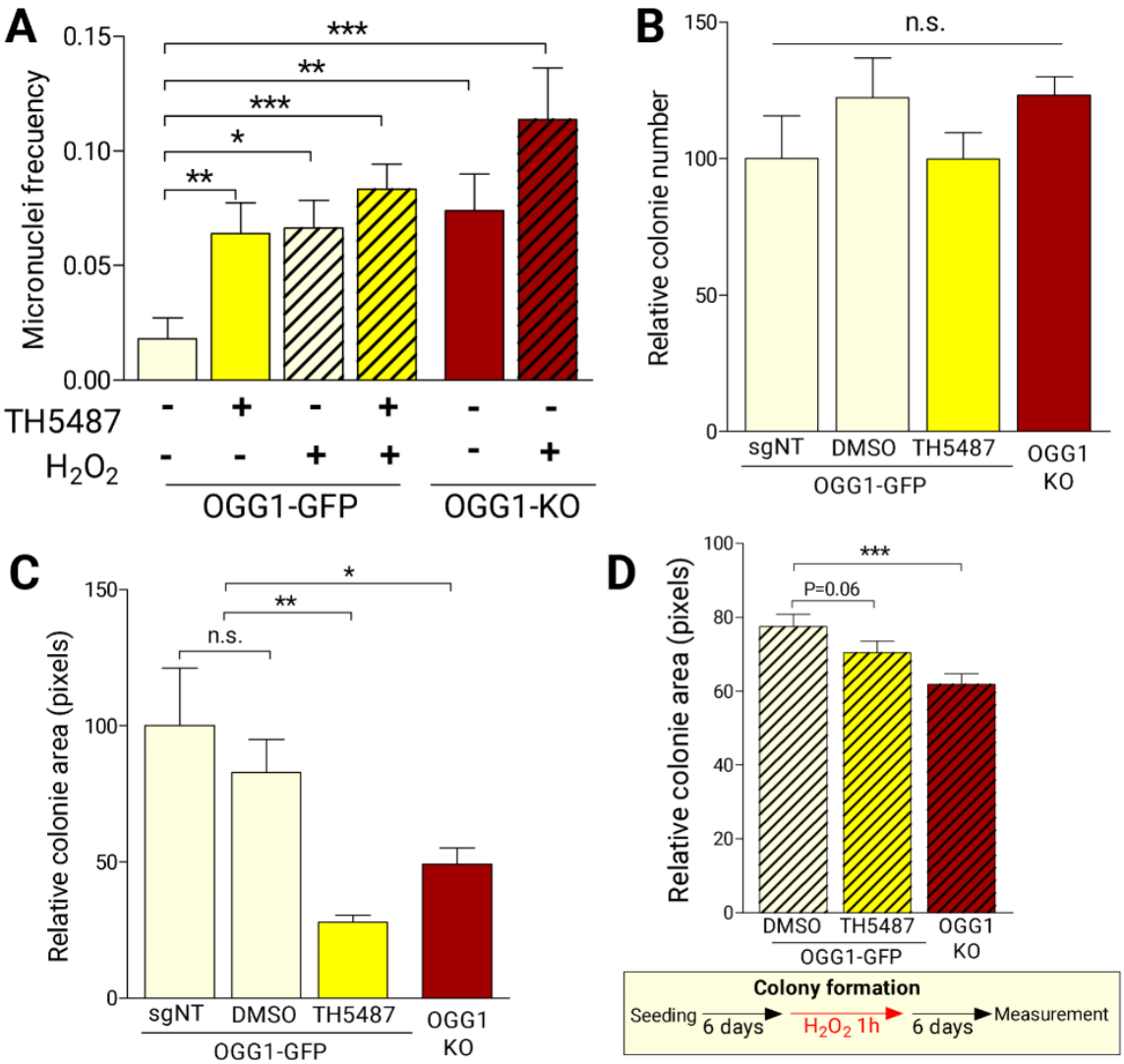

Figure 23 - OGG1 inactivation results in chromosome instability and proliferation defects. **A)** Comparative analysis of the micronuclei frequency for U2OS cells incubated with DMSO or TH5487 and for U2OS OGG1-KO cells at basal condition or during after oxidative treatment (H_2O_2 200 µM/1h). Data is the average of 2 independent experiments. More than 200 cells per condition were analysed. **B)** Comparative analysis of the clonogenic potential (colony number) after OGG1 inhibition (TH5487 5 µM) or depletion (OGG1-KO). **C)** Comparative analysis of cell proliferation (colony size) after OGG1 inhibition or depletion. U2OS OGG1-GFP transfected with non-targeting control (sgNT) cells were included as non-treated control in (B) and (C). **D)** Up, comparative analysis of the relative colony area when an oxidative pulse (H_2O_2 200uM/1h 6 days after seeding) was carried out during the colony formation. Down, summary for the schedule of the treatment. Significant differences were evaluated using the Mann-Whitney test for non-parametric distributions. Bars show the mean and the SEM. Data in (C) and (D) are average of the mean colony area values from three independent experiments.

RESULTS PART III

3. Synthetic lethal targeting of BRCA1-deficient cells by OGG1 inhibition

In the previous parts of this thesis, we have shown that cancer risk in *BRCA1/2* mutation carriers can be modified by genetic variants that modulate glycosylase expression, and that OGG1 could be rated as a potential novel therapeutic cancer target. Considering our results, and bearing in mind the synthetic lethal interaction between the *BRCA* genes and *PARP1*, also involved in the BER pathway, we aimed to explore the potential synthetic lethal interaction between *BRCA1* and *OGG1*. To achieve this objective, we treated BRCA1-proficient and deficient TNBC cells with the OGG1 inhibitor TH5487 (Visnes, Cázares-Körner, et al., 2018) and evaluated its effect on cell viability. Furthermore, we employed TH5487 in combination with the PARP inhibitor olaparib (Bochum et al., 2018) to analyse the possible synergistic interaction between the two inhibitors in the context of BRCA1 deficiency.

3.1 *BRCA1* silencing in MDA-MB-231 cell line confirms the synthetic lethal interaction between *BRCA1* and *PARP1*

In order to evaluate the potential synthetic lethal interaction between *BRCA1* and *OGG1*, *BRCA1* was silenced in the BRCA1-proficient TNBC cell line MDA-MB-231. We used CRISPR/Cas9 to target exon 11 of the *BRCA1* gene and several single colony clones were generated. Gene disruption in clones BRCA1ko1 and BRCA1ko2 was confirmed by DNA sequencing (**Supplementary Figure S1**). Additionally, the quantitative RT-PCR analysis showed a significantly lower *BRCA1* mRNA expression in BRCA1-KO clones compared to sgNT (**Figure 24A**), and Western blotting confirmed BRCA1 loss (**Figure 24B**).

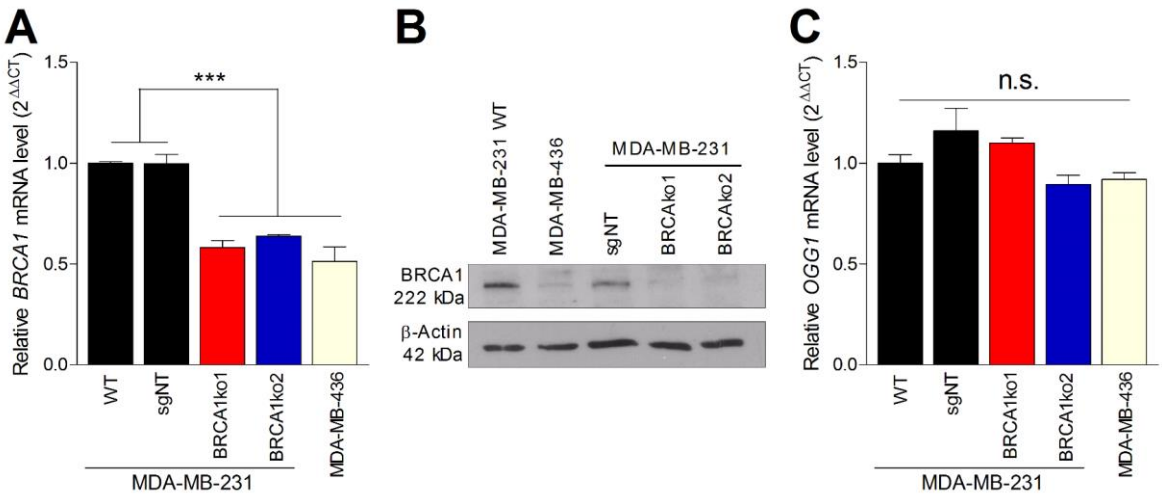

Figure 24 – *BRCA1* knockout validation in MDA-MB-231 cells. A) *BRCA1* mRNA relative level in parental (WT) MDA-MB-231 cells, the non-targeting control (sgNT), and two BRCA1-KO clones (BRCA1ko1 and BRCA1ko2). BRCA1-deficient TNBC cell line MDA-MB-436 was included as a negative control. **B)** Western blotting of BRCA1 in the different cells shown in (A). β-actin was used as a loading control. **C)** *OGG1* mRNA relative level in the different cells shown (A). Unpaired t-tests were used in (A) and (C). Bars show the mean and the SEM of three independent experiments.

It has been suggested that BRCA1 stimulates the expression of different BER enzymes, including OGG1 (Saha et al., 2010). Taking this into account, we determined *OGG1* mRNA expression to analyse whether BRCA1 silencing was associated with transcriptional down-regulation of OGG1. However, we did not find differences in OGG1 expression between BRCA1-proficient and deficient MDA-MB-231 cells (**Figure 24C**).

Besides, we wanted to validate the previously described synthetic lethal interaction between BRCA1 and PARP1 (Bryant et al., 2005; Farmer et al., 2005) by testing the PARP inhibitor olaparib in BRCA1-proficient and deficient MDA-MB-231 cells. In these cells, we evaluated the ability to form colonies (clonogenic assay) and changes in proliferation (MTT assay) in response to different olaparib concentrations. As expected, the two BRCA1-KO clones showed a significant relative lower number of colonies compared to BRCA1-proficient cells (sgNT) in the complete range of olaparib concentrations tested (**Figure 25A**). Consistently with these results, treatment with olaparib also markedly decreased proliferation of BRCA1-KO cells compared to BRCA1-proficient cells (**Figure 25B**). Moreover, we also determined the half-maximal olaparib inhibitory concentration (IC_{50}) values for BRCA1-proficient and BRCA1-KO clones, and these were more sensitive to olaparib (BRCA1ko1 = 0.645 µM and BRCA1ko2 = 0.457 µM) than control cells (sgNT = 2.138 µM). Together, these data confirm that PARP inhibition selectively causes a loss of viability and survival in BRCA1-deficient, but not in BRCA1-proficient TNBC cells.

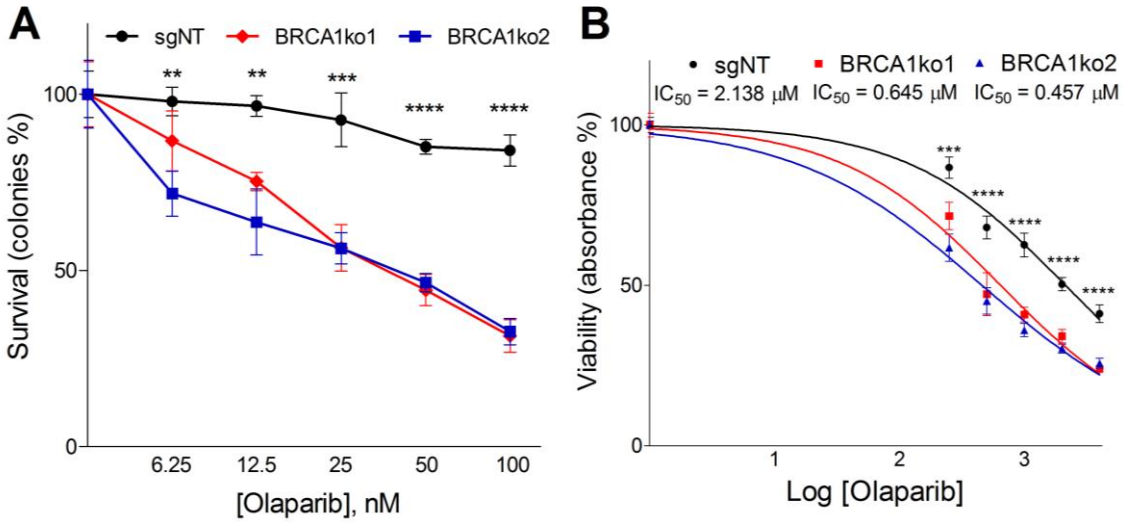

Figure 25 – *BRCA1* silencing sensitizes TNBC cells to PARP inhibition. A) Clonogenic survival of BRCA1-proficient (sgNT) and deficient (BRCA1ko1 and BRCA1ko2) MDA-MB-231 cells exposed to olaparib. Cells were incubated for 14 days in the presence of DMSO (control) or the indicated concentrations of olaparib, followed by colony enumeration. The values are normalized to untreated cells and represent a mean and standard deviation of three independent experiments. **B)** MTT assay displaying logarithm-transformed values and the viability curves of BRCA1-proficient (sgNT) and deficient (BRCA1ko1 and BRCA1ko2) MDA-MB-231 cells after treatment with olaparib for 72 hours. Six replicates for each concentration were used in two independent plates. IC_{50} calculated based on the resulting dose-response curves are shown. In (A) and (B), statistical significance at each olaparib concentration was determined by one-way ANOVA test.

3.2 BRCA1 knockout sensitizes TNBC cells to OGG1 inhibition

The capacity of PARP inhibitors to induce synthetic lethality in BRCA-deficient cancers implies that other factors within BER may be potential targets of synthetic lethality. In the view of our previous results suggesting OGG1 as a potential target for cancer treatment, we investigated the ability of the OGG1 inhibitor TH5487 to induce synthetic lethality in BRCA1-deficient cells.

To see whether BRCA1 knockout sensitizes TNBC cells to OGG1 inhibition, the effect of TH5487 on clonogenic potential was characterized by colony formation assays. We found that TH5487 caused a concentration-dependent loss of clonogenic potential significantly higher in *BRCA1* knockout clones compared to BRCA1-proficient cells (**Figure 26A**). In addition, in order to evaluate whether OGG1 inhibitors could selectively inhibit the growth of BRCA1-deficient TNBC cells, we also incubated BRCA1-proficient and deficient MDA-MB-231 cells with a dilution series of TH5487. BRCA1-KO clones displayed slower proliferation for up to 72 h (**Figure 26B**) and present substantially lower IC_{50} values for TH5487 (BRCA1ko1 = 3.710 µM and BRCA1ko2 = 3.393 µM) than control cells (sgNT = 6.744 µM), reflecting that BRCA1-deficient cells are more sensitive to TH5487. Overall, these data show that BRCA1 silencing increases sensitivity to OGG1 inhibition, supporting a synthetic lethal interaction between *BRCA1* and *OGG1*.

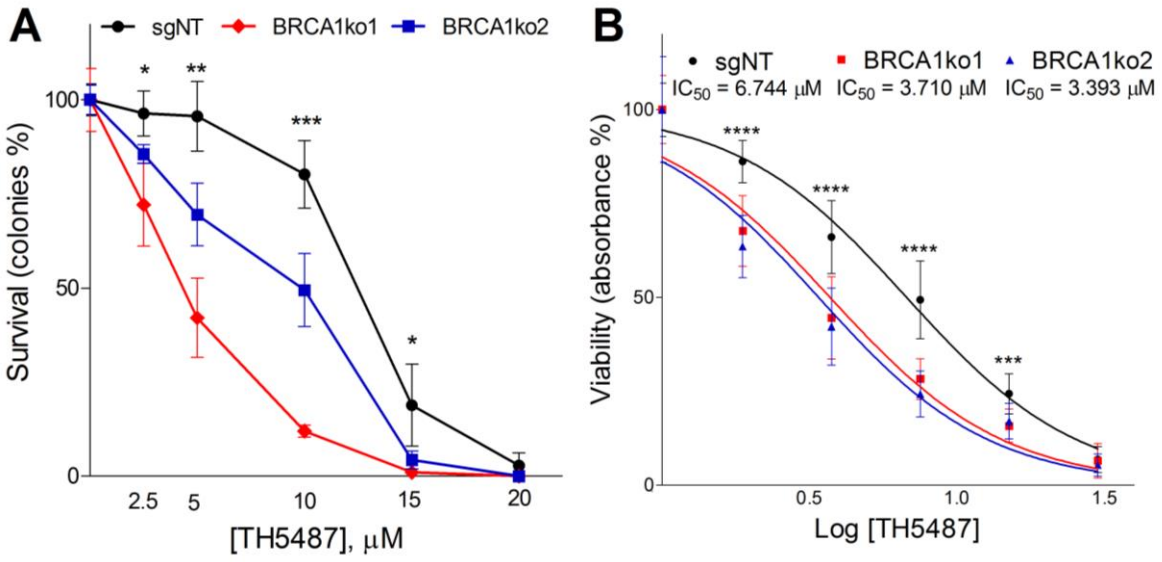

Figure 26 – *BRCA1* silencing sensitizes TNBC cells to OGG1 inhibition. A) Clonogenic survival of BRCA1-proficient (sgNT) and deficient (BRCA1ko1 and BRCA1ko2) MDA-MB-231 cells exposed to TH5487. Cells were incubated for 14 days in the presence of DMSO (control) or different concentrations (2.5, 5, 10, 15 and 20 µM) of TH5487, followed by colony enumeration. The values are normalized to untreated cells and represent a mean and standard deviation of three independent experiments. **B)** MTT assay displaying logarithm-transformed values and the viability curves of BRCA1-proficient (sgNT) and deficient (BRCA1ko1 and BRCA1ko2) MDA-MB-231 cells after treatment with TH5487 for 72 hours. Six replicates for each concentration were used in two independent plates. IC_{50} calculated based on the resulting dose-response curves are shown. In (A) and (B), statistical significance at each TH5487 concentration was determined by one-way ANOVA test.

3.3 OGG1 inhibition potentiates PARP inhibitor olaparib effects in BRCA1-deficient cells

Taking into account the two synthetic lethal interactions of *BRCA1* with the BER members *OGG1* and *PARP1*, we decided to analyse the possible synergistic interaction between the inhibitors of these two BER enzymes in BRCA1-deficient cells. To test this synergy, we selected sublethal concentrations of olaparib and TH5487 which caused a significantly higher impact on BRCA1-KO clones than BRCA1-proficient cells and evaluated their effect on the clonogenic potential (clonogenic assay) and cell proliferation (MTT assay).

According to the previous experiment, the treatment with TH5487 at 5 µM compared to DMSO treatment decreases the relative number of colonies in BRCA1-KO clones but not in control cells (sgNT) (**Figures 27A and 27B**). As expected, we also found a significantly higher decrease in clonogenic potential after olaparib treatment at 25 nM in BRCA1 knockout cells compared to BRCA1-proficient cells. Interestingly, the combined treatment with these two inhibitors notably diminishes the number of colonies compared to single-drug treatments in BRCA1-KO clones, while in BRCA1-proficient cells, TH5487 did not enhance the effect of the olaparib treatment alone (**Figures 27A and 27B**).

Furthermore, we analysed the effect of the two combined BER inhibitors on cell viability using the MTT assay (**Figure 27C**). Treatment with TH5487 did not increase sensitivity to olaparib in BRCA1-proficient cells. On the other hand, the combination of both inhibitors significantly decreased cell viability by a greater extent than each of the treatments alone in BRCA1 depleted cells (**Figure 27C**). These data support that the OGG1 inhibitor TH5487 selectively increases the sensitivity to the PARP1 inhibitor olaparib in BRCA1 depleted cells.

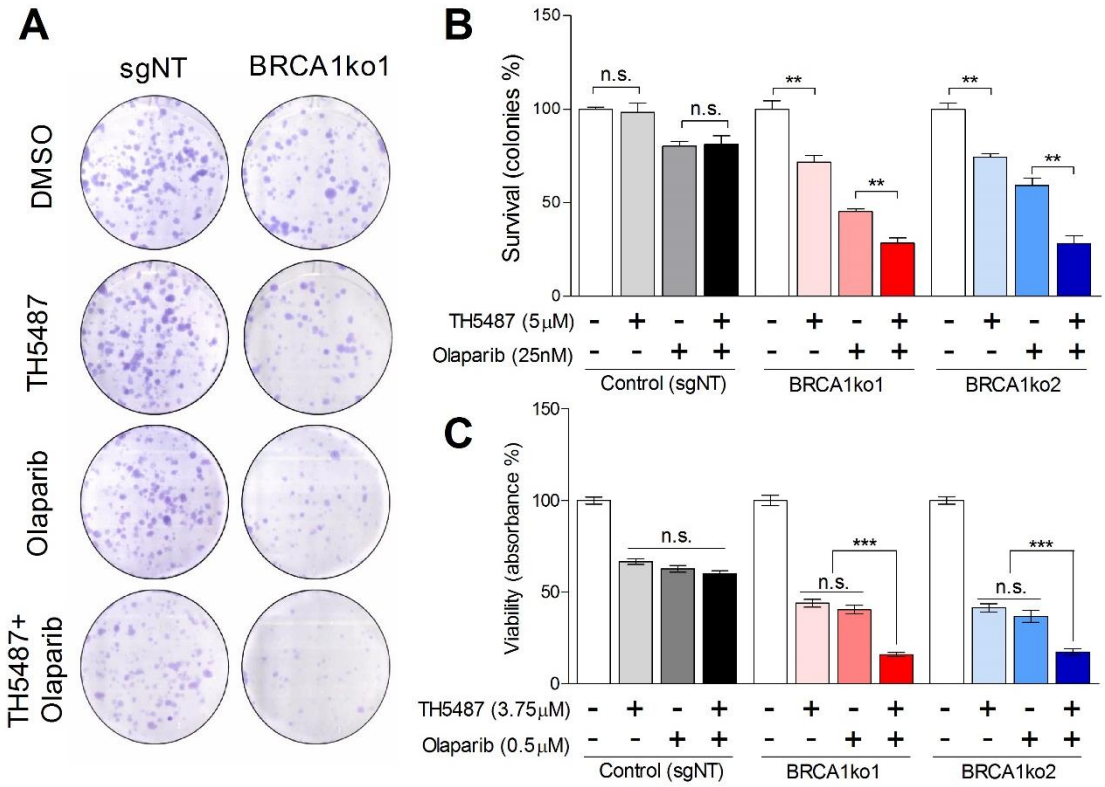

Figure 27 – OGG1 inhibition potentiates olaparib effects in BRCA1-deficient cells. A) Colony formation assays showing the effect of TH5487 and olaparib on MDA-MB-231 sgNT and BRCA1ko1 cell growth. A representative example of one of three independent experiments is shown for control (sgNT) and BRCA1ko1 cells. **B)** Clonogenic survival of BRCA1-proficient (sgNT) and deficient (BRCA1ko1 and BRCA1ko2) MDA-MB-231 cells exposed to TH5487 (5 µM), olaparib (25nM), or a combination of both. The values are normalized to untreated cells (DMSO) and represent a mean and standard deviation of three independent experiments. **C)** Cell viability assessment using MTT displaying proliferation changes of BRCA1-proficient (sgNT) and deficient (BRCA1ko1 and BRCA1ko2) MDA-MB-231 cells after single-drug (TH5487 3.75 µM or olaparib 0.5 µM) or combined treatments for 72 hours. Bars show the mean and the SEM of six replicates from two independent plates. Unpaired t-tests were used in (B) and (C).

Finally, we aimed to a gain better understanding of the molecular mechanisms behind the synthetic lethal interaction found between OGG1 and BRCA1. The widely accepted model for the well-characterized synthetic lethality caused by PARP inhibition in BRCA1-deficient cells is that PARP inhibition results in an increase in SSBs. These lesions are processed into DSBs during DNA replication being particularly cytotoxic in BRCA1-deficient cells owing to their reduced capacity for DSB repair (Farmer et al., 2005). We hypothesized that the inhibition of OGG1 can promote the accumulation of oxidative DNA lesions that may progress to SSB, and similarly to PARP inhibition, triggering genomic instability which lethal consequences in BRCA1-deficient cells. To analyse this premise, we assessed by high-throughput microscopy the pan-nuclear phosphorylated H2AX (γH2AX) staining as a commonly used indicator of DSBs (Burma et al., 2001) and replication stress (Ward and Chen, 2001), in MDA-MB-231 BRCA1-proficient and deficient cells.

BRCA1-KO clones showed a significantly higher level of mean γH2AX signal intensity as well as a higher percentage of γH2AX positive cancer cells (**Figure 28**), reflecting that BRCA1-deficient cells accumulate more DNA damage than control cells even under basal conditions. Next, we incubated MDA-MB-231 cells with the already determined sublethal concentrations of olaparib and TH5487 for 72 hours. Interestingly, TH5487 treatment increases the mean γH2AX signal intensity in both BRCA1-proficient and deficient cells, but the level of DNA damage was significantly more elevated in the BRCA1-KO clones, suggesting that OGG1 inhibition induces DSBs especially in the context of BRCA1 deficiency. As expected, the treatment with olaparib also increases the γH2AX signal, particularly for BRCA1-KO cells. Finally, we assessed the molecular consequences caused by the synergistic interaction between olaparib and TH5487. The combined treatment generates higher γH2AX signal intensity values than single-drug treatments both in BRCA1-proficient and deficient cells, indicating that OGG1 inhibition intensifies the accumulation of DNA damage caused by the treatment with olaparib. Furthermore, the effect on DNA damage attributed to the combined treatment was significantly more pronounced in BRCA1-deficient clones (**Figure 28**). This suggests that the impact on cell viability of PARP inhibition enhanced by TH5487 in BRCA1-deficient cells can be at least partially due to the accumulation of DNA damage resulting in selective cell death.

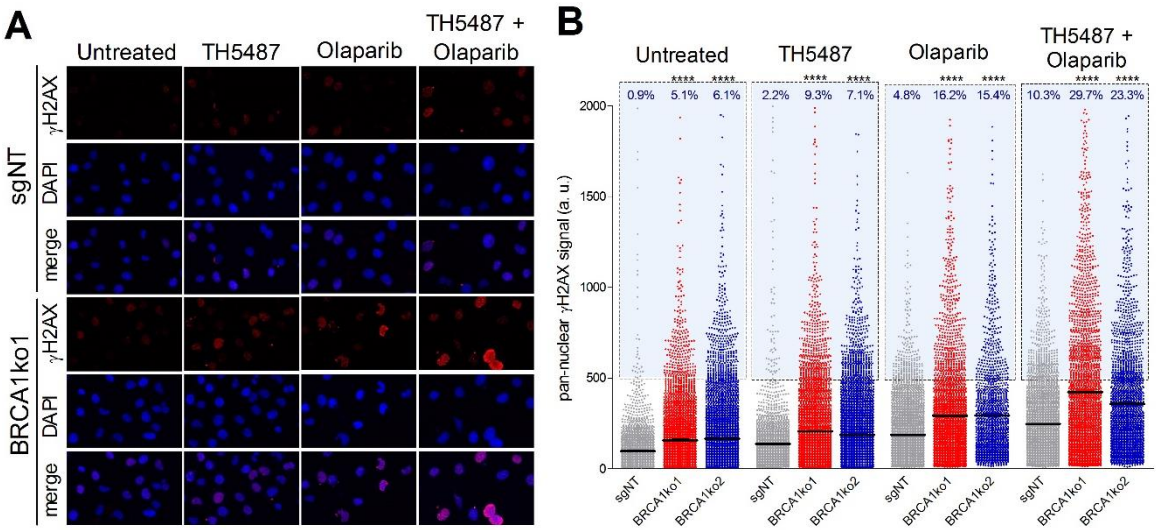

Figure 28 – Effect of OGG1 and PARP inhibitors on the level of DNA damage. A) Immunofluorescent staining of γH2AX. A representative confocal image example of one of three independent experiments is shown for control (sgNT) and BRCA1ko1 cells for each treatment condition. Cells were stained for γH2AX (red) and DAPI (blue) was used to stain cell nucleus. **B)** Pan-nuclear γH2AX signals of BRCA1-proficient (sgNT) and deficient (BRCA1ko1 and BRCA1ko2) MDA-MB-231 cells exposed to TH5487 (5 µM), olaparib (25nM), or a combination of both. Each dot represents the signal from one cell, horizontal lines indicate mean values, and the blue area delineates cells above an arbitrarily chosen threshold. Each condition incluides at least 2000 cells from 3 independent experiments. Statistical significance was determined by Mann-Whitney U test.

DISCUSSION

1. Clarifying by functional analyses the cancer risk modifier effect of SNPs in glycosylase genes in *BRCA1* and *BRCA2* mutation carriers.

Carrying an inherited mutation in the tumor suppressor genes *BRCA1* or *BRCA2* significantly increases individual´s lifetime risk to develop breast, ovarian and other cancers (Milne et al., 2008; Kuchenbaecker, Hopper, et al., 2017). Nevertheless, there is high variability in disease manifestation as consequence of environmental and genetic factors that can modify cancer risk (Friebel et al., 2014; Milne and Antoniou, 2016). Among other functions, the *BRCA* genes participate in the repair of DSBs by homologous recombination (Patel et al., 1998; Moynahan et al., 1990). As consequence, the cells which harbour pathogenic mutations in these genes are critically dependent on other DNA repair mechanisms (Gorodetska et al., 2019). In particular, a well-known synthetic lethal interaction was identified between *BRCA1* and *BRCA2* and *PARP1*, involved in the BER pathway (Bryant et al., 2005; Farmer et al., 2005).

Considering all this, it was proposed that genetic variation associated with impaired BER might thus increase breast or ovarian cancer risk (Osorio et al., 2011). In fact, several studies found some variants in BER which might affect breast cancer susceptibility (Roberts et al., 2011; Popanda et al., 2013). However, these studies were performed excluding HBOC cases. On the contrary, our research group carried out a candidate gene study focused on the BER genes to search for SNPs associated with cancer risk in *BRCA1/2* mutation carriers (Osorio et al., 2014). These analyses were carried out with the CIMBA series comprising 15,252 *BRCA1* and 8,211 *BRCA2* mutation carriers. As a result, were identified 11 candidate SNPs that were significantly associated ($p<0.05$) with breast and/or ovarian cancer. Interestingly, the three SNPs for which strongest evidence of association was detected were located in DNA glycosylase genes: rs2304277 in the *OGG1* gene, associated with ovarian cancer risk in *BRCA1* mutation carriers, rs804271 in the *NEIL2* gene, associated with breast cancer risk in *BRCA2* mutation carriers, and rs34259 in the *UNG* gene, associated with ovarian cancer risk in *BRCA2* mutation carriers (Osorio et al., 2014).

To our knowledge, only rs34259 had been previously studied as a potential candidate to alter the risk of developing breast (Marian et al., 2011) or lung cancer (Doherty et al., 2013). However, the *UNG* rs34259 association with cancer susceptibility was not confirmed in any of the studies. Moreover, the association of this SNP with ovarian cancer risk in *BRCA2* mutation carriers was initially interpreted with caution because the number of *BRCA2* carriers affected with ovarian cancer included in the series was four-fold lower than for *BRCA1* carriers. Therefore, the statistical power was more limited, which increased the probability of false-positives (Osorio et al., 2014). Nevertheless, the associations of the three glycosylase SNPs with cancer risk were later confirmed

in a different series of *BRCA1/2* mutation carriers from the OncoArray Consortium (Amos et al., 2017; Baquero et al., 2019).

Subsequently, our group proposed to carry out functional studies regarding these SNPs in order to validate their role as cancer risk modifiers. The SNP in *OGG1* has already been studied (Benitez-Buelga et al., 2016). This work reported that the cancer risk modifier effect of this variant could be due to the transcriptional down-regulation of *OGG1* associated with the SNP, which may exert a synergistic effect together with *BRCA1* or *BRCA2* mutations on DSBs generation and telomere instability. Nevertheless, the rest of the cancer risk modifiers SNPs discovered were lacking of functional validation. In the first part of the thesis, we aimed to gain a better understanding of the molecular basis of the cancer risk modifier effect in the context of *BRCA2* deficiency, exerted by the other two SNPs located in the glycosylase genes *NEIL2* and *UNG*. To this end, we studied the role of these polymorphisms in mRNA or protein expression, DNA damage accumulation, oxidative stress susceptibility, and TL regulation. These functional analyses were mainly performed in PBMCs from a collected FBOC series composed of *BRCA1* and *BRCA2* pathogenic mutation carriers, BRCAX cases, and controls. Additionally, a panel of LCLs derived from *BRCA1* patients and non-carriers relative controls, and a set of prophylactic oophorectomies from *BRCA1* and *BRCA2* mutation carriers were included as complementary series to validate some findings.

Given that both SNPs are located in regulatory regions and no better functional candidates in linkage disequilibrium were found, we first focused on the evaluation of their impact on expression levels of their corresponding genes. We found consistent results for the two SNPs in the FBOC series: the presence of the rs804271 is associated with *NEIL2* up-regulation, and the rs34259 is associated with *UNG* transcriptional down-regulation. However, we can not completely discard that these SNPs might be in linkage disequilibrium with other functional SNPs in the coding region of the genes, which could result in alterations in the function of their corresponding glycosylases.

The rs804271 is located 5' of the coding region of the *NEIL2* gene, within a strong positive regulatory domain of the *NEIL2* promoter (Kinslow et al., 2010). In line with our results, other formerly characterized SNPs located in this region have functional effects on *NEIL2* transcription (Kinslow et al., 2008), supporting that the rs804271 is associated with constitutive transcriptional activation of *NEIL2*. Besides, it was reported that genetic variations in the *NEIL2* promoter region can significantly alter the transcriptional response to OS (Kinslow et al., 2010).

On the other hand, the *UNG* variant rs34259 is located in the 3'UTR of the gene, into a region considered as a potential seed site for multiple human microRNAs (Hegre et al., 2013). These microRNAs down-regulate *UNG* expression by cleavage, degradation, or translational repression

(Lim et al., 2005; Djuranovic et al., 2012). Therefore, the presence of this SNP could modulate the interaction between miRNAs and *UNG* mRNA, which may explain the down-regulation of *UNG* associated with the SNP.

The cancer risk modifier effect of these SNPs is circumscribed to a particular cancer type (breast or ovarian). This could be due to the restricted statistical power because of the limited sample size (mainly for ovarian cancer and *BRCA2* mutation carriers) or, the fact that the effect sizes associated with the SNPs are relatively small (hazard ratio per copy of the minor allele <1.5). On the contrary, it also possible that the SNPs modulate in a tissue-specific manner gene expression. Indeed, *in silico* analyses with the GTEx data identified rs80427 and rs34259 as trans eQTL SNPs that modify *NEIL2* and *UNG* expression, respectively, in many different human tissues. However, there were notable differences in the impact of the SNPs between tissues. In particular, the two SNPs are classified as eQTLs in blood, the tissue from which the samples of the FBOC series were obtained. Besides, the rs804271 was significantly associated with increased *NEIL2* mRNA levels in breast, where the cancer risk modifier effect of this variant was found. Nevertheless, the rs34259 was not identified in GTEx as an eQTL SNP in ovarian tissue, likely due to the lower sample size analysed compared with blood (167 vs 670). Indeed, this SNP was associated with lower *UNG* mRNA expression in our series of prophylactic oophorectomies from *BRCA1/2* mutation carriers, but not in the panel of LCLs, supporting that the intensity of the SNP effect on transcriptional regulation could be tissue-specific.

The SNPs of DNA glycosylases that modulate expression levels may significantly impact the DNA repair capacity of the BER pathway, promote genomic instability, and contribute to the risk of disease (D'Errico et al., 2016). Interestingly, the cancer risk modifier effect of the two analysed variants is related to the regulation of gene expression likewise: the rs804271 increases *NEIL2* expression and breast cancer risk, while the rs34259 which decreases *UNG* expression exerts a protective effect for ovarian cancer. These results suggest that the over-expression of glycosylases, and not their down-regulation, may be deleterious and responsible for the increased or decreased cancer risk of the *NEIL2* and *UNG* SNPs, respectively.

Supporting this hypothesis, the rs804270, which is in high linkage disequilibrium (r^2=0.98) with the rs804271 and also upregulates *NEIL2* expression, has been found significantly associated to the increased susceptibility of gastric cancer (Elingarami et al., 2015) and cervical carcinoma (Ye et al., 2020). Moreover, it has been reported that *NEIL2* is commonly over-expressed in esophageal adenocarcinoma tumors (Goh et al., 2011), and those tumors with copy number gains of the *NEIL2* gene are associated with significant poor prognosis (Frankel et al., 2014). On the other side, triple

knock-out NEIL-deficient mice (*Neil1*$^{-/-}$ /*Neil2*$^{-/-}$ /*Neil3*$^{-/-}$) do not accumulate higher levels of oxidative DNA damage compared to WT mice and are not prone to cancer (Rolseth et al., 2017).

In the same line, it has been reported that *UNG* is upregulated in hepatocellular carcinoma tumors (Liu et al., 2019), or in small cell lung cancer and prostate adenocarcinoma tumoral cell lines (Vural et al., 2018). On the other hand, it has been shown that overexpression of human UNG in yeast induces DNA damage due to the generation of AP sites faster than they can be repaired (Elder et al., 2003), which could explain the deleterious effect of UNG overexpression. Therefore, considering also that uracil removal is the major rate-limiting step of BER (Visnes et al., 2008), the lower *UNG* expression associated with the rs34259 could prevent AP repair from becoming saturated, helping to explain the protective effect of this variant. In accordance with this idea, it has been shown that when cells are exposed to higher genotoxic stress, the tumor suppressor p53 decreases the expression level of *APE1*, which catalyzes the next BER step, (Poletto et al., 2016). This prevents the accumulation of additional SSB, giving the cell time to properly repair the DNA damage (Whitaker et al., 2017). Complementarily, an alternative consequence of glycosylase overexpression could be the loss of its substrate specificity (Zharkov et al., 2010), and consequently cause an accumulation of base lesions.

A different hypothesis postulates that increased *NEIL2* or *UNG* expression may contribute to mutagenesis through APOBEC3B regulation. APOBEC3B is a cytidine deaminase that is overexpressed in multiple cancer types, representing a key molecular driver inducing mutations by converting DNA cytosines to uracils (Zou et al., 2017). Surprisingly, it has been reported a positive correlation between APOBEC3B and *UNG* expression levels in tumors (Serebrenik et al., 2019). Moreover, it has been recently demonstrated that elevated expression of *NEIL2* in breast cancer cell lines facilitates APOBEC3B-mediated mutations and induces DSBs (Shen et al., 2020). Thereby, the cancer-protective effect linked to lower *UNG* expression or the increased risk associated with *NEIL2* overexpression could be indirectly due to their effect on APOBEC3B expression.

To evaluate whether these SNPs could alter glycosylase activity, we measured the accumulation of the lesions recognized by NEIL2 (oxidized bases) and UNG (uracil) at the telomeres. We decided to analyse this region because the telomeric DNA is especially susceptible to oxidation or uracil accumulation (Vallabhaneni et al., 2015; Barnes et al., 2019). Interestingly, *BRCA2* mutation carriers harbouring the rs804271 or the rs34259, present respectively higher DNA oxidation or lower uracil levels at their telomeres. This suggests that rs34259 might have a positive impact on UNG enzyme performance that could contribute to explain the protective effect of this SNP in *BRCA2* mutation carriers. Moreover, we found that the SNP impact on *UNG* expression also affects the mitochondrial

isoform (UNG1). Considering this, we cannot rule out that, apart from the telomeric DNA, the mitochondrial DNA of the carriers of this variant presents lower uracil levels, given that these lesions are repaired by UNG1 in the mitochondria (Akbari et al., 2007).

The accumulation of oxidative lesions could be particularly deleterious for BRCA1 or BRCA2-deficient cells, which are particularly sensitive to oxidative stress (Fridlich et al., 2015). In fact, *BRCA1* participates in OS regulation and its overexpression confers resistance while its deficiency increases the sensitivity to oxidizing agents (Bae et al., 2004; Yi et al., 2014). Consequently, it has been proposed that the tissue specificity of the cancer risk for *BRCA1/2* mutation carriers could be due to the elevated level of OS caused by hormonally regulated metabolism which the mammary and ovarian tissue are exposed (Malins et al., 1993; Gorrini, Baniasadi, et al., 2013; Fridlich et al., 2015). Indeed, BRCA1 and BRCA2 are both required for the transcription-coupled repair of the oxidative DNA lesions (Le Page et al., 2000). Therefore, these previous findings would contribute to explain why the cancer risk modification due to the SNPs would only be detected in the context of *BRCA2* mutation carriers and not in the general population.

Induction of ROS and OS conditions are involved in the pathogenesis of numerous chronic diseases, including cancer (Valko et al., 2006; Gill et al., 2016). To evaluate the relative levels of OS in the FBOC series, we measured protein carbonylation, a type of protein oxidation commonly used as a biomarker of chronic OS (Fedorova et al., 2013). We found lower protein oxidation in carriers of the rs34259, especially significant among the *BRCA2* patients. This association could be indicative of a lower chronic oxidative stress susceptibility and hence, may help to explain the lower cancer risk of *BRCA2* mutation carriers that harbour this SNP. However, this conclusion has some limitations because we did not have information for the possible existence of environmental factors, such as smoking, that have been linked to oxidative disturbances (Valavanidis et al., 2009).

Telomere length (TL) is regulated by shelterin-telomerase coordination. On the one hand, telomerase adds TTAGGG repeats to the chromosome ends, elongating the telomeres. Besides, the shelterin binding blocks the telomere lengthening by the telomerase (Hockemeyer and Collins, 2015). As expected, we observed a positive correlation between TL and telomerase activity in the FBOC series. Interestingly, we found a significantly shorter TL associated with the *UNG* SNP for *BRCA2* mutations carriers. The SNP effect on TL could be indirectly due to the lower accumulation of base lesions in the telomeric DNA, which can modulate telomere length (Wang et al., 2010). In particular, it has been reported that uracil accumulation in telomeric DNA weakens the binding affinity of the shelterin component POT1, increasing the accessibility of telomerase (Vallabhaneni et al., 2015). Besides, UNG deficienct mice show impair uracil removal that leads to telomere

lengthening (Vallabhaneni et al., 2015). Thus, according to this model, the shorter telomeres observed for the *BRCA2* mutation carriers harbouring the SNP could be explained by the lower uracil accumulation at their DNA which promotes shelterin binding and preventing telomerase from accessing and elongating the telomeres. Furthermore, a Mendelian randomization study shown that increased telomere length due to germline genetic variation is associated with an increased risk of ovarian serous tumors of low malignant potential (Haycock et al., 2017). This finding is consistent with the association between the short telomeres phenotype and the cancer-risk protective effect of the *UNG* SNP for *BRCA2* mutation carriers.

Overall, the results presented in this part of the thesis help to explain the association of these SNPs with cancer risk in *BRCA2* mutation carriers, mainly due to their impact on glycosylase expression, DNA damage levels, and telomere integrity. These findings highlight the importance of genetic changes in glycosylase genes as modifiers of cancer susceptibility for *BRCA1* and *BRCA2* mutation carriers. Consequently, the inclusion of the studied SNPs to generate more informative polygenic risk scores could improve screening and prevention strategies for breast and ovarian cancer.

2. OGG1 dysfunction blocks oxidative DNA damage repair at telomeres triggering genome instability

The majority of cancers maintain stable telomere length, which confers cell immortality (Srinivas et al., 2020). Therefore, telomeres and telomerase-based therapies are emerging as prospective cancer treatment strategies (Ivancich et al., 2017; Chow et al., 2018). Besides, telomere attrition is influenced by oxidative damage given that telomeric DNA represents a preferential target for suffering OS (Von Zglinicki, 2002). Consequently, telomeres are prone to accumulate 8-oxoG lesions, which are mainly removed by OGG1 (Rhee et al., 2011). In fact, several studies suggest that BER is critical for preserving telomeres, especially under elevated OS conditions (Fouquerel, Parikh, et al., 2016). Moreover, in the first part of this thesis we have shown that genetic variation in glycosylase genes can alter the levels of telomeric DNA damage, reflecting the importance of BER at the telomeres.

Taking into consideration all this information, we hypothesized that BER inhibitors could be employed as a tool to induce oxidative DNA damage at telomeres with potential implications for cancer treatment. To explore this hypothesis, we established a collaboration with the Thomas Helleday laboratory (Karolinska Institutet, Stockholm) where a specific small molecule inhibitor of OGG1 (TH5487) has recently been developed (Visnes, Cázares-Körner, et al., 2018). First, we selected the U2OS osteosarcoma cell line to generate OGG1-GFP cells which were used to

characterize the role of OGG1 at the telomeres at basal or upon OS conditions. Then, we treated the cells with the TH5487 and, in parallel, we generated a knockout for the *OGG1* gene to analyse the telomere and cellular defects associated with OGG1 dysfunction.

In line with previous studies (Rhee et al., 2011), we have found that telomeres are more prone to accumulate oxidative DNA damage than other genome regions, even in basal conditions. In comparison to the other evaluated regions, the *36B4* locus and the *MT-TF* mitochondrial gene, telomeric DNA harbours a relatively higher oxidative DNA damage. Transcriptionally active DNA is particularly subjected to the action of the DNA repair machinery (Marnef et al., 2017), which might explain the lowest amount of lesions found in the *36B4* locus. On the other hand, the relatively high DNA oxidation found in the mitochondrial gene could be caused by the prominent generation of ROS in the mitochondria (Balaban et al., 2005).

Moreover, when we measured the relative amount of oxidative lesions along the cell cycle, we obtained a differential accumulation among the phases, including a peak during the S phase. This finding could be explained by the dynamical changes of the telomeres throughout the cell cycle between the euchromatic and heterochromatic states (Ichikawa et al., 2015; Tardat and Déjardin, 2018). Usually, human telomeres are condensed heterochromatin structures concealing chromosome ends from repairing enzymes, preventing OGG1 accessibility to its substrate (Odell et al., 2013). However, telomere structure changes to an open or unprotected conformation in the S phase, enabling controlled access to DNA replication factors (Galati et al., 2013), and the recruitment of DNA damage factors during the G2 phase (Verdun et al., 2005). In consequence, the high accumulation of oxidative base lesions found during the S phase could be due to the unprotected status of these telomeres. Besides, the significant decrease in the amount of lesions found in the G2 phase would be attributed to the repair of telomeric DNA during S/G2 phases.

Further, we aimed to study BER at telomeres upon OS conditions. We performed an effective oxidative treatment that increases oxidized bases at telomeric DNA. OGG1 protein levels did not increase in response to OS, and also remained constant throughout the cell cycle, reflecting that OGG1 expression is not cell-cycle regulated, or induced by oxidative DNA damage, in accordance with earlier reports (Dhénaut et al., 2000; Mjelle et al., 2015). However, we observed by IF that oxidative DNA damage accumulation at telomeres promotes the recruitment of BER enzymes in these regions in order to repair local oxidative DNA damage (Amouroux et al., 2010).

It has been previously reported that prolonged treatments with the OGG1 inhibitor TH5487 do not increase genomic 8-oxoG global levels (Visnes, Cázares-Körner, et al., 2018). Nevertheless, since guanine nucleobase is enriched at promoters, UTR regions, or telomeres, these specific regions

would represent a hotspot for 8-oxoG detection after OGG1 inhibition (Pan et al., 2016; Ding et al., 2017). In fact, we have found that TH5487 causes a progressive accumulation of oxidized bases at telomeric DNA and blocks their repair by BER, supporting the consideration of the telomeres as a hotspot for oxidation (Ahmed and Lingner, 2018; Barnes et al., 2019). We also detected the increase in oxidized base levels in telomeric DNA in *OGG1* knockout human cancer cells as a consequence of OGG1 ablation, a result previously described in yeast (Lu and Liu, 2010) and mice (Wang et al., 2010). These findings validate the OGG1 inhibitor as a potential tool to induce persistent DNA damage at the telomeres in BER-proficient cells.

Persistent oxidative lesions at telomeric DNA induced by OS conditions lead to telomere dysfunction and chromosome instability (Coluzzi et al., 2014). Moreover, it has been recently shown that chronic OS conditions lead to genome instability through a telomere crisis-driven mechanism in OGG1-KO cells (Fouquerel et al., 2019). In this respect, we evaluate whether TH5487 treatment triggers a similar phenomenon. We found that cells lacking OGG1 or treated with TH5487 shown a significant increase in telomere losses and micronuclei formation, a hallmark of mitotic failure. These results are consistent with the phenotypes previously reported in OGG1 depleted cells and reflect the potential of OGG1 inhibition to induce telomere losses and micronucleus formation, evidencing the critical importance of BER to maintain telomere stability upon OS.

OGG1 plays an essential role in protecting cells against apoptosis induced by OS (Youn et al., 2007; Oka et al., 2008). In this regard, the telomeric defects that we report caused by OGG1 inhibition or depletion could contribute to understanding the molecular mechanisms that lead to cell death upon oxidative treatment. Ultimately, we evaluated whether these cellular defects caused by OGG1 inhibition or depletion could compromise cell viability. We reported that OGG1 dysfunction is associated with a mild impact on proliferation. It has been recently found that OGG1-initiated BER can lead to PARP1 overactivation (Wang et al., 2018). The hyperactivation of PARP1 mediates parthanatos, a caspase-independent cell death induced in response to extreme genomic stress (Yu et al., 2002). Consequently, cells lacking OGG1 showed increased resistance to OS induced parthanatos (Wang et al., 2018). Therefore, this fact may explain the limited effect on cell proliferation caused by OGG1 dysfunction that we found.

Additionally, the mild impact on proliferation associated with OGG1 inactivation could be attributed to the action of other active glycosylases. Apart from OGG1, in human cells, another five DNA glycosylases are implicated in the repair of oxidative DNA damage (Krokan and Bjøra, 2013). Regarding the potential complementary role of other glycosylases at the telomeres, NEIL3 has been reported to have an active role in this region along with OGG1 (Zhou et al., 2015) and its loss also

leads to telomere dysfunction and mitotic defects (Zhou et al., 2017). Particularly, NEIL3 is active in the telomeric overhang or the D-loop structure, where OGG1 cannot remove 8-oxoG (Zhou et al., 2013). In this regard, it has been recently published that although 8-oxoG is an epigenetic signal upregulating *NEIL3* gene expression, in OGG1-KO cells this upregulation is lost (Fleming et al., 2019). Hence, we should not rule out that telomere phenotypes reported in U2OS OGG1-KO cells could be partially consequence of *NEIL3* downregulation.

The generation of deficient mice for almost all glycosylase genes is compatible with life (Sampath, 2014). *OGG1* knockout mice harbour extensive accumulation of oxidative DNA damage but do not show apparent pathological changes (Minowa et al., 2000; Arai et al., 2006). On the contrary, the homozygous deletion of the core enzymes of BER (APE1, XRCC1, LIG1, and POL β) leads to lethality during embryogenesis in mice (Wilson and Thompson, 1997; Brenerman et al., 2014). This is because every step of BER generates intermediates (AP sites, 5'-dRP residues, and SSBs), which are both mutagenic and toxic to cells, whereas, the existence of oxidized bases is tolerable (Boiteux and Guillet, 2004; Kidane et al., 2014). Thus, inhibitors against the core component of BER may generate more severe telomere defects that could promote a telomere-driven crisis. In support, APE1 has been reported as an essential factor stabilizing telomeric DNA, and its deficiency causes telomere dysfunction, including multi-telomeric signals, telomere losses, chromosome end fragmentation, and chromosome fusions in U2OS cells (Madlener et al., 2013). Moreover, a previous study presented that the treatment with PARP inhibitors impairs telomere integrity in, inducing replicative and preventing cancer cells to escape from a telomere crisis (Ngo et al., 2018). In this regard, pharmacological inhibition of OGG1 to induce telomere instability might be especially relevant for combination therapies with other drugs, such as different BER inhibitors, as new anticancer drug regimens.

To summarize this second part, we have shown that OGG1-initiated BER is essential to maintain telomere integrity. The treatment with the OGG1 inhibitor TH5487 increases oxidative DNA damage accumulation in the telomeres, leading to telomere loss and post-mitotic defects (illustrated in **Figure 29**). These results recapitulate the phenotype previously reported in OGG1-KO cells (Fouquerel et al., 2019), reflecting the high selectivity of TH5487. In conclusion, our data not only illustrate the importance of BER in DNA oxidative DNA damage repair at telomeres but also show the effective use of OGG1 inhibitor TH5487 to induce telomere instability and proliferation defects, with potential implications in cancer treatment.

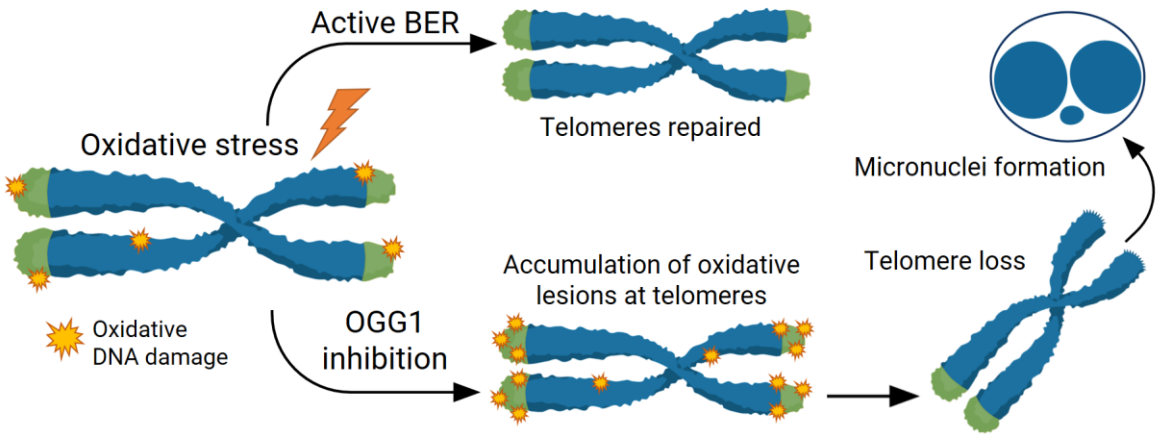

Figure 29 - A model for TH5487 mechanism of action at telomeres. Schematic representation of the oxidative DNA repair by BER and the cellular defects associated with OGG1 inhibition: accumulation of oxidative base lesions, telomere losses and micronuclei formation.

3. OGG1 inhibition triggers synthetic lethality and synergizes with the PARP inhibitor olaparib in BRCA1-deficient TNBC cells

The high ROS levels in cancer cells are balanced by their increased antioxidant capacity allowing tumorigenesis (Diehn et al., 2009). Hence, OS modulation in tumoral cells represents a potential anticancer strategy (Gorrini, Harris, et al., 2013). In this regard, targeting the hydrolase MTH1 has been proposed for anticancer therapy by sensitizing tumoral cells to endogenous OS (Gad et al., 2014). MTH1 sanitized the dNTP pool from 8-oxoGTP, preventing the incorporation of oxidized bases into replicating DNA. Initial studies using MTH1 inhibitors found that these molecules caused cytotoxicity in cancer cells (Gad et al., 2014; Huber et al., 2014). However, subsequent studies have shown that MTH1 is dispensable for cancer cell survival (Ellermann et al., 2017). It has been suggested that cancer cell death is triggered by the accumulation of oxidative base lesions, and, consequently, the lack of efficiency of MTH1 inhibitors is explained by their inability to introduce oxidized nucleotides into DNA (Berglund et al., 2016). This finding implies that targeting the glycosylases responsible for removing oxidized bases can be an interesting alternative or complementary strategy to MTH1 inhibition. Nonetheless, due to the low impact on cancer cell proliferation associated with OGG1 inhibition that we had observed (discussed in the previous section), we hypothesized that OGG1 inhibition could be particularly deleterious for those cancers extremely sensitive to OS. Considering that BRCA1 protects cells against OS (Fridlich et al., 2015), and the synthetic lethality that exists between the component of the BER pathway, *PARP1*, and *BRCA1*, we decided to use the novel OGG1 inhibitor TH5487 specifically in the context of *BRCA1* deficiency to study the potential synthetic lethality relationship between these two genes.

The dependence on compensatory repair pathways in cancer cells can be exploited as a therapeutic strategy in cancer therapy (Kelley et al., 2014). As previously mentioned, the synthetic lethal interaction between *BRCA1* and *BRCA2* with *PARP1* has led to the current use of several PARP inhibitors (PARPi) in the clinic, mainly for breast or ovarian cancers harbouring *BRCA1/2* germline mutations (Lord and Ashworth, 2017; Mateo et al., 2019). However, there are still unresolved concerns about the safety of long term PARPi (Yap and Sandhu, 2011). *BRCA* mutated tumors frequently acquire resistance to PARPi through multiple mechanisms (D'Andrea, 2018), and the clinical use of PARPi in combination with conventional doses of chemotherapy regimen is limited by the more-than-additive cytotoxicity (Dréan et al., 2016). Besides, given that most cancers are HR-proficient, the clinical potential of PARPi as monotherapy is very limited (Wang et al., 2020).

In view of the above, the identification of additional synthetic lethal partners of *BRCA* genes represents an emerging field, and the BER members are considered as potential candidates (Visnes, Grube, et al., 2018). In fact, it has been reported that APE1 inhibitors are synthetically lethal in BRCA1-deficient cells (Sultana et al., 2012). Nevertheless, bearing in mind that knockout mice for Ape1 are embryonic lethal, it has been suggested that the treatment with APE1 inhibitors might cause unforeseen on-target toxicities in normal tissues (Visnes, Grube, et al., 2018). On the contrary, since the deficiency of individual DNA glycosylases are relatively well-tolerated, these enzymes may be more promising candidates for drug development. In this regard, the results presented in this thesis provide the first evidence that OGG1 inhibition is a promising new synthetic lethality strategy in BRCA1-deficient cells.

A previous publication reported that BRCA1 does not regulate OGG1 incision activity, but indirectly stimulates early BER steps by transcriptional activation in different breast cancer cell lines (Saha et al., 2010). However, we did not find differences in *OGG1* mRNA expression between BRCA1-proficient and deficient MDA-MB-231 cells. This result rules out the possibility that the higher sensitivity to OGG1 inhibition in BRCA1-deficient cells was explained as a result of basal differences in OGG1 activity when BRCA1 is silenced. The dysregulation of redox homeostasis might be a more reasonable explanation for this synthetic lethality. Several reports, together with the results presented in the second part of this thesis, showed that the most direct consequence of OGG1 inhibition or depletion is the accumulation of oxidative DNA damage (Minowa et al., 2000; Arai et al., 2006). This accumulation of 8-oxoG is highly mutagenic (Ohno et al., 2014) and triggers distinct pathways of cell death (Oka et al., 2008). Thus, considering that both OGG1 and BRCA1 contribute to reducing intracellular OS (Saha et al., 2009), we hypothesized that OGG1 inhibition might generate more elevated ROS levels than BRCA1-deficient cells can handle. However,

differences regarding ROS levels between BRCA1-proficient and deficient cells should be subsequently evaluated.

OGG1 knockout and TH5487 treatment induce alterations in the expression of multiple genes, evidencing that OGG1 acts as a modulator of gene expression (Visnes, Cázares-Körner, et al., 2018). Therefore, apart from lead to excessive ROS accumulation, OGG1 inhibition could decrease the expression of certain essential genes for BRCA1-deficient cells survival. Interestingly, OGG1 binds to PARP1, stimulating its poly ADP-ribosylation activity and OGG1 knockout cells show decreased polyADP-ribose levels compared with wild type cells (Hooten et al., 2011). Hence, the severe effects of OGG1 inhibition in the context of *BRCA1* deficiency may result from indirect PARP1 inhibition. Complementary, it would also be interesting to evaluate the potential synthetic lethality between *OGG1* and *BRCA2*, given that BRCA2-deficient cells are also highly sensitive to PARP inhibition (Bryant et al., 2005). In fact, preclinical studies raise the possibility that BRCA2-knockout cells respond even better to PARP inhibition than BRCA1-deficient cells (Farmer et al., 2005; Turner et al., 2008).

Taking into consideration both synthetic lethal interactions of *BRCA1* with *PARP1* and *OGG1*, we combined PARP1 (olaparib) and OGG1 (TH5487) inhibitors to study is possible synergistic effects on BRCA1-deficient cells. We found that only for the *BRCA1*-knockout clones the combined treatment significantly decreases cell viability and the clonogenic potential compared to single-drug treatments. This finding could open new therapeutical opportunities for the treatment of HBOC. OGG1 inhibition may represent a potential way to maximize the clinical effectiveness of PARPi, for instance, overcoming the resistance to PARP inhibition or the unacceptable toxicity frequently reported when PARPi are combined with conventional chemotherapies (Dréan et al., 2016; D'Andrea, 2018).

On the other hand, a recent publication suggests that OGG1 inhibition would mitigate the impact of PARPi by preventing the formation of SSBs which are processed into DSBs during DNA replication, being particularly cytotoxic for BRCA1-deficient cells (Giovannini et al., 2019). Nevertheless, our results showed that TH5487 -alone or combined with olaparib- increases γH2AX signal, reflecting the generation of DSB as a consequence of OGG1 inhibition, and thus supporting the impairment of DNA damage repair as the principal mechanism underlying the synergy between TH5487 and olaparib. In addition, our results are consistent with several studies that have shown that selective attenuation of BER by knockdown or inhibition of their components sensitizes cells to PARP inhibition (Ström et al., 2011; Orta et al., 2014). In particular, it has been described that the knockdown of *OGG1* conferred sensitivity to PARP1 inhibition (Alli et al., 2009; Hooten et al., 2011).

Apart from in combination therapies with PARPi, OGG1 inhibitors may be used in the clinic together with inhibitors against other BER members or components of the DDR. Despite the moderate success in the development of BER inhibitors to date (Visnes, Grube, et al., 2018), there have been described different molecules targeting DDR or BER proteins whose combination with OGG1 inhibitors may provide positive results. For example, the combination of OGG1 with MTH1 inhibitors would facilitate the incorporation of 8-oxoGTP into DNA (Gad et al., 2014), and could trigger a synergistic effect. On the other hand, 8-oxoG is highly susceptible to suffer further oxidation (Neeley and Essigmann, 2006), resulting in the generation of other oxidative lesions that are not substrate for OGG1 and then are repaired by the NEIL glycosylases (Hailer et al., 2005). Consequently, the use of the small molecule inhibitors of NEIL1 (Jacobs et al., 2013) could increase the accumulation of oxidative DNA damage, intensifying the effects of OGG1 inhibition.

Another complementary strategy for cancer treatment through OGG1 inhibition can be its use in combination with chemo- and radiotherapeutic agents to sensitize cancer cells to therapy-induced DNA damage. Interestingly, this approach has been proven successful with other DNA glycosylases. As two examples, *NEIL1*-deficient cancer cells have hypersensitivity to psoralen (Couvé-Privat et al., 2007) and *UNG* depletion enhances the sensitivity to pemetrexed (Weeks et al., 2014). Besides, the combination of BER inhibitors with chemotherapy can expand their use to HR-proficient cancers, as has been already shown for PARPi (Wang et al., 2020).

In conclusion to this part, we showed that non-toxic doses of TH5487 markedly synergized with the PARP inhibitor olaparib to result in synthetic lethality in BRCA1-deficient cells. These data provide the first evidence that OGG1 inhibition is a promising new synthetic lethality strategy for HBOC. However, future preclinical studies will be needed before bringing the OGG1 inhibitors to the clinic.

The overexpression of BER factors observed in various types of solid cancers might represent an adaptive survival response for cancer cell survival in the tumor microenvironment (Seo and Kinsella, 2009; Gavande et al., 2016). Along this thesis, we have provided several results in line with this scenario. First, we found that SNPs in glycosylase genes that modify cancer risk in *BRCA1/2* mutation carriers were associated with alterations in glycosylase expression levels. Next, we showed that OGG1 inhibition promotes telomere instability in cancer cells and triggers synthetic lethality in BRCA1-deficient tumoral cells, supporting the indispensable role of BER in mediating cancer progression. Therefore, genetic variants that regulate BER expression, such as the studied SNPs, not only could modify cancer risk, but also have an impact on the response to therapies involving BER inhibitors, as in the case of PARPi for HBOC. In short, our results evidence the future

potential of targeting the BER pathway for cancer treatment. A summary of the knowledge derived from this thesis is shown in **Figure 30**.

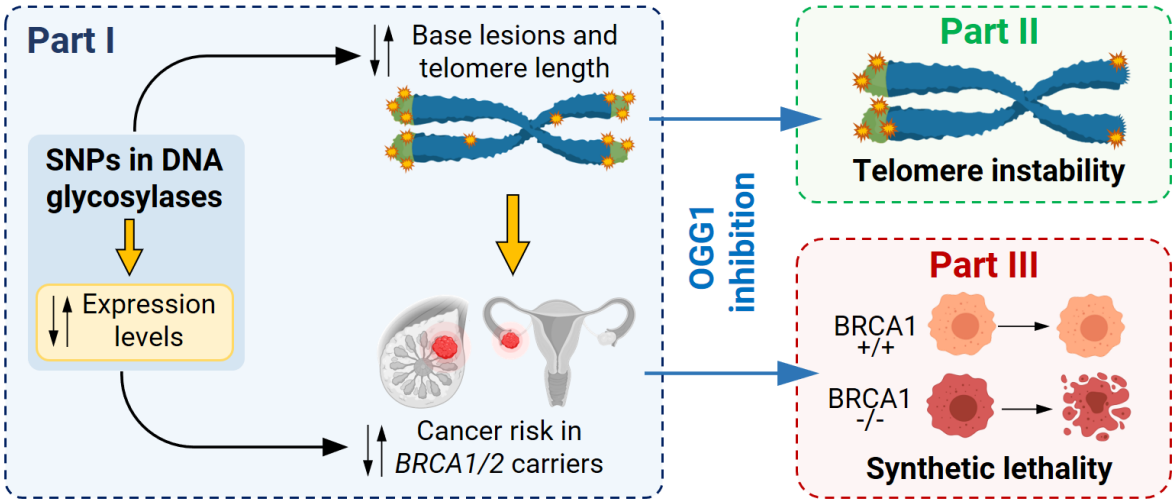

Figure 30 – Overview of the thesis. Schematic representation of the general conclusions regarding the three different part of this thesis.

CONCLUSIONS

1. The SNPs rs804271 and rs34259, located at regulatory regions of the *NEIL2* and *UNG* genes, respectively, represent functional variants that regulate the expression levels of their respective glycosylases. Our results highlight the molecular basis of the cancer risk modifier effect conferred by the studied variants for *BRCA2* mutation carriers. In particular, the overexpression of these glycosylases may be deleterious by being associated with an increase in the amount of telomeric DNA damage, which triggers telomere instability.

2. The OGG1-initiated base excision repair pathway plays an essential role in the maintenance of telomere integrity, especially under oxidative stress conditions. The inactivation of this pathway by the OGG1 inhibitor TH5487 increases the accumulation of oxidized bases at the telomeres, leading to telomere loss and post-mitotic defects. Consequently, pharmacological inhibition of OGG1 might be considered as a new tool to induce oxidative damage in the telomeric DNA of tumoral cells, with potential implications in cancer treatment.

3. The silencing of *BRCA1* in breast cancer cells increases their sensitivity to the OGG1 inhibitor TH5487, reflecting the possible synthetic lethal relationship between these genes. Furthermore, TH5487 enhances the activity of the PARP1 inhibitor olaparib on BRCA1-deficient cells. These preliminary results might represent the proof-of-concept for new alternative or complementary therapies for the treatment of hereditary breast and ovarian cancer.

.

CONCLUSIONES

1. Los SNPs rs804271 y rs34259, localizados en regiones reguladoras de los genes *NEIL2* y *UNG*, respectivamente, constituyen variantes funcionales que regulan los niveles de expresión de sus respectivas glicosilasas. Nuestros resultados ponen de manifiesto las bases moleculares del efecto modificador del riesgo de cancer atribuido a las variantes estudiadas para las portadoras de mutaciones en *BRCA2*. En particular, la sobreexpresión de estás glicosilasas podría resultar deletérea, al asociarse a un incremento en el nivel de daño en el ADN telomérico que desencadena inestabilidad telomérica.

2. La vía de reparación del ADN por escisión de bases, iniciada por la glicosilasa OGG1, ejerce un papel fundamental en el mantenimiento de la integridad telomérica, especialmente bajo condiciones de estrés oxidativo. La inactivación de esta vía mediante el inhibidor de OGG1 TH5487 aumenta la acumulación de bases oxidadas en los telómeros, conduciendo a pérdidas teloméricas y defectos post-mitóticos. En consecuencia, la inhibición farmacológica de OGG1 podría considerarse como una nueva herramienta para inducir daño oxidativo en el ADN telomérico de las células tumorales, con potenciales implicaciones en el tratamiento del cáncer.

3. El silenciamiento de *BRCA1* en celulas de cáncer de mama incrementa su sensibilidad frente al inhibidor de OGG1 TH5487, reflejando una posible relación de letalidad sintética entre ambos genes. Además, el inhibidor TH5487 potencia la acción del inhibidor de PARP1 olaparib sobre las células deficientes en BRCA1. Estos resultados preliminares podrían abrir la puerta hacia nuevas terapias alternativas o complementarias para el tratamiento del cáncer de mama y ovario hereditario.

REFERENCES

Ahmed, W., & Lingner, J. (2018). Impact of oxidative stress on telomere biology. *Differentiation*, *99*, 21–27. https://doi.org/10.1016/j.diff.2017.12.002

Akbari, M., Otterlei, M., & Krokan, H. E. (2007). Different organization of base excision repair of uracil in dna in nuclei and mitochondria and selective upregulation of mitochondrial uracil-dna glycosylase after oxidative stress. *Neuroscience*, *145,* 1201–1212. https://doi.org/10.1016/j.neuroscience.2006.10.010

Al-Attar, A., Gossage, L., Fareed, K. R., Shehata, M., Mohammed, M., Zaitoun, A. M., Madhusudan, S. (2010). Human apurinic/apyrimidinic endonuclease (APE1) is a prognostic factor in ovarian, gastro-oesophageal and pancreatico-biliary cancers. *British Journal of Cancer*, *102*(4), 704–709. https://doi.org/10.1038/sj.bjc.6605541

Aller, P., Ye, Y., Wallace, S. S., Burrows, C. J., & Doublié, S. (2010). Crystal structure of a replicative DNA polymerase bound to the oxidized guanine lesion guanidinohydantoin. *Biochemistry*, *49(*11), 2502–2509. https://doi.org/10.1021/bi902195p

Alli, E., & Ford, J. M. (2015). BRCA1: Beyond double-strand break repair. *DNA Repair*, *32,* 165–171. https://doi.org/10.1016/j.dnarep.2015.04.028

Alli, E., Sharma, V. B., Sunderesakumar, P., & Ford, J. M. (2009). Defective repair of oxidative DNA damage in triple-negative breast cancer confers sensitivity to inhibition of poly(ADP-ribose) polymerase. *Cancer Research*, *69*(8), 3589–3596. https://doi.org/10.1158/0008-5472.CAN-08-4016

Amente, S., Palo, G. Di, Scala, G., Castrignan, T., Gorini, F., Cocozza, S., Majello, B. (2019). Genome-wide mapping of 8-oxo-7 , 8-dihydro-2 -deoxyguanosine reveals accumulation of oxidatively-generated damage at DNA replication origins within transcribed long genes of mammalian cells. *Nucleic Acids Research, 47*(1), 221–236. https://doi.org/10.1093/nar/gky1152

Amos, C. I., Dennis, J., Wang, Z., Byun, J., Schumacher, F. R., Gayther, S. A., Easton, D. F. (2017). The oncoarray consortium: A network for understanding the genetic architecture of common cancers. *Cancer Epidemiology Biomarkers and Prevention*, *26*(1), 126–135. https://doi.org/10.1158/1055-9965.EPI-16-0106

Amos, W., Driscoll, E., & Hoffman, J. I. (2011). Candidate genes versus genome-wide associations: Which are better for detecting genetic susceptibility to infectious disease? *Proceedings of the Royal Society B: Biological Sciences*, *278*(1709), 1183–1188. https://doi.org/10.1098/rspb.2010.1920

Amouroux, R., Campalans, A., Epe, B., & Radicella, J. P. (2010). Oxidative stress triggers the preferential assembly of base excision repair complexes on open chromatin regions. *Nucleic Acids Research*, *38*(9), 2878–2890. https://doi.org/10.1093/nar/gkp1247

An, N., Fleming, A. M., White, H. S., & Burrows, C. J. (2015). Nanopore detection of 8-oxoguanine in the human telomere repeat sequence. *ACS Nano*, *9*(4), 4296–4307. https://doi.org/10.1021/acsnano.5b00722

Arai, T., Kelly, V. P., Minowa, O., Noda, T., & Nishimura, S. (2006). The study using wild-type and Ogg1 knockout mice exposed to potassium bromate shows no tumor induction despite an extensive accumulation of 8-hydroxyguanine in kidney DNA. *Toxicology*, *221*(2–3), 179–186. https://doi.org/10.1016/j.tox.2006.01.004

Ardlie, K. G., Deluca, D. S., Segre, A. V., Sullivan, T. J., Young, T. R., Gelfand, E. T., Dermitzakis, E. T. (2015). The Genotype-Tissue Expression (GTEx) pilot analysis: Multitissue gene regulation in humans. *Science*, *348*(6235), 648–660. https://doi.org/10.1126/science.1262110

Aviv, A., Anderson, J. J., & Shay, J. W. (2017). Mutations, Cancer and the Telomere Length Paradox. *Trends in Cancer*, *3*(4), 253–258. https://doi.org/10.1016/j.trecan.2017.02.005

Ba, X., & Boldogh, lstvan. (2018). 8-Oxoguanine DNA glycosylase 1: Beyond repair of the oxidatively modified base lesions. *Redox Biology*, *14*, 669–678. https://doi.org/10.1016/j.redox.2017.11.008

Bae, I., Fan, S., Meng, Q., Jeong, K. R., Hee, J. K., Hyo, J. K., Rosen, E. M. (2004). BRCA1 induces antioxidant gene expression and resistance to oxidative stress. *Cancer Research*, *64*(21), 7893–7909. https://doi.org/10.1158/0008-5472.CAN-04-1119

Bahcall, O. (2019). COGS project and design of the iCOGS array. *Nature Genetics*, 2011–2014. https://doi.org/10.1038/ngicogs.4

Balaban, R. S., Nemoto, S., & Finkel, T. (2005). Mitochondria, oxidants, and aging. *Cell*, *120*(4), 483–495. https://doi.org/10.1016/j.cell.2005.02.001

Baquero, J. M., Benítez-Buelga, C., Fernández, V., Urioste, M., García-Giménez, J. L., Perona, R., Benítez, R., Osorio, A. (2019). A common SNP in the UNG gene decreases ovarian cancer risk in BRCA2 mutation carriers. *Molecular Oncology*, *13*(5), 1110–1120. https://doi.org/10.1002/1878-0261.12470

Barnes, D. R., & Antoniou, A. C. (2012). Unravelling modifiers of breast and ovarian cancer risk for BRCA1 and BRCA2 mutation carriers: Update on genetic modifiers. *Journal of Internal Medicine*, *271*(4), 331–343. https://doi.org/10.1111/j.1365-2796.2011.02502.x

Barnes, R. P., Fouquerel, E., & Opresko, P. L. (2019). The impact of oxidative DNA damage and stress on telomere homeostasis. *Mechanisms of Ageing and Development*, *177*, 37–45. https://doi.org/10.1016/j.mad.2018.03.013

Beard, W. A., Horton, J. K., Prasad, R., & Wilson, S. H. (2019). Eukaryotic Base Excision Repair: New Approaches Shine Light on Mechanism. *Annual Review of Biochemistry*, *88*(1), 137–162. https://doi.org/10.1146/annurev-biochem-013118-111315

Benitez-Buelga, C., Sanchez-Barroso, L., Gallardo, M., Apellániz-Ruiz, M., Inglada-Pérez, L., Yanowski, K., Carrillo, J., García-Estébez, L., Calvo, I., Perona, R., Urioste, M., Osorio, A., Blasco, M. A., Rodríguez-Antona, C., Benitez, J. (2015). Impact of chemotherapy on telomere length in sporadic and familial breast cancer patients. *Breast Cancer Research and Treatment*, *149*(2), 385–394. https://doi.org/10.1007/s10549-014-3246-6

Benitez-Buelga, C., Vaclová, T., Ferreira, S., Urioste, M., Inglada-Perez, L., Soberón, N., Blasco, M. A., Osorio, A., Benitez, J. (2016). Molecular insights into the OGG1 gene, a cancer risk modifier in BRCA1 and BRCA2 mutations carriers. *Oncotarget*, *7*(18). https://doi.org/10.18632/oncotarget.8272

Berglund, U. W., Sanjiv, K., Gad, H., Kalderén, C., Koolmeister, T., Pham, T., Helleday, T. (2016). Validation and development of MTH1 inhibitors for treatment of cancer. *Annals of Oncology*, *27*(12), 2275–2283. https://doi.org/10.1093/annonc/mdw429

Blackburn, E. H. (2001). Switching and signaling at the telomere. *Cell*, *106*(6), 661–673. https://doi.org/10.1016/S0092-8674(01)00492-5

Blackburn, E. H., Epel, E. S., & Lin, J. (2015). Human telomere biology: A contributory and interactive factor in aging, disease risks, and protection. *Science, 350*(6265), 1193–1198. https://doi.org/10.1126/science.aab3389

Blasco, M. A. (2007). The epigenetic regulation of mammalian telomeres. *Nature Reviews Genetics*, *8*(4), 299–309. https://doi.org/10.1038/nrg2047

Bochum, S., Berger, S., & Martens, U. M. (2018). Olaparib. *Small Molecules in Oncology*, *211*, 217–233. https://doi.org/https://doi.org/10.1007/978-3-319-91442-8_15

Boiteux, S., & Guillet, M. (2004). Abasic sites in DNA: Repair and biological consequences in Saccharomyces cerevisiae. *DNA Repair*, *3*(1), 1–12. https://doi.org/10.1016/j.dnarep.2003.10.002

Bradbury, A. R., & Olopade, O. I. (2007). Genetic susceptibility to breast cancer. *Reviews in Endocrine and Metabolic Disorders*, *8*(3), 255–267. https://doi.org/10.1007/s11154-007-9038-0

Bray, F., Ferlay, J., Soerjomataram, I., Siegel, R. L., Torre, L. A., & Jemal, A. (2018). Global cancer statistics 2018: GLOBOCAN estimates of incidence and mortality worldwide for 36 cancers in 185 countries. *CA: A Cancer Journal for Clinicians*, *68*(6), 394–424. https://doi.org/10.3322/caac.21492

Brenerman, B. M., Illuzzi, J. L., & Wilson, D. M. (2014). Base excision repair capacity in informing healthspan. *Carcinogenesis*, *35*(12), 2643–2652. https://doi.org/10.1093/carcin/bgu225

Bryant, H. E., Schultz, N., Thomas, H. D., Parker, K. M., Flower, D., Lopez, E., Helleday, T. (2005). Specific killing of BRCA2-deficient tumours with inhibitors of poly(ADP-ribose) polymerase. *Nature*, *434*(7035), 913–917. https://doi.org/10.1038/nature03443

Burma, S., Chen, B. P., Murphy, M., Kurimasa, A., & Chen, D. J. (2001). ATM Phosphorylates Histone H2AX in Response to DNA Double-strand Breaks. *Journal of Biological Chemistry*, *276*(45), 42462–42467. https://doi.org/10.1074/jbc.C100466200

Cadet, J., & Richard Wagner, J. (2013). DNA base damage by reactive oxygen species, oxidizing agents, and UV radiation. *Cold Spring Harb Perspect Biol*, *5*(2), 1–18.

Cadet, Jean, Douki, T., & Ravanat, J. L. (2008). Oxidatively generated damage to the guanine moiety of DNA: Mechanistic aspects and formation in cells. *Accounts of Chemical Research*, *41*(8), 1075–1083. https://doi.org/10.1021/ar700245e

Canela, A., Vera, E., Klatt, P., & Blasco, M. A. (2007). High-throughput telomere length quantification by FISH and its application to human population studies. *Proceedings of the National Academy of Sciences*, *104*(13), 5300–5305. https://doi.org/10.1073/pnas.0609367104

Carey, M. F., Peterson, C. L., & Sinale, S. T. (2009). Chromatin Immunoprecipitation (ChIP). *Cold Spring Harbor Protocols*, *4*(9), 1–9. https://doi.org/10.1101/pdb.prot5279

Chakraborty, A., Wakamiya, M., Venkova-Canova, T., Pandita, R. K., Aguilera-Aguirre, L., Sarker, A. H., Hazra, T. K. (2015). Neil2-null mice accumulate oxidized DNA bases in the transcriptionally active sequences of the genome and are susceptible to innate inflammation. *Journal of Biological Chemistry*, *290*(41), 24636–24648. https://doi.org/10.1074/jbc.M115.658146

Chenevix-Trench, G., Milne, R. L., Antoniou, A. C., Couch, F. J., Easton, D. F., & Goldgar, D. E. (2007). An international initiative to identify genetic modifiers of cancer risk in BRCA1 and BRCA2 mutation carriers: The Consortium of Investigators of Modifiers of BRCA1 and BRCA2 (CIMBA). *Breast Cancer Research*, *9*(2), 4–7. https://doi.org/10.1186/bcr1670

Chow, T. T., Shi, X., Wei, J. H., Guan, J., Stadler, G., Huang, B., & Blackburn, E. H. (2018). Local enrichment of HP1alpha at telomeres alters their structure and regulation of telomere protection. *Nature Communications*, *9*(1). https://doi.org/10.1038/s41467-018-05840-y

Cipak, I., & Jantova, S. (2010). PARP-1 inhibitors: a novel genetically specific agents for cancer therapy. *Neoplasma*, *57*(5), 401–405. https://doi.org/10.4149/neo_2010_05_401

Coluzzi, E., Colamartino, M., Cozzi, R., Leone, S., Meneghini, C., O'Callaghan, N., & Sgura, A. (2014). Oxidative stress induces persistent telomeric DNA damage responsible for nuclear morphology change in mammalian cells. *PLoS ONE*, *9*(10). https://doi.org/10.1371/journal.pone.0110963

Cortizas, E. M., Zahn, A., Safavi, S., Reed, J. A., Vega, F., Di Noia, J. M., & Verdun, R. E. (2016). UNG protects B cells from AID-induced telomere loss. *The Journal of Experimental Medicine*, *213*(11), 2459–2472. https://doi.org/10.1084/jem.20160635

Couch, F. J., Nathanson, K. L., & Offit, K. (2014). Two decades after BRCA: Setting paradigms in personalized cancer care and prevention. *Science*, *343*(6178), 1466–1470. https://doi.org/10.1126/science.1251827

Couch, F. J., Wang, X., McGuffog, L., Lee, A., Olswold, C., Kuchenbaecker, K. B., Antoniou, A. C. (2013). Genome-Wide Association Study in BRCA1 Mutation Carriers Identifies Novel Loci Associated with Breast and Ovarian Cancer Risk. *PLoS Genetics*, *9*(3). https://doi.org/10.1371/journal.pgen.1003212

Couvé-Privat, S., Macé, G., Rosselli, F., & Saparbaev, M. K. (2007). Psoralen-induced DNA adducts are substrates for the base excision repair pathway in human cells. *Nucleic Acids Research*, *35*(17), 5672–5682. https://doi.org/10.1093/nar/gkm592

Crasta, K., Ganem, N. J., Dagher, R., Lantermann, A. B., Ivanova, E. V., Pan, Y., Pellman, D. (2012). DNA breaks and chromosome pulverization from errors in mitosis. *Nature*, *482*(7383), 53–58. https://doi.org/10.1038/nature10802

D'Andrea, A. D. (2018). Mechanisms of PARP inhibitor sensitivity and resistance. *DNA Repair*, *71,* 172–176. https://doi.org/10.1016/j.dnarep.2018.08.021

D'Errico, M., Parlanti, E., Pascucci, B., Fortini, P., Baccarini, S., Simonelli, V., & Dogliotti, E. (2016). Single nucleotide polymorphisms in DNA glycosylases: From function to disease. *Free Radical Biology and Medicine*, *107*, 78-291 . https://doi.org/10.1016/j.freeradbiomed.2016.12.002

Daly, M. B., Pilarski, R., Berry, M., Buys, S. S., Farmer, M., Friedman, S., Klein, C. (2017). CE NCCN Guidelines ® Insights Genetic Familial High-Risk Assessment: Breast and Ovarian. *NCCN Guidelines*, *15*(1).

De Bont, R., & van Larebeke, N. (2004). Endogenous DNA damage in humans: A review of quantitative data. *Mutagenesis*, *19*(3), 169–185. https://doi.org/10.1093/mutage/geh025

De Lange, T. (2005). Shelterin: The protein complex that shapes and safeguards human telomeres. *Genes and Development*, *19*(18), 2100–2110. https://doi.org/10.1101/gad.1346005

Deeks, E. D. (2015). Olaparib: First global approval. *Drugs*, *75*(2), 231–240. https://doi.org/10.1007/s40265-015-0345-6

Dhénaut, A., Boiteux, S., & Radicella, J. P. (2000). Characterization of the hOGG1 promoter and its expression during the cell cycle, *461*, 109–118.

Dianov, G. L., & Hübscher, U. (2013). Mammalian base excision repair: The forgotten archangel. *Nucleic Acids Research*, *41*(6), 3483–3490. https://doi.org/10.1093/nar/gkt076

Diehn, M., Cho, R. W., Lobo, N. A., Kalisky, T., Dorie, M. J., Kulp, A. N., Clarke, M. F. (2009). Association of reactive oxygen species levels and radioresistance in cancer stem cells. *Nature*, *458*(7239), 780–783. https://doi.org/10.1038/nature07733

Ding, Y., Fleming, A. M., & Burrows, C. J. (2017). Sequencing the Mouse Genome for the Oxidatively Modified Base 8-Oxo-7,8-dihydroguanine by OG-Seq. *Journal of the American Chemical Society*, *139*(7), 2569–2572. https://doi.org/10.1021/jacs.6b12604

Dizdaroglu, M. (2015). Oxidatively induced DNA damage and its repair in cancer. *Mutation Research - Reviews in Mutation Research*, *763*, 212–245. https://doi.org/10.1016/j.mrrev.2014.11.002

Dizdaroglu, M., Coskun, E., & Jaruga, P. (2017). Repair of oxidatively induced DNA damage by DNA glycosylases: Mechanisms of action, substrate specificities and excision kinetics. *Mutation Research - Reviews in Mutation Research*, *771*, 99–127. https://doi.org/10.1016/j.mrrev.2017.02.001

Djuranovic, S., Nahvi, A., & Green, R. (2012). miRNA-Mediated Gene Silencing, *336*(April), 237–241.

Doherty, J. A., Sakoda, L. C., Loomis, M. M., Barnett, M. J., Julianto, L., & Mark, D. (2013). DNA repair genotype and lung cancer risk in the beta- carotene and retinol efficacy trial. *Int J Mol Epidemiol Genet*, *4*(1), 11–34.

Dréan, A., Lord, C. J., & Ashworth, A. (2016). PARP inhibitor combination therapy. *Critical Reviews in Oncology/Hematology*, *108*, 73–85. https://doi.org/10.1016/j.critrevonc.2016.10.010

Drost, R., & Jonkers, J. (2014). Opportunities and hurdles in the treatment of BRCA1-related breast cancer. *Oncogene*, *33*(29), 3753–3763. https://doi.org/10.1038/onc.2013.329

Easton, D. F., Pharoah, P. D. P., Antoniou, A. C., Tischkowitz, M., Tavtigian, S. V, Nathanson, K. L., Foulkes, W. D. (2015). Gene-panel sequencing and the prediction of breast-cancer risk. *New England Journal of Medicine*, *372*(23), 2243–2257. https://doi.org/10.1056/NEJMsr1501341

Elder, R. T., Zhu, X., Priet, S., Chen, M., Yu, M., Navarro, J. M., Zhao, Y. (2003). A fission yeast homologue of the human uracil-DNA-glycosylase and their roles in causing DNA damage after overexpression. *Biochemical and Biophysical Research Communications*, *306*(3), 693–700. https://doi.org/10.1016/S0006-291X(03)01036-2

Elingarami, S., Liu, H., Kalinjuma, A. V., Hu, W., Li, S., & He, N. (2015). Polymorphisms in NEIL-2, APE-1, CYP2E1 and MDM2 genes are independent predictors of gastric cancer risk in a Northern Jiangsu population (China). *Journal of Nanoscience and Nanotechnology*, *15*(7), 4815–4828. https://doi.org/10.1166/jnn.2015.10028

Ellermann, M., Eheim, A., Rahm, F., Viklund, J., Guenther, J., Andersson, M., Gorjánácz, M. (2017). Novel Class of Potent and Cellularly Active Inhibitors Devalidates MTH1 as Broad-Spectrum Cancer Target. *ACS Chemical Biology*, *12*(8), 1986–1992. https://doi.org/10.1021/acschembio.7b00370

Faraoni, I., & Graziani, G. (2018). Role of BRCA mutations in cancer treatment with poly(ADP-ribose) polymerase (PARP) inhibitors. *Cancers*, *10*(12). https://doi.org/10.3390/cancers10120487

Farmer, H., McCabe, N., Lord, C. J., Tutt, A. N. J., Johnson, D. A., Richardson, T. B., Ashworth, A. (2005). Targeting the DNA repair defect in BRCA mutant cells as a therapeutic strategy. *Nature*, *434*(7035), 917–921. https://doi.org/10.1038/nature03445

Fedorova, M., Bollineni, R., & Hoffmann, R. (2013). Protein Carbonylation as a major hallmark of oxidative damage: update of analytical strategies. *Mass Spectrom Rev*, *33*(2), 79–97. https://doi.org/10.1002/mas

Ferreira, M. A., Gamazon, E. R., Al-Ejeh, F., Aittomäki, K., Andrulis, I. L., Anton-Culver, H., Chenevix-Trench, G. (2019). Genome-wide association and transcriptome studies identify target genes and risk loci for breast cancer. *Nature Communications*, *10*(1), 1–18. https://doi.org/10.1038/s41467-018-08053-5

Fouquerel, E., Barnes, R. P., Uttam, S., Watkins, S. C., Bruchez, M. P., & Opresko, P. L. (2019). Targeted and Persistent 8-Oxoguanine Base Damage at Telomeres Promotes Telomere Loss and Crisis. *Molecular Cell*, *75*(May). https://doi.org/10.1016/j.molcel.2019.04.024

Fouquerel, E., Lormand, J., Bose, A., Lee, H. T., Kim, G. S., Li, J., Opresko, P. L. (2016). Oxidative guanine base damage regulates human telomerase activity. *Nature Structural and Molecular Biology*, *23*(12), 1092–1100. https://doi.org/10.1038/nsmb.3319

Fouquerel, E., Parikh, D., & Opresko, P. (2016). DNA damage processing at telomeres: The ends justify the means. *DNA Repair*, *44*, 159–168. https://doi.org/10.1016/j.dnarep.2016.05.022

Fradet-Turcotte, A., Sitz, J., Grapton, D., & Orthwein, A. (2016). BRCA2 functions: From DNA repair to replication fork stabilization. *Endocrine-Related Cancer*, *23*(10), T1–T17. https://doi.org/10.1530/ERC-16-0297

Frankel, A., Armour, N., Nancarrow, D., Krause, L., Hayward, N., Lampe, G., Barbour, A. (2014). Genome-Wide Analysis of Esophageal Adenocarcinoma Yields Specific Copy Number Aberrations that Correlate with Prognosis. *Genes and Development*, *53*, 324–338. https://doi.org/10.1002/gcc

Fridlich, R., Annamalai, D., Roy, R., Bernheim, G., & Powell, S. N. (2015). BRCA1 and BRCA2 protect against oxidative DNA damage converted into double-strand breaks during DNA replication. *DNA Repair*, *30*, 11–20. https://doi.org/10.1016/j.dnarep.2015.03.002

Friebel, T. M., Domchek, S. M., & Rebbeck, T. R. (2014). Modifiers of cancer risk in BRCA1 and BRCA2 mutation carriers: Systematic review and meta-analysis. *Journal of the National Cancer Institute*, *106*(6). https://doi.org/10.1093/jnci/dju091

Gad, H., Koolmeister, T., Jemth, A. S., Eshtad, S., Jacques, S. A., Ström, C. E., Helleday, T. (2014). MTH1 inhibition eradicates cancer by preventing sanitation of the dNTP pool. *Nature*, *508*(7495), 215–221. https://doi.org/10.1038/nature13181

Galati, A., Micheli, E., & Cacchione, S. (2013). Chromatin Structure in Telomere Dynamics. *Frontiers in Oncology*, *3*(March), 1–16. https://doi.org/10.3389/fonc.2013.00046

García-Giménez, J. L., Ledesma, A. M. V., Esmoris, I., Romá-Mateo, C., Sanz, P., Viña, J., & Pallardó, F. V. (2012). Histone carbonylation occurs in proliferating cells. *Free Radical Biology and Medicine*, *52*(8), 1453–1464. https://doi.org/10.1016/j.freeradbiomed.2012.01.022

Gavande, N. S., Vandervere-Carozza, P. S., Hinshaw, H. D., Jalal, S. I., Sears, C. R., Pawelczak, K. S., & Turchi, J. J. (2016). DNA repair targeted therapy: The past or future of cancer treatment? *Pharmacology and Therapeutics*, *160*, 65–83. https://doi.org/10.1016/j.pharmthera.2016.02.003

Gill, J. G., Piskounova, E., & Morrison, S. J. (2016). Cancer, oxidative stress, and metastasis. *Cold Spring Harbor Symposia on Quantitative Biology*, *81*(1), 163–175. https://doi.org/10.1101/sqb.2016.81.030791

Giovannini, S., Weller, M. C., Repmann, S., Moch, H., & Jiricny, J. (2019). Synthetic lethality between BRCA1 deficiency and poly(ADP-ribose) polymerase inhibition is modulated by processing of endogenous oxidative DNA damage. *Nucleic Acids Research*, *47*(17), 9132–9143. https://doi.org/10.1093/nar/gkz624

Girolimetti, G., Perrone, A. M., Santini, D., Barbieri, E., Guerra, F., Ferrari, S., Turchetti, D. (2014). BRCA-associated ovarian cancer: from molecular genetics to risk management. *Biomed Res Int*, *2014*, 787143. https://doi.org/10.1155/2014/787143

Goh, X. Y., Rees, J. R. E., Paterson, A. L., Chin, S. F., Marioni, J. C., Save, V., Fitzgerald, R. C. (2011). Integrative analysis of array-comparative genomic hybridisation and matched gene expression profiling data reveals novel genes with prognostic significance in oesophageal adenocarcinoma. *Gut*, *60*(10), 1317–1326. https://doi.org/10.1136/gut.2010.234179

González-Santiago, S., Ramón y Cajal, T., Aguirre, E., Alés-Martínez, J. E., Andrés, R., Balmaña, J., the SEOM Hereditary Cancer Working Group. (2020). SEOM clinical guidelines in hereditary breast and ovarian cancer (2019). *Clinical and Translational Oncology*, *22*(2), 193–200. https://doi.org/10.1007/s12094-019-02262-0

Gorodetska, I., Kozeretska, I., & Dubrovska, A. (2019). BRCA genes: The role in genome stability, cancer stemness and therapy resistance. *Journal of Cancer*, *10*(9), 2109–2127. https://doi.org/10.7150/jca.30410

Gorrini, C., Baniasadi, P. S., Harris, I. S., Silvester, J., Inoue, S., Snow, B., Gauthier, M. L. (2013). BRCA1 interacts with Nrf2 to regulate antioxidant signaling and cell survival. *Journal of Experimental Medicine*, *210*(8), 1529–1544. https://doi.org/10.1084/jem.20121337

Gorrini, C., Harris, I. S., & Mak, T. W. (2013). Modulation of oxidative stress as an anticancer strategy. *Nature Reviews Drug Discovery*, *12*(12), 931–947. https://doi.org/10.1038/nrd4002

Gu, H., Marth, J. D., Orban, P. C., Mossmann, H., & Rajewsky, K. (1994). Deletion of a DNA polymerase β gene segment in T cells using cell type-specific gene targeting. *Science*, *265*(5168), 103–106. https://doi.org/10.1126/science.8016642

Hailer, M. K., Slade, P. G., Martin, B. D., Rosenquist, T. A., & Sugden, K. D. (2005). Recognition of the oxidized lesions spiroiminodihydantoin and guanidinohydantoin in DNA by the mammalian base excision repair glycosylases NEIL1 and NEIL2. *DNA Repair*, *4*(1), 41–50. https://doi.org/10.1016/j.dnarep.2004.07.006

Haycock, P. C., Burgess, S., Nounu, A., Zheng, J., Okoli, G. N., Bowden, J., Davey Smith, G. (2017). Association between telomere length and risk of cancer and non-neoplastic diseases a mendelian randomization study. *JAMA Oncology*, *3*(5), 636–651. https://doi.org/10.1001/jamaoncol.2016.5945

Hegde, M. L., Hazra, T. K., & Mitra, S. (2008). Early steps in the DNA base excision/single-strand interruption repair pathway in mammalian cells. *Cell Research*, *18*(1), 27–47. https://doi.org/10.1038/cr.2008.8

Hegre, S. A., Sætrom, P., Aas, P. A., Pettersen, H. S., Otterlei, M., & Krokan, H. E. (2013). Multiple microRNAs may regulate the DNA repair enzyme uracil-DNA glycosylase. *DNA Repair*, *12*(1), 80–86. https://doi.org/10.1016/j.dnarep.2012.10.007

Hewitt, G., Jurk, D., Marques, F. D. M., Correia-Melo, C., Hardy, T., Gackowska, A., Passos, J. F. (2012). Telomeres are favoured targets of a persistent DNA damage response in ageing and stress-induced senescence. *Nature Communications*, *3*, 708. https://doi.org/10.1038/ncomms1708

Hockemeyer, D., & Collins, K. (2015). Control of telomerase action at human telomeres. *Nature Structural and Molecular Biology*, *22*(11), 848–852. https://doi.org/10.1038/nsmb.3083

Hooten, N. N., Kompaniez, K., Barnes, J., Lohani, A., & Evans, M. K. (2011). Poly(ADP-ribose) polymerase 1 (PARP-1) binds to 8-oxoguanine-DNA glycosylase (OGG1). *Journal of Biological Chemistry*, *286*(52), 44679–44690. https://doi.org/10.1074/jbc.M111.255869

Huber, K. V. M., Salah, E., Radic, B., Gridling, M., Elkins, J. M., Stukalov, A., Superti-Furga, G. (2014). Stereospecific targeting of MTH1 by (S)-crizotinib as an anticancer strategy. *Nature*, *508*(7495), 222–227. https://doi.org/10.1038/nature13194

Ichikawa, Y., Nishimura, Y., Kurumizaka, H., & Shimizu, M. (2015). Nucleosome organization and chromatin dynamics in telomeres. *Biomolecular Concepts*, *6*(1), 67–75. https://doi.org/10.1515/bmc-2014-0035

Ivancich, M., Schrank, Z., Wojdyla, L., Leviskas, B., Kuckovic, A., Sanjali, A., & Puri, N. (2017). Treating cancer by targeting telomeres and telomerase. *Antioxidants*, *6*(1). https://doi.org/10.3390/antiox6010015

Jacobs, A. C., Calkins, M. J., Jadhav, A., Dorjsuren, D., Maloney, D., Simeonov, A., Stephen Lloyd, R. (2013). Inhibition of DNA glycosylases via small molecule purine analogs. *PLoS ONE*, *8*(12). https://doi.org/10.1371/journal.pone.0081667

Jasin, M., & Rothstein, R. (2013). Repair of strand breaks by homologous recombination. *Cold Spring Harbor Perspectives in Biology*, *5*(11), 1–18. https://doi.org/10.1101/cshperspect.a012740

Jeggo, P. A., Pearl, L. H., & Carr, A. M. (2016). DNA repair, genome stability and cancer: A historical perspective. *Nature Reviews Cancer*, *16*(1), 35–42. https://doi.org/10.1038/nrc.2015.4

Jia, P., Her, C., & Chai, W. (2015). DNA excision repair at telomeres. *DNA Repair*, *36*, 137–145. https://doi.org/10.1016/j.dnarep.2015.09.017

Karlan, B. Y., Berchuck, A., & Mutch, D. (2007). The role of genetic testing for cancer susceptibility in gynecologic practice. *Obstetrics and Gynecology*, *110*(1), 155–167. https://doi.org/10.1097/01.AOG.0000269050.79143.84

Kelley, M. R., Logsdon, D., & Fishel, M. L. (2014). Targeting DNA repair pathways for cancer treatment: What's new? *Future Oncology*, *10*(7), 1215–1237. https://doi.org/10.2217/fon.14.60

Kidane, D., Murphy, D. L., & Sweasy, J. B. (2014). Accumulation of abasic sites induces genomic instability in normal human gastric epithelial cells during Helicobacter pylori infection. *Oncogenesis*, *3*(11). https://doi.org/10.1038/oncsis.2014.42

Kinslow, C. J., El-Zein, R. A., Hill, C. E., Wickliffe, J. K., & Abdel-Rahman, S. Z. (2008). Single Nucleotide Polymorphisms 5' Upstream the Coding Region of the NEIL2 Gene Influence Gene Transcription Levels and Alter Levels of Genetic Damage. *Genes, Chromosomes & Cancer*, *47*(January), 923–932. https://doi.org/10.1002/gcc

Kinslow, C. J., El-Zein, R. A., Rondelli, C. M., Hill, C. E., Wickliffe, J. K., & Abdel-Rahman, S. Z. (2010). Regulatory regions responsive to oxidative stress in the promoter of the human DNA glycosylase gene NEIL2. *Mutagenesis*, *25*(2), 171–177. https://doi.org/10.1093/mutage/gep058

Kobayashi, H., Ohno, S., Sasaki, Y., & Matsuura, M. (2013). Hereditary breast and ovarian cancer susceptibility genes (Review). *Oncology Reports*, *30*(3), 1019–1029. https://doi.org/10.3892/or.2013.2541

Kotsopoulos, J. (2018). BRCA mutations and breast cancer prevention. *Cancers*, *10*(12), 1–15. https://doi.org/10.3390/cancers10120524

Krishnakumar, R., & Kraus, W. L. (2010). The PARP Side of the Nucleus: Molecular Actions, Physiological Outcomes, and Clinical Targets. *Molecular Cell*, *39*(1), 8–24. https://doi.org/10.1016/j.molcel.2010.06.017

Krokan, H. E., & Bjøra, M. (2013). Base Excision Repair. *Cold Spring Harb Perspect Biol*, *5*, 1–22. https://doi.org/10.1101/cshperspect.a012583

Krokan, H. E., Drabløs, F., & Slupphaug, G. (2002). Uracil in DNA – occurrence, consequences and repair. *Oncogene*, *21*(58), 8935–8948. https://doi.org/10.1038/sj.onc.1205996

Kuchenbaecker, K. B., Hopper, J. L., Barnes, D. R., Phillips, K. A., Mooij, T. M., Roos-Blom, M. J., Antoniou, A. C. (2017). Risks of breast, ovarian, and contralateral breast cancer for BRCA1 and BRCA2 mutation carriers. *JAMA - Journal of the American Medical Association*, *317*(23), 2402–2416. https://doi.org/10.1001/jama.2017.7112

Kuchenbaecker, K. B., McGuffog, L., Barrowdale, D., Lee, A., Soucy, P., Dennis, J., Lester, J. (2017). Evaluation of polygenic risk scores for breast and ovarian cancer risk prediction in BRCA1 and BRCA2 mutation carriers. *Journal of the National Cancer Institute*, *109*(7), 1–15. https://doi.org/10.1093/jnci/djw302

Larsen, E., Gran, C., Saether, B. E., Seeberg, E., & Klungland, A. (2003). Proliferation Failure and Gamma Radiation Sensitivity of Fen1 Null Mutant Mice at the Blastocyst Stage. *Molecular and Cellular Biology*, *23*(15), 5346–5353. https://doi.org/10.1128/mcb.23.15.5346-5353.2003

Le Page, F., Randrianarison, V., Marot, D., Cabannes, J., Perricaudet, M., Feunteun, J., & Sarasin, A. (2000). BRCA1 and BRCA2 are necessary for the transcription-coupled repair of the oxidative 8-oxoguanine lesion in human cells. *Cancer Research*, *60*(19), 5548–5552.

Lee, A., Mavaddat, N., Wilcox, A. N., Cunningham, A. P., Carver, T., Hartley, S., Antoniou, A. C. (2019). BOADICEA: a comprehensive breast cancer risk prediction model incorporating genetic and nongenetic risk factors. *Genetics in Medicine*, *21*(8), 1708–1718. https://doi.org/10.1038/s41436-018-0406-9

Lee, K. J., Piett, C. G., Andrews, J. F., Mann, E., Nagel, Z. D., & Gassman, N. R. (2019). Defective base excision repair in the response to DNA damaging agents in triple negative breast cancer. *PLoS ONE*, *14*(10), 1–23. https://doi.org/10.1371/journal.pone.0223725

Lee, T. H., & Kang, T. H. (2019). DNA oxidation and excision repair pathways. *International Journal of Molecular Sciences*, *20*(23). https://doi.org/10.3390/ijms20236092

Lesueur, F., Mebirouk, N., Jiao, Y., Barjhoux, L., Belotti, M., Laurent, M., Stoppa-Lyonnet, D. (2018). GEMO, a national resource to study genetic modifiers of breast and ovarian cancer risk in BRCA1 and BRCA2 pathogenic variant carriers. *Frontiers in Oncology*, *8*(OCT), 1–8. https://doi.org/10.3389/fonc.2018.00490

Lheureux, S., Gourley, C., Vergote, I., & Oza, A. M. (2019). Epithelial ovarian cancer. *The Lancet*, *393*(10177), 1240–1253. https://doi.org/10.1016/S0140-6736(18)32552-2

Lilyquist, J., Ruddy, K. J., Vachon, C. M., & Couch, F. J. (2018). Common genetic variation and breast cancer Risk—Past, present, and future. *Cancer Epidemiology Biomarkers and Prevention*, *27*(4), 380–394. https://doi.org/10.1158/1055-9965.EPI-17-1144

Lim, L. P., Lau, N. C., Garrett-Engele, P., Grimson, A., Schelter, J. M., Castle, J., Johnson, J. M. (2005). Microarray analysis shows that some microRNAs downregulate large numbers of-target mRNAs. *Nature*, *433*(7027), 769–773. https://doi.org/10.1038/nature03315

Liu, W., Wu, J., Yang, F., Ma, L., Ni, C., Hou, X., Cao, G. (2019). Genetic polymorphisms predisposing the interleukin 6-induced APOBEC3B-UNG imbalance increase HCC risk via promoting the generation of APOBEC-signature HBV mutations. *Clinical Cancer Research*, *25*(18), 5525–5536. https://doi.org/10.1158/1078-0432.CCR-18-3083

Lord, C. J., & Ashworth, A. (2017). PARP inhibitors: Synthetic lethality in the clinic. *Science*, *355*(March), 1152–1158. https://doi.org/10.2307/j.ctt211qvxv.13

Lu, H. M., Li, S., Black, M. H., Lee, S., Hoiness, R., Wu, S., Elliott, A. (2019). Association of Breast and Ovarian Cancers with Predisposition Genes Identified by Large-Scale Sequencing. *JAMA Oncology*, *5*(1), 51–57. https://doi.org/10.1001/jamaoncol.2018.2956

Lu, J., & Liu, Y. (2010). Deletion of Ogg1 DNA glycosylase results in telomere base damage and length alteration in yeast. *The EMBO Journal*, *29*(2), 398–409. https://doi.org/10.1038/emboj.2009.355

Lu, Y., Beeghly-Fadiel, A., Wu, L., Guo, X., Li, B., Schildkraut, J. M., Long, J. (2018). A transcriptome-wide association study among 97,898 women to identify candidate susceptibility genes for epithelial ovarian cancer risk. *Cancer Research*, *78*(18), 5419–5430. https://doi.org/10.1158/0008-5472.CAN-18-0951

Maciejowski, J., & De Lange, T. (2017). Telomeres in cancer: Tumour suppression and genome instability. *Nature Reviews Molecular Cell Biology*, *18*(3), 175–186. https://doi.org/10.1038/nrm.2016.171

Madlener, S., Ströbel, T., Vose, S., Saydam, O., Price, B. D., Demple, B., & Saydam, N. (2013). Essential role for mammalian apurinic/apyrimidinic (AP) endonuclease Ape1/Ref-1 in telomere maintenance. *Proceedings of the National Academy of Sciences of the United States of America*, *110*(44), 17844–17849. https://doi.org/10.1073/pnas.1304784110

Mah, L. J., El-Osta, A., & Karagiannis, T. C. (2010). γh2AX: A sensitive molecular marker of DNA damage and repair. *Leukemia*, *24*(4), 679–686. https://doi.org/10.1038/leu.2010.6

Malins, D. C., Holmes, E. H., Polissar, N., & Gunselman, S. J. (1993). The etiology of breast cancer characteristic alterations in hydroxyl radical-induced dna base lesions during oncogenesis with potential for evaluating incidence risk. *Cancer*, *71*(10), 3036–3043.

Marian, C., Tao, M., Mason, J. B., Goerlitz, D. S., Nie, J., Chanson, A., Shields, P. G. (2011). Single nucleotide polymorphisms in uracil-processing genes, intake of one-carbon nutrients and breast cancer risk. *European Journal of Clinical Nutrition*, *65*(6), 683–689. https://doi.org/10.1038/ejcn.2011.29

Marnef, A., Cohen, S., & Legube, G. (2017). Transcription-Coupled DNA Double-Strand Break Repair: Active Genes Need Special Care. *Journal of Molecular Biology*, *429*(9), 1277–1288. https://doi.org/10.1016/j.jmb.2017.03.024

Mateo, J., Lord, C. J., Serra, V., Tutt, A., Balmaña, J., Castroviejo-Bermejo, M., De Bono, J. S. (2019). A decade of clinical development of PARP inhibitors in perspective. *Annals of Oncology*, *30*(9), 1437–1447. https://doi.org/10.1093/annonc/mdz192

Mavaddat, N., Antoniou, A. C., Easton, D. F., & Garcia-Closas, M. (2010). Genetic susceptibility to breast cancer. *Molecular Oncology*, *4*(3), 174–191. https://doi.org/10.1016/j.molonc.2010.04.011

Mavaddat, N., Michailidou, K., Dennis, J., Lush, M., Fachal, L., Lee, A., Easton, D. F. (2019). Polygenic Risk Scores for Prediction of Breast Cancer and Breast Cancer Subtypes. *American Journal of Human Genetics*, *104*(1), 21–34. https://doi.org/10.1016/j.ajhg.2018.11.002

Maynard, S., Schurman, S. H., Harboe, C., de Souza-Pinto, N. C., & Bohr, V. A. (2009). Base excision repair of oxidative DNA damage and association with cancer and aging. *Carcinogenesis*, *30*(1), 2–10. https://doi.org/10.1093/carcin/bgn250

Mechetin, G. V., Endutkin, A. V., Diatlova, E. A., & Zharkov, D. O. (2020). Inhibitors of DNA glycosylases as prospective drugs. *International Journal of Molecular Sciences*, *21*(9), 1–30. https://doi.org/10.3390/ijms21093118

Melchor, L., & Benítez, J. (2013). The complex genetic landscape of familial breast cancer. *Human Genetics*, *132*(8), 845–863. https://doi.org/10.1007/s00439-013-1299-y

Michailidou, K., Lindström, S., Dennis, J., Beesley, J., Hui, S., Kar, S., Easton, D. F. (2017). Association analysis identifies 65 new breast cancer risk loci. *Nature*, *551*(7678), 92–94. https://doi.org/10.1038/nature24284

Miki, Y., Swensen, J., Shattuck-Eidens, D., Futreal, P. A., Harshman, K., Tavtigian, S., Skolnick, M. H. (1994). A strong candidate for the breast and ovarian cancer susceptibility gene BRCA1. *Science*, *266*(5182), 66–71. https://doi.org/10.1126/science.7545954

Milne, R. L., & Antoniou, A. C. (2011). Genetic modifiers of cancer risk for BRCA1 and BRCA2 mutation carriers. *Annals of Oncology*, *22*(SUPPL. 1), 11–17. https://doi.org/10.1093/annonc/mdq660

Milne, Roger L., & Antoniou, A. C. (2016). Modifiers of breast and ovarian cancer risks for BRCA1 and BRCA2 mutation carriers. *Endocrine-Related Cancer*, *23*(10), T69–T84. https://doi.org/10.1530/ERC-16-0277

Milne, Roger L., Osorio, A., Cajal, T. R. Y., Vega, A., Llort, G., De La Hoya, M., Benítez, J. (2008). The average cumulative risks of breast and ovarian cancer for carriers of mutations in BRCA1 and BRCA2 attending genetic counseling units in Spain. *Clinical Cancer Research*, *14*(9), 2861–2869. https://doi.org/10.1158/1078-0432.CCR-07-4436

Mimouni, A., Rouleau, E., Saulnier, P., Marouani, A., Abdelali, M. L., Filali, T., Satta, D. (2020). Association of TERT, OGG1, and CHRNA5 Polymorphisms and the Predisposition to Lung Cancer in Eastern Algeria. *Pulmonary Medicine*, *2020*, 1–12. https://doi.org/10.1155/2020/7649038

Minowa, O., Arai, T., Hirano, M., Monden, Y., Nakai, S., Fukuda, M., Noda, T. (2000). Mmh/Ogg1 gene inactivation results in accumulation of 8-hydroxyguanine in mice. *Proceedings of the National Academy of Sciences of the United States of America*, *97*(8), 4156–4161. https://doi.org/10.1073/pnas.050404497

Mjelle, R., Hegre, S. A., Aas, P. A., Slupphaug, G., Drabløs, F., Sætrom, P., & Krokan, H. E. (2015). Cell cycle regulation of human DNA repair and chromatin remodeling genes. *DNA Repair*, *30*, 53–67. https://doi.org/10.1016/j.dnarep.2015.03.007

Molenaar, C., Wiesmeijer, K., Verwoerd, N. P., Khazen, S., Eils, R., Tanke, H. J., & Dirks, R. W. (2003). Visualizing telomere dynamics in living mammalian cells using PNA probes, *22*(24), 6631–6641.

Moynahan, M. E., Chiu, J. W., Koller, B. H., Jasin, M., Hill, C., & Carolina, N. (1990). Brca1 Controls Homology-Directed DNA Repair University of North Carolina at Chapel Hill. *Molecular Cell*, *4*(4), 511–518.

Müezzinler, A., Zaineddin, A. K., & Brenner, H. (2013). A systematic review of leukocyte telomere length and age in adults. *Ageing Research Reviews*, *12*(2), 509–519. https://doi.org/10.1016/j.arr.2013.01.003

Nakabeppu, Y. (2014). Cellular levels of 8-oxoguanine in either DNA or the nucleotide pool play pivotal roles in carcinogenesis and survival of cancer cells. *International Journal of Molecular Sciences*, *15*(7), 12543–12557. https://doi.org/10.3390/ijms150712543

Neeley, W. L., & Essigmann, J. M. (2006). Mechanisms of formation, genotoxicity, and mutation of guanine oxidation products. *Chemical Research in Toxicology*, *19*(4), 491–505. https://doi.org/10.1021/tx0600043

Ngo, G., Hyatt, S., Grimstead, J., Jones, R., Hendrickson, E., Pepper, C., & Baird, D. (2018). PARP inhibition prevents escape from a telomere-driven crisis and inhibits cell immortalisation. *Oncotarget*, *9*(101), 37549–37563. https://doi.org/10.18632/oncotarget.26499

Nilsen, H., Otterlei, M., Haug, T., Solum, K., Nagelhus, T. A., Skorpen, F., & Krokan, H. E. (1997). Nuclear and mitochondrial uracil-DNA glycosylases are generated by alternative splicing and transcription from different positions in the UNG gene. *Nucleic Acids Research*, *25*(4), 750–755. https://doi.org/10.1093/nar/25.4.750

O'Callaghan, N. J., Dhillon, V. S., Thomas, P., & Fenech, M. (2008). A quantitative real-time PCR method for absolute telomere length. *BioTechniques*, *44*(6), 807–809. https://doi.org/10.2144/000112761

O'Connor, M. J. (2015). Targeting the DNA Damage Response in Cancer. *Molecular Cell*, *60*(4), 547–560. https://doi.org/10.1016/j.molcel.2015.10.040

O'Neil, N. J., Bailey, M. L., & Hieter, P. (2017). Synthetic lethality and cancer. *Nature Reviews Genetics*, *18*(10), 613–623. https://doi.org/10.1038/nrg.2017.47

O'Sullivan, R. J., & Karlseder, J. (2010). Telomeres: protecting chromosomes against genome instability. *Nature Reviews Molecular Cell Biology*, *11*(mARCH). https://doi.org/10.1038/nrm2848

Odell, I. D., Wallace, S. S., & Pederson, D. S. (2013). Rules of engagement for base excision repair in chromatin. *Journal of Cellular Physiology*, *228*(2), 258–266. https://doi.org/10.1002/jcp.24134

Ohno, M., Sakumi, K., Fukumura, R., Furuichi, M., Iwasaki, Y., Hokama, M., Nakabeppu, Y. (2014). 8-Oxoguanine causes spontaneous de novo germline mutations in mice. *Scientific Reports*, *4*, 1–9. https://doi.org/10.1038/srep04689

Oikawa, S., & Kawanishi, S. (1999). Site-specific DNA damage at GGG sequence by oxidative stress may accelerate telomere shortening. *FEBS Letters*, *453*(3), 365–368. https://doi.org/10.1016/S0014-5793(99)00748-6

Oka, S., Ohno, M., Tsuchimoto, D., Sakumi, K., Furuichi, M., & Nakabeppu, Y. (2008). Two distinct pathways of cell death triggered by oxidative damage to nuclear and mitochondrial DNAs. *EMBO Journal*, *27*(2), 421–432. https://doi.org/10.1038/sj.emboj.7601975

Okamoto, K., & Seimiya, H. (2019). Revisiting Telomere Shortening in Cancer. *Cells*, *8*(2), 107. https://doi.org/10.3390/cells8020107

Opresko, P. L., Fan, J., Danzy, S., Wilson, D. M., & Bohr, V. A. (2005). Oxidative damage in telomeric DNA disrupts recognition by TRF1 and TRF2. *Nucleic Acids Research*, *33*(4), 1230–1239. https://doi.org/10.1093/nar/gki273

Orta, M. L., Höglund, A., Calderón-Montaño, J. M., Domínguez, I., Burgos-Morón, E., Visnes, T., Helleday, T. (2014). The PARP inhibitor Olaparib disrupts base excision repair of 5-aza-2'-deoxycytidine lesions. *Nucleic Acids Research*, *42*(14), 9108–9120. https://doi.org/10.1093/nar/gku638

Osorio, A., Milne, R. L., Alonso, R., Pita, G., Peterlongo, P., Teulé, A., Benítez, J. (2011). Evaluation of the XRCC1 gene as a phenotypic modifier in BRCA1/2 mutation carriers. Results from the consortium of investigators of modifiers of BRCA1/BRCA2. *British Journal of Cancer*, *104*(8), 1356–1361. https://doi.org/10.1038/bjc.2011.91

Osorio, Ana, Milne, R. L., Kuchenbaecker, K., Vaclová, T., Pita, G., Alonso, R., Benitez, J. (2014). DNA Glycosylases Involved in Base Excision Repair May Be Associated with Cancer Risk in BRCA1 and BRCA2 Mutation Carriers. *PLoS Genetics*, *10*(4). https://doi.org/10.1371/journal.pgen.1004256

Pan, L., Zhu, B., Hao, W., Zeng, X., Vlahopoulos, S. A., Hazra, T. K., Boldogh, I. (2016). Oxidized guanine base lesions function in 8-oxoguanine DNA glycosylase-1-mediated epigenetic regulation of nuclear factor κB-driven gene expression. *Journal of Biological Chemistry*, *291*(49), 25553–25566. https://doi.org/10.1074/jbc.M116.751453

Panier, S., & Boulton, S. J. (2014). Double-strand break repair: 53BP1 comes into focus. *Nature Reviews Molecular Cell Biology*, *15*(1), 7–18. https://doi.org/10.1038/nrm3719

Patel, K. J., Yu, V. P. C. C., Lee, H., Corcoran, A., Thistlethwaite, F. C., Evans, M. J., Venkitaraman, A. R. (1998). Involvement of Brca2 in DNA repair. *Molecular Cell*, *1*(3), 347–357. https://doi.org/10.1016/S1097-2765(00)80035-0

Phelan, C. M., Kuchenbaecker, K. B., Tyrer, J. P., Kar, S. P., Lawrenson, K., Winham, S. J., Pharoah, P. D. P. (2017). Identification of 12 new susceptibility loci for different histotypes of epithelial ovarian cancer. *Nature Genetics*, *49*(5), 680–691. https://doi.org/10.1038/ng.3826

Poetsch, A. R. (2020). The genomics of oxidative DNA damage, repair, and resulting mutagenesis. *Computational and Structural Biotechnology Journal*, *18*, 207–219. https://doi.org/10.1016/j.csbj.2019.12.013

Poletto, M., Legrand, A. J., Fletcher, S. C., & Dianov, G. L. (2016). P53 coordinates base excision repair to prevent genomic instability. *Nucleic Acids Research*, *44*(7), 3165–3175. https://doi.org/10.1093/nar/gkw015

Pooley, K. A., Bojesen, S. E., Weischer, M., Nielsen, S. F., Thompson, D., Amin Al Olama, A., Nordestgaard, B. G. (2013). A genome-wide association scan (GWAS) for mean telomere length within the COGS project: Identified loci show little association with hormone-related cancer risk. *Human Molecular Genetics*, *22*(24), 5056–5064. https://doi.org/10.1093/hmg/ddt355

Popanda, O., Seibold, P., Nikolov, I., Oakes, C. C., Burwinkel, B., Hausmann, S., Schmezer, P. (2013). Germline variants of base excision repair genes and breast cancer: A polymorphism in DNA polymerase gamma modifies gene expression and breast cancer risk. *International Journal of Cancer*, *132*(1), 55–62. https://doi.org/10.1002/ijc.27665

Prakash, A., Doublié, S., & Wallace, S. S. (2012). The Fpg/Nei family of DNA Glycosylases: Substrates, structures, and search for damage. *Progress in Molecular Biology and Translational Science*, *110*, 71–91. https://doi.org/10.1016/B978-0-12-387665-2.00004-3

Prakash, R., Zhang, Y., Feng, W., & Jasin, M. (2015). Homologous Recombination and Human Health. *Perspectives in Biology*, 1–29. https://doi.org/10.1101/cshperspect.a016600

Puebla-Osorio, N., Lacey, D. B., Alt, F. W., & Zhu, C. (2006). Early Embryonic Lethality Due to Targeted Inactivation of DNA Ligase III. *Molecular and Cellular Biology*, *26*(10), 3935–3941. https://doi.org/10.1128/mcb.26.10.3935-3941.2006

Ray Chaudhuri, A., & Nussenzweig, A. (2017). The multifaceted roles of PARP1 in DNA repair and chromatin remodelling. *Nature Reviews Molecular Cell Biology*, *18*(10), 610–621. https://doi.org/10.1038/nrm.2017.53

Rebbeck, T. R., Mitra, N., Wan, F., Sinilnikova, O. M., Healey, S., McGuffog, L., Andrulis, I. (2015). Association of type and location of BRCA1 and BRCA2 mutations with risk of breast and ovarian cancer. *JAMA - Journal of the American Medical Association*, *313*(13), 1347–1361. https://doi.org/10.1001/jama.2014.5985

Reid, B. M., Permuth, J. B., & Sellers, T. A. (2017). Epidemiology of ovarian cancer: a review. *Cancer Biology and Medicine*, *14*(1), 9–32. https://doi.org/10.20892/j.issn.2095-3941.2016.0084

Rhee, D. B., Ghosh, A., Lu, J., Bohr, V. A., & Liu, Y. (2011). Factors that influence telomeric oxidative base damage and repair by DNA glycosylase OGG1. *DNA Repair*, *10*(1), 34–44. https://doi.org/10.1016/j.dnarep.2010.09.008

Roberts, M. R., Shields, P. G., Ambrosone, C. B., Nie, J., Marian, C., Krishnan, S. S., Freudenheim, J. L. (2011). Single-nucleotide polymorphisms in DNA repair genes and association with breast cancer risk in the web study. *Carcinogenesis*, *32*(8), 1223–1230. https://doi.org/10.1093/carcin/bgr096

Rolseth, V., Luna, L., Olsen, A. K., Suganthan, R., Scheffler, K., Neurauter, C. G., Bjørås, M. (2017). No cancer predisposition or increased spontaneous mutation frequencies in NEIL DNA glycosylases-deficient mice. *Scientific Reports*, *7*(1), 1–12. https://doi.org/10.1038/s41598-017-04472-4

Rouleau, M., Patel, A., Hendzel, M. J., Kaufmann, S. H., & Poirier, G. G. (2010). PARP inhibition: PARP1 and beyond. *Nature Reviews Cancer*, *10*(4), 293–301. https://doi.org/10.1038/nrc2812

Roy, R., Chun, J., & Powell, S. N. (2012). BRCA1 and BRCA2: Different roles in a common pathway of genome protection. *Nature Reviews Cancer*, *12*(1), 68–78. https://doi.org/10.1038/nrc3181

Rudolph, A., Chang-Claude, J., & Schmidt, M. K. (2016). Gene-environment interaction and risk of breast cancer. *British Journal of Cancer*, *114*(2), 125–133. https://doi.org/10.1038/bjc.2015.439

Saha, T., Rih, J. K., & Rosen, E. M. (2009). BRCA1 down-regulates cellular levels of reactive oxygen species. *FEBS Letters*, *583*(9), 1535–1543. https://doi.org/10.1016/j.febslet.2009.04.005

Saha, T., Rih, J. K., Roy, R., Ballal, R., & Rosen, E. M. (2010). Transcriptional regulation of the base excision repair pathway by BRCA1. *Journal of Biological Chemistry*, *285*(25), 19092–19105. https://doi.org/10.1074/jbc.M110.104430

Samadder, N. J., Giridhar, K. V., Baffy, N., Riegert-Johnson, D., & Couch, F. J. (2019). Hereditary Cancer Syndromes—A Primer on Diagnosis and Management: Part 1: Breast-Ovarian Cancer Syndromes. *Mayo Clinic Proceedings*, *94*(6), 1084–1098. https://doi.org/10.1016/j.mayocp.2019.02.017

Sampath, H. (2014). Oxidative DNA Damage in Disease - Insights Gained from Base Excision Repair Glycosylase-Deficient Mouse Models. *Environmental and Molecular Mutagenesis*, *55*, 689–703. https://doi.org/DOI 10.1002/em.21886

Schipler, A., & Iliakis, G. (2013). DNA double-strand-break complexity levels and their possible contributions to the probability for error-prone processing and repair pathway choice. *Nucleic Acids Research*, *41*(16), 7589–7605. https://doi.org/10.1093/nar/gkt556

Seo, Y., & Kinsella, T. J. (2009). Essential role of DNA base excision repair on survival in an acidic tumor microenvironment. *Cancer Research*, *69*(18), 7285–7293. https://doi.org/10.1158/0008-5472.CAN-09-0624

Serebrenik, A. A., Starrett, G. J., Leenen, S., Jarvis, M. C., Shaban, N. M., Salamango, D. J., Harris, R. S. (2019). The deaminase APOBEC3B triggers the death of cells lacking uracil DNA glycosylase. *Proceedings of the National Academy of Sciences of the United States of America*, *116*(44), 22158–22163. https://doi.org/10.1073/pnas.1904024116

Sfeir, A., & de Lange, T. (2012). Removal of Shelterin Reveals the Telomere End-Protection Problem. *Science*, *336*(6081), 593–597. https://doi.org/10.1126/science.1218498

Shankar, K., & Mehendale, H. M. (2014). *Oxidative Stress*. *Encyclopedia of Toxicology: Third Edition* (Third Edit, Vol. 3). Elsevier. https://doi.org/10.1016/B978-0-12-386454-3.00345-6

Shay, J. W. (2016). Role of telomeres and telomerase in aging and cancer. *Cancer Discovery*, *6*(6), 584–593. https://doi.org/10.1158/2159-8290.CD-16-0062

Shay, J. W., & Wright, W. E. (2019). Telomeres and telomerase: three decades of progress. *Nature Reviews Genetics*, *20*(5), 299–309. https://doi.org/10.1038/s41576-019-0099-1

Shen, B., Chapman, J. H., Custance, M. F., Tricola, G. M., & Jones, C. E. (2020). Perturbation of base excision repair sensitizes breast cancer cells to APOBEC3 deaminase-mediated mutations. *ELife*, *9*, 1–22. https://doi.org/10.7554/eLife.51605

Slade, D. (2020). PARP and PARG inhibitors in cancer treatment. *Genes and Development*, *34*(5), 360–394. https://doi.org/10.1101/gad.334516.119

Sousa, F. G., Matuo, R., Soares, D. G., Escargueil, A. E., Henriques, J. A. P., Larsen, A. K., & Saffi, J. (2012). PARPs and the DNA damage response. *Carcinogenesis*, *33*(8), 1433–1440. https://doi.org/10.1093/carcin/bgs132

Srinivas, N., Rachakonda, S., & Kumar, R. (2020). Telomeres and telomere length: A general overview. *Cancers*, *12*(3), 1–29. https://doi.org/10.3390/cancers12030558

Stoppa-Lyonnet, D. (2016). The biological effects and clinical implications of BRCA mutations: Where do we go from here? *European Journal of Human Genetics*, *24*(S1), S3–S9. https://doi.org/10.1038/ejhg.2016.93

Ström, C. E., Johansson, F., Uhlén, M., Szigyarto, C. A. K., Erixon, K., & Helleday, T. (2011). Poly (ADP-ribose) polymerase (PARP) is not involved in base excision repair but PARP inhibition traps a single-strand intermediate. *Nucleic Acids Research*, *39*(8), 3166–3175. https://doi.org/10.1093/nar/gkq1241

Sultana, R., McNeill, D. R., Abbotts, R., Mohammed, M. Z., Zdzienicka, M. Z., Qutob, H., Madhusudan, S. (2012). Synthetic lethal targeting of DNA double-strand break repair deficient cells by human apurinic/apyrimidinic endonuclease inhibitors. *International Journal of Cancer*, *131*(10), 2433–2444. https://doi.org/10.1002/ijc.27512

Tahara, Y. K., Auld, D., Ji, D., Beharry, A. A., Kietrys, A. M., Wilson, D. L., Kool, E. T. (2018). Potent and Selective Inhibitors of 8-Oxoguanine DNA Glycosylase. *Journal of the American Chemical Society*, *140*(6), 2105–2114. https://doi.org/10.1021/jacs.7b09316

Takaoka, M., & Miki, Y. (2018). BRCA1 gene: function and deficiency. *International Journal of Clinical Oncology*, *23*(1), 36–44. https://doi.org/10.1007/s10147-017-1182-2

Tardat, M., & Déjardin, J. (2018). Telomere chromatin establishment and its maintenance during mammalian development. *Chromosoma*, *127*(1), 3–18. https://doi.org/10.1007/s00412-017-0656-3

Tebbs, R. S., Flannery, M. L., Meneses, J. J., Hartmann, A., Tucker, J. D., Thompson, L. H., Pedersen, R. A. (1999). Requirement for the Xrcc1 DNA base excision repair gene during early mouse development. *Developmental Biology*, *208*(2), 513–529. https://doi.org/10.1006/dbio.1999.9232

Tomasova, K., Cumova, A., Seborova, K., Horak, J., Koucka, K., Vodickova, L., Vodicka, P. (2020). DNA repair and ovarian carcinogenesis: Impact on risk, prognosis and therapy outcome. *Cancers*, *12*(7), 1–37. https://doi.org/10.3390/cancers12071713

Torres-ruiz, R., Martinez-lage, M., Martin, M. C., Garcia, A., Bueno, C., Castan, J., Rodriguez-perales, S. (2017). Efficient Recreation of t(11;22) EWSR1-FLI1+ in Human Stem Cells Using CRISPR/Cas9. *Stem Cell Reports*, *8*, 1408–1420. https://doi.org/10.1016/j.stemcr.2017.04.014

Toyokuni, S., Okamoto, K., Yodoi, J., & Hiai, H. (1995). Persistent oxidative stress in cancer. *FEBS Letters*, *358*(1), 1–3. https://doi.org/10.1016/0014-5793(94)01368-B

Turner, N. C., Lord, C. J., Iorns, E., Brough, R., Swift, S., Elliott, R., Ashworth, A. (2008). A synthetic lethal siRNA screen identifying genes mediating sensitivity to a PARP inhibitor. *EMBO Journal*, *27*(9), 1368–1377. https://doi.org/10.1038/emboj.2008.61

Vaclova, T., Gomez-Lopez, G., Setien, F., Bueno, J. M. G., Macias, J. A., Barroso, A., Osorio, A. (2015). DNA repair capacity is impaired in healthy BRCA1 heterozygous mutation carriers. *Breast Cancer Research and Treatment*, *152*(2), 271–282. https://doi.org/10.1007/s10549-015-3459-3

Valavanidis, A., Vlachogianni, T., & Fiotakis, K. (2009). Tobacco smoke: Involvement of reactive oxygen species and stable free radicals in mechanisms of oxidative damage, carcinogenesis and synergistic effects with other respirable particles. *International Journal of Environmental Research and Public Health*, *6*(2), 445–462. https://doi.org/10.3390/ijerph6020445

Valko, M., Rhodes, C., Moncol, J., Izakovic, M., & Mazur, M. (2006). Free radicals, metals and antioxidants in oxidative stress-induced cancer. *Chem Biol Interact*, *160(1)*, 1–40.

Vallabhaneni, H., Zhou, F., Maul, R. W., Sarkar, J., Yin, J., Lei, M., Liu, Y. (2015). Defective repair of uracil causes telomere defects in mouse hematopoietic cells. *Journal of Biological Chemistry*, *290*(9), 5502–5511. https://doi.org/10.1074/jbc.M114.607101

Verdun, R. E., Crabbe, L., Haggblom, C., & Karlseder, J. (2005). Functional human telomeres are recognized as DNA damage in G2 of the cell cycle. *Molecular Cell*, *20*(4), 551–561. https://doi.org/10.1016/j.molcel.2005.09.024

Visnes, T., Akbari, M., Hagen, L., Slupphaug, G., & Krokan, H. E. (2008). The rate of base excision repair of uracil is controlled by the initiating glycosylase. *DNA Repair*, *7*(11), 1869–1881. https://doi.org/10.1016/j.dnarep.2008.07.012

Visnes, T., Cázares-Körner, A., Hao, W., Wallner, O., Masuyer, G., Loseva, O., Helleday, T. (2018). Small-molecule inhibitor of OGG1 suppresses proinflammatory gene expression and inflammation. *Science*, *362*(6416), 834–839. https://doi.org/10.1126/science.aar8048

Visnes, T., Doseth, B., Pettersen, H. S., Hagen, L., Sousa, M. M. L., Akbari, M., Krokan, H. E. (2009). Uracil in DNA and its processing by different DNA glycosylases. *Philosophical Transactions of the Royal Society B: Biological Sciences*, *364*(1517), 563–568. https://doi.org/10.1098/rstb.2008.0186

Visnes, T., Grube, M., Hanna, B. M. F., Benitez-Buelga, C., Cázares-Körner, A., & Helleday, T. (2018). Targeting BER enzymes in cancer therapy. *DNA Repair*, *71*(August), 118–126. https://doi.org/10.1016/j.dnarep.2018.08.015

Von Zglinicki, T. (2002). Oxidative stress shortens telomeres. *Trends in Biochemical Sciences*, *27*(7), 339–344. https://doi.org/10.1016/S0968-0004(02)02110-2

Vural, S., Simon, R., & Krushkal, J. (2018). Correlation of gene expression and associated mutation profiles of APOBEC3A, APOBEC3B, REV1, UNG, and FHIT with chemosensitivity of cancer cell lines to drug treatment. *Human Genomics*, *12*(1), 1–21. https://doi.org/10.1186/s40246-018-0150-x

Waks, A. G., & Winer, E. P. (2019). Breast Cancer Treatment: A Review. *JAMA - Journal of the American Medical Association*, *321*(3), 288–300. https://doi.org/10.1001/jama.2018.19323

Wallace, S. S. (2014). Base excision repair: A critical player in many games. *DNA Repair*, *19*, 14–26. https://doi.org/10.1016/j.dnarep.2014.03.030

Wallace, S. S., Murphy, D. L., & Sweasy, J. B. (2012). Base excision repair and cancer. *Cancer Letters*, *327*(1–2), 73–89. https://doi.org/10.1016/j.canlet.2011.12.038

Wang, H., Zhang, S., Song, L., Qu, M., & Zou, Z. (2020). Synergistic lethality between PARP-trapping and alantolactone-induced oxidative DNA damage in homologous recombination-proficient cancer cells. *Oncogene*, *39*(14), 2905–2920. https://doi.org/10.1038/s41388-020-1191-x

Wang, R., Li, C., Qiao, P., Xue, Y., Zheng, X., Chen, H., Ba, X. (2018). OGG1-initiated base excision repair exacerbates oxidative stress-induced parthanatos. *Cell Death and Disease*, *9*(6). https://doi.org/10.1038/s41419-018-0680-0

Wang, Z. Q., Auer, B., Stingl, L., Berghammer, H., Haidacher, D., Schweiger, M., & Wagner, E. F. (1995). Mice lacking ADPRT and poly(ADP-ribosyl)ation develop normally but are susceptible to skin disease. *Genes and Development*, *9*(5), 509–520. https://doi.org/10.1101/gad.9.5.509

Wang, Z., Rhee, D. B., Lu, J., Bohr, C. T., Zhou, F., Vallabhaneni, H., Liu, Y. (2010). Characterization of oxidative guanine damage and repair in mammalian telomeres. *PLoS Genetics*, *6*(5), 28. https://doi.org/10.1371/journal.pgen.1000951

Ward, I. M., & Chen, J. (2001). Histone H2AX Is Phosphorylated in an ATR-dependent Manner in Response to Replicational Stress. *Journal of Biological Chemistry*, *276*(51), 47759–47762. https://doi.org/10.1074/jbc.C100569200

Ward, L. D., & Kellis, M. (2012). HaploReg: A resource for exploring chromatin states, conservation, and regulatory motif alterations within sets of genetically linked variants. *Nucleic Acids Research*, *40*(D1), 930–934. https://doi.org/10.1093/nar/gkr917

Weeks, L. D., Zentner, G. E., Scacheri, P. C., & Gerson, S. L. (2014). Uracil DNA glycosylase (UNG) loss enhances DNA double strand break formation in human cancer cells exposed to pemetrexed. *Cell Death and Disease*, *5*(2). https://doi.org/10.1038/cddis.2013.477

Wendt, C., & Margolin, S. (2019). Identifying breast cancer susceptibility genes–a review of the genetic background in familial breast cancer. *Acta Oncologica*, *58*(2), 135–146. https://doi.org/10.1080/0284186X.2018.1529428

Westra, H.-J., Peters, M. J., Esko, T., Yaghootkar, H., Schurmann, C., Kettunen, J., Franke, L. (2013). Systematic identification of trans eQTLs as putative drivers of known disease associations. *Nature Genetics*, *45*(10), 1238–1243. https://doi.org/10.1038/ng.2756

Whitaker, A. M., Schaich, M. A., Smith, M. S., Flynn, T. S., & Freudenthal, B. D. (2017). Base excision repair of oxidative DNA damage: From mechanism to disease. *Frontiers in Bioscience - Landmark*, *22*(9), 1493–1522. https://doi.org/10.2741/4555

Willoughby, A., Andreassen, P. R., & Toland, A. E. (2019). Genetic testing to guide risk-stratified screens for breast cancer. *Journal of Personalized Medicine*, *9*(1). https://doi.org/10.3390/jpm9010015

Wilson, D. M., & Thompson, L. H. (1997). Commentary Life without DNA repair, *94*(November), 12754–12757.

Wooster, R., Neuhausen, S. L., Mangion, J., Quirk, Y., Ford, D., Collins, N., Stratton, M. R. (1994). Localization of a breast cancer susceptibility gene, BRCA2, to chromosome 13q12-13. *Science*, *265*(5181), 2088–2090. https://doi.org/10.1126/science.8091231

Xanthoudakis, S., Smeyne, R. J., Wallace, J. D., & Curran, T. (1996). The redox/DNA repair protein, Ref-1, is essential for early embryonic development in mice. *Proceedings of the National Academy of Sciences of the United States of America*, *93*(17), 8919–8923. https://doi.org/10.1073/pnas.93.17.8919

Yang, X., Leslie, G., Doroszuk, A., Schneider, S., Allen, J., & Decker, B. (2020). Cancer Risks Associated With Germline PALB2 Pathogenic Variants : An International Study of 524 Families rapid communications abstract, *38*(7), 674–685.

Yap, T. A., Plummer, R., Azad, N. S., & Helleday, T. (2019). The DNA Damaging Revolution: PARP Inhibitors and Beyond. *American Society of Clinical Oncology Educational Book*, (39), 185–195. https://doi.org/10.1200/edbk_238473

Yap, T., & Sandhu, S. (2011). Poly (ADP-Ribose) polymerase (PARP) inhibitors: Exploiting a synthetic lethal strategy in the clinic. *CA: A Cancer Journal for Clinicians*, *61*(1), 31–49. https://doi.org/10.3322/caac.20095.Available

Ye, F., Liu, J., Wang, H., Chen, X., Cheng, Q., & Chen, H. (2020). Cervical carcinoma risk associate with genetic polymorphisms of NEIL2 gene in Chinese population and its significance as predictive biomarker. *Scientific Reports*, *10*(1), 1–13. https://doi.org/10.1038/s41598-020-62040-9

Yi, Y. W., Kang, H. J., & Bae, I. (2014). BRCA1 and oxidative stress. *Cancers*, *6*(2), 771–795. https://doi.org/10.3390/cancers6020771

Youn, C. K., Song, P. I., Kim, M. H., Jin, S. K., Hyun, J. W., Choi, S. J., Ho, J. Y. (2007). Human 8-oxoguanine DNA glycosylase suppresses the oxidative stress-induced apoptosis through a p53-mediated signaling pathway in human fibroblasts. *Molecular Cancer Research*, *5*(10), 1083–1098. https://doi.org/10.1158/1541-7786.MCR-06-0432

Yu, S. W., Wang, H., Poitras, M. F., Coombs, C., Bowers, W. J., Federoff, H. J., Dawson, V. L. (2002). Mediation of poty(ADP-ribose) polymerase-1 - Dependent cell death by apoptosis-inducing factor. *Science*, *297*(5579), 259–263. https://doi.org/10.1126/science.1072221

Zámborszky, J., Szikriszt, B., Gervai, J. Z., Pipek, O., Póti, Á., Krzystanek, M., Szüts, D. (2017). Loss of BRCA1 or BRCA2 markedly increases the rate of base substitution mutagenesis and has distinct effects on genomic deletions. *Oncogene*, *36*(6), 746–755. https://doi.org/10.1038/onc.2016.243

Zerbino, D. R., Achuthan, P., Akanni, W., Amode, M. R., Barrell, D., Bhai, J., Flicek, P. (2018). Ensembl 2018. *Nucleic Acids Research*, *46*(D1), D754–D761. https://doi.org/10.1093/nar/gkx1098

Zharkov, D. O., Mechetin, G. V., & Nevinsky, G. A. (2010). Uracil-DNA glycosylase: Structural, thermodynamic and kinetic aspects of lesion search and recognition. *Mutation Research - Fundamental and Molecular Mechanisms of Mutagenesis*, *685*(1–2), 11–20. https://doi.org/10.1016/j.mrfmmm.2009.10.017

Zhou, J., Chan, J., Lambelé, M., Yusufzai, T., Stumpff, J., Opresko, P. L., Wallace, S. S. (2017). NEIL3 Repairs Telomere Damage during S Phase to Secure Chromosome Segregation at Mitosis. *Cell Reports*, *20*(9), 2044–2056. https://doi.org/10.1016/j.celrep.2017.08.020

Zhou, J., Fleming, A. M., Averill, A. M., Burrows, C. J., & Wallace, S. S. (2015). The NEIL glycosylases remove oxidized guanine lesions from telomeric and promoter quadruplex DNA structures. *Nucleic Acids Research*, *43*(8), 4039–4054. https://doi.org/10.1093/nar/gkv252

Zhou, J., Liu, M., Fleming, A. M., Burrows, C. J., & Wallace, S. S. (2013). Neil3 and NEIL1 DNA glycosylases remove oxidative damages from quadruplex DNA and exhibit preferences for lesions in the telomeric sequence context. *Journal of Biological Chemistry*, *288*(38), 27263–27272. https://doi.org/10.1074/jbc.M113.479055

Zou, J., Wang, C., Ma, X., Wang, E., & Peng, G. (2017). APOBEC3B, a molecular driver of mutagenesis in human cancers. *Cell and Bioscience*, *7*(1), 1–7. https://doi.org/10.1186/s13578-017-0156-4

APPENDIX I:
Supplementary Tables and Figures

Supplementary Tables

Supplementary Table S1 - FBOC series description

	BRCA1	*BRCA2*	BRCAX	Controls	Total
Average age	48.5	50.2	50.3	48.7	**49.5**
Families	32	31	110	-	**173**
***BRCA1/2* healthy carriers**	25	34	-	-	**59**
Cancer cases	26	28	120	-	**174**
rs804271 genotying	40	46	-	80	**166**
rs34259 genotyping	51	63	120	110	**344**
***NEIL2* mRNA expression**	24	30	-	29	**83**
***UNG* mRNA expression**	37	53	104	83	**277**
UNG protein expression	-	20	-	10	**30**
Uracil at telomeres	42	63	115	108	**328**
Telomere oxidation	23	19	68	62	**172**
Protein carbonylation	29	27	31	20	**107**
Telomere length	36	32	85	91	**244**
Telomerase activity	13	15	38	47	**113**

Supplementary Table S2 - Panel of LCLs (n=20)

LCL ID[a]	*BRCA1* mutation[b]	BRCA1 Exon	Age[c]	rs804271 genotype	rs34259 genotype
06S179-L	WT	-	31	GT	GG
09S797-L[1]	WT	-	27	TT	GG
10S889-L[2]	WT	-	20	GT	GG
11S66-L[3]	WT	-	30	GT	GG
11S534-L[4]	WT	-	50	GT	GC
11S954-L	WT	-	35	GT	GC
11S375-L	WT	-	23	GT	GG
10S890-L[2]	c.5123C>A; p.Ala1708Glu	18	25	GT	GG
10S1202-L	c.5123C>A; p.Ala1708Glu	18	53	GT	GC
11S65-L[5]	c.5117G>A; p.Gly1706Glu	18	31	GT	GG
11S67-L[5]	c.5117G>A; p.Gly1706Glu	18	34	GG	GC
07S1291-L	c.3239T>A; p.Leu1080X	11	34	GT	GC
09S798-L[1]	c.2410C>T; p.Gln804X	11	24	GG	GC
09S546-L	c.212+1G>A; p.?	5	42	TT	GG
11S376-L[6]	c.212+1G>A; p.?	5	39	GT	GG
11S384-L[6]	c.212+1G>A; p.?	5	75	GT	GG
09S491-L	c.815_824dup10; p.Thr276fs	11	24	GT	GG
10S44-L	c.4309delT; p.Ser1437fs	13	22	GG	GC
10S1177-L[3]	c.68_69delAG; p.Glu23fs	2	27	TT	GG
11S1004-L[4]	c.981_982delAT; p.Cys328X	11	25	GT	GG

[a]1-6 indicate which LCLs were established from relatives (sisters or mother/daughter)
[b]Mutation nomenclature based on GenBank reference sequences NM_007294.3 with numbering starting at the A of the first ATG, following the journal guidelines (www.hgvs.org/mutnomen); p.?, unknown protein nomenclature (variant causing skipping of exon 5 of *BRCA1*)
[c]Age of women at the time of blood extraction to establish LCL

Supplementary Table S3 - Set of prophylactic oophorectomies (n=17)

Sample ID	Gene	Mutation[a]	rs34259 genotype
06N196	*BRCA2*	Not reported	GG
OV050707	*BRCA2*	Not reported	GG
OV070807	*BRCA1*	Not reported	GG
OV140108	*BRCA1*	c.1240delCAinsT	GC
OV110408	*BRCA1*	c.3450-3453delCAAG	GG
OV060608	*BRCA2*	Not reported	GC
OV120608	*BRCA1*	Not reported	GG
OV061008	*BRCA1*	Not reported	GC
10NN1	*BRCA1*	Not reported	GG
11NN1	*BRCA2*	c.658_659delGT; p.Val220fs	GG
11NN2	*BRCA1*	c.1790delA; p.K558 fsX13	GG
13NN24	*BRCA1*	c.470_471del; p.Ser157X	GG
13NN27	*BRCA2*	c.9026_9030del; p.Tyr3009Serfs	GC
14NN29	*BRCA2*	c.5350_5351delinsT; p.Asn1784	GG
15NN33	*BRCA2*	c.2957delA; p.Asn986fs	GC
15NN34	*BRCA2*	Not reported	GG
16NN38	*BRCA1*	c.4107_4110dupATCT; p.Gly1371	GG

[a]Mutation nomenclature based on HGVS-nomenclature (*http://varnomen.hgvs.org/)*

Supplementary Table S4 - Cell lines authentication by STR profiling

Cell line	**U2OS**		**MDA-MB-231**		**MDA-MB-436**	
GenePrint10 Marker	Ref. Sample (CVCL_0042)	Test Sample	Ref. Sample (CVCL_0062)	Test Sample	Ref. Sample (CVCL_0623)	Test Sample
TH01	6, 9.3	6, 9.3	7, 9.3	7, 9.3	9.3	9.3
D21S11	31	31	30, 33.2	30, 33.2	30, 31.2	30, 31.2
D5S818	8, 11	8, 11	12	12	13	13
D13S317	13	13	13	13	10	10
D7S820	11, 12	11, 12	8, 9	8, 9	10	10
D16S539	11, 12	11, 12	12	12	9, 11	9, 11
CSF1PO	12, 13	12, 13	12, 13	12, 13	12	12
AMEL	X	X	X	X	X	X
vWA	14, 18	14, 18	15, 18	15, 18	14, 20	14, 20
TPOX	11, 12	11, 12	8, 9	8, 9	8	8
Percent Match (PM)[a]	100%		100%		100%	

[a]PM= (shared alleles)*2*100/[Total alleles in (Test Sample + Reference Sample)]

Supplementary Table S5 - Specific conditions for glycosylase incubations

Glycosylase	Concentration	Incubation Time (h)	DNA amount (ng)
UNG	0,13 µM	0,5	130
NEIL2	5,6 µM	4	200
OGG1	2,4 µM	4	40
FPG	12 Units	12	400

Supplementary Table S6 - Primers used in this Doctoral Thesis

Primer pair	5'-3' Forward primer	5'-3' Reverse primer
GAPDH-cDNA	CCTGCACCACCAACTGCTTA	CCATCACGCCACAGTTTCC
NEIL2-cDNA	GTCACACCCACCTGTGACAT	GCACTCAGGACTGAACCGAG
UNG-cDNA	TTGTTCATCCTGGCCATGGA	ACTGCCCTTCTTCTGAGCAT
UNG1-cDNA	ATGGGCGTCTTCTGCCTTG	CTCTGGATCCGGTCCAACTG
UNG2-cDNA	CCTCCTCAGCTCCAGGATGA	TCGCTTCCTGGCGGG
OGG1-cDNA	GGAGGCTCATCTCAGGAAGC	AGTTCCTTGTTGGTCTGGGG
BRCA1-cDNA	GAAGCAGCATCTGGGTGTGA	ATTTCGCAGGTCCTCAAGGG
OGG1-exon2	CGCCATGCCCGGTTAAATTT	CCTCTTGGAAGTGGGAGTCC
BRCA1-exon11A	AGTTGGTTGATTTCCACCTC	CCAGTGATCCTCATGAGGCT
36B4 loci	CAGCAAGTGGGAAGGTGTAATCC	CCCATTCTATCATCAACGGGTACAA
MT-TF	CCCCTCCCCAATAAAGCTAA	TGTGGCTCGTAGTGTTCTGG
Telomeric DNA	CGGTTTGTTTGGGTTTGGGTTTGG GTTTGGGTTTGGGTT	GGCTTGCCTTACCCTTACCCTTACCC TTACCCTTACCCT

Supplementary Table S7- Linear regression analysis in *BRCA1/2* carriers regarding cancer status

Dependent variables	Independent variable	β coefficient[a]	p-value[b]	95% C. I. ((Lower) - (Upper limit))
***NEIL2* mRNA expression**	Cancer	0.231	0.091	((-0.585)-(0.811))
***UNG* mRNA expression**	Cancer	0.029	0.773	((-0.269)-(0.201))
Adjusted TL	Cancer	-0.109	0.373	((-1.244)-(0.473))
% Short telomeres	Cancer	0.209	0.081	((-0.422)-(7.002))
Telomere oxidation	Cancer	-0.218	0.156	((-4.381)-(0.437))
Uracil at telomeres	Cancer	-0.014	0.889	((-0.393)-(0.341))
Telomerase activity	Cancer	-0.237	0.072	((-55.006)-(2.415))
Carbonylation	Cancer	-0.234	0.078	((-0.033)-(0.605))

[a]β coefficients quantify how much the independent variable (cancer status) modify the dependent variables. [b]Unpaired *t*-test was used to check the significance of individual regression coefficients in the multiple linear regression model

Supplementary Table S8 - Variants within the block of linkage disequilibrium (LD) > 0.9 with rs804271 or rs34259

Variant	Ref	Alt	Position	Gene	Location[a]	r^2 (LD)
rs804271	**C**	**A**	**11:769705**	***NEIL2***	**5'-UTR**	**-**
rs804270	G	C	11:770112	*NEIL2*	5'-UTR	0.91
rs2740435	C	T	11:770962	*NEIL2*	intronic	0.93
rs804266	A	T	11:772343	*NEIL2*	intronic	0.93
rs804265	A	T	11:772572	*NEIL2*	intronic	0.93
rs804263	C	T	11:773406	*NEIL2*	intronic	0.93
rs804261	A	G	11:774053	*NEIL2*	intronic	0.91
rs34259	**G**	**C**	**12:109113428**	***UNG***	**3' UTR**	-
rs34261	G	A	12:109114490	*UNG*	3' UTR	0.971065
rs34262	C	T	12:109114670	*UNG*	3' UTR	0.971065
rs34263	A	G	12:109115044	*UNG*	3' UTR	1
rs2436630	G	A	12:109124655	*UNG*	3' UTR	0.918382

[a]In some cases, the SNPs can reside in more than one location, depending on the isoform of the gene. Only one gene location is shown in the table

Supplementary Table S9 - Summary of information in the GTEx portal regarding SNPs effect on transcriptional regulation in different tissues.

Gene	SNP	P-Value	Effect size	Tissue
NEIL2	rs804271	6.3e-50	0.48	Nerve - Tibial
NEIL2	rs804271	1.7e-27	0.34	Heart - Atrial Appendage
NEIL2	rs804271	1.5e-23	0.32	Artery - Tibial
NEIL2	rs804271	5.2e-22	0.29	Adipose - Subcutaneous
NEIL2	rs804271	3.0e-20	0.26	Thyroid
NEIL2	rs804271	2.5e-17	0.25	Adipose - Visceral (Omentum)
NEIL2	rs804271	2.9e-17	0.29	Whole Blood
NEIL2	rs804271	5.2e-17	0.24	Muscle - Skeletal
NEIL2	rs804271	1.5e-16	0.32	Artery - Aorta
NEIL2	rs804271	2.8e-16	0.43	Pituitary
NEIL2	rs804271	1.3e-15	0.50	Ovary
NEIL2	rs804271	1.5e-13	0.28	Cells - Cultured fibroblasts
NEIL2	rs804271	1.7e-12	0.21	Heart - Left Ventricle
NEIL2	rs804271	5.5e-11	0.22	Breast - Mammary Tissue
NEIL2	rs804271	8.0e-10	0.36	Brain - Putamen (basal ganglia)
NEIL2	rs804271	1.4e-9	0.25	Colon - Sigmoid
NEIL2	rs804271	2.1e-9	0.29	Artery - Coronary
NEIL2	rs804271	3.4e-9	0.18	Esophagus - Muscularis
NEIL2	rs804271	5.0e-9	0.31	Brain - Caudate (basal ganglia)
NEIL2	rs804271	5.2e-9	0.27	Esophagus - Gastroesophageal Junction
NEIL2	rs804271	1.0e-8	0.35	Brain - Hypothalamus
NEIL2	rs804271	1.7e-7	0.41	Uterus
NEIL2	rs804271	1.9e-7	0.37	Vagina
NEIL2	rs804271	2.2e-7	0.26	Brain - Hippocampus
NEIL2	rs804271	2.6e-7	0.35	Prostate
NEIL2	rs804271	0.0000021	0.30	Brain - Cortex
NEIL2	rs804271	0.0000027	0.27	Liver
NEIL2	rs804271	0.0000036	0.21	Pancreas
NEIL2	rs804271	0.0000052	0.17	Stomach
NEIL2	rs804271	0.0000056	0.27	Brain - Nucleus accumbens
NEIL2	rs804271	0.0000079	0.43	Brain - Spinal cord (cervical c-1)
NEIL2	rs804271	0.000022	0.22	Adrenal Gland
NEIL2	rs804271	0.000029	0.17	Lung
NEIL2	rs804271	0.00007	0.282	Brain - Amygdala
NEIL2	rs804271	0.00008	0.298	Brain - Substantia nigra
NEIL2	rs804271	0.000094	0.258	Brain - Frontal Cortex
NEIL2	rs804271	0.00022	0.181	Small Intestine - Terminal Ileum
NEIL2	rs804271	0.0003	0.255	Brain - Cerebellum
NEIL2	rs804271	0.0012	0.262	Cells - EBV-transformed lymphocytes
NEIL2	rs804271	0.0013	0.102	Testis
NEIL2	rs804271	0.0014	0.260	Minor Salivary Gland
NEIL2	rs804271	0.0016	0.230	Brain - Anterior cingulate cortex
NEIL2	rs804271	0.0044	0.180	Spleen
NEIL2	rs804271	0.008	0.0867	Colon - Transverse
NEIL2	rs804271	0.009	0.365	Kidney - Cortex
NEIL2	rs804271	0.04	0.125	Brain - Cerebellar Hemisphere
UNG	rs34259	6.8e-16	-0.184	Whole Blood
UNG	rs34259	2.5e-4	-0.198	Adrenal Gland
UNG	rs34259	5.5e-4	-0.0870	Muscle - Skeletal
UNG	rs34259	3.3e-3	-0.195	Liver
UNG	rs34259	4.6e-3	-0.0964	Lung
UNG	rs34259	4.7e-3	-0.0828	Adipose - Subcutaneous
UNG	rs34259	0.02	-0.151	Artery - Coronary
UNG	rs34259	0.03	-0.0793	Adipose - Visceral (Omentum)
UNG	rs34259	0.03	-0.112	Pancreas
UNG	rs34259	0.03	-0.284	Kidney - Cortex
UNG	rs34259	0.03	-0.0606	Colon - Transverse
UNG	rs34259	0.03	-0.141	Pituitary
UNG	rs34259	0.04	-0.119	Brain - Cerebellum

Supplementary Figures

MDA-MB-231 BRCA1-KO clons

BRCA1ko1

```
     Wild type AATACTCATGCCAGCTCATTACAGCATGAGAACAGCAGTTTATTACTCACTAAAGACAGAAT…
Modification 1 AATACTCATGCCAGCT***********GAGAACAGCAGTTTATTACTCACTAAAGACAGAAT…
Modification 2 AATACTCATGCCAGCT**TTACAGCATGAGAACAGCAGTTTATTACTCACTAAAGACAGAAT…
Modification 3 AATA***************************ACAGCAGTTTATTACTCACTAAAGACAGAAT…
Modification 4 AA***************************GAACAGCAGTTTATTACTCACTAAAGACAGAAT…
```

BRCA1ko2

```
     Wild type AATACTCATGCCAGCTCATTACAGCATGAGAACAGCAGTTTATTACTCACTAAAGACAGAAT…
Modification 1 AATACTCATGCCAGCT*ATTACAGCATGAGAACAGCAGTTTATTACTCACTAAAGACAGAAT…
Modification 2 AATAC************ATTACAGCATGAGAACAGCAGTTTATTACTCACTAAAGACAGAAT…
Modification 3 AATACT************TTACAGCATGAGAACAGCAGTTTATTACTCACTAAAGACAGAAT…
Modification 1 AATACTCATGCCAGC*CATTACAGCATGAGAACAGCAGTTTATTACTCACTAAAGACAGAAT…
```

Supplementary Figure S1 – DNA sequencing confirm *BRCA1* gene disruption in BRCA-KO clones. Deleted and inserted nucleotides in BRCA1-KO clones giving rise to premature termination codons in the *BRCA1* open reading frame. Sequences of guide RNA are indicated in green letters and red (*) indicate nucleotide deletion.

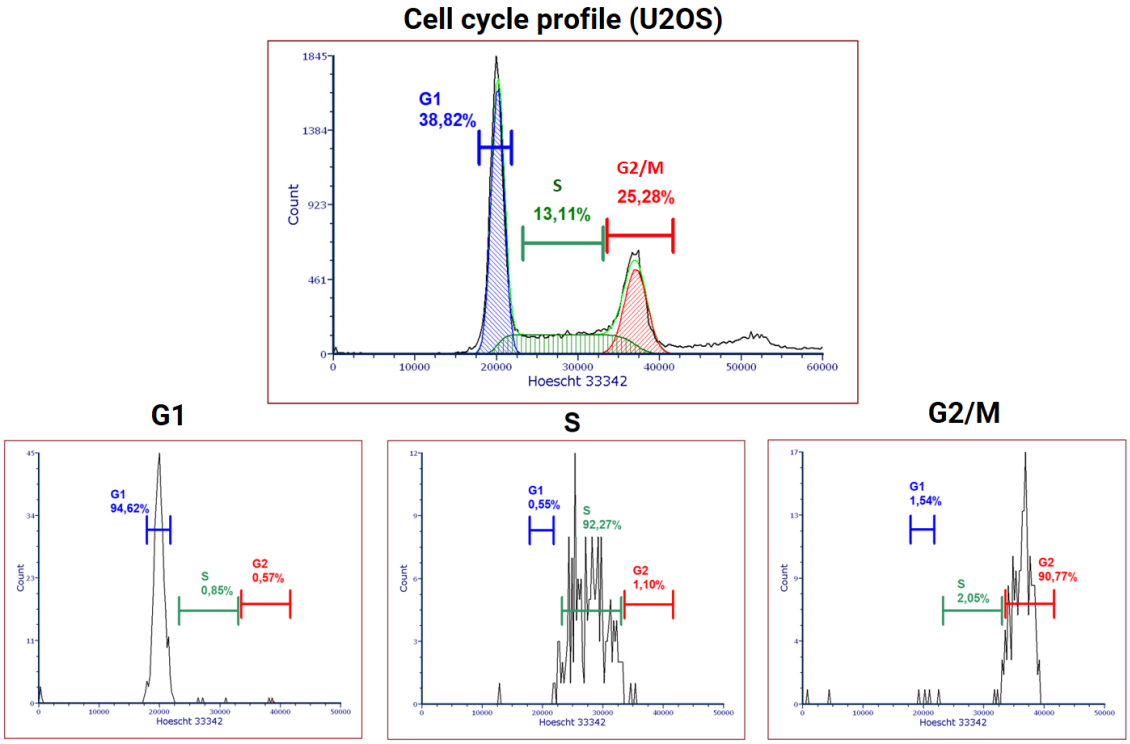

Supplementary Figure S2 – U2OS cells sorting by cell cycle phase. U2OS cell cycle profile and the establishment of sorted-cells populations according to cell cycle phases (G1, S, G2/M). Post-sort purity check of the resulting sorted populations. The purity was higher than 90% in all cases.

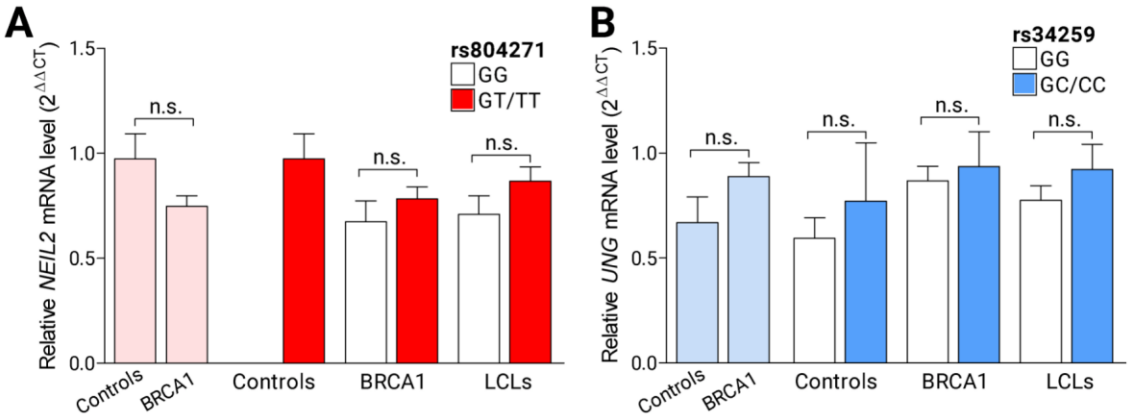

Supplementary Figure S3 - *NEIL2* and *UNG* mRNA levels in the panel of LCLs. A) Comparative analysis of *NEIL2* mRNA expression according to the *NEIL2* SNP rs804271 status [(non-carriers (GG) Vs carriers (GT/TT)]. **B)** Comparative analysis of *UNG* mRNA expression according to the *UNG* SNP rs34259 status [(non-carriers (GG) Vs carriers (GC/CC)]. Bars represent the mean and the SEM for each group. Unpaired student t-test was used to test for potential significant differences between means.

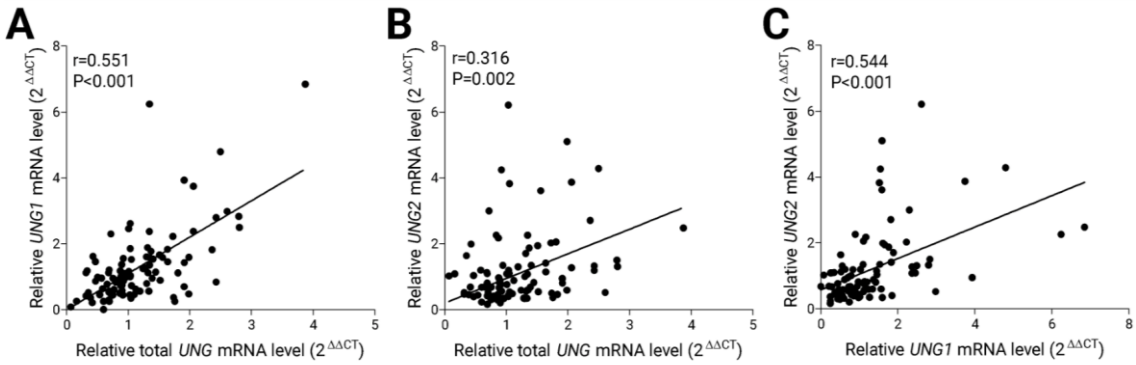

Supplementary Figure S4 – Correlations regarding UNG mRNA expression levels in the FBOC series. A) Correlation analysis between total *UNG* mRNA expression and *UNG1* mRNA expression. **B)** Correlation analysis between total *UNG* mRNA expression and *UNG2* mRNA expression. **C)** Correlation analysis between *UNG1* mRNA and *UNG2* mRNA expression. Spearman's test was used to assess the significance of the correlations.

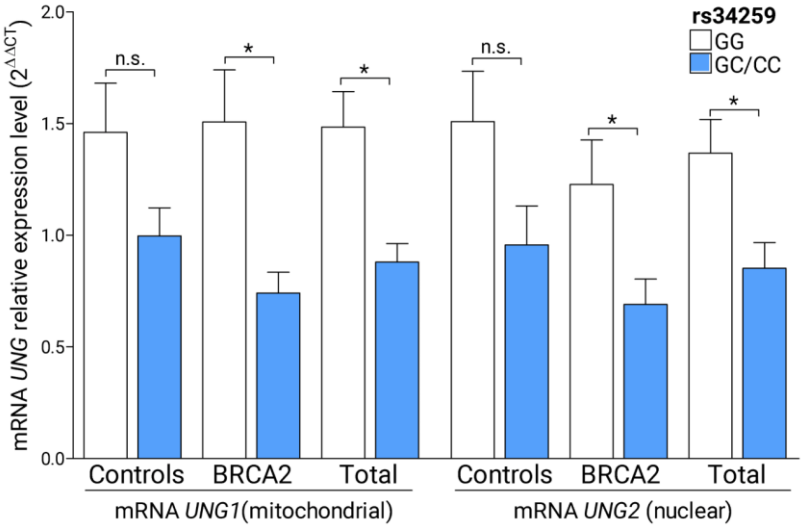

Supplementary Figure S5 - mRNA expression levels of specific isoforms of *UNG* in *BRCA2* mutation carriers and controls from the FBOC series. *UNG1* (mitochondrial) and *UNG2* (nuclear) mRNA expression according to the presence or absence of the UNG SNP rs34259 [non-carriers (GG)/carriers (GC/CC)]. Bars reflect the mean and the SEM. Unpaired t-tests were performed for statistical significance.

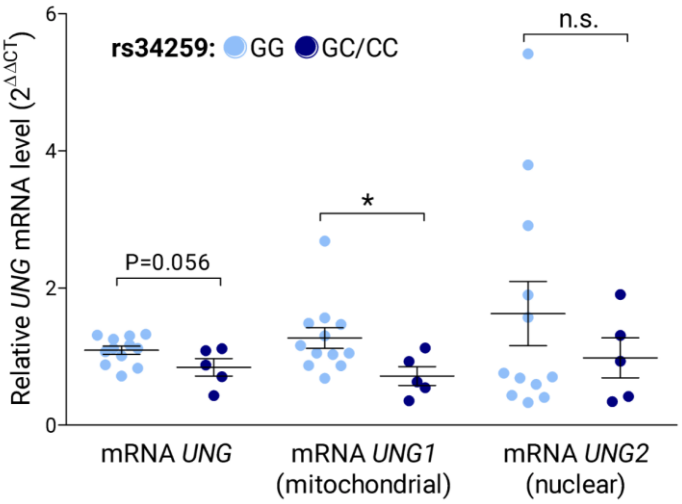

Supplementary Figure S6 – *UNG* mRNA expression levels in ovarian biopsies. Total *UNG*, *UNG1* (mitochondrial) and *UNG2* (nuclear) mRNA expression according to the *UNG* SNP rs34259 [non-carriers (GG)/carriers (GC/CC)]. Bars reflect the mean and the SEM. Unpaired t-tests were performed for statistical significance.

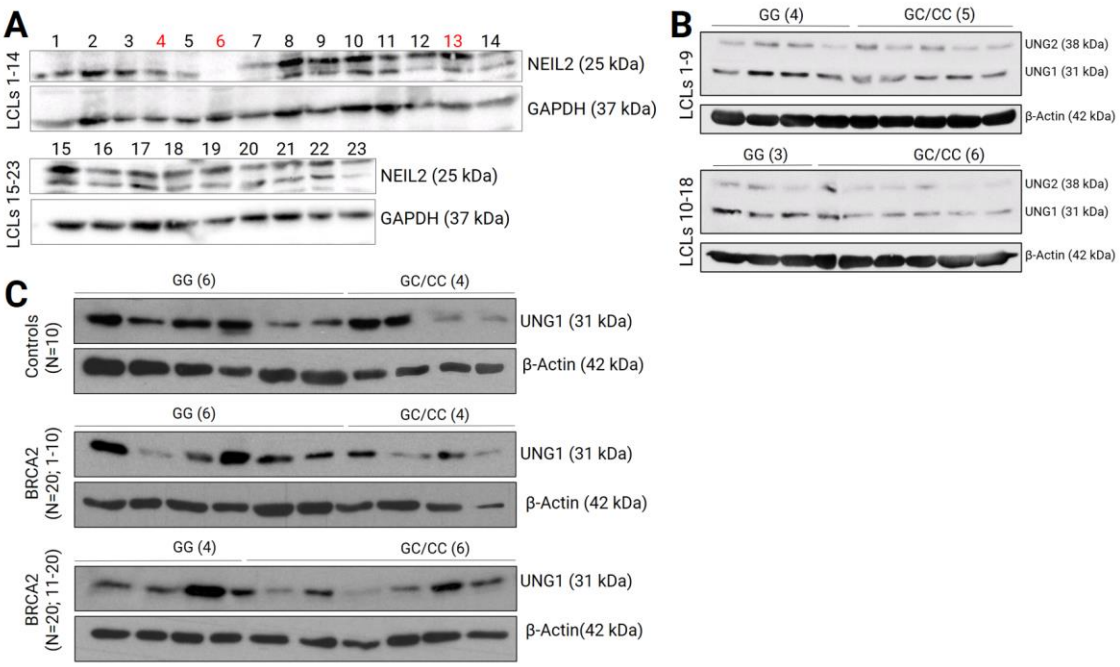

Supplementary Figure S7 - NEIL2 and UNG relative protein expression by Western blotting. A) NEIL2 expression in the panel of LCLs. In red 3 LCLs (4,6,13) that could not be included in different analyses. **B)** UNG1 and UNG2 expression in the panel of LCLs (n=18) according to the *UNG* SNP genotype [non-carriers (GG)/carriers (GC/CC)]. **C)** UNG1 protein levels in a subset of controls (n = 10) and *BRCA2* mutation carriers (n = 20) from the FBOC series according to the *UNG* SNP genotype.

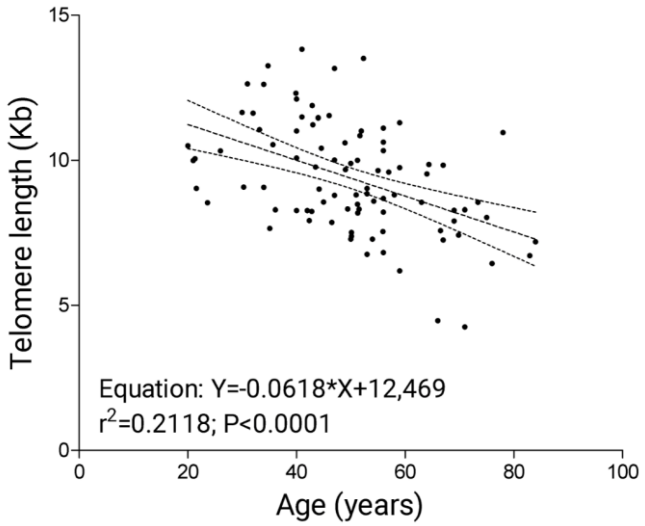

Supplementary Figure S8 – Telomere length adjusted by age. TL distribution in PBMC from the controls of the FBOC series (n=91) as a function of age. The regression line is shown (y= -0.0618 x age + 12.469; r2=0.212; p<0.0001).

APPENDIX II:
Publications

www.impactjournals.com/oncotarget/ Oncotarget, 2017, Vol. 8, (No. 70), pp: 114626-114636

Research Paper

Genetic variation in the *NEIL2* DNA glycosylase gene is associated with oxidative DNA damage in *BRCA2* mutation carriers

Carlos Benítez-Buelga[1], Juan Miguel Baquero[1], Tereza Vaclova[1], Victoria Fernández[1], Paloma Martín[1,4], Lucia Inglada-Perez[2,4], Miguel Urioste[3,4], Ana Osorio[1,4] and Javier Benítez[1,4]

[1]Human Genetics Group, Spanish National Cancer Research Center (CNIO), Madrid, Spain

[2]Endocrine Cancer Group, Spanish National Cancer Research Center (CNIO), Madrid, Spain

[3]Familial Cancer Unit, Spanish National Cancer Research Center (CNIO), Madrid, Spain

[4]Spanish Network on Rare Diseases (CIBERER), Madrid, Spain

Correspondence to: Javier Benítez, **email:** jbenítez@cnio.es

Keywords: *BRCA1 and BRCA2; NEIL2 polymorphism cancer risk modifier; mRNA levels; oxidative DNA damage*

Received: *March 28, 2017* ***Accepted:*** *October 27, 2017* ***Published:*** *November 23, 2017*

ABSTRACT

In this report, we have tried to gain molecular insight into a single nucleotide polymorphism (SNP) in the *NEIL2* gene previously identified as "cancer risk modifier" for *BRCA2* mutation carriers.

To that end, we studied the role of this SNP (rs804271) on *NEIL2* transcriptional regulation, oxidative DNA damage and genome instability in two independent set of samples: The first one was a series of eighty-six *BRCA1* and *BRCA2* mutation carriers and eighty non-carrier controls in which we evaluated the effect of the SNP on *NEIL2* gene expression and oxidative DNA damage accumulation. The second was a set of twenty lymphoblastoid cell lines (LCLs), thirteen *BRCA1* mutation carriers and seven non-carriers control, that were used to analyze the correlation between *NEIL2* mRNA and/or protein levels, the oxidative and the double stranded break (DSB) DNA damage levels.

Our results suggest that an excessive production of NEIL2 enzyme, associated with the SNP, may have a deleterious effect modifying cancer risk susceptibility in *BRCA2* mutation carriers. We hypothesize that due to the SNP impact on *NEIL2* transcriptional upregulation, a cascade of events may converge in the accumulation of oxidative DNA damage and its posterior conversion into DSBs for this specific group of patients.

INTRODUCTION

The tumor suppressor genes *BRCA1* and *BRCA2* maintain genomic stability through their involvement in homologous recombination (HR) double-stranded break DNA repair among other processes [1].

Carrying a mutation in the *BRCA1* or *BRCA2* genes increases a woman's lifetime risk of developing breast and ovarian cancer, although there are considerable differences in disease manifestation. At the age of 80, cumulative cancer risk for *BRCA1* and *BRCA2* mutation carriers ranges from 72% to 69% for breast cancer development, and from 44% to 17% for ovarian cancer [2]. This high variability may be explained by other genetic modifiers and/or environmental factors.

Given the relation of synthetic lethality that exists between one of the components of the Base Excision Repair (BER) pathway, *PARP1* (poly[ADP-ribose] polymerase 1), and both *BRCA1* and *BRCA2* genes [3], it is likely that other members of the BER pathway exhibit a similar behavior. We hypothesized that common genetic variants in genes involved in BER might modify a woman's lifetime risk of developing breast and ovarian cancer if she is a *BRCA1* or *BRCA2* mutation carrier. In particular, two Single Nucleotide Polymorphisms (SNPs) in the *OGG1* and *NEIL2* genes were identified as cancer

risk modifiers for *BRCA1* and *BRCA2* mutation carriers, respectively [4]. Although the molecular mechanism underlying these associations is not clear yet, both SNP_S were in transcriptional regulatory regions of genes encoding DNA glycosylase enzymes which play an important role in the first steps of the pathway.

The BER pathway corrects base lesions from deamination, oxidation or methylation [5, 6] which represent the majority of endogenous DNA damage due to chemical reactions during cellular metabolism [7]. There are 11 DNA glycosylases which have the ability of recognizing a wide variety of lesions thanks to a DNA binding domain, the helix-hairpin helix DNA binding motif (like OGG1) [8] and the helix-2turn-helix domain (like NEIL2) [9]. In bi-functional DNA glycosylases, like OGG1 or NEIL2, base lesions are excised from the DNA thanks to its glycosylase activity and AP lyase activity, although they may have different DNA-structure/substrate affinities. For example, the OGG1 incises DNA at 8-oxoG residues, and is active only on duplex DNAs [10]. In contrast, NEIL2 shows preferential activity on bubble DNA or single-stranded DNA regions [11] and present high incising activity for several cytosine-derived lesions with robust activity for 5-hydroxyuracil and weaker activity for dihydrouracil, 5-hydroxycytosine, thymine glycol and 8-oxoG [10] .

If they are not repaired, these lesions may evolve into mutation (C:G→T transversions [12] or DNA single-strand [7] or double-strand breaks (DSBs) [13, 14], which are the principal source of genomic instability [15, 16].

Certain SNPs in DNA glycosylase genes could affect negatively to the general performance of the BER pathway and contribute by increasing the levels of genome instability and hence to a higher cancer risk, especially in presence of a defective *BRCA1* or *BRCA2* background. As an example, we previously identified that the single nucleotide polimorphism "rs2304277", located 1.8Kb downstream the 3'-untranslated region (UTR) of *OGG1* gene, was associated with an increased ovarian cancer risk for *BRCA1* mutation carriers [4]. We tried to explain this cancer association at a molecular level and we discovered that the SNP was associated with a constitutive *OGG1* transcriptional down-regulation, which contributed to a higher genome and telomere instability, especially in those individuals harboring mutations in *BRCA1* [17].

Similarly, the SNP rs804271, localized within the *NEIL2* promoter region, is associated with increased breast cancer risk for *BRCA2* mutation carriers [4]. This SNP forms part of several transcription-factor binding motifs that are responsive to oxidative stress [18]. It has previously been reported that SNPs 5´- UTR upstream the coding region of the *NEIL2* gene influence gene transcription levels and alter levels of genetic damage [19]. In this study, we have explored in two independent set of samples with different BRCA status the role of this SNP at transcriptional level and its possible implication on DNA damage and genome instability to explain its cancer risk modifier effect.

RESULTS

SNP frequency in FBOC series

We genotyped the rs804271 in FBOC (familial breast and ovarian cancer) individuals, and we found a SNP allelic frequency of 0.39, similar as reported for European population 0.41 in Ensembl data base (http://www.ensembl.org). No significant differences in the genotypic frequencies were detected among the different BRCA and control groups (Supplementary Table 1).

NEIL2 mRNA levels are activated by rs804271 SNP: *In silico* studies (HaploReg and GTEX public data), FBOC series and LCLs

The SNP rs804271 is located at the 5′- UTR region of the *NEIL2* gene, within a transcriptional regulatory domain at Transcriptional Start Site (TSS) of the gene. We explored the possible phenotypic effects of this SNP by using HaploReg Database web server [20] and we found that 18 proteins are predicted to interact within TSS and 3 binding motifs for transcription factors TFs (E2F1, SIN3A and YY1) are predicted to be altered in the presence of this specific SNP (rs804271), (Supplementary Table 2).

Because transcriptional changes could be expected due to the modifications by this SNP at the TSS, we used the GTEx eQTL web server [21] (http://www.gtexportal.org) to test whether rs804271 was associated with changes on *NEIL2* mRNA levels in different tissues. Overall, we found significant increased *NEIL2* mRNA levels for 30 tissues, including breast ($p = 1*10^{-4}$), ovary ($p = 1.4 * 10^{-14}$), and blood ($p = 6.6 * 10^{-13}$), Supplementary Table 3 although in some of them, such as "Cells - EBV-transformed lymphocytes (LCLs)" the effect was "moderated" (Supplementary Figure 1).

In parallel, we measured *NEIL2* mRNA expression levels in FBOC series considering both, the BRCA mutational status and the presence or absence of the NEIL2- variant to stratify and compare expression values among groups. We found no significant differences in the *NEIL2* mRNA levels between *BRCA1* and/or *BRCA2* mutation carriers compared to controls (Figure 1A). In contrast, when we stratified by the presence of the SNP we detected a common *NEIL2* mRNA up-regulation pattern that was similar for each BRCA mutational group (Figure 1B). We performed linear regression analysis to confirm that the rs804271 was associated with significant higher *NEIL2* mRNA levels ($\beta = 0.24$; $p = 0.01$) among the FBOC individuals.

Finally, we measured *NEIL2* mRNA basal levels among the 20 LCLs considering the BRCA and SNP status. Although we detected higher *NEIL2* mRNA levels

for those LCLs harboring the SNP, these differences were not significant (Supplementary Figure 2). This result confirmed the tissue variability previously observed in the data provided by GTEX (Supplementary Figure 1).

NEIL2 mRNA and protein levels are correlated and both predict NEIL2-derived DNA damage

Because protein sample from FBOC series was not available, we decided to use the LCL panel ($n = 20$) to test NEIL2 protein levels (Supplementary Figure 3). Spearman correlation analysis confirmed that *NEIL2* mRNA and protein levels were significantly correlated among LCLs in basal conditions ($r = 0.51$; $p = 0.02$), Figure 2A.

In parallel, we measured in the DNA extracted from the same LCLs ($n = 20$), the amount of base lesions that are recognized and processed by NEIL2 (NEIL2-lesions) at telomeres (detailed information in the material and methods section). We selected this region because NEIL-protein family members have been described to be active at telomeres [22]. Then, we performed a correlation analysis between the *NEIL2* mRNA/ protein levels and the relative number of "NEIL2-lesions" detected, independently of the BRCA or the SNP status. We found that both *NEIL2* mRNA and NEIL2 protein levels were significantly correlated with the relative number of telomeric "NEIL2-lesions¨ ($r = 0.65$; $p = 0.001$ and $r = 0.51$; $p = 0.01$, respectively), (Figure 2B and 2C).

The rs804271 is associated to higher levels of NEIL2-lesions at telomeres in FBOC series

When considering the BRCA status and NEIL2 genotypes, we found significantly higher amount of "NEIL2-lesions" in *BRCA1* and *BRCA2* mutation carriers compared with controls ($p = 0.01$ and $p < 0.0001$ respectively), (Figure 3A). Moreover, when we considered the presence of the SNP (rs804271) we found that those individuals presenting both genetic events (BRCA mutation together with the SNP) presented significantly higher levels of "NEIL2-lesions", compared to their *BRCA1/ BRCA2* counterparts without the SNP or controls ($p < 0.05$), (Figure 3B).

Because FPG (formamidopyrimidine [fapy]-DNA glycosylase) (e. *coli*) recognizes specifically oxidative purines lesions (8-oxoG/methylFapyG) [23], we measured in the DNA from our FBOC individuals the relative amount of "FPG-lesions". Then, we performed correlation analysis between ("FPG-lesions" and "NEIL2-lesions") and we detected a significant correlation between both type of lesions ($r = 0.40$; $p = 0{,}03$), (Supplementary Figure 4A), which suggest that that from the wide range of lesions that NEIL2 can recognize [10], the presence of the SNP among *BRCA1* and *BRCA2* mutation carriers lead preferentially to the accumulation of purine lesions (8-oxoG or methylFapyG).

Because telomeres are susceptible to uracil miss incorporation which is primarily recognized and removed by the uracil DNA glycosylase (UNG) [24], we have

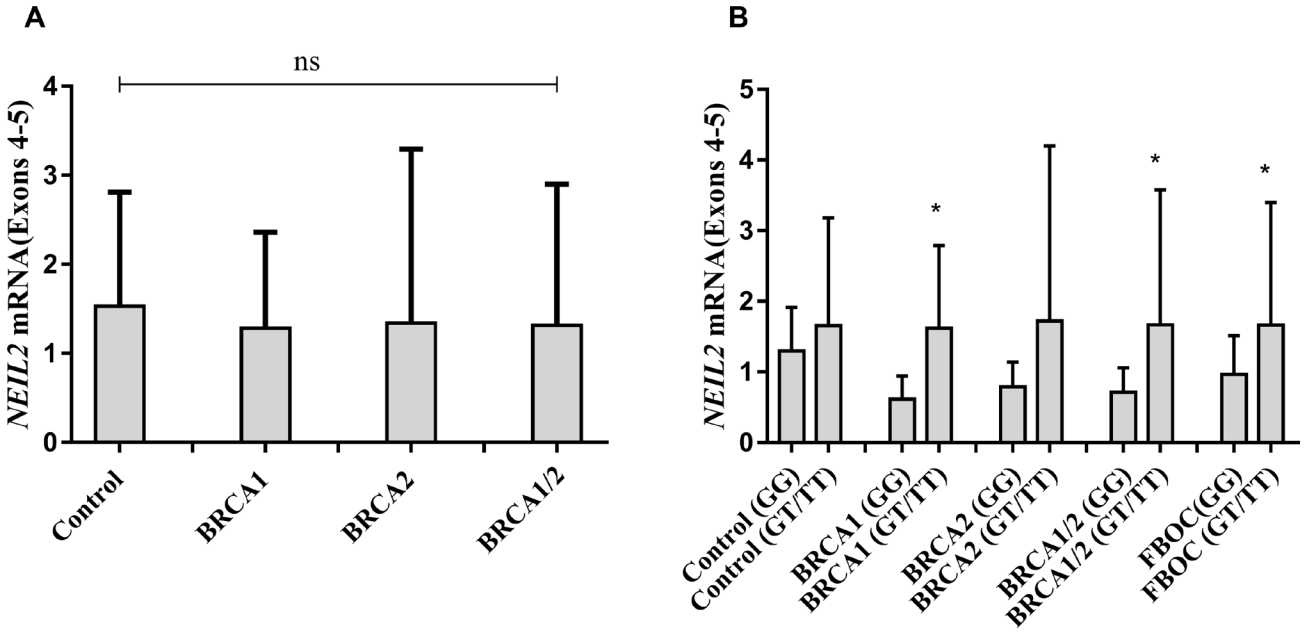

Figure 1: (**A**) Comparative analysis of *NEIL2* mRNA expression according BRCA mutational status in FBOC series (*BRCA1* and *BRCA2* mutation carriers are compared with Controls). (**B**) Comparative analysis of *NEIL2* mRNA expression according the SNP status ((Carriers (GT/TT) *Vs* Non-carriers (GG)) among the different FBOC groups (*BRCA1, BRCA2* mutation carriers and *BRCA1/BRCA2* non-carrier Controls). Bars represent the mean and the standard deviation for each group. Unpaired student t test was used to test for potential significant differences between means. ($^*p < 0.05$).

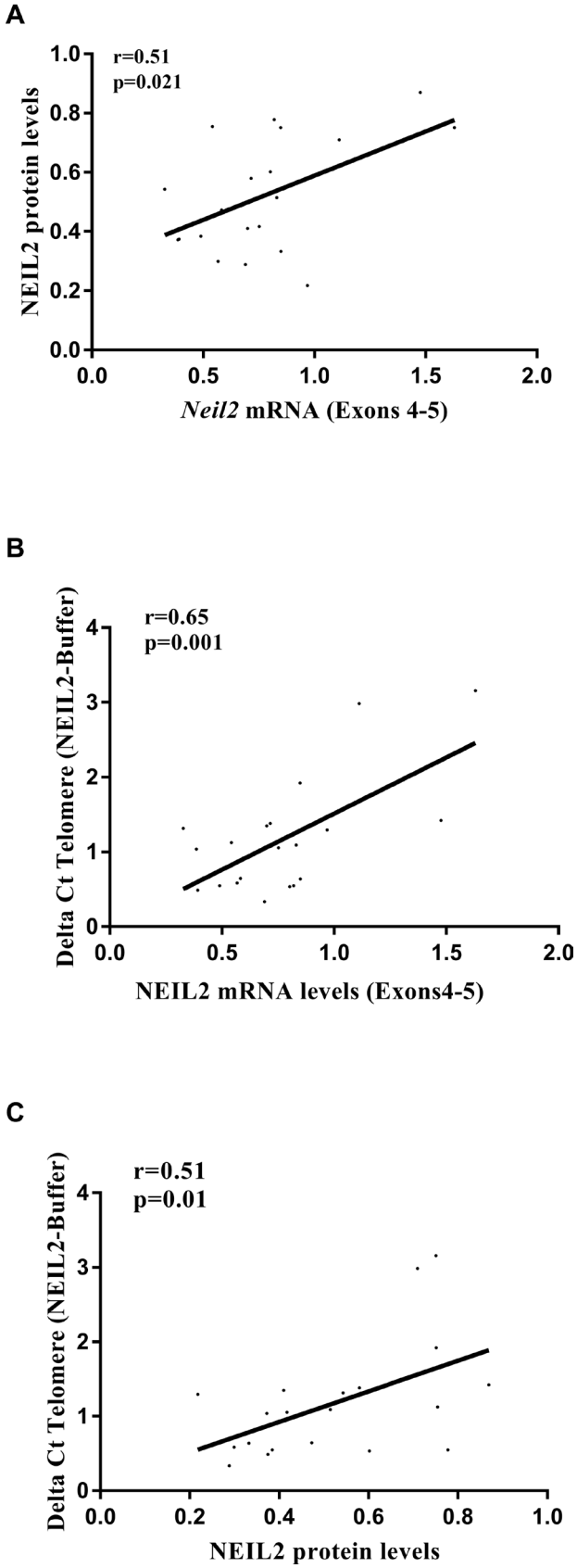

Figure 2: (**A**) Correlation analysis between *NEIL2* mRNA and protein levels. (**B**) Correlation analysis between *NEIL2* mRNA levels and the relative amount of "NEIL2-lesions". (**C**) Correlation analysis between the NEIL2 protein levels and the relative amount of "NEIL2-lesions". Spearman test, was used to test whether correlation is significant. significant p-value when ($p < 0.05$).

measured the relative amount of uracil miss incorporation at the telomere region as NEIL2 is not able to recognize/process this type of lesions. We performed correlation analysis between "Uracil-lesions" and "NEIL2-lesions" and we found no significant correlation between them (Supplementary Figure 4B)

NEIL2-derived DNA damage correlates with γH2AX intensity signal

We measured the γH2AX signal intensity in the cell nucleus of the 20 LCLs (as a marker of DSBs) at basal conditions. We found a direct correlation between the relative amount of "NEIL2-lesions¨ and the nuclear γH2AX intensity signal independently of the BRCA or SNP status ($r = 0.31$; $p = 0.09$), (Figure 4).

DISCUSSION

In the present study, we have tried to gain molecular insights into a common genetic variant (rs804271) previously reported by our group to be associated with increased breast cancer risk in *BRCA2* mutation carriers [4]. For that, we have used two independent set of samples to test the SNP effect on *NEIL2* transcriptional regulation and its possible implication on genome instability.

This SNP is localized within the TSS of *NEIL2* gene. Previous characterization of the *NEIL2* promoter region showed that *NEIL2* transcription is influenced by certain SNPs located 5′ upstream of the start site [19]. Indeed, *in silico* analysis predicted that this polymorphism is located within a binding motif for several transcription factors (Supplementary Table 2), and transcriptional modifications due to this SNP may be expected.

Data from Gtex confirmed that the presence of rs804271 was associated with a significant mRNA upregulation in 30 tissues including breast ($p = 0.00001$), ovary ($p = 1.4 * 10^{-14}$), and blood ($p = 6.6 * 10^{-13}$), (Supplementary Table 3). However, for some tissues, such as "Cells - EBV-transformed lymphocytes (LCLs)", this effect was "moderate" (Supplementary Figure 1), suggesting that the intensity of the SNP effect may be tissue specific. We validated these results in our FBOC series and we found, independently of the BRCA status, significantly increased *NEIL2* mRNA levels in the blood from FBOC individuals harboring the SNP ($\beta = 0.24$; $p = 0.01$), suggesting that it is associated *per se* with transcriptional activation of the *NEIL2* gene. In contrast, we were not able to detect a significant *NEIL2* mRNA upregulation associated to the SNP in the 20 LCL analyzed, confirming the tissue specificity found in the GTEX data. All these results suggest that rs804271 is indeed associated with constitutive transcriptional activation of the *NEIL2* gene.

A recent work in which NEIL1 and NEIL2 (Neil1 −/− /Neil2 −/−) double and NEIL1, NEIL2 and NEIL3 (Neil1 −/− /Neil2 −/− /Neil3 −/−) triple knock-out mouse models have been characterized, no accumulation of oxidative DNA damage, no changes in the mutation frequencies under normal physiological conditions and more importantly, no cancer predisposition for these mice has been observed [25]. This would agree with our results in which it is *NEIL2* "excess" and not its "absence" that

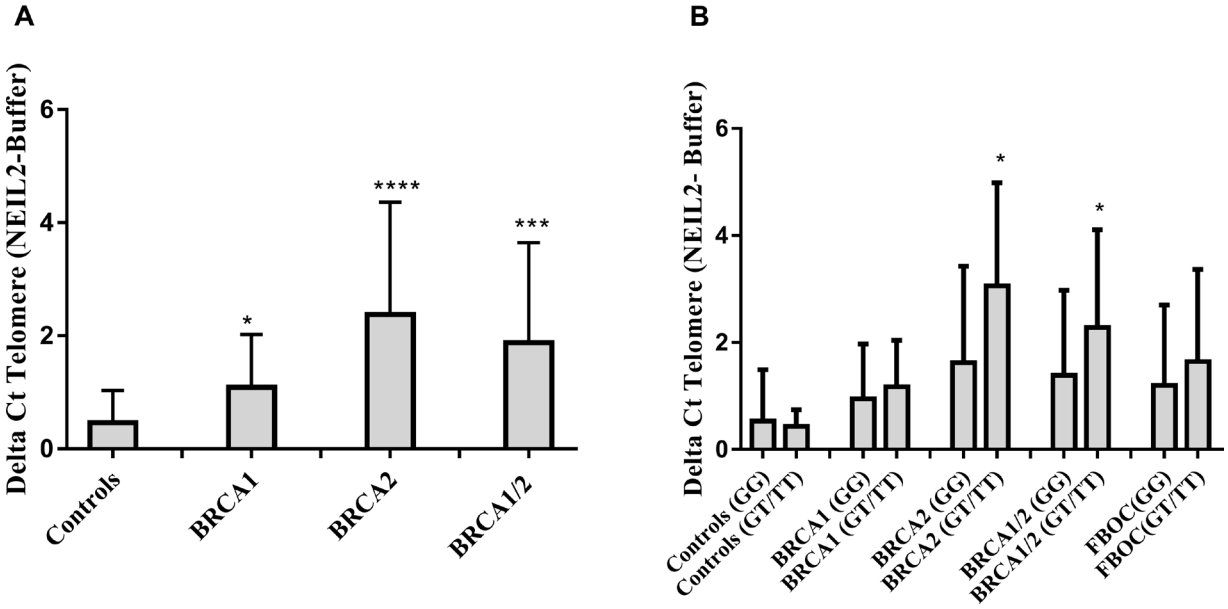

Figure 3: (**A**) Comparative analysis of the relative number of NEIL2-lesions found at telomeres according BRCA mutational status in FBOC series (*BRCA1* and *BRCA2* mutation carriers are compared with Controls). (**B**) Comparative analysis of the relative amount of "NEIL2-lesions" found at telomeres according the SNP status ((Carriers (GT/TT) *Vs* Non-carriers (GG)) among the different BRCA mutational groups in FBOC series (*BRCA1, BRCA2* mutation carriers and *BRCA1/BRCA2* non-carrier Controls). Unpaired student *t* test was used to test for potential significant differences. ($^{*}p < 0.05$, $^{**}p < 0.01$, $^{***}p < 0.001$, $^{****}p < 0.0001$).

may be deleterious and responsible for the increased risk effect of this SNP in *BRCA2* mutation carriers.

In the line of this hypothesis, it has been previously described that *NEIL2* gene is frequently amplified in esophageal adenocarcinoma and that tumors with copy number gains of *NEIL2* gene present significant poor prognosis [26, 27]. In addition, we have observed that *NEIL2* gene is frequently upregulated in several tumor types (Supplementary Figure 5A), and more importantly that *NEIL2* mRNA upregulation or copy number amplification has prognostic value for some of those tumors (Supplementary Figure 5B).

The molecular mechanism by which *NEIL2* mRNA upregulation could be deleterious for *BRCA2* mutation carriers is unclear. However, high expression levels of BER related enzymes have been associated with tissue oxidative DNA base damage [12]. In addition, it was described that rs804271 (previously ss74800505) was associated with both NEIL2 transcriptional modifications and significantly increased mutagen-induced genetic damage [19]. In fact, in LCLs we found a significant positive correlation between the amount of *NEIL2* mRNA or protein levels and "NEIL2-lesions" ($r = 0.65$; $p = 0.001$ and $r = 0.51$; $p = 0.02$, respectively) (Figure 2B). Moreover, in FBOC the SNP was also associated with higher amount of "NEIL2-lesions" compared to their counterparts without the SNP, although it was only significant for *BRCA1* and *BRCA2* mutation carriers ($p = 0.03$) (Figure 3B).

A possible explanation for this result, could be that the NEIL2 enzyme "excess" as consequence of the SNP could lead to the recognition and binding to DNA lesions for which normally it presents low excision activity, like 8-oxoG [10]. Indeed, we found a significant correlation between "NEIL2-lesions" and "FPG-lesions" ($r = 0.40$; $p = 0.003$) (Supplementary Figure 4A), which mostly correspond to purine bases lesions (8-oxoG/methylFapyG). This could lead to a delay in the repair and to the accumulation of "NEIL2-lesions" in the DNA.

In the context of *BRCA1* and *BRCA2* deficiency, this accumulation of base lesions would be deleterious since both enzymes are involved in transcription-coupled repair of 8-OxoG [28] and protect against oxidative DNA damage converted into DSBs [14]. Indeed, our results in the LCLs confirmed that the relative number of "NEIL2-lesions" at the telomere was correlated with nuclear γH2AX intensity signal (a marker for DSBs) independently of the BRCA or SNP status ($r = 0.31$; $p = 0.09$) (Figure 4).

In summary, our hypothesis would be that this SNP activates at transcriptional level *NEIL2* gene expression leading to a cascade of events that converge in the accumulation of unresolved "NEIL2-lesions" that may be converted into DSBs. In a system with a defective HR DNA repair, as it is the case for *BRCA2* mutation carriers, this SNP would contribute to higher genome instability and finally to a higher cancer risk for this specific group of patients.

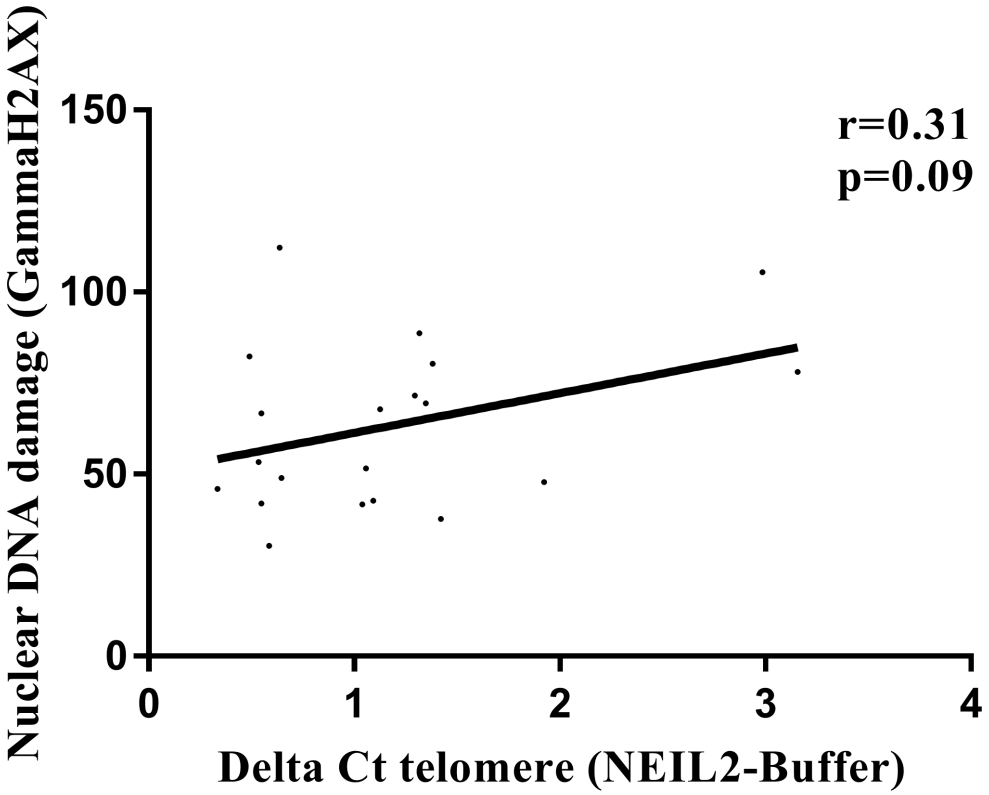

Figure 4: Correlation analysis between relative amount of "NEIL2-lesions" and the γH2AX nuclear intensity signal (DSBs). Spearman test, was used to test whether correlation is significant. significant *p*-value when ($p < 0.05$).

MATERIALS AND METHODS

Familial breast and ovarian cancer (FBOC) series

We studied a group composed of 166 individuals belonging to 51 families meeting high-risk criteria, and screened for deleterious mutations in the *BRCA1* and *BRCA2* genes, as reported previously [29]. Of these families, 25 carried a deleterious mutation in the *BRCA1* gene, 25 in *BRCA2*.

Eighty individuals were used as non-carrier controls: they were relatives of *BRCA1/2* mutation carriers who did not have personal cancer antecedents and did not harbor the corresponding familial mutation in the *BRCA1* or *BRCA2* genes.

All cases and controls signed an appropriate informed consent form and the ethics committee of the hospital involved (Fuenlabrada University Hospital) approved the proposal.

We used this set of samples to calculate the SNP frequency, to quantify *NEIL2* mRNA levels in peripheral blood and to measure the accumulation of oxidative DNA damage at telomeres (NEIL2-lesions, FPG-lesions, uracil accumulation) in blood DNA. (Table 1).

Lymphoblastoid cell lines

A second set of 20 LCLs was established by Epstein-Barr virus transformation of peripheral blood lymphocytes from thirteen healthy women carrying heterozygous mutations in *BRCA1* and seven non-carrier relatives used as controls. Mutational analysis had been performed by Sanger sequencing (BRCA status) or Taqman probe (rs804271) (Supplementary Table 4). None of the women included in the study had personal antecedents of cancer. This LCL panel has been previously described by our group [30]. Cell lines were cultured in RPMI-1640 media (Sigma-Aldrich) supplemented with non-heat-inactivated 20% fetal bovine serum (Sigma-Aldrich), penicillin-streptomycin (Gibco) and Fungizone (Gibco). The cultures were carried out in 25 cm^2 flasks (Corning) at 37°C in 5% CO2 atmosphere and cell lines were maintained in exponential growth by daily dilution to 106 cells/ml of full media.

We used this sample set to analyze the correlation between *NEIL2* mRNA – protein levels, the relative number of "NEIL2-lesions" found at DNA, and the relative number of double stranded brakes (DSB) at DNA.

SNP genotyping (rs804271)

Single Nucleotide Polymorphism rs1466785, located in the *NEIL2* gene is a cancer risk modifier for *BRCA2* mutation carriers [4]. Imputation using *1000 Genomes* data showed that there were several SNPs in strong linkage disequilibrium (LD) with rs1466785, the original SNP reported in Osorio *et al.* [4]. Of these, we considered rs804271 to be the best candidate, given that it showed the most significant associations and that there existed functional data supporting its putative role in cancer [19].

DNA was extracted from peripheral blood of FBOC patients or LCLs using MagNAPure LC 2.0 (Roche Diagnostics, Indianapolis, Indiana) following the manufacturer's instructions. DNA quantification and quality were assessed by NanoDrop® (ND-1000 V3.7.1). A specific Taqman probe for rs804271 was used to genotype the presence/absence of the polymorphism among the sample collection. Allelic discrimination assays were conducted using the 7900HT Fast Real-Time PCR System (Applied Biosystems). Probe design for rs804271 is (G>T) instead of (C>A). Along the manuscript we refer to the variant as G>T.

NEIL2 mRNA expression analysis

RNA was extracted from peripheral blood cells using TRIzol Reagent (Ambion®, Life Techonogies) according to the manufacturer's instructions. NanoDrop® (ND-1000 V3.7.1) was used to assess both RNA quantity and quality. Two microliters of cDNA at a final concentration of 10-20 ng/µl were mixed in triplicate with GoTaq® qPCR MasterMix 1x (Promega), *NEIL2* cDNA primers (F/R) and GAPDH cDNA primers (F/R) at final concentrations of 500nM. Primers used were: *NEIL2 4-5 exons* (F: GTCACACCCACCTGTGACAT; R: GCACTCAGGACTGAACCGAG) and *GAPDH* (F: CCTGCACCACCAACTGCTTA; R: CCATCACGCCACAGTTTCC).All reagents were used following the manufacturer's instructions. qPCR was done using the QuantStudio S6 system (Applied Biosystems).

NEIL2 protein quantification

The expression level of endogenous NEIL2 protein was analyzed by western blot. Briefly, cell lysates were prepared in RIPA buffer (Sigma) and protease inhibitors cocktail (Roche). Protein content was determined by Lowry analysis (Bio-Rad). Eighty micrograms of proteins were analyzed by SDS-PAGE on polyacrylamide gels and transferred to Immobilon-FL membranes (Millipore). Membranes were blocked in TBS-T (50 mM Tris-HCl, 150 mM NaCl, pH 7.5 plus 0.1% Tween 20) and 5% nonfat milk for 1 hour at RT. Blots were probed with following primary antibodies: rabbit anti-NEIL2 (Atlas Antibibodies, #HPA064460) at 1/1000 dilution or mouse anti-GAPDH (manufactured by the monoclonal antibodies core nit from the Spanish National Cancer Research Centre) at 1/3000 dilution in TBS-T containing 5% nonfat milk. The secondary antibodies were HRP-conjugated (Dako) and the immunoblots were developed using the

Table 1: FBOC series information

	Families (n)	Healthy carriers (n)		Cancer cases (n)	rs804271 genotyped (n)	NEIL2 mRNA (n)	NEIL2-lesions	FPG-lesions	uracil-lesions
BRCA1	25	21		19	40	24	25	14	14
BRCA2	25	23		23	46	30	35	18	18
Controls	na	0		0	80	29	25	20	20

Information regarding number of healthy *BRCA1* and *BRCA2* mutation carriers or cancer cases and the sample size for each experimental section.

ECL system (GE Healthcare). ImageLab software version 4.1 (Bio-Rad) was used for image acquisition and images were analyzed using ImageJ software for quantification of signal intensity/area for both proteins.

Oxidative DNA damage studies "NEIL2-lesions"

We used a qPCR-based method to evaluate the oxidative DNA damage within telomeric DNA [32], based on differences in PCR kinetics between DNA template digested by formamidopyrimidine-DNA glycosylase (FPG) and undigested DNA. Quantitative real-time amplification of genomic DNA was performed as described by O'Callaghan et al. [31].

Measurement of telomere damage

Oxidative DNA damage within telomeres

We used a qPCR-based method to evaluate the oxidative stress within telomeric DNA. We followed the procedure described by O'Callaghan *et al.* based on differences in PCR kinetics between DNA template digested by formamidopyrimidine-DNA-glycosylase (FPG) and undigested DNA [32]. Briefly, FPG is a bacterial DNA glycosylase that recognizes and cuts the oxidized bases from DNA, principally 8-oxoG, AP sites that are converted in single-strand breaks (SSBs) by its AP-lyase activity. These SSBs reduce amplification efficiency, thus, the ΔCq after digesting DNA by FPG (Cq digested – Cq undigested) is proportional to the oxidative damage in the amplified region. The incubation and qPCR amplification of genomic DNA was performed as described by O'Callaghan et al. [31].

Quantification of "NEIL2-lesions" accumulation at telomeres

The telomere oxidation protocol previously described can be potentially adapted to quantify the accumulation of different base lesions incubating the DNA with other glycosylases that are sensitive to other specific base lesions. Following this premise, we used NEIL2 enzyme to measure the "NEIL2-lesions" accumulation (5hydroxyuracildihydrouracil, 5-hydroxycytosine, thymine glycol and 8-oxoG) at telomeres [9]. We optimized the protocol using a low NEIL2 concentration, decreasing DNA amount and incubation time. 200 ng of genomic DNA was incubated with 5,6 µM NEIL2 (provided by Dr. Thomas Helleday, Karolinska Institutet, Stockholm, Sweden) or without (replaced with H20) in a buffer (25 mM TrisHcl pH 8.0, 15 mM NaCl, 2 Mm MgCl2 and 0.0025% Tween 20) for 4 hours at 37°C. The reaction was stopped by incubation at 95°C for 5 min. qPCR analysis was performed on 10 ng of digested or undigested genomic DNA following the same reagents and conditions that in the original protocol for FPG [31].

Quantification of uracil accumulation at telomeres

Following this premise, we used UNG to measure the accumulation of uracil at telomeres that is recognized and excised by this enzyme [33]. We optimized the protocol using a low UNG concentration, decreasing DNA amount and incubation time. 180 ng of genomic DNA was incubated with 130 nM UNG (provided by Dr. Thomas Helleday, Karolinska Institutet, Stockholm, Sweden) or without (replaced with H20) in a buffer (25 mM TrisHcl pH 8.0, 15 mM NaCl, 2 Mm MgCl2 and 0.0025% Tween 20) for 30 min at 37°C. The reaction was stopped by incubation at 95°C for 5 min. qPCR analysis was performed on 10 ng of digested or undigested genomic DNA following the same reagents and conditions that in the original protocol for FPG [31].

DNA damage

LCLs were cultured 4 hours before fixation with 4% paraformaldehyde (Electron Microscopy Sciences, Hatfield, Philadelphia, USA). Two hours before fixation, cells were counted and seeded into a poly-L-lysine-coated (Sigma-Aldrich) µCLEAR bottom 96-well plate (Greiner Bio-One) at a density of 75,000 cells per 100ul full media per well. LCL were then left for 2 hours to attach to the surface of the wells, fixed for 15 min at room temperature, permeabilized in 0.5% Triton X-100 in PBS for 20 minutes at 4°C and stained with primary and secondary antibodies and 4′,6-Diamidino-2-phenylindole dihydrochloride (DAPI) to visualize nuclei. To detect γ-H2AX we used

mouse monoclonal anti-phospho-histone H2AX antibody (Millipore; #05-636). Alexa Fluor 488 from molecular probes (Invitrogen; #A-11034) was used, and fluorescent images were automatically taken for each well of the 96-well plate using an Opera High-Content Screening System (Perkin Elmer). Pictures were taken under non-saturating conditions using a 40x magnification lens to calculate the γ-H2AX nuclear signal intensity.

Statistical analysis

Pearson's chi-squared test was used to calculate whether differences in the frequency of the SNP among the FBOC groups were significant (Supplementary Table 1).

We performed linear regression analysis to test whether cancer antecedents in *BRCA1* and *BRCA2* mutation carriers were associated with any of the variables we evaluated in this report, but we did not find significant differences (Significant p-values < 0.05) between healthy *BRCA1* and *BRCA2* carriers or cancer cases. Hence, we did not stratify for cancer status in these groups (Supplementary Table 5).

We considered heterozygotes and homozygotes (GT/TT) as a single group, to evaluate the effect of the SNP for each of the studied variables, as the cancer modifier effect of rs804271 is dominant for *BRCA2* mutation carriers [4].

Significant differences for the different comparative analysis were stablished by unpaired t test analysis (SNP effect on *NEIL2* mRNA levels or NEIL2 derived base damage accumulation, Figure 1 and Figure 3, respectively).

Spearman correlation was used to assess for significant correlations between *NEIL2* mRNA levels, protein levels and NEIL2 derived base damage accumulation at telomeres (Figure 3). Also, to assess whether NEIL2-lesions correlates with "FPG-lesions", "UNG-lesions" and γ-H2AX nuclear signal intensity in FBOC and LCLs respectively (Supplementary Figure 4A and Figure 4B).

Statistical calculations were done using SPSS version 18 (SPSS Inc., Chicago, Illinois) and GraphPad Prism 5.03 (San Diego, California); graphs were made using GraphPad Prism 5.03.

ACKNOWLEDGMENTS

We thank Alicia Barroso her technical assistance. Also to Dr. Thomas Helleday, (Karolinska Institutet, Stockholm, Sweden) that kindly provided NEIL2 and UNG purified enzymes.

The Genotype-Tissue Expression (GTEx) Project was supported by the Common Fund of the Office of the Director of the National Institutes of Health. Additional funds were provided by the NCI, NHGRI, NHLBI, NIDA, NIMH, and NINDS. Donors were enrolled at Biospecimen Source Sites funded by NCI/SAIC-Frederick, Inc. (SAIC-F) subcontracts to the National Disease Research Interchange (10XS170), Roswell Park Cancer Institute (10XS171), and Science Care, Inc. (X10S172). The Laboratory, Data Analysis, and Coordinating Center (LDACC) were funded through a contract (HHSN268201000029C) to The Broad Institute, Inc. Biorepository operations were funded through an SAIC-F subcontract to the Van Andel Institute (10ST1035). Additional data repository and project management were provided by SAIC-F (HHSN261200800001E). The Brain Bank was supported by supplements to University of Miami grants DA006227 & DA033684 and to contract N01MH000028. Statistical Methods development grants were made to the University of Geneva (MH090941 & MH101814), the University of Chicago (MH090951, MH090937, MH101820, MH101825), the University of North Carolina - Chapel Hill (MH090936 & MH101819), Harvard University (MH090948), Stanford University (MH101782), Washington University St Louis (MH101810), and the University of Pennsylvania (MH101822). The data used for the analyses described in this manuscript were obtained from: [insert, where appropriate] the GTEx Portal on 01/12/2015 and/or dbGaP accession number phs000424.v7.p2 on 01/10/2017.

CONFLICTS OF INTEREST

None.

FUNDING

J.B.'s laboratory is partially funded by the Spanish Ministry of Health PI12/00070, supported by FEDER funds, and the Spanish Research Network on Rare diseases (CIBERER). C.B-B is supported by FIS PI12/00070. J.M.B is supported by grant FPU15/01978 from the Spanish Ministry of Education, Culture and Sport. MU is supported by the Spanish Ministry of Health PI14/00459 with FEDER funds. The study was partially supported by the Spanish Ministry of Economy and Competitiveness (MINECO) SAF2014-57680-R.

REFERENCES

1. Roy R, Chun J, Powell SN. BRCA1 and BRCA2: different roles in a common pathway of genome protection. Nat Rev Cancer. 2012; 12:68–78. https://doi.org/10.1038/nrc3181.
2. Kuchenbaecker KB, Hopper JL, Barnes DR, Phillips KA, Mooij TM, Roos-Blom MJ, Jervis S, van Leeuwen FE, Milne RL, Andrieu N, Goldgar DE, Terry MB, Rookus MA, et al, and BRCA1 and BRCA2 Cohort Consortium. Risks of Breast, Ovarian, and Contralateral Breast Cancer for BRCA1 and BRCA2 Mutation Carriers. JAMA. 2017; 317:2402–16. https://doi.org/10.1001/jama.2017.7112.
3. Helleday T, Petermann E, Lundin C, Hodgson B, Sharma RA. DNA repair pathways as targets for cancer therapy. Nat Rev. 2008; 8:193–204. https://doi.org/10.1038/nrc2342.

4. Osorio A, Milne RL, Kuchenbaecker K, Vaclová T, Pita G, Alonso R, Peterlongo P, Blanco I, de la Hoya M, Duran M, Díez O, Ramón Y Cajal T, Konstantopoulou I, et al. DNA glycosylases involved in base excision repair may be associated with cancer risk in BRCA1 and BRCA2 mutation carriers. PLoS Genet. 2014; 10:e1004256.
5. Dizdaroglu M, Coskun E, Jaruga P. Repair of oxidatively induced DNA damage by DNA glycosylases: Mechanisms o f action, substrate specificities and excision kinetics. Mutat Res. 2017; 771:99–127. https://doi.org/10.1016/j.mrrev.2017.02.001.
6. Dianov GL, Hübscher U. Mammalian base excision repair: The forgotten archangel. Nucleic Acids Res. 2013; 41:3483–90. https://doi.org/10.1093/nar/gkt076.
7. Lindahl T. Instability and decay of the primary structure of DNA. Nature. 1993; 362:709–15. https://doi.org/10.1038/362709a0.
8. Arai K, Morishita K, Shinmura K, Kohno T, Kim SR, Nohmi T, Taniwaki M, Ohwada S, Yokota J. Cloning of a human homolog of the yeast OGG1 gene that is involved in the repair of oxidative DNA damage. Oncogene. 1997; 14:2857–61. https://doi.org/10.1038/sj.onc.1201139.
9. Hazra TK, Kow YW, Hatahet Z, Imhoff B, Boldogh I, Mokkapati SK, Mitra S, Izumi T. Identification and characterization of a novel human DNA glycosylase for repair of cytosine-derived lesions. J Biol Chem. 2002; 277:30417–20. https://doi.org/10.1074/jbc.C200355200.
10. Hazra TK, Das A, Das S, Choudhury S, Kow YW, Roy R. Oxidative DNA damage repair in mammalian cells: A new perspective. DNA Repair (Amst). 2007; 6:470–80. https://doi.org/10.1016/j.dnarep.2006.10.011.
11. Dou H, Mitra S, Hazra TK. Repair of Oxidized Bases in DNA Bubble Structures by Human DNA Glycosylases NEIL1 and NEIL2. J Biol Chem. 2003; 278:49679–84. https://doi.org/10.1074/jbc.M308658200.
12. Whitaker AM, Schaich MA, Smith MR, Flynn TS, Freudenthal BD. Base excision repair of oxidative DNA damage: from mechanism to disease. Front Biosci (Landmark Ed). 2017; 22:1493–1522. http://dx.doi.org/10.2741/4555.
13. Woodbine L, Brunton H, Goodarzi AA, Shibata A, Jeggo PA. Endogenously induced DNA double strand breaks arise in heterochromatic DNA regions and require ataxia telangiectasia mutated and Artemis for their repair. Nucleic Acids Res. 2011; 39:6986–97. https://doi.org/10.1093/nar/gkr331.
14. Fridlich R, Annamalai D, Roy R, Bernheim G, Powell SN. BRCA1 and BRCA2 protect against oxidative DNA damage converted into double-strand breaks during DNA replication. DNA Repair (Amst). 2015; 30:11–20. https://doi.org/10.1016/j.dnarep.2015.03.002.
15. Caldecott KW. Single-strand break repair and genetic disease. Nat Rev Genet. 2008; 9:619–31. https://doi.org/10.1038/nrg2380.
16. Khanna KK, Jackson SP. DNA double-strand breaks: signaling, repair and the cancer connection. Nat Genet. 2001; 27:247–54. https://doi.org/10.1038/85798.
17. Benítez-Buelga C, Vaclová T, Ferreira S, Urioste M, Inglada-Perez L, Soberón N, Blasco MA, Osorio A, Benítez J. Molecular insights into the OGG1 gene, a cancer risk modifier in BRCA1 and BRCA2 mutations carriers. Oncotarget. 2016; 7:25815–25. https://doi.org/10.18632/oncotarget.8272.
18. Kinslow CJ, El-Zein RA, Rondelli CM, Hill CE, Wickliffe JK, Abdel-Rahman SZ. Regulatory regions responsive to oxidative stress in the promoter of the human DNA glycosylase gene NEIL2. Mutagenesis. 2010; 25:171–7. https://doi.org/10.1093/mutage/gep058.
19. Kinslow CJ, El-Zein RA, Hill CE, Wickliffe JK, Abdel-Rahman SZ. Single nucleotide polymorphisms 5??? upstream the coding region of the NEIL2 gene influence gene transcription levels and alter levels of genetic damage. Genes Chromosom Cancer. 2008; 47:923–32. https://doi.org/10.1002/gcc.20594.
20. Ward LD, Kellis M. HaploReg: A resource for exploring chromatin states, conservation, and regulatory motif alterations within sets of genetically linked variants. Nucleic Acids Res. 2012; 40. https://doi.org/10.1093/nar/gkr917.
21. Lonsdale J, Thomas J, Salvatore M, Phillips R, Lo E, Shad S, Hasz R, Walters G, Garcia F, Young N, Foster B, Moser M, Karasik E, et al. The Genotype-Tissue Expression (GTEx) project. Nat Genet. 2013; 45:580–5. https://doi.org/10.1038/ng.2653.
22. Zhou J, Fleming AM, Averill AM, Burrows CJ, Wallace SS. The NEIL glycosylases remove oxidized guanine lesions from telomeric and promoter quadruplex DNA structures. Nucleic Acids Res. 2015; 43:4039–54. https://doi.org/10.1093/nar/gkv252.
23. Tchou J, Bodepudi V, Shibutani S, Antoshechkin I, Miller J, Grollman AP, Johnson F. Substrate Specificity of Fpg Protein: Recognition and cleavage of oxidatively damaged DNA. J Biol Chem. 1994; 269:15318–24. https://doi.org/10.1021/bi1014453.
24. Vallabhaneni H, Zhou F, Maul RW, Sarkar J, Yin J, Lei M, Harrington L, Gearhart PJ, Liu Y. Defective repair of uracil causes telomere defects in mouse hematopoietic cells. J Biol Chem. 2015; 290:5502–11. https://doi.org/10.1074/jbc.M114.607101.
25. Rolseth V, Luna L, Olsen AK, Suganthan R, Scheffler K, Neurauter CG, Esbensen Y, Kuśnierczyk A, Hildrestrand GA, Graupner A, Andersen JM, Slupphaug G, Klungland A, et al. No cancer predisposition or increased spontaneous mutation frequencies in NEIL DNA glycosylases-deficient mice. Sci Rep. 2017; 7:4384. https://doi.org/10.1038/s41598-017-04472-4.
26. Frankel A, Armour N, Nancarrow D, Krause L, Hayward N, Lampe G, Smithers BM, Barbour A. Genome-wide analysis of esophageal adenocarcinoma yields specific copy number aberrations that correlate with prognosis. Genes Chromosom Cancer. 2014; 53:324–38. https://doi.org/10.1002/gcc.22143.
27. Goh XY, Rees JRE, Paterson AL, Chin SF, Marioni JC, Save V, O'Donovan M, Eijk PP, Alderson D, Ylstra B, Caldas C,

Fitzgerald RC. Integrative analysis of array-comparative genomic hybridisation and matched gene expression profiling data reveals novel genes with prognostic significance in oesophageal adenocarcinoma. Gut. 2011; 60:1317–26. https://doi.org/10.1136/gut.2010.234179.

28. Le Page F, Randrianarison V, Marot D, Cabannes J, Perricaudet M, Feunteun J, Sarasin A. BRCA1 and BRCA2 are necessary for the transcription-coupled repair of the oxidative 8-oxoguanine lesion in human cells. Cancer Res. 2000; 60:5548–52.

29. Milne RL, Osorio A, Cajal TRY, Vega A, Llort G, De La Hoya M, Díez O, Carmen Alonso M, Lazaro C, Blanco I, Sánchez-de-Abajo A, Caldés T, Blanco A, et al. The average cumulative risks of breast and ovarian cancer for carriers of mutations in BRCA1 and BRCA2 attending genetic counseling units in Spain. Clin Cancer Res. 2008; 14:2861–9. https://doi.org/10.1158/1078-0432.CCR-07-4436.

30. Vaclová T, Gómez-López G, Setién F, Bueno JM, Macías JA, Barroso A, Urioste M, Esteller M, Benítez J, Osorio A. DNA repair capacity is impaired in healthy BRCA1 heterozygous mutation carriers. Breast Cancer Res Treat. 2015; 152:271–82. https://doi.org/10.1007/s10549-015-3459-3.

31. O'Callaghan NJ, Dhillon VS, Thomas P, Fenech M. A quantitative real-time PCR method for absolute telomere length. Biotechniques. 2008; 44:807–9. https://doi.org/10.2144/000112761.

32. O'Callaghan N, Baack N, Sharif R, Fenech M. A qPCR-based assay to quantify oxidized guanine and other FPG-sensitive base lesions within telomeric DNA. Biotechniques. 2011; 51:403–12. https://doi.org/10.2144/000113788.

33. Doseth B, Visnes T, Wallenius A, Ericsson I, Sarno A, Pettersen HS, Flatberg A, Catterall T, Slupphaug G, Krokan HE, Kavli B. Uracil-DNA glycosylase in base excision repair and adaptive immunity: Species differences between man and mouse. J Biol Chem. 2011; 286:16669–80. https://doi.org/10.1074/jbc.M111.230052.

Molecular Oncology

FEBS PRESS

A common SNP in the *UNG* gene decreases ovarian cancer risk in *BRCA2* mutation carriers

Juan Miguel Baquero[1], Carlos Benítez-Buelga[2], Victoria Fernández[1], Miguel Urioste[3,4], Jose Luis García-Giménez[3,5], Rosario Perona[3,6], the CIMBA Consortium[7], Javier Benítez[1,3,8] and Ana Osorio[1,3]

1 Human Genetics Group, Spanish National Cancer Research Centre (CNIO), Madrid, Spain
2 Helleday Laboratory, Department of Oncology-Pathology, Karolinska Institutet, Solna, Sweden
3 Spanish Network on Rare Diseases (CIBERER), Madrid, Spain
4 Familial Cancer Clinical Unit, Spanish National Cancer Research Centre (CNIO), Madrid, Spain
5 Department of Physiology, Faculty of Medicine and Dentistry, Universitat de Valencia, Mixed Unit CIPF-INCLIVA, Spain
6 Biomedical Research Institute Alberto Sols (CSIC-UAM), Madrid, Spain
7 Consortium of Investigators of Modifiers of BRCA1/2
8 Genotyping Unit (CEGEN), Spanish National Cancer Research Centre (CNIO), Madrid, Spain

Keywords
BRCA2; cancer risk modifier; DNA damage; oxidative stress susceptibility; telomere damage; uracil-DNA glycosylase

Correspondence
A. Osorio, Human Cancer Genetics Programme, Spanish National Cancer Research Centre (CNIO), C/Melchor Fernández Almagro 3, Madrid 29029, Spain
Tel: +34917328002
E-mail: aosorio@cnio.es

(Received 11 October 2018, revised 5 February 2019, accepted 5 February 2019, available online 1 March 2019)

doi:10.1002/1878-0261.12470

Single nucleotide polymorphisms (SNPs) in DNA glycosylase genes involved in the base excision repair (BER) pathway can modify breast and ovarian cancer risk in *BRCA1* and *BRCA2* mutation carriers. We previously found that SNP rs34259 in the uracil-DNA glycosylase gene (*UNG*) might decrease ovarian cancer risk in *BRCA2* mutation carriers. In the present study, we validated this finding in a larger series of familial breast and ovarian cancer patients to gain insights into how this *UNG* variant exerts its protective effect. We found that rs34259 is associated with significant *UNG* downregulation and with lower levels of DNA damage at telomeres. In addition, we found that this SNP is associated with significantly lower oxidative stress susceptibility and lower uracil accumulation at telomeres in *BRCA2* mutation carriers. Our findings help to explain the association of this variant with a lower cancer risk in *BRCA2* mutation carriers and highlight the importance of genetic changes in BER pathway genes as modifiers of cancer susceptibility for *BRCA1* and *BRCA2* mutation carriers.

1. Introduction

Women carrying germline mutations in the *BRCA1* and *BRCA2* genes have a high lifetime risk of developing breast, ovarian, and other cancers (Milne *et al.*, 2008). However, mutation carriers show considerable differences in disease manifestation, and this suggests the existence of other genetic or environmental factors that modify the risk of cancer development. BRCA proteins are involved in double-strand break (DSB) DNA repair through the homologous recombination pathway (O'Donovan and Livingston, 2010), and cells harboring mutations in these genes are dependent on other DNA repair mechanisms. In this regard, we have shown that single nucleotide polymorphisms (SNPs) in genes from the base excision repair (BER) pathway can modify breast or ovarian cancer susceptibility in *BRCA1* and *BRCA2* mutation carriers (Osorio *et al.*, 2014).

The BER pathway corrects base lesions that result from deamination, oxidation, or methylation (Xue

Abbreviations
AP, apurinic/apyrimidinic; BER, base excision repair; DSB, double-strand break; dTTP, deoxythymidine triphosphate; dUTP, deoxyuridine triphosphate; FBOC, familial breast and ovarian cancer; FPG, formamidopyrimidine-DNA glycosylase; HR, hazard ratio; LCLs, lymphoblastoid cell lines; PARP, poly(ADP-ribose) polymerase; SNP, single nucleotide polymorphism; TL, telomere length; UNG, uracil-DNA glycosylase.

et al., 2016). BER is initiated by DNA glycosylases that cleave the *N*-glycosylic bond between the sugar and the base, and release the damaged base to form an abasic site, also termed an apurinic/apyrimidinic (AP) site (Maynard *et al.*, 2009). A deficiency in BER can give rise to an accumulation of DSBs, which in the presence of a defective *BRCA1* or *BRCA2* background can persist and lead to cell cycle arrest or cell death. A synthetic lethal interaction was described between the *BRCA1/2* genes and poly(ADP-ribose) polymerase (*PARP1*) involved in the BER pathway, with BRCA-deficient cells being extremely sensitive to PARP1 inhibitors (Bryant *et al.*, 2005; Farmer *et al.*, 2005).

On the other hand, the BER pathway is essential for maintaining telomere integrity in mammals (Jia *et al.*, 2015). Telomeres are susceptible to uracil misincorporation, which is primarily recognized and removed by the uracil-DNA glycosylase (UNG) (Cortizas *et al.*, 2016). Due to the presence of long arrays of TTAGGG repeats, uracil can appear in telomeric DNA by misincorporation of deoxyuridine triphosphate (dUTP) instead of deoxythymidine triphosphate (dTTP) opposite adenine or by deamination of cytosine to uracil opposite guanine (Krokan *et al.*, 2002). Accumulation of uracil interferes with telomere homeostasis, and UNG-initiated BER is necessary for the preservation of telomere integrity (Vallabhaneni *et al.*, 2015).

In view of the above, we hypothesized that SNPs in DNA glycosylase genes might interfere with telomere maintenance and thus contribute to the risk of developing cancer. Supporting this idea, we reported that variant rs2304277, located in the 3′-UTR of the glycosylase gene *OGG1*, is associated with higher ovarian cancer risk in *BRCA1* mutation carriers, probably due to transcriptional downregulation of *OGG1* and increased DNA damage and telomere instability (Benítez-Buelga *et al.*, 2016). Similarly, we analyzed variant rs804271, previously associated with increased breast cancer risk in *BRCA2* mutation carriers (Osorio *et al.*, 2014), which is located within the promoter region of the glycosylase gene *NEIL2*. The modifier effect of this variant may be due to its negative impact on the performance of the NEIL2 enzyme, leading to an accumulation of oxidative lesions at telomeres (Benítez-Buelga *et al.*, 2017).

In the present study, we aimed to explain the molecular basis of the protective effect exerted by a SNP located in the 3′-UTR of the *UNG* gene (rs34259) in *BRCA2* mutation carriers (Osorio *et al.*, 2014). For that purpose, we explored the effects of the SNP on UNG activity and expression levels, and its possible involvement in telomere integrity.

2. Materials and methods

2.1. Patients and healthy controls

The study was performed in accordance with the principles of the Declaration of Helsinki. All patients and controls signed an appropriate informed consent form, and the proposal was approved by the ethics committee at the Fuenlabrada University Hospital, Madrid, Spain.

We studied a familial breast and ovarian cancer (FBOC) series of 344 individuals from 173 families meeting high-risk criteria, and screened for deleterious mutations in the *BRCA1* and *BRCA2* genes, as reported previously (Milne *et al.*, 2008). Thirty-two families carried a deleterious mutation in *BRCA1*, 31 in *BRCA2*, and 110 did not carry any mutation in either of these two genes (BRCAX families). One hundred eleven controls were included who were relatives of *BRCA1/2* mutation carriers, did not have personal cancer antecedents, and did not harbor the corresponding familial mutation in the *BRCA1* or *BRCA2* genes. The different traits studied in this series are detailed in Table 1.

2.2. DNA extraction and genotyping of SNP rs34259

DNA was extracted from peripheral blood of FBOC patients using the Maxwell® FSC Instrument

Table 1. Characteristics of the FBOC series and the number of persons studied for the indicated traits.

	BRCA1	BRCA2	BRCAX[a]	Controls[b]	Total (FBOC)
Families	32	31	110	–	173
Healthy carriers	25	34	–	–	59
Cancer cases	26	28	120	–	174
SNP rs34259 genotyping	51	63	120	110	344
UNG mRNA expression	37	53	104	83	277
UNG protein expression	–	20	–	10	30
Uracil at telomeres	42	63	115	108	328
Telomere oxidation	23	19	68	62	172
Protein carbonylation	29	27	31	20	107
Telomere length	36	32	85	61	214
Telomerase activity	13	15	–	47	75

[a] Non-BRCA1/2 families. [b] Controls were relatives without cancer antecedents and negative for BRCA1/2 mutations.

(Promega, Madison, WI, USA) following the manufacturer's instructions and quantified by the PicoGreen® fluorometric assay (Thermo Fisher Scientific, Waltham, MA, USA).

Single nucleotide polymorphism genotyping was carried out using a KASPar probe specifically designed for rs34259 (LGC Genomics, Berlin, Germany). Allelic discrimination assays were performed in duplicate using the 7900HT Fast Real-Time PCR System (Applied Biosystems, Foster City, CA, USA) and the Abi QuantStudio 6 Flex Real-Time PCR System (Applied Biosystems) following the instrument-specific conditions detailed by the manufacturer (LGC Genomics).

2.3. RNA expression analysis

RNA was extracted from peripheral blood mononuclear cells using TRIzol® Reagent (Thermo Fisher Scientific). RNA quantity and quality were assessed by NanoDrop® (ND-1000 V3.7.1; Thermo Fisher Scientific). The High-Capacity cDNA Reverse Transcription Kit (Applied Biosystems) was utilized for cDNA synthesis following the manufacturer's instructions.

The human *UNG* gene encodes both nuclear (UNG2) and mitochondrial (UNG1) forms of uracil-DNA glycosylase (Nilsen *et al.*, 1997). We designed specific primers to quantify total *UNG* mRNA expression and the relative expression of each isoform. Two microliters of cDNA at a final concentration of 10 $ng \cdot \mu L^{-1}$ was mixed with GoTaq® qPCR MasterMix 1× (Promega) and 1 μM cDNA primers of each pair of primers (F/R) in a final volume reaction of 10 μL. Primers used are listed in Table S1. The amplification conditions consisted of an initial step at 95 °C for 10 min, followed by 40 cycles of 10 s at 95 °C and 1 min at 65 °C. Each qPCR was performed in triplicate including no-template controls in an Abi QuantStudio 6 Flex Real-Time PCR System (Applied Biosystems). Relative *UNG*/*UNG1*/*UNG2* mRNA expression was calculated using the $2^{\Delta\Delta C_t}$ method for qPCR analysis after normalization with the housekeeping gene *GAPDH* using the QUANTSTUDIO™ Real-Time PCR Software (Applied Biosystems).

2.4. Western blotting

The expression of UNG1 was quantified by western blot analysis in a subset of controls ($n = 10$) and *BRCA2* mutation carriers ($n = 20$) from the FBOC series. Briefly, peripheral blood mononuclear cells were isolated from whole blood using TRIzol® Reagent (Thermo Fisher Scientific) according to manufacturer's instructions. Cell lysates were prepared in RIPA buffer (Sigma-Aldrich, San Luis, MO, USA) in the presence of a protease inhibitor cocktail (Roche, Basel, Switzerland). Total protein concentration was determined using the Pierce BCA Protein Assay Kit (Thermo Fisher Scientific) following the manufacturer's instructions. Sixty micrograms of protein was analyzed by SDS/PAGE and transferred to Immobilon-FL membranes (Millipore, Burlington, MA, USA). Membranes were blocked in TBS-T (50 mM Tris/HCl, 150 mM NaCl, pH 7.5 plus 0.2% Tween-20) and 5% nonfat milk for 1 h at RT. Blots were probed with the following primary antibodies: mouse anti-UNG (#TA503563; OriGene, Rockville, MD, USA) at 1/1000 dilution and mouse anti-actin (A2228; Sigma-Aldrich) at 1/10 000 dilution in TBS-T containing 5% nonfat milk. Anti-mouse IgG-HRP (Dako, Glostrup, Denmark) was used as the secondary antibody, and the immunoblots were developed using Immobilon Classico Western HRP substrate (Millipore). Each western blot was performed in quadruplicate. Images were analyzed using IMAGEJ software (NIH Image, Bethesda, MD, USA), and UNG1 protein level was normalized by actin.

In parallel, given that UNG2 protein levels in peripheral blood mononuclear cells from the FBOC series were too low to analyze their relative expression, we also performed western blot analyses of a previously described set of 18 lymphoblastoid cell lines (LCLs) (Vaclová *et al.*, 2015) proceeding from *BRCA1* mutation carriers and controls following the same protocol.

2.5. Measurement of telomere damage

2.5.1. Oxidative DNA damage within telomeres

We used a qPCR-based method previously described to evaluate the accumulation of oxidative lesions within telomeric DNA based on differences in PCR kinetics between template DNA digested by formamidopyrimidine-DNA glycosylase (FPG) and undigested DNA (O'Callaghan *et al.*, 2011). Incubation and qPCR amplification of genomic DNA were performed as described by O'Callaghan *et al.* (2011) to estimate oxidative DNA damage levels at telomeres and the 36B4 locus.

2.5.2. Quantification of uracil accumulation at telomeres

The telomere oxidation protocol (O'Callaghan *et al.*, 2011) can be adapted to quantify the accumulation of different base lesions by incubating the DNA with other glycosylases that are sensitive to other specific

base lesions. We used UNG to measure the accumulation of uracil, which is recognized and excised by this enzyme (Hegde *et al.*, 2008), at telomeres.

Due to the high affinity of UNG for DNA (Zharkov *et al.*, 2010), we optimized the protocol using a low UNG concentration and decreasing DNA amounts and incubation times. One hundred and eighty nanograms of genomic DNA was incubated in the absence or presence of 130 nM UNG (provided by T. Helleday, Karolinska Institutet, Stockholm, Sweden) in reaction buffer (25 mM Tris/HCl pH 8.0, 15 mM NaCl, 2 mM $MgCl_2$, and 0.0025% Tween-20) for 30 min at 37 °C. The reaction was stopped by incubation at 95 °C for 5 min. qPCR analysis was performed on 10 ng of digested or undigested genomic DNA using the same reagents and conditions as described in the original protocol for FPG (O'Callaghan *et al.*, 2011).

2.6. Immunodetection of oxidized proteins

Oxidized proteins in plasma samples were detected by measuring the levels of carbonylated proteins as previously described (García-Giménez *et al.*, 2012). Carbonylated proteins are a widely used biomarker of chronic oxidative stress (Fedorova *et al.*, 2013).

2.7. Telomere length measurement

Telomere length (TL) was quantified by high-throughput quantitative fluorescence *in situ* hybridization (HT-QFISH) with automated fluorescence microscopy as previously described (Canela *et al.*, 2007). Because TL is strongly heritable (Pooley *et al.*, 2013), BRCA status, the presence or absence of the SNP, and TL were assessed in the same member of each family. Whenever possible, we used the index case, and if this sample was not available, we used the most recently genotyped individual. As we previously demonstrated that chemotherapy affects TL (Benítez-Buelga *et al.*, 2015), we excluded patients from the analysis who were undergoing this treatment.

2.8. Telomerase assay

Protein extracts were obtained from peripheral blood mononuclear cells cultured in RPMI supplemented with 20% fetal bovine serum and phytohemagglutinin during 4–5 days, according to the recommendations of the manufacturer of the TRAPeze telomerase detection kit (Millipore). The average telomerase activity was determined in each sample using 0.5, 0.25, and 0.125 μg of protein extract and normalized with the internal control included in the assay. Because telomerase activity can be affected by chemotherapeutic agents (Benítez-Buelga *et al.*, 2015), we excluded all patients who received chemotherapy at any time during their lifetime.

2.9. Statistical analysis

To evaluate the effect of the SNP for each of the studied variables, we considered heterozygotes and homozygotes (GC/CC) as a single group, as the cancer modifier effect of rs34259 acts in a dominant fashion in *BRCA2* mutation carriers (Osorio *et al.*, 2014).

Pearson's chi-squared test was used to calculate whether the frequency of the SNP among the FBOC groups was significantly different from the frequency reported in the 1000 Genomes Project for the Iberian subpopulation (Zerbino *et al.*, 2018). The Spearman correlation test was used to establish whether correlations between variables were statistically significant. We performed linear regression analysis to test whether cancer antecedents in *BRCA1* and *BRCA2* mutation carriers were associated with any of the variables evaluated in this study, but we did not find significant differences ($P < 0.05$) between healthy *BRCA1* and *BRCA2* carriers or cancer cases. Hence, we did not stratify for cancer status in these groups (Table S2).

The Kolmogorov–Smirnov test was used to evaluate whether the data sets were normally distributed. For comparative analyses, statistically significant differences were assessed by an unpaired *t*-test for normal distributions and the Mann–Whitney *U*-test for non-normal distributions. Linear regression analysis including the *UNG* SNP as explanatory variable was run to test whether this SNP affected the variables studied. The effect size of the studied variant was defined as the slope of the linear regression line and was computed as the effect of the alternative allele (C) relative to the reference allele (G).

Statistical calculations and graphs were done using the SPSS software package version 19.0 (IBM, Armonk, NY, USA) and GRAPHPAD PRISM 5.03 (GraphPad Software Inc, San Diego, CA, USA). In all analyses, a 2-tailed P value < 0.05 was considered statistically significant.

3. Results

3.1. Association study, validation, and fine mapping

In a previous study, using a tagging SNP approach in a large series of *BRCA1* and *BRCA2* mutation carriers

(n = 23 463) from the CIMBA consortium, we found that SNP rs34259 showed the strongest association with ovarian cancer risk among all SNPs covering the *UNG* gene (tagged or imputed): HR: 0.80, 95% CI: 0.69–0.94, $P = 7.6 \times 10^{-3}$ (Osorio *et al.*, 2014). This association was confirmed in a larger series of *BRCA2* mutation carriers (4291 new cases) from the OncoArray Consortium (Amos *et al.*, 2017) (HR: 0.84, $P = 7.6 \times 10^{-3}$).

SNP rs34259 is located in the 3′UTR of the *UNG* gene, 2.4 kb downstream of the translation termination codon. Using HAPLOREG v4.1 (Ward and Kellis, 2012), we were not able to detect a more plausible causal SNP among those in high linkage disequilibrium with rs34259 according to their predicted regulatory features (Table S3). Indeed, rs34259 has been identified as a *trans* expression quantitative trait locus (eQTL) SNP that decreased *UNG* gene expression in two independent eQTL studies (Ardlie *et al.*, 2015; Westra *et al.*, 2013) and we considered it the best candidate.

We genotyped SNP rs34259 in the FBOC sample set to evaluate its association with the studied variables. Genotype distributions were in Hardy–Weinberg equilibrium ($\chi^2 = 0.03$; $P = 0.86$). The different groups of cases and controls presented similar genotype and allele frequencies, not statistically different from the frequencies reported in the *1000 Genomes Project* for the Iberian subpopulation (Zerbino *et al.*, 2018) (Table S4).

3.2. rs34259 is associated with lower *UNG* mRNA and protein levels

We first analyzed the SNP effect on transcriptional regulation in different tissues using the GTEx eQTL web server (Carithers *et al.*, 2015). We found significantly decreased *UNG* mRNA levels associated with SNP rs34259 in several tissues, including breast (effect size = −0.17; $P = 0.023$) and blood (effect size = −0.19; $P < 0.0001$; Table S5).

In parallel, we analyzed *UNG* mRNA levels in the FBOC series considering the BRCA status and the presence or absence of the *UNG* variant (Fig. 1A). First, we confirmed in a subgroup of samples (n = 97) that the mRNA levels of both *UNG* isoforms (UNG1 and UNG2) were highly correlated ($r = 0.551$; $P < 0.001$) and that total *UNG* mRNA expression was correlated with each of the two isoforms and, therefore, representative of both (Fig. S1). We detected significantly lower *UNG* mRNA expression in individuals harboring the variant (effect size = −0.209; $P < 0.001$). The effect was more pronounced in the *BRCA2* group (effect size = −0.366; $P = 0.007$) and remained significant when analyzing both isoforms separately (Fig. S2).

Given that the SNP protective effect is for ovarian cancer, we also determined *UNG* mRNA expression in tissues of 17 prophylactic oophorectomies from *BRCA1* and *BRCA2* mutation carriers. In this cohort, we also found a trend toward lower total *UNG* mRNA expression associated with the studied SNP ($P = 0.056$; Fig. S3), which was significant for the *UNG1* isoform ($P = 0.045$).

To confirm whether this downregulation was translated into lower expression of the protein, we determined UNG1 protein expression by western blotting (WB) in 10 controls, of which 4 were carriers of the SNP, and in 20 *BRCA2* carriers, of which 10 were carriers of the SNP (Fig. 1B). Quantification showed that *BRCA2* carriers harboring SNP rs34259 had lower UNG1 protein levels ($P = 0.023$) when controls and *BRCA2* carriers were combined, and the effect of SNP rs34259 on UNG1 protein levels remained significant ($P = 0.021$; Fig. 1C). *UNG1* mRNA levels correlated significantly with UNG protein levels in these patients ($r = 0.791$; $P < 0.001$) (Fig. 1D). Finally, we performed WB of both UNG1 and UNG2 in a set of 18 LCLs and confirmed that both UNG isoforms remained highly correlated at the protein level ($r = 0.829$; $P < 0.001$; Fig. S4A,B). Despite the reduced sample size, we also found a trend toward lower UNG1 and UNG2 protein levels in the LCL series associated with the *UNG* variant (Fig. S4C).

3.3. Accumulation of DNA damage at the telomeres

We analyzed the accumulation of two kinds of lesions: 8-oxoguanine and uracil, which are detected by FPG and UNG glycosylases, respectively.

3.3.1. SNP rs34259 is associated with lower oxidative DNA damage

When analyzing the accumulation of 8-oxoguanine, we observed significantly lower oxidation levels in individuals harboring the variant ($P = 0.008$) (Fig. 2A). We were not able to detect significant differences within each mutational group. However, a statistically significant lower oxidative DNA damage associated with the SNP was found in controls ($P = 0.009$), suggesting that the SNP is associated with lower oxidative damage accumulation at telomeres independently of the *BRCA* status.

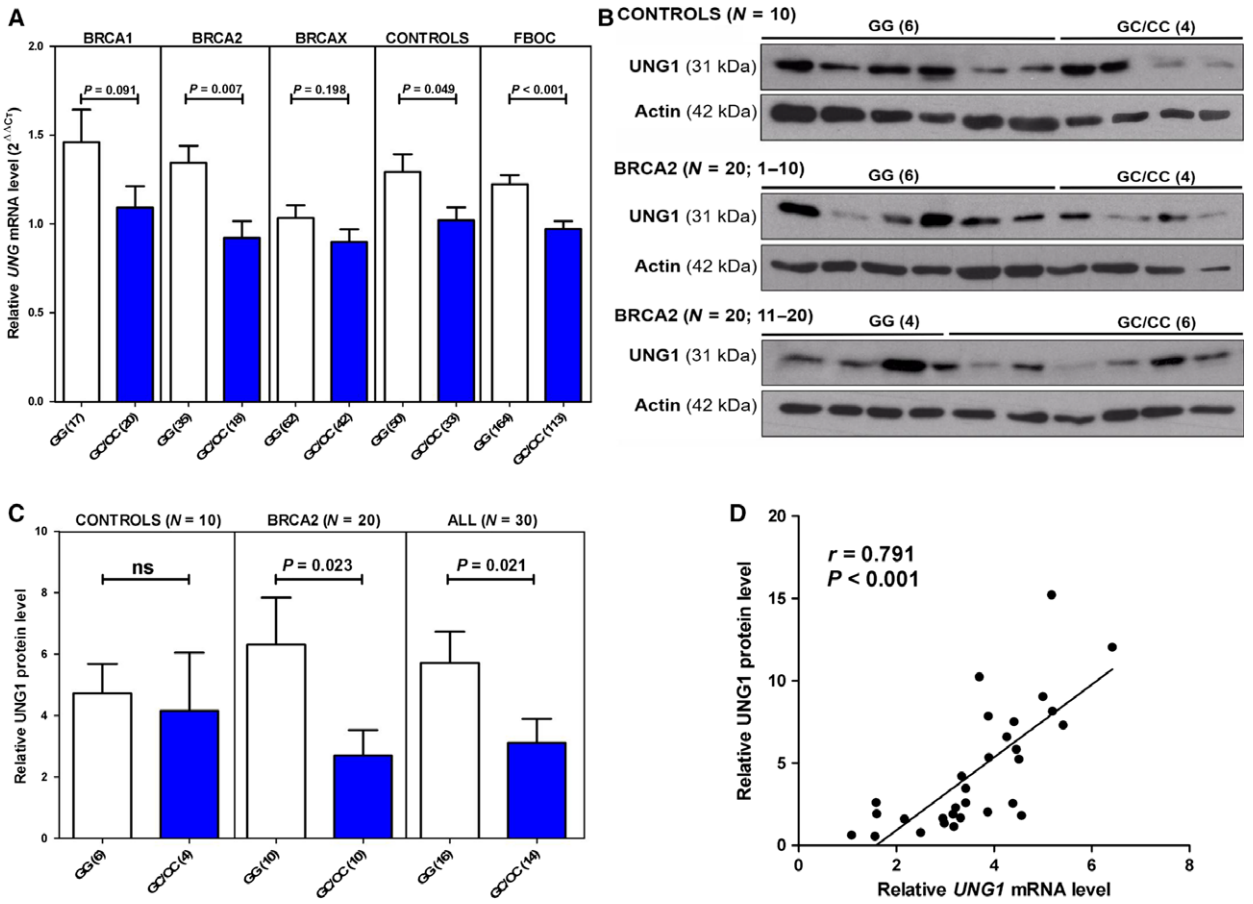

Fig. 1. *UNG* mRNA and protein levels. (A) *UNG* mRNA levels in the various FBOC groups according to the presence or absence of the SNP [noncarriers (GG)/carriers (GC/CC)]. (B) UNG1 protein levels in controls ($n = 10$) and *BRCA2* mutation carriers ($n = 20$) according to the presence or absence of the SNP [noncarriers (GG)/carriers (GC/CC)]. Actin levels were used to normalize for protein loading. (C) Quantification of UNG1 protein levels of the western blot shown in (B). Bars show the mean and the standard error of the mean (SEM). Numbers in brackets indicate sample size. (D) Correlation analysis between *UNG1* mRNA and protein levels in the patients shown in (B). Unpaired *t*-tests were performed for statistical significance in (A) and (C), Spearman's test was used to test the significance of the correlation in panel (D).

3.3.2. *BRCA2* mutation carriers harboring SNP rs34259 show lower uracil accumulation at the telomeres

After treatment with UNG, telomeric DNA showed an average decrease of 54% in PCR amplification compared to a 22% decrease observed when amplifying the 36B4 control locus ($P < 0.0001$), reflecting a predominant presence of uracil in telomeres (Fig. S5).

We did not find significant differences in uracil levels at telomeres among BRCA groups or controls. However, when we stratified according to the SNP (Fig. 2B), we detected a significantly lower uracil accumulation at telomeres when the variant was present for *BRCA2* mutation carriers ($P = 0.01$). This result suggests that the protective effect for ovarian cancer risk associated with SNP rs34259 in *BRCA2* mutation carriers could be due to an increased UNG activity, leading to less accumulation of uracil at the telomere region.

3.4. Lower protein carbonylation level in individuals harboring SNP rs34259

No significant differences were found in carbonylation levels in relation to the BRCA status. Notwithstanding, we found a trend toward lower carbonylation levels in all FBOC individuals with the variant ($P = 0.052$). In addition, for *BRCA2* mutation carriers harboring the SNP we detected a significantly lower carbonylation level ($P = 0.016$) (Fig. 3). These results suggest that the SNP in *UNG* is associated with lower oxidative stress susceptibility that becomes pronounced in *BRCA2* mutation carriers.

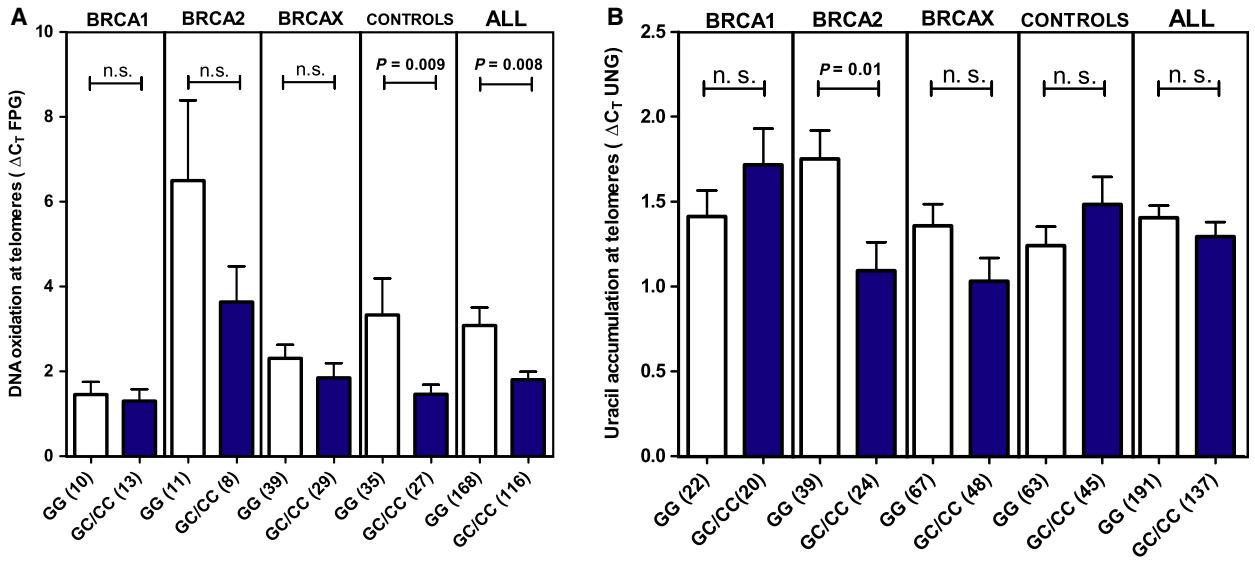

Fig. 2. Telomere DNA damage in the various FBOC groups according to the presence or absence of the *UNG* SNP. (A) DNA oxidation at telomeres. (B) Detection of uracil at telomeres in FBOC patients. Bars show the mean and the SEM. Numbers in brackets indicate sample size. Mann–Whitney *U*-test was used in (A), unpaired *t*-test was used in (B).

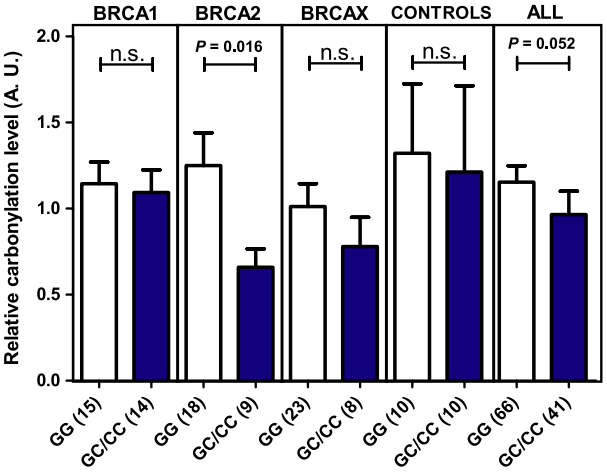

Fig. 3. Immunodetection of protein-bound carbonyl groups in plasma samples from the FBOC series. Carbonylation levels in the different groups stratified according to the presence or absence of SNP rs34259 in *UNG* [noncarriers (GG)/carriers (GC/CC)]. Bars show the mean and the SEM. Numbers in brackets indicate sample size. Unpaired *t*-tests were performed for statistical significance. A.U., arbitrary units.

3.5. Shorter telomeres in *BRCA2* mutation carriers harboring the SNP

We first evaluated TL distribution in 91 healthy women as a function of age to obtain a regression line to adjust TL in the FBOC samples. As expected, we found a decrease in TL with age (Fig. S6). When the effect of rs34259 was analyzed for each BRCA mutation group, we only found a significant effect among *BRCA2* mutation carriers: In this group, SNP carriers had a reduced age-adjusted TL ($P = 0.018$; Fig. 4A) and showed a trend toward accumulation of short telomeres ($P = 0.067$; Fig. 4B).

3.6. Telomerase activity

We found a significant correlation between telomerase activity and telomere length ($r = 0.313$; $P < 0.001$). Mean telomerase activity was lower when the SNP was present in all groups, but it did not reach statistical significance (Fig. S7).

4. Discussion

The SNP rs34259 in the 3′UTR of the *UNG* gene may decrease ovarian cancer risk in *BRCA2* mutation carriers (Osorio *et al.*, 2014). However, the molecular mechanism underlying this association is unknown. In the present report, we show that rs34259 is associated with significant *UNG* downregulation and with lower levels of oxidative DNA damage at telomeres. In addition, we found that for *BRCA2* mutation carriers the SNP is associated with significantly lower oxidative stress susceptibility and lower uracil accumulation at telomeres.

As it has been previously demonstrated that the region where the variant is located is a potential seed

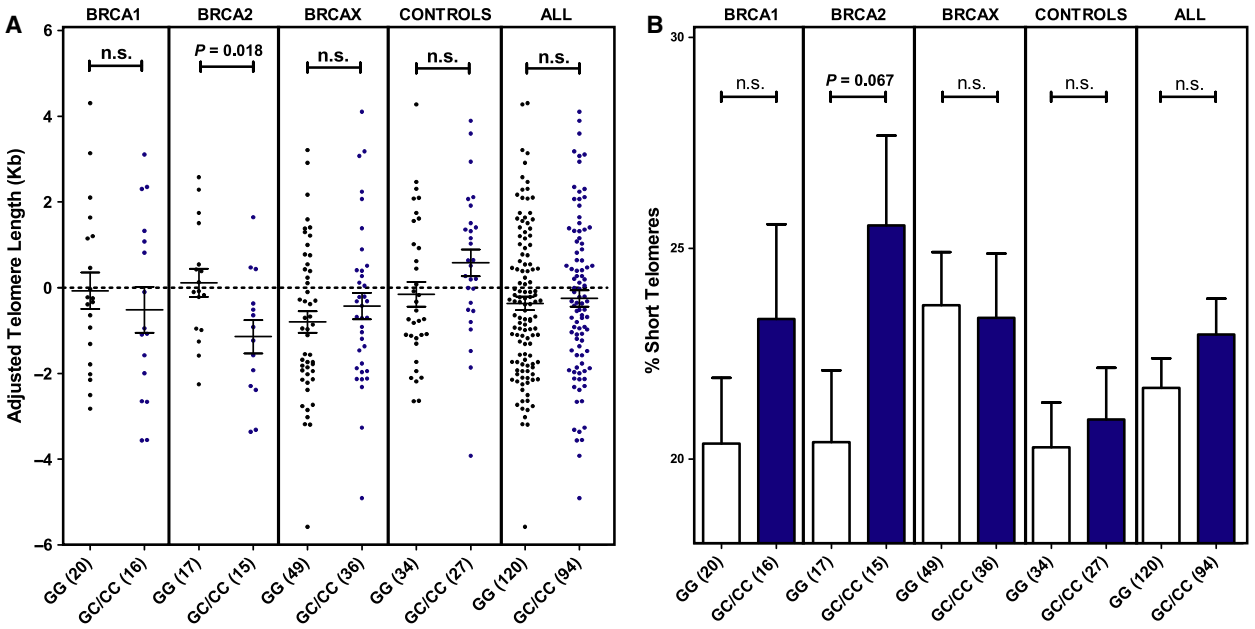

Fig. 4. Telomere length and percentage of short telomeres. (A) Distribution of telomere length (kb) values adjusted for age in the FBOC series according to the presence or absence of the *UNG* SNP [noncarriers (GG)/carriers (GC/CC)]. (B) Comparative analysis of FBOC groups regarding the percentage of short (< 3 kb) telomeres. Bars show the mean and the SEM. Numbers in brackets indicate sample size. Unpaired *t*-tests were performed for statistical significance.

site for microRNAs that downregulate *UNG* expression (Hegre *et al.*, 2013), we decided to explore the effect of this SNP on *UNG* mRNA and protein levels. We detected significantly lower *UNG* mRNA and UNG1 protein levels associated with SNP rs34259, which became pronounced in *BRCA2* mutation carriers. It has been shown that overexpression of human UNG in yeast causes DNA damage due to the generation of AP sites faster than they are repaired (Elder *et al.*, 2003). In this regard, the lower UNG expression associated with rs34259 may prevent AP repair from becoming saturated, and this may in part explain its protective effect.

Given the dominant role of UNG for processing uracil at telomeres (Cortizas *et al.*, 2016), we evaluated uracil accumulation and observed that this was higher in telomeric DNA than in other genomic regions (Fig. S5), confirming that telomeres are prone to uracil accumulation (Vallabhaneni *et al.*, 2015). When we analyzed the SNP effect, we found significantly lower uracil accumulation when the SNP was present, but only for *BRCA2* carriers (Fig. 2B). This suggests that rs34259 could have a positive impact on UNG enzyme performance that may help to explain the protective effect of this SNP in *BRCA2* carriers.

Furthermore, we explored the impact of this SNP on other features related to telomere biology, such as oxidative damage. Because telomeres are especially susceptible to DNA oxidation (O'Callaghan *et al.*, 2011; Von Zglinicki *et al.*, 2000), we evaluated the accumulation of 8-oxoguanine as a measure of oxidative damage. We observed significantly lower 8-oxoguanine levels in individuals harboring the variant (Fig. 2A), suggesting that the SNP is associated with lower oxidative DNA damage accumulation at the telomeres.

We found that the SNP impact on *UNG* expression affects both nuclear (UNG2) and mitochondrial (UNG1) isoforms (Fig. S2). Therefore, apart from the telomeres, it is probable that mitochondrial DNA of patients harboring the SNP presents lower damage, given that oxidative base lesions in mitochondria are repaired by UNG1 (Akbari *et al.*, 2007). In addition, we analyzed whether the lower levels of oxidative DNA damage associated with the SNP could be related to lower chronic oxidative stress susceptibility. We found lower protein carbonylation levels when rs34259 was present (Fig. 3), and this was more pronounced in *BRCA2* mutation carriers. These results suggest that the SNP in *UNG* is associated with lower oxidative stress susceptibility, especially for *BRCA2* carriers. Oxidative stress plays an important role in the development and progression of cancer (Valko *et al.*, 2006), and therefore, the lower oxidative stress

associated with the SNP may help to explain the lower cancer risk of *BRCA2* carriers that harbor the SNP.

We also found a significantly shorter TL associated with the SNP in carriers of *BRCA2* mutations (Fig. 4A). TL is regulated by the shelterin protein complex that protects telomeres (De Lange, 2005) and by telomerase, a ribonucleoprotein complex that adds TTAGGG repeats to the chromosome ends (Blackburn, 2001). Our data reflect this expected positive correlation between TL and telomerase activity. The accumulation of uracil in telomeres weakens the binding affinity of the shelterin component POT1, increasing the accessibility of telomerase. Thus, UNG deficiency causes defective uracil removal that can lead to lengthening of telomeres, as has been demonstrated in mice (Vallabhaneni *et al.*, 2015). According to this model, the short telomeres phenotype observed in *BRCA2* carriers harboring the SNP could be due to the lower uracil accumulation at telomeres, also associated with this group, which facilitates shelterin binding.

5. Conclusions

We have found that the ovarian cancer risk modifier SNP rs34259 may have a positive impact on UNG enzyme performance and is associated with lower oxidative levels in *BRCA2* carriers, which may explain the cancer-protective effect attributed to this SNP in this group. Taken together, our findings support the importance of genetic changes in BER pathway genes as modifiers of cancer susceptibility for *BRCA1* and *BRCA2* mutation carriers.

Acknowledgements

We thank the patients and healthy volunteers who participated in this study. We thank Dr Thomas Helleday (Karolinska Institutet, Stockholm, Sweden) for providing the UNG enzyme. We thank all members of the Human Cancer Genetics Program of the Spanish National Cancer Research Centre for their support. JMB is supported by grant FPU15/01978 from the Spanish Ministry of Education, Culture, and Sport. CB-B is supported by the Spanish Ministry of Health FIS PI12/00070. This study was partially funded by the Spanish Ministry of Economy and Competitiveness (MINECO) SAF2014-57680-R. JB's laboratory is partially funded by FIS PI16/00440 supported by FEDER funds and the Spanish Network on Rare Diseases (CIBERER). MU is supported by grant PI14/00459 from the European Regional Development Fund (ERDF). RP's laboratory is funded by grant P14-01495 (Fondo de Investigaciones Sanitarias, Instituto de Salud Carlos III, Spain) supported by FEDER funds. JLG-G thanks the Instituto de Salud Carlos III for grant number PI16/01031, cofinanced by the European Regional Development Fund (ERDF).

Conflict of interest

The authors declare no conflict of interest.

Author contributions

JB and AO contributed to study conception and design. JMB, CB-B, VF, MU, JLG-G, and RP involved in acquisition of data. JMB, CB-B, JB, and AO contributed to analysis and interpretation of data. JMB and CB-B drafted the manuscript. JB and AO critically revised the manuscript. All authors read and approved the final manuscript.

References

Akbari M, Otterlei M, Peña-Diaz J and Krokan HE (2007) Different organization of base excision repair of uracil in DNA in nuclei and mitochondria and selective upregulation of mitochondrial uracil-DNA glycosylase after oxidative stress. *Neuroscience* **145**, 1201–1212.

Amos CI, Dennis J, Wang Z, Byun J, Schumacher FR, Gayther SA, Casey G, Hunter DJ, Sellers TA, Gruber SB *et al.* (2017) The Oncoarray Consortium: a network for understanding the genetic architecture of common cancers. *Cancer Epidemiol Biomarkers Prev* **26**, 26–36.

Ardlie KG, Deluca DS, Segre AV, Sullivan TJ, Young TR, Gelfand ET, Trowbridge CA, Maller JB, Tukiainen T, Lek M *et al.* (2015) The Genotype-Tissue Expression (GTEx) pilot analysis: multitissue gene regulation in humans. *Science* **348**, 648–660.

Benítez-Buelga C, Baquero JM, Vaclová T, Fernández V, Martín P, Inglada-Pérez L, Urioste M, Osorio A and Benítez J (2017) Genetic variation in the NEIL2 DNA glycosylase gene is associated with oxidative DNA damage in BRCA2 mutation carriers. *Oncotarget* **8**, 114626–114636.

Benítez-Buelga C, Sanchez-Barroso L, Gallardo M, Apellániz-Ruiz M, Inglada-Pérez L, Yanowski K, Carrillo J, Garcia-Estevez L, Calvo I, Perona R *et al.* (2015) Impact of chemotherapy on telomere length in sporadic and familial breast cancer patients. *Breast Cancer Res Treat* **149**, 385–394.

Benítez-Buelga C, Vaclová T, Ferreira S, Urioste M, Inglada-Pérez L, Soberón N, Blasco M, Osorio A and Benitez J (2016) Molecular insights into the OGG1 gene, a cancer risk modifier in BRCA1 and BRCA2 mutations carriers. *Oncotarget* **7**, 25815–25825.

Blackburn EH (2001) Switching and signaling at the telomere. *Cell* **106**, 661–673.

Bryant HE, Schultz N, Thomas HD, Parker KM, Flower D, Lopez E, Kyle S, Meuth M, Curtin NJ and Helleday T (2005) Specific killing of BRCA2-deficient tumours with inhibitors of poly (ADP-Ribose) polymerase. *Nature* **434**, 913–917.

Canela A, Vera E, Klatt P and Blasco MA (2007) High-throughput telomere length quantification by FISH and its application to human population studies. *Proc Natl Acad Sci USA* **104**, 5300–5305.

Carithers LJ, Ardlie K, Barcus M, Branton PA, Britton A, Buia SA, Compton CC, DeLuca DS, Peter-Demchok J, Gelfand ET *et al*. (2015) A novel approach to high-quality postmortem tissue procurement: the GTEx project. *Biopreserv Biobank* **13**, 311–319.

Cortizas EM, Zahn A, Safavi S, Reed JA, Vega F, Di Noia JM and Verdun RE (2016) UNG protects B cells from AID-induced telomere loss. *J Exp Med* **213**, 2459–2472.

De Lange T (2005) Shelterin: the protein complex that shapes and safeguards human telomeres. *Genes Dev* **19**, 2100–2110.

Elder RT, Zhu X, Priet S, Chen M, Yu M, Navarro JM, Sire J and Zhao Y (2003) A fission yeast homologue of the human Uracil-DNA-glycosylase and their roles in causing DNA damage after overexpression. *Biochem Biophys Res Commun* **306**, 693–700.

Farmer H, McCabe N, Lord CJ, Tutt ANJ, Johnson DA, Richardson TB, Santarosa M, Dillon KJ, Hickson I, Knights C *et al*. (2005) Targeting the DNA repair defect in BRCA mutant cells as a therapeutic strategy. *Nature* **434**, 917–921.

Fedorova M, Bollineni RC and Hoffmann R (2013) Protein carbonylation as a major hallmark of oxidative damage: update of analytical strategies. *Mass Spectrom Rev* **33**, 79–97.

García-Giménez JL, Velázquez-Ledesma AM, Esmoris I, Romá-Mateo C, Sanz P, Viña J and Federico Pallardó FV (2012) Histone carbonylation occurs in proliferating cells. *Free Radic Biol Med* **52**, 1453–1464.

Hegde ML, Hazra TK and Mitra S (2008) Early steps in the DNA base excision/single-strand interruption repair pathway in mammalian cells. *Cell Res* **18**, 27–47.

Hegre SA, Sætrom P, Aas PA, Pettersen HS, Otterlei M and Krokan HE (2013) Multiple microRNAs may regulate the DNA repair enzyme uracil-DNA glycosylase. *DNA Repair* **12**, 80–86.

Jia P, Chengtao H and Chai W (2015) DNA excision repair at telomeres. *DNA Repair* **36**, 137–145.

Krokan HE, Drabløs F and Slupphaug G (2002) Uracil in DNA – occurrence, consequences and repair. *Oncogene* **21**, 8935–8948.

Maynard S, Schurman SH, Harboe C, de Souza-Pinto NC and Bohr VA (2009) Base excision repair of oxidative DNA damage and association with cancer and aging. *Carcinogenesis* **30**, 2–10.

Milne RL, Osorio A, Cajal TR, Vega A, Llort G, De La Hoya M, Díez O, Alonso MC, Lazaro C, Blanco I *et al*. (2008) The average cumulative risks of breast and ovarian cancer for carriers of mutations in BRCA1 and BRCA2 attending genetic counseling units in Spain. *Clin Cancer Res* **14**, 2861–2869.

Nilsen H, Otterlei M, Haug T, Solum K, Nagelhus TA, Skorpen F and Krokan HE (1997) Nuclear and mitochondrial uracil-DNA glycosylases are generated by alternative splicing and transcription from different positions in the UNG gene. *Nucleic Acids Res* **25**, 750–755.

O'Callaghan N, Baack N, Sharif R and Fenech M (2011) A qPCR-based assay to quantify oxidized guanine and other FPG-sensitive base lesions within telomeric DNA. *Biotechniques* **51**, 403–412.

O'Donovan PJ and Livingston DM (2010) BRCA1 and BRCA2: breast/ovarian cancer susceptibility gene products and participants in DNA double-strand break repair. *Carcinogenesis* **31**, 961–967.

Osorio A, Milne RL, Kuchenbaecker K, Vaclová T, Pita G, Alonso R, Peterlongo P, Blanco I, de la Hoya M, Duran M *et al*. (2014) DNA glycosylases involved in base excision repair may be associated with cancer risk in BRCA1 and BRCA2 mutation carriers. *PLoS Genet* **10**, e1004256.

Pooley KA, Bojesen SE, Weischer M, Nielsen SF, Thompson D, Olama AA, Michailidou K, Tyrer JP, Benlloch S, Brown J *et al*. (2013) A Genome-Wide Association Scan (GWAS) for mean telomere length within the COGS project: identified loci show little association with hormone-related cancer risk. *Hum Mol Genet* **22**, 5056–5064.

Vaclová T, Gómez-López G, Setién F, Garcia-Bueno JM, Macias JA, Barroso A, Urioste M, Esteller M, Benítez J and Osorio A (2015) DNA repair capacity is impaired in healthy BRCA1 heterozygous mutation carriers. *Breast Cancer Res Treat* **152**, 271–282.

Valko M, Rhodes CJ, Moncol J, Izakovic M and Mazur M (2006) Free radicals, metals and antioxidants in oxidative stress-induced cancer. *Chem Biol Interact* **160**, 1–40.

Vallabhaneni H, Zhou F, Maul RW, Sarkar J, Yin J, Lei M, Harrington L, Gearhart PJ and Liu Y (2015) Defective repair of uracil causes telomere defects in mouse hematopoietic cells. *J Biol Chem* **290**, 5502–5511.

Von Zglinicki T, Pilger R and Sitte N (2000) Accumulation of single-strand breaks is the major cause of telomere shortening in human fibroblasts. *Free Radic Biol Med* **28**, 4–74.

Ward LD and Kellis M (2012) HaploReg: a resource for exploring chromatin states, conservation, and

regulatory motif alterations within sets of genetically linked variants. *Nucleic Acids Res* **40**, 930–934.

Westra HJ, Peters MJ, Esko T, Yaghootkar H, Schurmann C, Kettunen J, Christiansen MW, Fairfax BP, Schramm K, Powell JE *et al.* (2013) Systematic identification of trans eQTLs as putative drivers of known disease associations. *Nat Genet* **45**, 1238–1243.

Xue JH, Xu GF, Gu TP, Chen GD, Han BB, Xu ZM, Bjørås M, Krokan HE, Xu GL and Du YR (2016) Uracil-DNA glycosylase UNG promotes Tet-mediated DNA demethylation. *J Biol Chem* **291**, 731–738.

Zerbino DR, Achuthan P, Akanni W, Amode MR, Barrell D, Bhai J, Billis K, Cummins C, Gall A, Girón CG *et al.* (2018) Ensembl 2018. *Nucleic Acids Res* **46**, 754–761.

Zharkov DO, Mechetin GV and Nevinsky GA (2010) Uracil-DNA glycosylase: structural, thermodynamic and kinetic aspects of lesion search and recognition. *Mutat Res* **685**, 11–20.

Supporting information

Additional supporting information may be found online in the Supporting Information section at the end of the article.

Fig. S1. (A) Correlation analysis between total *UNG* mRNA expression and *UNG1* mRNA expression. (B) Correlation analysis between total *UNG* mRNA expression and *UNG2* mRNA expression. (C) Correlation analysis between *UNG1* mRNA and *UNG2* mRNA expression. Spearman's test was used to assess the significance of the correlations.

Fig. S2. Expression levels of specific isoforms of *UNG* mRNA according to the presence or absence of the SNP (noncarriers (GG)/carriers (GC/CC)).

Fig. S3. Expression levels of specific isoforms of *UNG* mRNA according to the presence or absence of the SNP (noncarriers (GG)/carriers (GC/CC)) in ovarian tissue from *BRCA1* and *BRCA2* patients ($n = 17$).

Fig. S4. (A) Western blot of UNG1 and UNG2 in a panel of 18 established lymphoblastoid cell lines (LCLs) (Vaclová *et al.*, 2015). Briefly, the LCLs were established by Epstein-Barr virus transformation of peripheral blood lymphocytes from eleven healthy women carrying heterozygous mutations in *BRCA1* and seven noncarrier relatives (controls). None of the women included in the study had personal antecedents of cancer. Cells were cultured in RPMI-1640 media (Sigma-Aldrich) supplemented with 20% non-heat-inactivated fetal bovine serum (Sigma-Aldrich), penicillin-streptomycin (Gibco) and Fungizone (Gibco). Cells were cultured at 37 °C in a 5% CO_2 atmosphere and were maintained in exponential growth by daily dilution to 10^6 cells·mL^{-1} complete media. Protein extraction and western blotting were performed as described in the Materials and Methods section. (B) Correlation analysis between UNG1 and UNG2 protein expression levels in LCLs. Spearman's test was used to assess the significance of the correlation. (C) UNG1 and UNG2 expression levels in the LCL series according to the presence or absence of the SNP (noncarriers (GG)/carriers (GC/CC)). Bars show the mean and the standard error of the mean (SEM). Numbers in brackets indicate sample size. Unpaired *t*-tests were performed for statistical significance. DNA extraction and SNP genotyping were performed as are described in the Materials and Methods section.

Fig. S5. PCR amplification efficiency at the untreated and UNG-treated telomeric and *36B4* loci.

Fig. S6. Telomere length (TL) distribution in peripheral blood leukocytes as a function of age for the control population ($n = 91$), measured by HT QFISH.

Fig. S7. Comparative analysis of telomerase activity in the FBOC series according to the presence or absence of the *UNG* SNP (noncarriers (GG)/carriers (GC/CC)).

Table S1. Primers used for *UNG* RNA expression analysis.

Table S2. Linear regression analysis in *BRCA* 1/2 mutation carriers.

Table S3. Variants within the block of linkage disequilibrium (LD) > 0.8 with SNP rs34259.

Table S4. Frequency distribution of the *UNG* variant rs34259 among FBOC groups.

Table S5. Summary of information in the GTEx eQTL server regarding transcriptional downregulation of *UNG* in 16 different tissues when rs34259 is present.